Identification of Low Order Models for Large Scale Processes

PROEFSCHRIFT

ter verkrijging van de graad van doctor aan de
Technische Universiteit Eindhoven,
op gezag van de rector magnificus, prof.dr.ir. C.J. van Duijn,
voor een commissie aangewezen door het College voor
Promoties in het openbaar te verdedigen op
maandag 8 februari 2010 om 16.00 uur

door

Satyajit Kishanrao Wattamwar

geboren te Manwath, India

Dit proefschrift is goedgekeurd door de promotor:

prof.dr.ir. A.C.P.M. Backx

Copromotor:
dr. S. Weiland

A catalogue record is available from the Eindhoven University of Technology Library

ISBN 978-90-386-2154-8

to my family

Eerste promotor: prof.dr.ir. A.C.P.M. Backx

Copromotor: dr. Siep Weiland

Kerncommissie:

Prof.ir. O.H. Bosgra
Prof.Dr.-Ing. Wolfgang Marquardt
Prof. S. Skogestad

This PhD work was financially supported by Eindhoven University of Technology and the European Union within the Marie-Curie Training Network PROMATCH under the grant number MRTN-CT-2004-512441.

The Ph.D. work forms a part of the research program of the Dutch Institute of Systems and Control (DISC).

Summary

Many industrial chemical processes are complex, multi-phase and large scale in nature. These processes are characterized by various nonlinear physio-chemical effects and fluid flows. Such processes often show coexistence of fast and slow dynamics during their time evolutions. The increasing demand for a flexible operation of a complex process, a pressing need to improve the product quality, an increasing energy cost and tightening environmental regulations make it rewarding to automate a large scale manufacturing process. Mathematical tools used for process modeling, simulation and control are useful to meet these challenges. Towards this purpose, development of process models, either from the first principles (conservation laws) i.e. the rigorous models or the input-output data based models constitute an important step. Both types of models have their own advantages and pitfalls. Rigorous process models can approximate the process behavior reasonably well. The ability to extrapolate the rigorous process models and the physical interpretation of their states make them more attractive for the automation purpose over the input-output data based identified models. Therefore, the use of rigorous process models and rigorous model based predictive control (R-MPC) for the purpose of online control and optimization of a process is very promising. However, due to several limitations e.g. slow computation speed and the high modeling efforts, it becomes difficult to employ the rigorous models in practise. This thesis work aims to develop a methodology which will result in smaller, less complex and computationally efficient process models from the rigorous process models which can be used in real time for online control and dynamic optimization of the industrial processes. Such methodology is commonly referred to as a methodology of Model (order) Reduction. Model order reduction aims at removing the model redundancy from the rigorous process models.

The model order reduction methods that are investigated in this thesis, are applied to two benchmark examples, an industrial glass manufacturing process and a tubular reactor. The complex, nonlinear, multi-phase fluid flow that is observed in a glass manufacturing process offers multiple challenges to any model reduction technique. Often, the rigorous first principle models of these benchmark examples are implemented in a discretized form of partial differential equations and their solutions are computed using the Computational Fluid Dynamics (CFD) numerical tools. Although these models are

reliable representations of the underlying process, computation of their dynamic solutions require a significant computation efforts in the form of CPU power and simulation time.

The glass manufacturing process involves a large furnace whose walls wear out due to the high process temperature and aggressive nature of the molten glass. It is shown here that the wearing of a glass furnace walls result in change of flow patterns of the molten glass inside the furnace. Therefore it is also desired from the reduced order model to approximate the process behavior under the influence of changes in the process parameters. In this thesis the problem of change in flow patterns as result of changes in the geometric parameter is treated as a bifurcation phenomenon. Such bifurcations exhibited by the full order model are detected using a novel framework of reduced order models and hybrid detection mechanisms. The reduced order models are obtained using the methods explained in the subsequent paragraphs.

The model reduction techniques investigated in this thesis are based on the concept of Proper Orthogonal Decompositions (POD) of the process measurements or the simulation data. The POD method of model reduction involves spectral decomposition of system solutions and results into arranging the spatio-temporal data in an order of increasing importance. The spectral decomposition results into spatial and temporal patterns. Spatial patterns are often known as POD basis while the temporal patterns are known as the POD modal coefficients. Dominant spatio-temporal patterns are then chosen to construct the most relevant lower dimensional subspace. The subsequent step involves a Galerkin projection of the governing equations of a full order first principle model on the resulting lower dimensional subspace.

This thesis can be viewed as a contribution towards developing the data-based nonlinear model reduction technique for large scale processes. The major contribution of this thesis is presented in the form of two novel identification based approaches to model order reduction. The methods proposed here are based on the state information of a full order model and result into linear and nonlinear reduced order models. Similar to the POD method explained in the previous paragraph, the first step of the proposed identification based methods involve spectral decomposition. The second step is different and does not involve the Galerkin projection of the equation residuals. Instead, the second step involves identification of reduced order models to approximate the evolution of POD modal coefficients. Towards this purpose, two different methods are presented. The first method involves identification of locally valid linear models to represent the dynamic behavior of the modal coefficients. Global behavior is then represented by 'blending'

the local models. The second method involves direct identification of the nonlinear models to represent dynamic evolution of the model coefficients.

In the first proposed model reduction method, the POD modal coefficients, are treated as outputs of an unknown reduced order model that is to be identified. Using the tools from the field of system identification, a black-box reduced order model is then identified as a linear map between the plant inputs and the modal coefficients. Using this method, multiple local reduced LTI models corresponding to various working points of the process are identified. The working points cover the nonlinear operation range of the process which describes the global process behavior. These reduced LTI models are then blended into a single Reduced Order-Linear Parameter Varying (RO-LPV) model. The weighted blending is based on nonlinear splines whose coefficients are estimated using the state information of the full order model. Along with the process nonlinearity, the nonlinearity arising due to the wear of the furnace wall is also approximated using the RO-LPV modeling framework.

The second model reduction method that is proposed in this thesis allows approximation of a full order nonlinear model by various (linear or nonlinear) model structures. It is observed in this thesis, that, for certain class of full order models, the POD modal coefficients can be viewed as the states of the reduced order model. This knowledge is further used to approximate the dynamic behavior of the POD modal coefficients. In particular, reduced order nonlinear models in the form of tensorial (multi-variable polynomial) systems are identified. In the view of these nonlinear tensorial models, the stability and dissipativity of these models is investigated.

During the identification of the reduced order models, the physical interpretation of the states of the full order rigorous model is preserved. Due to the smaller dimension and the reduced complexity, the reduced order models are computationally very efficient. The smaller computation time allows them to be used for online control and optimization of the process plant. The possibility of inferring reduced order models from the state information of a full order model alone i.e. the possibility to infer the reduced order models in the absence of access to the governing equations of a full order model (as observed for many commercial software packages) make the methods presented here attractive. The resulting reduced order models need further system theoretic analysis in order to estimate the model quality with respect to their usage in an online controller setting.

Samenvatting

Processen in de chemische industrie zijn doorgaans complex, multi-fase en grootschalig. Dergelijke processen worden gekarakteriseerd door diverse niet-lineariteiten in fysische en chemische verschijnselen, en door stromingen van vloeistoffen of gassen. In de tijd-evolutie van deze processen zijn doorgaans zowel snelle als trage dynamische fenomenen te onderkennen. De complexiteit van deze processen wordt verder beinvloed door de moeilijkheid om 'in-situ' metingen aan het proces uit te kunnen voeren. Door de toenemende vraag naar een flexibele bedrijfsvoering van dergelijke complexe processen, de noodzaak om kwaliteitsverbetering van produkten te realiseren, en door de toenemende vraag naar duurzaamheid en verminderd energiegebruik, is het noodzakelijk om produktie-processen tot in hoge mate te automatiseren. Om deze uitdaging aan te gaan zijn mathematische modellen noodzakelijk voor het beschrijven, simuleren en besturen van processen, De ontwikkeling van rigoreuze mathematische modellen op grond van elementaire fysische begrippen of de ontwikkeling van empirische modellen op grond van waargenomen data vormen hierbij een belangrijke stap. Beide types modellen hebben voor- en nadelen. Rigoreuze modellen geven doorgaans goede benaderingen van proces gedrag. De fysisch relevante interpretatie van variabelen in deze modellen zijn doorgaans zeer bruikbaar voor automatische besturingen. Het gebruik van rigoreuze procesmodellen is met name van belang bij toepassingen in model-voorspellende regelingen (MPC) waar proces optimalisatie en on-line procesbesturingen een rol spelen. De complexiteit en rekenintensiteit van rigoreuze modellen vormt daarentegen een serieuze belemmering voor on-line toepassingen.

Het is de doelstelling van dit onderzoek om methodologieen te ontwikkelen voor de constructie van vereenvoudigde, minder rekenintensieve modellen die toepasbaar zijn als substitutiemodellen voor on-line toepassingen van optimalisatie en automatische besturingen in de proces industrie. Dit proefschrift heeft tot doel om dergelijke methodologieen voor model reductie te ontwikkelen en te valideren. Model reductie heeft daarmee tot doel om redundantie uit bestaande modellen te verwijderen, waardoor vereenvoudigde modellen worden gecreeerd die relevant zijn voor proces optimalisatie en automatische procesbesturingen.

De model reductie technieken die in dit proefschrift worden ontwikkeld worden toegepast op een tweetal voorbeelden: een industriele oven voor glas-

productie en een buis-reactor voor een chemische applicatie. De complexe, niet-lineaire en multi-fase vloeistofstromingen die in een glasoven plaatsvinden maken de glasoven bij uitstek geschikt voor het toepassen van model reductie technieken. Deze processen worden doorgaans numeriek geimplementeerd als gediscretiseerde partiele differentiaal vergelijkingen en gesimuleerd door geavanceerde CFD ("computational fluid dynmaics") technieken. Ofschoon deze simulatiemodellen nauwkeurig zijn, vereisen de berekening van sinmulatietrajecten een substantiele hoeveelheid rekentijd.

Het glasoven proces dat in dit proefschrift is beschreven betreft en grote oven waarvan de wanden door corrosie en hoge proces temperaturen aan verandering onderhevig zijn. De verandering van geometrie in de oven veroorzaakt op haar beurt een verandering van het stromingsprofiel van gesmolten glas in de oven. Modelreductie technieken dienen derhalve in staat te zijn deze veranderingen van procesdynamika te kunnen beschrijven. In dit proefschrift worden deze parametergevoeligheden gemodelleerd als bifurcatieverschijnselen. Doel van dit onderzoek is o.m. om dergelijke bifurcaties zo nauwkeurig mogelijk in gereduceerde modellen te representeren.

In dit proefschrift staat de POD ("proper orthogonal decomposition") techniek centraal voor de constructievan gereduceerde modellen. Deze techniek is gebaseerd op een spectraaldecompositie van de procesvariabelen waarin een scheiding wordt aangebracht van spatiele en temporele variabelen. De spatiele patronen (de POD basis functies) en de temporele patronen (POD modale coefficienten) worden empirisch bepaald uit gemeten of gesimuleerde data. De dominante spatiele-temporele patronen zijn vervolgens de basis voor de constructie van het gereduceerde model. Het gereduceerde model komt daarbij tot stand door een Galrkin projectie uit te voeren op de residueen van het rigoreuze proces model.

Dit proefschrift vormt een bijdrage voor het uitvoeren van data-gebaseerde model reductie voor grootschalige processen. De belangrijkste contributies in dit werk zijn een tweetal nieuwe identificatie-gebaseerde technieken voor het bepalen van gereduceerde modellen. Deze technieken zijn gebaseerd op informatie over de toestand van het volle orde model en resulteren lineaire of niet-lineaire gereduceerde modellen. Vergelijkbaar met de POD techniek wordt als eerste een spectraal decompositie uitgevoerd op gemeten of gesimuleerde data. In een tweede stap wordt een identificatie technieken toegepast om te komen tot een beschrijving van de tijd-evolutie van de POD modale coefficienten. Voor dit laatste worden in dit proefschrift twee technieken voorgesteld en vergeleken. In de eerste identificatie methode worden diverse lokaal relevante lineaire modellen samengevoegd door een 'blending' techniek tot een globaal relevant model. In de tweede identificatie methode wordt een

niet-lineair model direkt geïdentificeerd.

In de eerste model reductie procedure worden de POD modale coefficienten beschouwd als uitgangen van een vooralsnog onbekend model dat geïdentificeerd dient te worden. Via 'black-box' identificatie technieken wordt een lineair model bapaald dat de proces ingangen relateert aan de POD modale coefficienten. Deze lineaire modellen worden geidentificeerd in iverse werkpunten van het proces. De werkpunten worden representatief verondersteld over de dynamische bandbreedte van het proces. Via een 'blending' techniek worden de lokale modellen vervolgens samengevoegd tot één enkel gereduceerd lineair parameter afhankelijk (RO-LTV) model. De blending techniek maakt gebruik van splines waarvan coefficienten geschat worden op grond van toestandsinformatie van het volle orde model.

In de tweede model redcutie procedure wordt het volle orde model direkt benaderd door diverse lineaire of niet-lineaire gereduceerde modellen. Hierbij worden de POD modale coefficienten geinterpreteerd als toestanden van gereduceerde modellen waarvan de tijd-afhankelijke dynamica wordt beschreven door lage orde niet lineaire model structuren. In het bijzonder zijn identificatie-technieken uitgewerkt voor nieut lineiare tensor-modellen. de stabiliteit en dissipativiteit van deze modellen is verder onderzocht.

Bij de identificatie van gereduceerde modellen blijft de fysische interpretatie van de toestand van het rigoreuze model behouden. De diverse gereduceerde modellen zijn aanzienlijk sneller in rekentijd dan de volle orde modellen. Deze versnelling in rekentijd maakt deze modellen geschikt voor on-line toepassingen en voor verdere proces optimalisatie. De mogelijkheid om gereduceerde modellen te identificeren maakt de in dit proefschrift beschreven technieken aantrekkelijk voor toepassingen waar een comleet mathematische model van het proces niet, of slechts ten dele voorhanden is. Voor de geidenficeerde lage orde modellen is verdere analyse noodzakelijk om de kwaliteit van de modellen te kwantificeren voor on-line regel doeleinden.

Contents

List of Figures

1

Introduction

This thesis presents novel ways to solve the problem of model order reduction for large scale systems as they occur in real life applications. The methods proposed here have been applied to an industrial glass manufacturing process. The glass manufacturing process is characterized by multidimensional, nonlinear, multi-phase reactive fluid flows. Such a process is typically modeled by Computational Fluid Dynamics tools. Depending on the required accuracy, this results into very large order process models. The model reduction techniques presented here are aimed at providing control oriented models for such large scale processes that can be used online for model based control and optimization purposes. The methods proposed in this thesis constitute the combination of tools available from literature like spectral decomposition, parameter estimation, and modeling and identification. Spectral decomposition techniques are used to separate spatial and temporal patterns. Temporal patterns are approximated by using a modeling framework of linear parameter varying systems and of nonlinear forms. The thesis has three major contributions; First- Hybrid detection mechanisms based on reduced order models to detect the discontinuous process behavior as result of continuous parameter variations. Second- A linear parameter varying reduced order modeling framework. Third- a reduced order nonlinear modeling framework involving tensorial decompositions. The methods that are proposed here formulate the model reduction problem as an identification problem. The outcome of the methods proposed here has reduced the number of equations with a factor of at least 100 while, an increase in computation speed is established by a factor of more than 1000 times. The possibility of approximating the nonlinear effects by the reduced order models has greatly enhanced the usability of these methods. Faster compu-

tation of the resulting reduced order models allow them to be used for online purpose of control and optimization.

1.1 General introduction

It is human psyche to observe, to study and to influence the nature around him. The ability to think and to act rationally has made human being the most powerful species on this planet. The inquisitive human nature has transformed him from the stone age to the digital age of present time. It took ages to invent the sharp tools and the use of metals, but their availability greatly transformed the compatibility of early humans. Similarly, the invention of wheel increased human efficiency by many times. Now, we are at the stage in human history where we almost double our efficiency every year in the form of computation speed. The continuous pursuit towards betterment, excellence and innovation are some of the reasons behind this transformation. The zeal towards the improvement of human life is also reflected in the form of infinite number of man-made machines, instruments, processes etc. Towards the similar aim, in the last century, mathematical modeling of our physical surrounding and the human invented machines has emerged as the important tool for understanding and therefore influencing them in some desired way. In the present time, mathematical modeling accompanied by the vast computational power forms an integral part of research and development in almost every scientific pursuit. Together with Control and Optimization, mathematical modeling constitute a wise attempt in order to influence the man-made processes. Next subsections elaborates more on the need for mathematical modeling and control of physical processes.

1.1.1 Modeling

Modeling of dynamical features of a process is an important step to understand the process in a better way. Usually modeling involves the task to discover and express the relation between measurable and quantifiable process variables and external effects. Modeling of a process or a physical device is necessary to condense the knowledge, to understand, to predict and to control it in a desired way. Modeling of physical phenomena has a very long standing tradition. It has helped mankind to understand the relation between cause and effect for a large variety of physical (natural and man

made) systems. Usually the intension is to express different physical effects in the form of mathematical equations. This art of expressing the behavior of a system in terms of mathematical expression is referred to as modeling. The contribution of many legendary personalities like Pythagoras, Newton, Euler, Gauss, Einstein etc. has made this field an interesting and motivating one to explore new ideas.

Similar to other physical phenomena, chemical processes are often modeled in order to understand the relations among different variables. This understanding is then used to design the process operation, its equipment in some optimal way. There are different possible ways to model a process. Usually most of the chemical unit operations are modeled as lumped systems. A lumped system assumes that the raw material that is undergoing certain changes is perfectly mixed and there is no spatial variation inside the process equipement. This assumption simplifies the modeling considerably. In fact, the only variable that remains independent is time. Mathematical models of such lumped processes are based on laws of conservation and they are described by Ordinary Differential Equations (ODEs) or by Differential Algebraic Equations (DAEs). Dynamics of many chemical processes can be approximately described by equations of DAE or ODE form. Such type of process modeling is usually referred to as the First Principle or the Mechanistic or the Rigorous Process Modeling. In such models, the physical effects are often expressed by nonlinear relations. Solutions of such lumped nonlinear first principle models are obtained at each time instant by applying a combination of different numerical integration schemes and these solutions are commonly referred to as the 'states' of a model. As the first principle models are derived from the laws of physics, their states have a physical interpretation. Depending on the type of a nonlinear model, the numerical scheme and the efficiency of involved hardware and software structures, the simulation time of such a model can vary a lot. With advancements in computer efficiency, many commercial software packages can easily simulate rigorous process models quite efficiently.

As an alternative to the class of lumped parameter systems, we mention here the class of Distributed Parameter Systems (DPS) or simply Distributed Processes. The term distributed refers to the distribution in space. Therefore such process models have at least two (often space and time) or more independent variables. Although, most of the processes belong to this class, only the processes whose dynamic behavior can not be effectively modeled as 'lumped in space' systems are usually modeled as DPS. Modeling tech-

niques for DPS need rigorous mathematical treatments and result into model equations of the form which are commonly referred to as Partial Differential Equations (PDEs).

The common approach to numerically solve spatio-temporal systems amounts to using a discretization of the spatial configuration space by means of finite element or finite volume methods. With appropriate choices of discretization (mesh) densities, this approach leads to approximating the original partial differential equations by a finite, but usually large set of implicit or explicit PDEs. A popular spatial discretization technique is the Galerkin or Petrov-Galerkin projection method, where the original infinite dimensional system is projected on a finite dimensional space spanned by some orthonormal basis functions. After projection, the resultant system is represented by ordinary differential equations and in this thesis such a model obtained from spatial discretization is referred as a full order model. Full order model is then simulated by different numerical integration schemes, see Antoulas (2005a), Lapidus and Pinder (1982).

The work that is presented in this thesis is applied to industrial glass manufacturing process which belongs to the class of DPS involving nonlinear reaction kinetics and fluid flows. It is typical to use the tools from Computational Fluid Dynamics (CFD) to solve such a DPS. Therefore, such full order models are also referred to as CFD models. Depending upon the required accuracy and the dimension of the spatial configuration space, these spatial discretizations may lead to large mesh sizes, and consequently large number of ODEs. For a glass manufacturing process simulation model, spatial discretization for a sufficient accuracy of solutions may easily lead to about 10^6 to 10^8 equations, which needs to be solved at every time step. A dynamic simulation of such a model therefore need tremendous computational efforts in the form of CPU power and simulation time. In spite of the advancement in computation power over the years, it is still impossible for a normal configured PC to meet the above mentioned computational requirements in real time.

1.1.2 Process control and optimization

As explained in section 1.1.1, modeling of a physical process can be useful for analyzing its dynamic performance. Moreover, modeling of physical processes can also be used to predict its behavior and to control in some desired

way. The field of engineering which studies the aspects of control of chemical processes is usually referred to as process control. The role of a controller in a process plant is to drive a process towards a desired goal in a stable and optimal way. In the last few decades process control has made many advancements in controlling chemical processes. Especially model based predictive control (MPC) has proved its usability in many applications. A model based controller allows to meet the constraints which are necessary for operation of many chemical processes. Often, the MPC is accompanied by an optimizer which provides an optimum set point or a desirable or optimal trajectory of the process. Based on such a set point and measurements from the plant, MPC predicts an optimal future control input at each time instance. Such an optimal process input trajectory drives the plant towards the desired set point in presence of the disturbances. Both, the optimizer and MPC involve some sort of optimization problem which rely on evaluation of the process model at each time instance. If the given process model is complex and difficult to evaluate in real time, then it is different to use MPC as a controller for the plant. Therefore, the bottleneck in achieving a desired performance of a model based process controller lies in the quality and computational speed of the process model.

1.1.3 Modeling and model reduction for control

It is explained in section 1.1.2 that the rigorous process models can be useful for the purpose of control of chemical processes in a real time. Unfortunately the modeling of a physical process from conservation laws is a time consuming, expensive and laborious process. Sometimes, even with the availability of a reliable first principle model for a DPS, due to its forbidding computational efforts, it is hardly possible to use such models for the model based control purposes. To overcome this problem, the control community has developed some system identification tools which are based on plant input and output data. Such data need to be obtained by exciting the plant in some smart way so as to excite the dynamics from a control viewpoint. Although such models are good for model based control, the identification test performed on the plant can be very expensive. The states of such a model do not have any physical interpretation. Moreover the validity range of such a model is limited to the window of the excitation signals used during the identification step. Therefore, the solution to the problem of obtaining reliable models for the purpose of model based control lies in inferring computationally efficient models from the first principle models. As the required

computational efforts for dynamic simulations are proportional to the system order (number of states), reduction in computational efforts amounts to reduction in system order. This step is usually known as model order reduction (MOR). For a DPS, computationally efficient approximate or reduced order models obtained by simplification of first principle model can be very promising for model based controller and optimizer design. Some model reduction work in similar directions is presented in Gay and Ray (1995), Antoulas (2005b), Hoo and Zheng (2002), Marquardt (1990), Antoulas (2005a), or Shvartsman and Kevrekidis (1998).

Among many different model order reduction techniques, the method of Proper Orthogonal Decomposition (POD) (or the Karhunen-Loève method) is widely used for deriving lower dimensional approximations of first principle models. The POD method searches for the dominant subspace in which the dynamics of the full order model evolve. Such a space is spanned by orthonormal POD basis functions. Using Galerkin type of projections of full order model equations, a reduced order model can be inferred. The method of POD and Galerkin projection is discussed in chapter 3.

1.2 Thesis objectives and problem formulation

In this section we present the thesis objectives that led to the present research. The thesis objectives are formulated as the research problems. The overall objective can be briefly formulated in generic terms as "To develop the methodologies to infer low dimensional, computationally efficient, accurate models for large scale complex processes. Such reduced order models should be significantly less complex than the full order models". As the terms 'complex', 'fast', 'accurate', 'low' and 'large' are relative, in following paragraphs the thesis objectives are explained in more detail by quantifying these relative terms. The notion of complexity is divided in terms of - system order, computation speed, ease in modeling and implementation. Some of these objectives are inherently contradictory to each other, e.g. order and accuracy of reduced order model. The research work presented in this thesis aims to meet these objectives simultaneously by finding appropriate tradeoffs among the various objectives. Consider an original (full order) dynamic process model represented by $M \in \mathbb{M}$ where $\mathbb{M}$ is a certain model class. This thesis aims at identifying an approximate model M_r in the same class, i.e. $M_r \in \mathbb{M}$ with some properties. These properties are itemized as follows:

- *Reduction in model complexity.*

  Given a model class $\mathbb{M}$, the complexity of a model $M \in \mathbb{M}$, is the real number $c(M)$ where $c : \mathbb{M} \rightarrow \mathbb{R}$ is the "complexity" function. Reduction in complexity implies $c(M_r) \leq c(M)$ where M_r is a less complex approximate model. Typical examples include when $\mathbb{M}$ is the class of LTI systems with finite dimensional state vector. In that case, $c\,(M) = n\,(M)$, i.e. the state dimension of one (and hence all) minimal state representations of M. For the model class of Distributed Parameter Systems (DPS), i.e. $\mathbb{M}$ is DPS, the complexity is a combination of many factors like system order, computation time, type of nonlinear source or sink term etc. Therefore in that case, complexity is a vector such that $c : \mathbb{M} \rightarrow \mathbb{R}^q$, where q is the number of factors that influence the complexity. It the becomes imperative to compare the i^{th} complexity factor in $c(M)$of original model, i.e. $c_i(M)$ and an approximate model $c_i(M_r)$ in the same model class $\mathbb{M}$.

  All following objectives can be seen as the form of complexity reduction.

- *Reduction in model order.*

  Similar to the LTI systems, the model order is also one of the factors that influences the complexity of processes modeled as DPS, i.e. $c_i(M) = n(M)$. Therefore, one of the objectives of this thesis is to reduce the system order, i.e. $n\,(M_r) < n\,(M)$.

  Explanation: It is the primary aim of this thesis to develop model reduction techniques which can be used to approximate the large scale process models, especially to solve problems involving fluid flows and reactions. Such processes are usually categorized under the class of Distributed Processes or Distributed Parameter Systems and modeled by using Computational Fluid Dynamic (CFD) tools. CFD tools employ Finite Element or Finite Volume techniques to transform the DPS into (non)-linear discrete time state evolutions for which the complexity is again the state dimension. Therefore, $c_i(M) = n(M)$. Where, $M \in \mathbb{M}$, $\mathbb{M}$ is a class of Ordinary Difference Equation (ODE) models formed as an outcome of Finite Element implementation of the DPS model. Such an FE implementation results in a high order process model. By large we mean models approximately of order $10^6 - 10^8$. Due to such a large state dimension, applicability of most of the model approximation (reduction) techniques is very limited for such a process. Therefore, the aim of this thesis is to investigate a methodology

which is not only applicable to academic examples, but can be used to deduce reduced order approximate models for real life applications. The application considered in this thesis is a glass manufacturing process whose process models fit the above mentioned description of full order process models.

- *Maintaining the model accuracy.*

  Model accuracy is defined in terms of a distance measure $\mathrm{d} : \mathbb{M} \times \mathbb{M} \rightarrow \mathbb{R}$, measuring the (approximation) mismatch $\mathrm{d}(M, M_r)$ between the two models M and M_r in the same model class $\mathbb{M}$ as defined in the introduction of this section, with a property. Then the problem of model approximation with maintaining the accuracy amounts to

  $$M_r = \arg \min_{M_r \in \mathbb{M}; c(M_r) < c(M)} \mathrm{d}(M, M_r)$$

  That is, the aim is to find an approximate model with less complexity, which can minimize the mismatch d.

  Explanation: It is desired that for the model class of DPS the trajectories of the approximate model M_r should not deviate substantially from the trajectories of the original model M.

- *Improved computational efficiency.*

  For the DPS, belonging to the model class $\mathbb{M}$ the computational efficiency can be expressed in terms of simulation time that is required by an original model and an approximate model for a given configuration of solver and numerical scheme, such that for a simulation horizon T of the real process, the full order model needs time T_f and the approximate model M_r needs time T_r. The computational efficiency then implies that $T_r < T_f$ and $T_r << T$. Moreover if the fastest time constant of the process is T_d then computational efficiency also implies that $T_r < T_d$. Here the reduction in complexity is viewed as the reduction in simulation time, i.e. $c_i(M) = T(M)$, where $T(M)$ is the simulation time of a model M in a class $\mathbb{M}$, in a specified simulation scenario.

  Explanation: Galerkin type of projection techniques in combination with Proper Orthogonal Decomposition as a model approximation technique, results into a low order but dense system model such that the original sparse structure of the full order model is lost. Loss of the sparse structure, in spite of the smaller dimension of the reduced

model, leads to significant computational cost and then the reduced order model can not be used for the purpose of real time process control and optimization. It is an objective of this thesis to develop an approximate model for systems belonging to DPS, which can be used to compute the system trajectories in real time (few seconds). Such an objective demands that the simulation time needs to be in order of 1000 times shorter than the time needed for a full order CFD model, simulated over the same simulation horizon.

- *To develop approximate process models which are optimal in some sense.*

  Explanation: The optimality is explained such that for given process conditions, the solutions of the reduced order models reside in a space spanned by basis functions which are optimal in some sense.

- *To develop a model approximation technique which can approximate bifurcation behavior nearby critical parameter values as exhibited by the original process model and to detect its occurrence.*

  Consider an original parameterized model $M(\theta) \in \mathbb{M}$ with θ a parameter, belonging to a parameter space Θ. Hence a model $M : \Theta \rightarrow \mathbb{M}$ is a function defined on a parameter set Θ. Suppose that the model has a qualitative property $P_1 \in P$ for $\theta \in \Theta_1$ and $P_2 \in P$ for $\theta \in \Theta_2$, where $\Theta_1 \subseteq \Theta$ and $\Theta_2 \subseteq \Theta$ define a partition of Θ. We call $\theta^* \in \Theta$ a bifurcation value, if θ^* lies on the boundary $\partial\Theta_1 \cap \partial\Theta_2$ where, $\partial\Theta_i$ is boundary of $\Theta_i \subseteq \Theta$. Property sets P_1 and P_2 are disjoint sets. Typically P_1 and P_2 denote different stability properties of fixed point/limit cycles/regions or orbits in phase plane of $M(\theta)$. A bifurcation is defined as a discontinuous (from one set to another) change in the property P as result of a continuous change in θ. The aim is to find an approximate, less complex, parameterized model $M_r : \Theta \rightarrow \mathbb{M}$ of complexity $c(M_r(\theta)) < c(M(\theta))$, such that if θ^* is bifurcation of $M(\theta)$ then θ^* is a bifurcation of $M_r(\theta)$.

  Explanation: Many chemical processes show discontinuous dependence (form of bifurcations) on process parameters. It becomes difficult to approximate the behavior of a process with parametric uncertainty by using an approximate model. The application that is presented here, results in bifurcation type of a behavior as result of the changes in geometry of the plant equipment. It is one of the objectives of this thesis to develop a model approximation technique which can approximate the bifurcation type of a process behavior.

- *To infer an approximate model in the absence of an explicit mathematical expression of the model.*

  Explanation: It is an objective of this thesis to investigate a data based model approximation technique which is able to infer an approximate model in the absence of governing mathematical equations. E.g. for many commercial software packages, it is possible to get access to the states of a full order model, but the access to the governing equations is not possible. In such case one can not employ projection based or physical insight based model approximation techniques.

- *Model approximation with preservation of the qualitative system properties.*

  Explanation: It is desired for the approximate model to preserve the invariant properties of the original model, with respect to stability, robustness, conservation of physical quantities, physical constraints, dissipativity, system gains, controllability, observability, achievable performance etc.

- *Development of model approximation technique as an alternative to the physical insight based model approximation techniques.*

  Explanation: Some of the model approximation techniques which do not require projection of equations includes physical insight based methods like wave theory, compartmental methods, approximate inertial manifolds, etc. It is imperative to have a good understanding of the underlying process for such model approximation techniques and therefore they are not very generic and they are difficult to implement as an algorithmic routine. It is one of the objectives of this thesis to develop a data based model reduction technique which will not need projection of equation residuals as usually explored in the method of Proper Orthogonal Decomposition. Data based technologies are often referred to as the generic technologies due to wide applicability of these methods to different processes irrespective of the underlying physics.

- *To develop model approximation techniques with minimum implementation efforts.*

  Explanation: Most of the nonlinear model approximation techniques need significant programming efforts and theoretical understanding of the mathematics behind the technology. Especially for very large scale systems, these efforts can be laborious and expensive. This is undesirable and can hinder the applicability of even a good model approx-

imation technique on real life applications. It is therefore an intention of this thesis to develop a method, which can be easily applied with minimum efforts for various applications modeled as systems which are distributed in space. It is desired that the proposed model approximation technique, in its algorithmic form, should be easily distributed as a tool-box or as a programming routine.

Apart from the objectives mentioned above there are several other objectives which are somewhat difficult to quantify but are interesting e.g. maintaining the physical interpretation of the states, maintaining the interpretation of physical relations among process variables, inventing structures of the approximate model which are suitable for system theoretic analysis of notions like stability, convexity, controller design, closed loop performance etc. Often, the objectives are related, e.g. it is seen that accuracy and simulation time of the reduced order models are functions of the order of the reduced model which again is a function of the input excitation signal and the intensity of physical effects which are manifested in the full order models as non-linear functions.

1.3 Overview and organization

The main contributions of this thesis are briefly explained at the beginning of this chapter. The details of the proposed model reduction ideas and the results of their implementation on the benchmark examples are explained in subsequent chapters. The overview and the organization of the thesis in the form of major contents of each chapter is presented in this section.

In Chapter 2 some examples of large scale processes which occur in chemical process industry are presented. Specifically, the benchmark examples depicting a one dimensional tubular reactor and a glass manufacturing process are presented. Both the benchmarks are examples of Distributed Parameter Systems (DPS) which need to be solved by using combination of different numerical tools for spatial discretization and integration. The full order model of the tubular reactor, contrary to the glass manufacturing process, is easy to understand, easy to model and easy to simulate. Only the mass and energy balance of the tubular reactor are modeled. Due to its less complex nature, the tubular reactor is easier to validate the performance of model reduction

techniques.

The prime interest of this thesis is to develop model reduction techniques, especially suitable for large scale process like glass manufacturing. The CFD model of the glass manufacturing process depicting the reality is very complex and is often of order approximately in the range of $10^6 - 10^8$. Therefore it becomes difficult to test the effectiveness of a model reduction technique due to the large efforts that are involved with a real life model of a glass furnace. To overcome these difficulties, a 2 dimensional model (very small third dimension) of a glass furnace is developed. This model is used as a replacement of the 3D model throughout this thesis. The 2D model offers most of the features of a 3D model, but it is relatively easier to work and to implement the new technologies. Although the efforts required for the 2D model are small in comparison to a 3D model, they are still significant when compared to the efforts that are required for the tubular reactor.

Chapter 3 presents modeling tools and an extensive literature survey on the theory applicable to the problem of model reduction. One of the contributions in this chapter amounts to reformulating and re-interpreting the MOR problem as an identification problem. Specifically, chapter 3 presents the tools which are often used in subsequent chapters while proposing a new idea. Tools from system identification theory like subspace state space method and the tools from projection and model reduction theory like Proper Orthogonal Decomposition are presented. The main contribution of this thesis is to solve the problem of reduced order modeling by formulating it as an identification problem. Some earlier work on relation between model order reduction and system identification is also presented in this chapter. Based on the available literature and the aims of this thesis, possible research directions from literature overview is presented at the end of this chapter.

Chapter 4 addresses the problem of model reduction from the perspective of parameter uncertainty. Model approximation (reduction) is an important step towards the construction of model based controllers. However, model reduction methods hardly take model uncertainties and parameter variations into account. As such, reduced order models are not well equipped when uncertain system parameters vary in time. It is shown in this chapter, that the performance of reduced order models inferred from Galerkin projections and proper orthogonal decompositions can deteriorate considerably when system parameters vary over bifurcation points. Motivated by these

observations, detection mechanisms based on reduced order models obtained by the proper orthogonal decompositions is proposed. Using the reduced order models, the mechanisms allow to characterize the influence of parameter variations around a bifurcation value. The ideas are applied on the example of a tubular reactor. In particular, this chapter discusses the difficulties in approximating the transition from extinction to the ignited state in a tubular reactor.

In Chapter 5 we apply a combination of the method of spectral decompositions and system identification to identify a low dimensional model of a benchmark example representing an Industrial Glass Manufacturing Process (IGMP). The proposed model reduction method does not need the access to the governing equations and relies only on the state information of the full order model. In particular, we infer a reduced model by identifying the linear map from process inputs to the POD modal coefficients by a subspace state-space identification method. Reduced models obtained from such a method are not well equipped to capture the process behavior with time varying uncertain process parameters. For this reason a hybrid detection mechanism, which has been introduced in Chapter 4 is used to approximate the glass manufacturing process (benchmark CFD model) exhibiting non-smooth geometric parameter dependence (corrosion and wear) by using lower dimensional models. Given the state or the output information this mechanism detects the process parameter operation regime and suggests a computationally faster, lower dimensional model as an approximate for the real process.

In Chapter 6 a novel procedure for obtaining low dimensional models for large scale fluid flow systems is proposed. The approach is based on the combination of methods of spectral decomposition, black box system identification techniques and nonlinear spline based blending of the local black box models to create a reduced order linear parameter varying model. The proposed method is of empirical nature and gives computationally very efficient low order process models for large scale processes, which are modeled by computational fluid dynamic tools. Similar to the method proposed in chapter 5, the method proposed here does not need the usual Galerkin type of projection of equation residuals to obtain the reduced order model and the method is of generic nature. The efficiency of the proposed approach is illustrated on a benchmark problem of an industrial glass manufacturing

process where the process non-linearity and non-linearity arising due to the corrosion of refractory materials is approximated using a linear parameter varying model. The results show good performance of the proposed model reduction framework.

In Chapter 7, another novel procedure for obtaining low order linear and low order non-linear models of large scale systems is proposed. The approach is based on the combination of the methods of spectral decomposition of system solutions, and non-linear system identification techniques. There, the model reduction problem for non-linear processes is formulated as a parameter estimation problem. The first step of this model reduction technique is similar to the one proposed in other chapters and involves separation of spatial and temporal patterns. The second step of the model reduction procedure explores the observation made in the third chapter that the POD modal coefficients can be viewed as the states of the reduced order model that is to be identified. In the second step, with the knowledge of the states of a reduced model (POD modal coefficients) and process inputs, different model structures are proposed to relate the input and the states of reduced model. In particular, a tensorial (multi-variable polynomial) representation of the vector field of the system is proposed in order to describe the linear and non-linear evolutions. This generalizes the usual LTI setting in a nice manner to a different model class of nonlinear systems. An ordinary least squares method is then used to efficiently estimate the model parameters. The simplicity of the proposed method gives computationally very efficient linear and non-linear low order process models for large scale processes. During the whole procedure the physical interpretation of the states is preserved. The method is of generic nature. The efficiency of the identification method is illustrated on large scale benchmark examples of an industrial tubular reactor and a glass manufacturing process. Chapter 7 also presents a sufficient condition for the Lyapunov stability of the tensorial system at a fixed point. The tools from the Linear Matrix Inequalities (LMI) and the semi-definite programming are used to establish these conditions. Moreover, Chapter 7 also presents a sufficient condition for the dissipativity of the tensorial systems for a quadratic supply function.

Chapter 8 concludes this thesis by emphasizing the major conclusions and the insights obtained in this thesis. Along with the major contributions, the chapter will provide few research recommendations for the future. The recommendations are based on experiences in model reduction that have been gained during the research work that is presented in this thesis.

2

Benchmark Applications

2.1 Introduction

This chapter presents examples of large scale processes in the field of chemical process industry. The benchmark examples depict a one dimensional tubular reactor and a glass manufacturing furnace. Both the benchmarks are examples of Distributed Parameter Systems (DPS), with time and space as independent variables that need to be solved by using the Computational Fluid Dynamics (CFD) simulation tools. The full order model of the tubular reactor, in comparison to the glass manufacturing process, is easy to understand, easy to model and easy to simulate. Only the mass and energy balance of the tubular reactor are modeled. Due to its less complex nature, it is easier to test the model reduction technique on the tubular reactor.

The prime interest of this thesis is to develop model reduction techniques, especially suitable for large scale processes like glass manufacturing. A CFD model of a glass manufacturing process depicting a 3-dimensional real process is highly complex and often it is approximately of order $10^6 - 10^8$. Therefore it becomes difficult to evaluate the performance of a model reduction techniques due to the large efforts that are involved in obtaining a good quality data from the 3 dimensional models. To overcome these difficulties, a 2-dimensional model (actually a 3D model of very small width) of a glass furnace is developed and it is used as a replacement of a 3D model throughout this thesis. The 2D model offers similar complexity that of a 3D model is relatively easier to model, to simulate, to extract and to process the data. Although the efforts required for a 2D model are smaller in comparison to

the 3D model, they are still significantly larger when compared to the efforts that are needed for the tubular reactor.

2.2 Tubular reactor

2.2.1 Introduction to tubular reactor

Tubular reactors are widely used in the chemical process industry for carrying out various reactions and they contribute significantly to the continuous production. The raw material enters through one end and the product leaves via the other end of the reactor. Due to the absence of any moving part they are often preferred in the chemical process industry. Highly exothermic reactions, e.g. polymerization reactions, are often carried out in such a reactor so that they can be effectively cooled. Effective cooling is possible due to a large ratio of surface to the volume of a tubular reactor. To overcome the disadvantages of smaller volumes, tubular reactors sometimes appear in bundels of many tubes placed next to each other with a common inlet and outlet port. Sometimes they also appear in the form of coils.

Due to the large value of the ratio of surface to the volume, the length of the tubular reactor is more important for deciding its dynamic behavior. This distinguishes them from other unit reactors like batch and continuous stirred tank reactors (CSTR), where the dynamics are assumed to be lumped (perfectly mixed) without any significant spatial variation of the dynamic behavior. Therefore, the dynamics of a tubular reactor are function of space and time, that is, the concentration and the temperature of its content is different at each location. Such a reactor is therefore modeled by using Partial Differential Equations. In the past, when computing power was limited, the dynamic solution (concentration, temperature, etc.) of the governing partial differential equations was computed by approximating the space as a lumped variable or by dividing the tubular reactor into a chain of a few CSTRs. This eliminated the need of computing over the complete length of the reactor. With advancement in computing power and numerical techniques, in order not to loose the spatially varying information, the continuous space is approximated by dividing it in a large number of small volumes, usually referred to as 'spatial discretization'. Numerical schemes of Finite Element or Finite Volume type are often used to perform such a spatial discretization. The resulting model of the tubular reactor, therefore can

consists of large number of Ordinary Differential Equations (ODEs) whose temporal solution is computed using several types of numerical integration schemes.

Depending on the initial conditions, boundary conditions, underlying reaction kinetics (usually nonlinear) and values of the process parameters, dynamic behavior of the tubular reactor is difficult to understand and needs big efforts to properly study it. Nevertheless, it has been used as a benchmark for many different purposes and there are many tools to characterize the dynamics of the tubular reactor. In this thesis, the tubular reactor is used as a benchmark example to investigate the performance of the reduced order modeling techniques developed in this thesis. For numerical computation purpose, the tubular reactor model is discretized using the method of lines and integrated using *ODE suite* from *Matlab*.

In Chapter 4 the benchmark example of the tubular reactor is used to study the bifurcations, while in Chapter 7 it is used to study the performance of proposed nonlinear model reduction technique. The generic appearance of a tubular reactor is shown in Figure 2.1.

2.2.2 Modeling of a tubular reactor

The dynamical model of a tubular reactor is of the form (2.1).

$$\frac{\partial T}{\partial t} = \frac{1}{P_{\text{eh}}}\frac{\partial^2 T}{\partial z^2} - \frac{1}{L_e}\frac{\partial T}{\partial z} + \nu C e^{\gamma\left(1-\frac{1}{T}\right)} + \mu(T_{\text{wall}} - T) \tag{2.1a}$$

$$\frac{\partial C}{\partial t} = \frac{1}{P_{\text{em}}}\frac{\partial^2 C}{\partial z^2} - \frac{\partial C}{\partial z} - D_{\text{a}} C e^{\gamma\left(1-\frac{1}{T}\right)} \tag{2.1b}$$

which are subject to the mixed boundary conditions

$$\text{left side: } \begin{cases} \frac{\partial T}{\partial z} = P_{\text{eh}}(T - T_i) \\ \frac{\partial C}{\partial z} = P_{\text{em}}(C - C_i) \end{cases} \quad \text{right side: } \begin{cases} \frac{\partial T}{\partial z} = 0 \\ \frac{\partial C}{\partial z} = 0 \end{cases}$$

The model represents a reactor with both diffusion and convection phenomena and a nonlinear heat generation term. The model is governed by coupled partial differential equations. The system of equations can be classified as non-self adjoint, parabolic PDEs. Many tubular reactor models that occur in literature can be adequately represented by this dimensionless model. The model explains material and energy balances in the reactor. The model

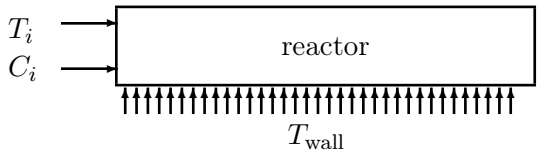

Figure 2.1: Tubular reactor

---

with its parameter values are taken from Zheng and Hoo (2002), which has been originally taken from Gay (1989). First order reaction kinetics of the reaction $A \rightarrow B$ are assumed here. $T(z,t)$ and $C(z,t)$ are dimensionless temperature and concentration state variables, respectively, which are functions of time t and position z. Here, $t \in \mathbb{R}_+$ is the temporal independent variable and $z \in \Omega := [0,1]$ is the spatial independent variable. Inputs to the model are $u(t) = (T_{\text{wall}}(t))$ which are the wall temperature influenced by a heating/cooling jacket divided into three parts. The disturbances are $(T_{\text{i}}(t), C_{\text{i}}(t))$, i.e. inflow temperature and the inflow concentration, respectively. Initial conditions at time instant $t = 0$ are set to $T_0(z) = T_{ss}$ and $C_0(z) = C_{ss}$, where T_{ss}, C_{ss} are steady states profiles. The physical parameters of the system are given in the table below.

Peclet number (energy)	Peh	5
Peclet number (mass)	Pem	5
Lewis number	Le	1.0
Damkohler number	Da	0.875
Adiabatic temperature rise	B	10.0
Activation energy	γ	20.0
Heat of reaction	ν	0.8375
Heat transfer coefficient	μ	13.0

2.3 Glass manufacturing process

The discussion that follows in this section is applicable to the glass manufacturing process. In subsequent subsections, the process, its operation, characteristics, modeling, control and challenges offered by the process for the model reduction are discussed. The general description is followed by the description of a specific glass furnace model that is developed during this thesis. The model is referred to as 2D glass furnace model and it is

extensively used to validate the results of the model reduction techniques that are developed during this thesis.

2.3.1 Introduction

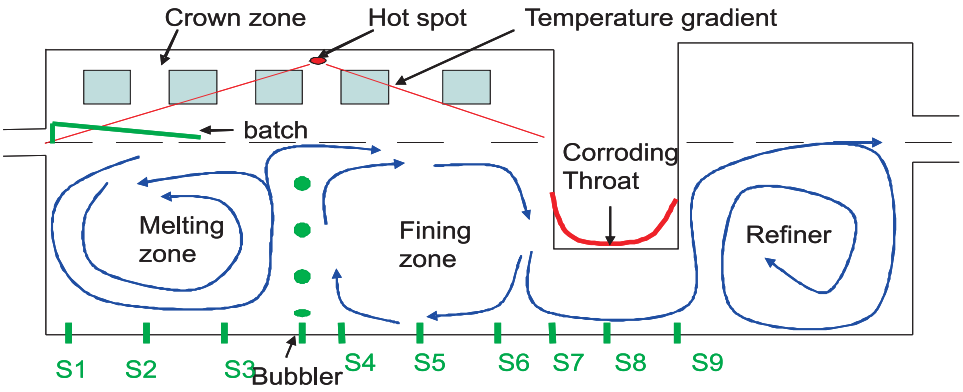

Figure 2.2: Glass Manufacturing Furnace, a 2D view

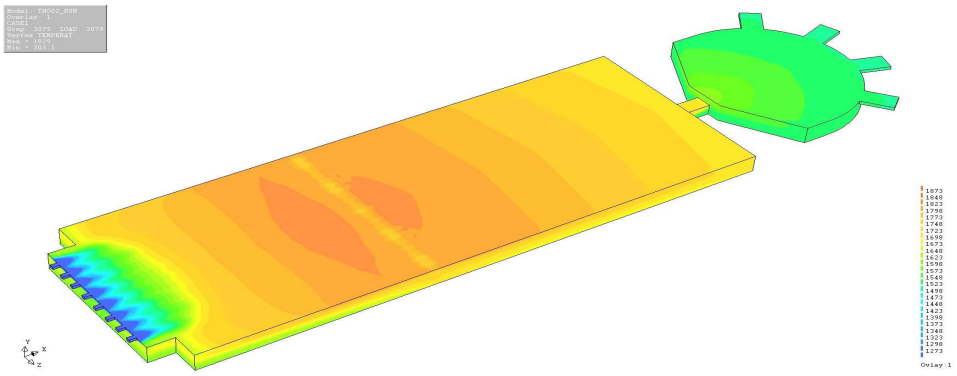

Figure 2.3: Glass Manufacturing Furnace, a 3D view

Glass manufacturing is one of the oldest technologies known to the mankind. There are some references to the glass production which go back to 1000 BC in some old civilizations. The process that is used in practise now-a-days differs a lot from the process that was commonly used to be in the past. Advancement in equipment design, furnace material, instrumentation and novel process design makes the industrial glass manufacturing process (IGMP) as one of the advanced process industry. Various types of high end glasses like

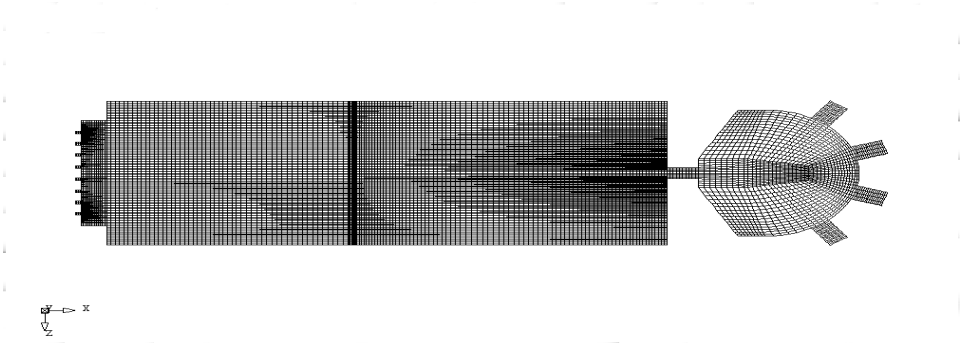

Figure 2.4: Distribution of grid cells in 3D tank

float glass, LCD glass, Solar glass etc. has redefined the age old operation of glass manufacturing. This is accompanied by the increased process manufacturing demand, increased process complexity, interacting process variables, varying raw material properties, nonlinear multi-phase reactions, novel product types, need of flexible process operations, demand for improved product quality, tightening environmental regulations, increasing energy costs that make IGMP very challenging from point of process modeling and control.

IGMP is usually carried out in large furnace. Figure 2.2 shows a schematic of the process along the furnace length. The raw material is fed in the form of a batch blanket. Depending on the glass type, the batch material may contain different minerals (mostly silica based) or it may content recycled glass, or a combination of both. High-end glasses like optical, solar and LCD glass need precise knowledge of the content of the raw material and sometimes known artificial chemicals are preferred over the minerals as the raw material. The raw material enters from the inlet (on the left side) which is usually referred to as a dog house, in the form of a batch blanket to float on the molten glass. The batch material melts from the top side by the heat supplied by burners. The hot glass that is already present in the tank melts the glass blanket from the bottom. After circulating through the glass furnace for many (nearly 8-40) hours, glass passes through the throat, circulates for some more time in the refiner section and then finally leaves via the outlet commonly referred to as the feeder or the working end.

Based on the type of a glass product, type of the furnace and the desired process characteristics, the process operation varies a lot. But often, there are roughly three regimes - melting, fining and refining. All these zones are

shown in the Figure 2.2. A 3-dimensional view of the furnace sometimes resembles a swimming pool filled with the molten glass. Figure 2.3 shows a typical glass furnace without a combustion chamber, whereas the division of geometry of a 3D furnace model into number of small grids is shown in Figure 2.4.

- *Melting*

  Melting of the raw material predominantly takes place in the melting zone. Melting is a highly nonlinear process and involves multi-phase reactions. That is, during the transition from solid to the liquid phase, many gases are released and at the same time, depending on the type of raw material, various chemical reactions take place simultaneously. Glass temperature varies between $1100 - 1650\ ^0$C in the melting zone. Spatially varying heat distribution from the top combustion chamber induces a gradient in glass temperature in different parts of the furnace. This temperature gradient leads to a strong natural convection in the furnace. The convective currents (flow patterns) characterize the process operation. In an average glass manufacturing process, glass make 4-5 circulation loops in the melting zone and then enters into the fining zone. The length of the melting zone is determined by the hot spot location.

- *Fining*

  Melting is followed by the fining process, which is necessary to remove the high concentration of the dissolved gases from the molten glass. Sometimes, fining agents are added which help to remove the gases from the molten glass. Fining zone is mostly necessary for the high purity glass. Depending on the type of the furnace, glass may make couple of loops in the fining zone.

- *Refining*

  Fining is followed by the refining process, which is necessary to dissolve and to distribute the remaining undissolved gases during the fining process. The glass coming out of the refiner has a low concentration of the dissolved gases. The molten glass is cooled to an appropriate temperature for glass forming by letting it go through a feeder. The glass is then dosed into the equipment that form the glass in different shapes.

2.3.2 Process characteristics

- *Large scale, complex process.*

  Glass manufacturing is one of the largest, energy intensive, industrial chemical processes. The process is characterized by complex, multi-phase reactive fluid flow. A large number of interdependent variables like temperature, velocity, pressure, thermal conductivity, etc. make the process difficult to understand. Moreover, the presence of three dimensional flow patterns carries the effects from one operation zone in the furnace to the other.

- *Presence of multiple physical effects.*

  Increased demand for better quality, flexible operation, varied glass types and demanding economic constraints have resulted into inclusion of various physical effects into the glass manufacturing process. Apart from melting, fining and refining many other physical effects like bubbling, boosting, stirring, bottom wall heating/cooling etc. are also present in the furnace. For a constant heat supply, bubbling and electrical boosting are often used to influence the flow patterns inside the furnace.

- *Presence of dynamics with different time scales.*

  The process exhibit dynamics in the range of few minutes to days. The effects of change in heat input are observed in half to two hours, whereas the effects of change in pull-rate (feed amount) need many hours to days to see its effect. The residence time of the glass in the furnace is kept larger than the largest time constant of the process. Usually the time constant of the changes in pull-rate is the largest for a glass furnace. The furnace dynamics are characterized by the residence time of the glass. Residence time of an average furnace is around 40-60 hours. A residence time analysis also helps to compare the performance of different furnaces. The intensity of the observed effects and the time constants associated with various inputs/disturbances is different in each region of the furnace. Usually the dynamics of externally supplied heat changes has the largest influence in the top layers of the molten glass. The dynamics in the fining zone are the most critical and they show intermediate behavior in comparison to the behavior in melting and the refining section. In comparison to other unit operations in chemical process industry, the dynamic behavior of a glass manufacturing process can be viewed as a series combination

of ideal plug flow reactor (PFR) and a continuous stirrer tank reactors (CSTR). The effect of the furnace input/distrubances is not just limited to the residence time of glass or the flow pattern in the tank, but it also influences the life of furnace material. The effect on the furnace material is prominent if the pressure inside the furnace fluctuates a lot. The variation of pressure inside the furnace results into the switching between condensation and evaporation of metal oxide vapors which further induces the corrosion of the furnace walls. Due to the difficult process operation, it is desired to operate the furnace as stable as possible. Stability implies that the furnace is operated around some steady state working point without any significant changes in the operating conditions.

- *Limited measurement information.*

  Corrosive nature of the glass at higher temperatures make it difficult to access any process information by placing sensors inside the furnace. The measurements are therefore limited to a few thermocouple placed in the bottom wall of the furnace. Apart form the temperature sensors, there are few level sensors to measure the glass depth.

- *Operating conditions.*

  The process is operated at around $1400 - 1650^0$C. The top layer is hotter than the lower layers. Temperature keeps on decreasing along the length of the furnace. Depending on the type of furnace usually the production capacity varies between 50-200 tons/day. Similarly, the average residence time varies from 40-60 hours.

- *Quality criteria.*

  Usually the concentration of undissolved gas in the molten glass, transparency of the product glass, its strength, breaking index, porosity, color, chemical inertness etc. serve as the quality criteria.

- *Control variables.*

  In order to run the process smoothly, the control variables of interest are temperature distributions, flow patterns in the tank, depth of molten glass, concentration of the dissolved gases, pressure in the tank, NO_x and CO_2 formation in the exhaust, quality of the product glass etc. Many of these variables are related to each other, e.g. quality of glass is a function of flow pattern, which is a function of temperature distribution, which is again a function of heat distribution.

- *Manipulated variables.*

  In order to bound the variations of control variables in a certain range, manipulated variables like external heat supply, bubbling, stirring, boosting etc. are used. The values of the manipulated variables are determined by either the logic used in a control system, or they are based on the experience of the plant operators.

- *Disturbances.*

  Usually the batch (raw material) amount, batch compositions, batch melting rate, outside environmental conditions, aging/corroding furnace and the refractory walls, depleting insulation layers are the major disturbances to the process operation.

- *Optimization variables.*

  Optimization variables are total product throughput, minimization of the fuel consumption, minimization of the product loss, minimization of NO_x quantity in the exhaust, maximization of lifespan of a furnace etc.

2.3.3 Process modeling and open questions

Process modeling and simulation

Similar to many other processes involving fluid flows, the transport of physical quantities in a glass furnace is modeled with reasonable accuracy by a set of Navier-Stokes equations of the form

$$\frac{\partial (\rho\phi)}{\partial t} + \operatorname{div}(\phi\rho\upsilon) = \operatorname{div}(\Gamma \operatorname{grad}\phi) + q_\phi \tag{2.2}$$

where ρ is the mass density, υ is the velocity, div is the divergence operator, Γ is the diffusion coefficient, q_ϕ is source/sink term. When $\phi = 1$ we have continuity equation, for $\phi = \upsilon$ we have momentum equation and for $\phi = H$, i.e. enthalpy, we have energy balance equation. The source/sink term is the major contributor to the process non-linearity. It is the term which represents the contribution of physical effects like bubbling, boosting, reactions, melting, combustion etc. Various mathematical models of the physical effects are presented in Krause and Loch (2002) and in the user manual of glass process modeling software GTM-X. See, TNO (2008) for more details.

The physical contact with external environment at various surfaces of the furnace are approximated by appropriate boundary conditions of type Drichlet, Neumann, Robin etc. Usually the initial condition for such models are taken close to the steady state operating conditions of the glass furnace.

Simulation of a glass manufacturing process usually is performed by using the Computational Fluid Dynamics (CFD) tools which involves discretization of the spatial geometry in Navier-Stoke's equation in (2.2). It is common to employ the finite element or the finite volume discretization of the spatial domain. Such spatial discretization for a model depicting a real furnace can easily lead to a few hundred or million grid cells. During a simulation run, solution of all time dependent variables is evaluated at each grid cell. Often, the spatial geometry is divided into few blocks to facilitate the computations. Each block may then consists of many discrete grid elements/volumes. Combination of several numerical schemes are used to obtain reliable simulation results. Simulation of residence time of glass in the furnace is performed by simulating the flow patterns of large number of particles fed into the furnace via inlet.

Some more details about mathematical modeling of glass manufacturing process can be found in Patankar (1980), Post (1988), Krause and Loch (2002), Huisman (2005) and in TNO (2008). Control and optimization oriented modeling of the glass process is provided in Carvalho et al. (1997) and Backx (2002).

Open modeling questions

Mathematical modeling of a glass manufacturing process has greatly evolved over the years. With advancement in computer simulation techniques, such models are increasingly finding their place as an important tool to understand, to analyze, to predict and to control the glass manufacturing process. Nevertheless, there are still many open questions in modeling of glass manufacturing process. Few open question in modeling are listed below.

- There is a need to develop rigorous mathematical models that represent physical effects like corrosion, reaction kinetics at micro level, melting of the batch blanket, radiation effects for the clear (low absorption) glass types, etc. Availability of these models and their simulations can significantly improve the performance of glass manufacturing process.

- Rigorous mathematical models have to be adjusted with respect to the actual furnace behavior. This makes mathematical modeling and parameter tuning for the existing furnaces an expensive process.

- The simulation techniques used for simulating the glass furnace models need to become efficient especially to compute the transient (dynamic) behavior of glass. further advances in developing the mathematical models and the numerical schemes to evaluate the dynamic changes in the residence time of glass as function of different process variables can be very rewarding.

- The existing mathematical models and the numerical schemes are computationally very inefficient and there is lot of scope for further improvement.

- The models which can explain the uncertainties in the plant and in the process operation are still unavailable.

- The mathematical models of the process that are currently available are not suitable to analyze the system theoretic notions like controllability, observability, stability, robustness etc. Therefore it becomes difficult to extend the concepts from system and control theory to a glass manufacturing process.

2.3.4 Control of glass furnace

In the first chapter of this thesis, the advantages and need for advanced model based control of chemical processes is explained. Similar to any other large scale chemical process, advanced control of glass manufacturing process offers many intensives in term of improved performance, flexible process operation, better process understanding, longer lifespan of the furnace equipment and improved economic gain. The next subsection presents the scope and challenges for the development of advanced controllers for the glass manufacturing process. A model based controller using either a black-box type of a model or a rigorous first principle model can drastically improve the performance of a furnace. Currently there are more than 5000 furnaces all over the world and they consume approximately $50 \times 10^9 [m^3/year]$ of natural gas. Even a small fraction of this if saved using modern process control, it would translate into a big financial gain and a reduced process emission.

Scope for model based process control

- To automate the overall glass manufacturing process and make wiser decisions while manipulating the process variables.
- To minimize the effects of uncertainties and disturbances during the process operation.
- To stabilize the operation for a given disturbance in the form of changes in working point (load, color,batch amount etc.)
- To minimize the emission of the polluting exhaust gases.
- Approximately 50% energy usage in a glass manufacturing process is for melting of raw glass. Improved performance in melting can save a substantial amount of energy.
- Reproducibility of the results, stability of process operation and flexible control of the process.
- Anticipate, understand and nullify the effect of disturbances, effect of interaction among time varying variable and effect of operator interference.
- Novel glass types like solar glass, LCD glass and other engineering application glasses need good understanding of the process with very tight control of dynamic variables. Due to the increased interaction among variables such processes need complete automation and can no longer be easily controlled only with 'past experience'.
- To make decisions in terms of solution to mathematical problems of plant's economic objectives, control objectives, objectives with respect to emissions etc.

Challenges for model based process control of glass furnaces

Although the last subsection has described the advantages of advanced model based predictive control (MPC) of glass manufacturing process, there are still many challenges to its complete automation.

- The complex, nonlinear nature and interaction among the time varying variables of glass melting makes it difficult to control by model

based controllers based on linear black-box type of models. Rigorous first principle models too cannot be used in MPC due to their large state dimension and involved complexity. Such models need significant computation time to simulate, which makes them unapplicable to be used in MPC.

- Identification of data driven models that can be used in MPC need expensive identification tests which are not easily permitted in the glass industry due to the inherent economic losses during the identification tests.

2.3.5 Model reduction

As explained in the introductory chapter of this thesis, model order reduction can be very useful for inferring lower dimensional mathematical models for glass manufacturing process. Model order reduction can be seen as a solution to the problem of having reliable, but computationally slow first principle models on one hand, and, not very reliable (beyond the identification domain) but computationally fast black-box models identified from the plant input-output data. Model order reductions aims at reducing the complexity (order, computation time, etc.) of full order first principle models which happen to be Computational Fluid Dynamic (CFD) models for glass. This part of the chapter discusses glass manufacturing in perspective of model order reduction.

Scope for model reduction

- Reliable reduced order models can be used for the process analysis, design, control and optimization purposes for glass manufacturing process.
- The advantages of having a Rigorous Model based Predictive Controller (R-MPC) can be realized only through the availability of reduced order models for a glass manufacturing process.
- Reduced order, computationally efficient models obtained from the first principle models can be used as a replacement of an original process if they are reliable and accurate enough. This will eliminate the need of having an expensive identification test in the plant in order to identify a good black-box model.

- Unlike the black-box identified models which are obtained from plant tests, depending upon the model reduction method used, the states of the reduced order model may have a physical interpretation and therefore they can have better acceptance among users of the reduced order models.

Challenges for model reduction

Although, the reduced order models can be of great use for online control and optimization purpose of glass manufacturing process, there are many problems in inferring the reduced order models from full order first principle CFD models. Some of them are listed below.

- Unlike other chemical processes, glass manufacturing is characterized by its complex nature, very large state dimension of the full order models ($10^5 - 10^8$ states), interaction among several physical variables and a combination of many physical effects.

- Applicability of physical insight based model reduction techniques like time scale based separation, compartmental methods or approximate inertial manifolds is limited due to the complex process nature and large state dimension of the full order process model.

- Projection based model reduction techniques can lead to a dense structure of the reduced order models and might not offer any specific advantage in term of computational gain over the full order CFD model.

- Multidimensional geometry, non-Cartesian grids, model uncertainty and limited sensor information can further pose challenges to construct an effective reduced order model.

- For the extension of the notions from system theory like stability, robustness, optimality, controllability, observability, controller design, etc. need suitable structure of a model and therefore reduced order modeling need to consider these issues while inferring an approximate model for the glass manufacturing process.

Current status of model reduction

Although there are many references in the literature about control of glass furnace by using black-box type of identified models, the idea of inferring a reduced order model of a glass manufacturing process from the CFD models for the purpose of controller design is relatively new. Some early work in this direction include work from Astrid (2004) and Huisman (2005). Astrid (2004) has proposed a model reduction technique involving proper orthogonal decomposition and Galerkin type of projections of full order model equations. The proposed technique is tried on industrial model of a glass feeder. Moreover, it proposes a novel way, a technique of 'Missing Point Estimation' (MPE) to infer computationally efficient reduced order models from full order CFD model. In the work of Huisman (2005), he proposes a reduced order modeling technique based on the tools like spectral decompositions and system identification.

There are some drawbacks of both the approaches. Unlike feeder, a glass furnace is more complex and it has melting, fining and refining of glass which makes furnace operation a highly nonlinear process. Application of technique like Missing Point Estimation (see, Astrid et al. (2008) and Astrid (2004)) which is based on the principles of interpolation for reconstruction of the missing data might not be very promising to infer reduced order computationally efficient models of a glass furnace. Applicability of MPE will be limited due to relatively complex nature of furnace which is characterized by a large spatial variation of the physical variables inside the glass furnace. Moreover the reduced models inferred by classical POD (see, chapter 3) or by MPE do not have a structure that is suitable for an easy extension of the notions from system theory mentioned in previous subsection.

The method proposed by Huisman (2005) results in Linear Time Invariant (LTI) model structure of reduced order models. Unfortunately, for a high quality glass (with two circulation loops) the glass furnace shows highly nonlinear behavior and a linear model, in general, is not sufficient. One needs a richer model structure to accommodate the complex nonlinearities. Not withstanding to the drawbacks, the result shown in the PhD thesis of Huisman (2005) and Astrid (2004) are encouraging and have paved the way to further investigate model reduction for glass furnaces from the perspective of controller design.

Contribution of this thesis

Continuing the work on the ideas proposed in Huisman (2005) and Astrid (2004), this thesis has proposed some new approaches towards inferring a low order, less complex, approximate model of a glass melting furnace. The main contribution is already mentioned in the beginning of the first chapter and in the thesis overview discussed in the section 1.3. To approximate the nonlinearities in the glass furnace, this thesis has proposed two different reduced order model structures. The first reduced order model structure is of Linear Parameter Varying (LPV) type and is suited to approximate the process nonlinearities. It's closeness to the LTI model structure inherits many advantages offered by LTI model structure. With the same LPV reduced order modeling structure, the nonlinear effect due to the uncertainties in the furnace in the form of corrosion of a furnace wall is approximated. The second reduced order model structure is of tensorial (multi-variable polynomial) form. Such a structure allows process nonlinearities and at the same time it is much more amenable to extend the notions from system theory that have been developed for LTI models. More information about the thesis overview can be found in section 1.3.

2.3.6 2D Glass furnace model

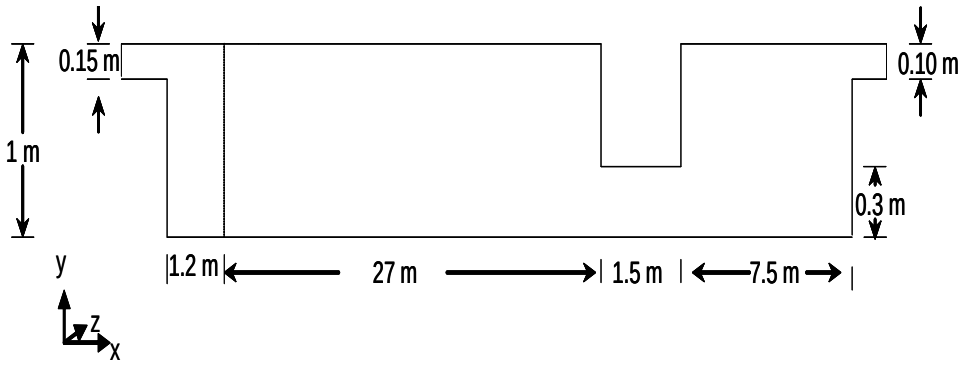

Figure 2.5: Dimensions of 2D furnace model

This thesis aims at developing reduced order models specifically for a glass manufacturing process. To invent, to develop and to validate any model reduction technique needs large number of simulation experiments in order to

collect a representative data from a full order model. Full order CFD models of glass furnace are approximately of order $10^5 - 10^8$. Such a high order and inclusion of nonlinear source/sink terms make these models computationally very slow and it often needs many days of simulation to estimate the steady state solution of such a model. Dynamic (transient) simulation of such a model also takes considerably more time. Such a large simulation time can hinder the progress of developing model reduction techniques which are suitable for applications like glass manufacturing process. To overcome this problem of simulation time associated with a full order model , a 2 dimensional (small third dimension) model of glass furnace is developed.

The $2D$ glass furnace mimics the vertical cross section along the length of $3D$ glass furnace and has only 2 grid cells in z-direction (width). In total, the 2D furnace geometry was divided into approximately 6000 grid cells. The 2D model needs much smaller simulation time in comparison to the full order model. Similar to a 3D model, the simulation time of such a model is function of convergence threshold of various parameters, physical effects that are modeled, combination of numerical integration schemes, overall distribution of grid cells, real time simulation horizon, etc. For steady state simulations with the same settings of numerical parameters, the 2D model needs half an hour on normal configured PC. The CFD software that is used to build and simulate glass furnace model is GTM-X, which is developed by TNO. See, TNO (2008) for further details.

The PC configuration that is used for the research presented in this thesis is; Manufacturer - Aragorn, Pentium 4 CPU, dual core converted to a single core, 3.2gHz, 3 GB of RAM and Microsoft Windows XP professional version 2002, service pack 3.

A 2D view of a typical furnace is shown in Figure 2.2. Bottom wall has sensor $S1$ to $S9$. Although, the research results about model reduction presented here are based on the simulations, the sensor positions $S1$ to $S9$ depicts real life sensor positions and they are useful while comparing the outcome of specific model reduction strategies that are explained in subsequent chapters. The figure also shows different stages (melting, fining, refining) during manufacturing of glass. The details of these operations are already discussed in the introductory section of a glass manufacturing process. The dimensions of the 2D tank are shown in Figure 2.5, while the temperature distribution in the 2D tank is shown in Figure 2.7. Figure 2.7 shows that the temperature is highest in the top layer due to the heating from flames. The temperature in the lower part and along the length of the furnace keeps on decreasing.

The throat height in Figure 2.5 is equal to $0.3[m]$. It has big influence on the overall dynamic behavior of the furnace and it is discussed in next subsection. The average residence time of glass in the 2D furnace is similar to that of a 3D furnace and it is around 40-60 hours. The plot in Figure 2.6 is a simulated residence time plot. The residence time is evaluated by analyzing how long the trace particles fed through the inlet stays in the glass furnace. The number of particles considered were 10000 and the average residence time is of practical interest. The minimum residence time among these particles characterize the poorest quality of glass. As it is difficult to observe the path of all the particles in the tank, usually the flow path of the particle corresponding to the minimum and maximum residence time is analyzed. Figure 2.8 shows the particle path of a random particle in the furnace, which characterizes the average flow pattern of the molten glass in the tank. The figure confirms that glass enters from the left end, mixes for some time in the melting zone as shown by few circulation loops and then enters into the fining zone. Again it makes few rotations there and then finally leaves through the throat zone and enters into the refining zone. Sometimes to get rid of all the remaining bubbles and to homogenize the glass, it is preferred that the glass make few loops in the refining zone as well. Finally glass leaves via the outlet situated at the top right corner of the furnace.

The physical effects that are modeled in the simulation of 2D glass furnace are - flow, energy, melting of raw material (batch), and a bubbler. The heating is provided only from the top surface and the heat input profile of the 2D furnace model was kept similar to an average 3D model and schematically it was close to the one shown in Figure 2.2. In most of the real life cases, the hot spot location, its heat intensity and the distribution of heat are used to adjust the first loop (melting) while bubbler is used more to induce local mixing in a cold glass at the bottom and to get rid of the smaller gas bubbles formed as result of reactions. In the 2D furnace model, due to its small width, the bubbler was playing a major role by inducing mixing in the furnace while the hot spot location, its heat intensity and distribution of heat were not very effective in controlling the flow pattern and mixing in the furnace. The time varying variables that are calculated are - temperature, velocity in three directions, pressure, viscosity, density, thermal conductivity, energy, force, specific heat and batch concentration.

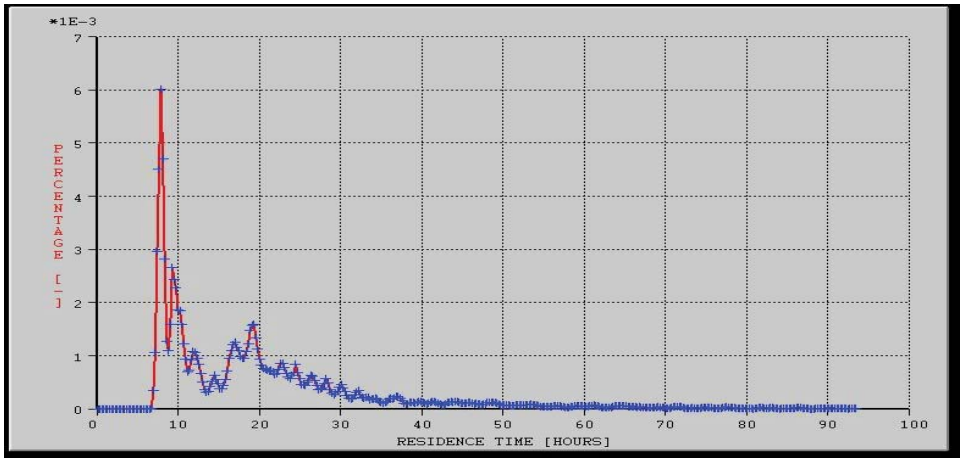

Figure 2.6: Residence time distribution in 2D tank

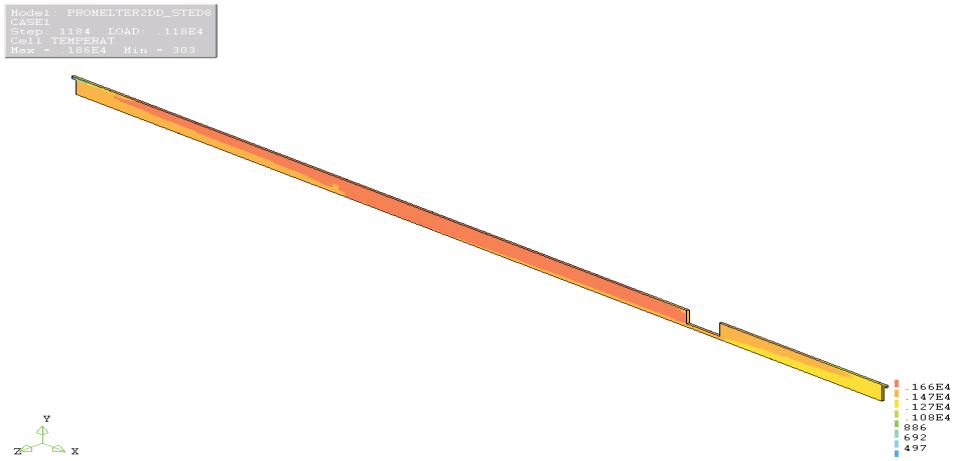

Figure 2.7: Temperature distribution in 2D glass furnace model

---

Step response of the 2D furnace model

Figure 2.9 shows the step response of the $2D$ model in different regions of the furnace. The step response characterizes the overall dynamic behavior of the glass in different regions of 2D furnace. The input signal chosen for the excitation is the feed rate of raw glass, which is also equal to the product removal rate called as *pull-rate* in the glass industry. The step amplitude was equal to 1% of the nominal value of 3.5 tons/day. The convergence threshold

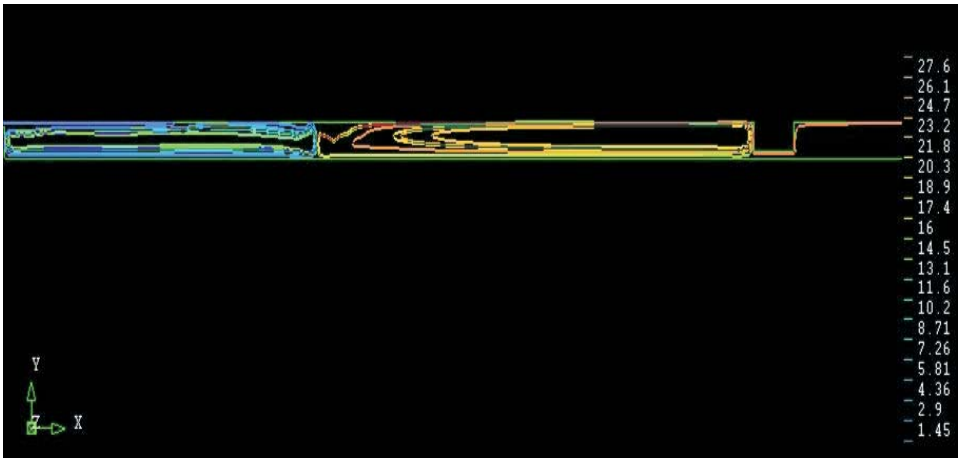

Figure 2.8: Particle Trace: Flow pattern of a random particle in the furnace

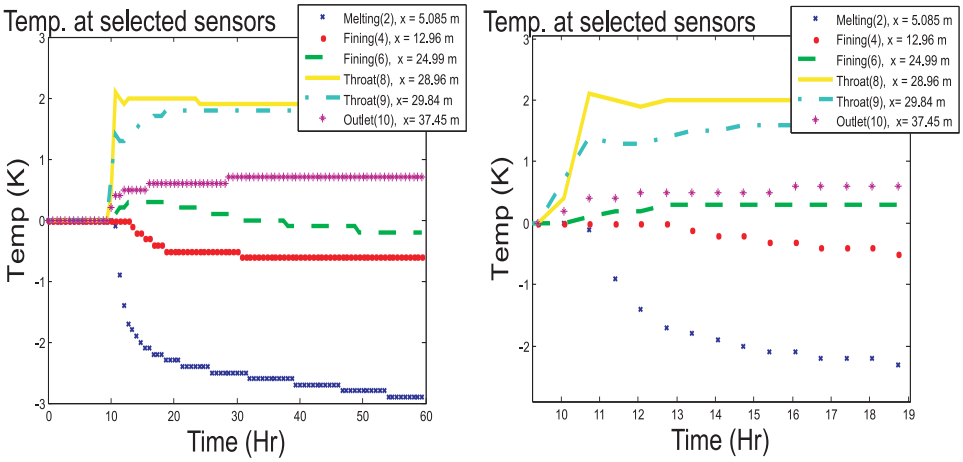

Figure 2.9: Step response of 2D furnace: Temp. change as result of step change in feed rate. Right, zoomed version.

---

of the solutions during the simulation was 10^{-5}.

The outputs that are analyzed are the temperatures at few sensor locations which are shown in figure 2.2. The figure also shows the location of sensors with respect to the bottom left corner of the tank. It is clear from Figure 2.9 that for a 2D furnace model the glass behave differently in each region. Most of the regions show relatively slow response due to the large ratio of tank capacity (≈ 4 ton) to the feed rate (≈ 3.5 ton/day). The characteristic

properties like rise time, settling time are different in each region. The melting and the refining region shows opposite behavior because raw material is added in the melting region whereas glass as a finished product is taken away from the refiner. The fining zone shows a mixed behavior as this region has first influence of melting section and later after long time, it has influence of refining section (a colder region), due to the back-flow of glass from the refining zone. Therefore the glass behavior in fining zone is the most difficult to be approximated by a linear model. For high quality glass, fining zone is necessary. The response of changes in the pull-rate is more evident and fast in the throat region as compared to other regions. Glass behaves linearly in the throat region. The average time constant (63% of steady state value) is 4-5 hours for the 2D tank. This analysis of the dynamics of 2D tank was useful in designing proper excitation signals during the identification of reduced order models in subsequent chapters.

Software architecture

The overall software architecture that is used to simulate the 2D CFD model of a glass furnace and the steps involved in processing of its data are shown in Figure[1] 2.10. The software architecture can also be used for the 3D CFD model. The glass furnace simulation software that is used to build a full order model is GTM-X and it is a CFD based software tool from TNO (2008). The software has different parts for different purposes. A Batch file is used to generate the furnace geometry by using a user interface X-GUI. Along with the generated geometry (grid) file a default model description file called *case file* is generated, which is later needs to be modified by the user. It is the *case file* where the initial conditions, the boundary conditions, the model constants, the numerical schemes and their parameters, the heating profile, types of governing models etc. are mentioned. Using the simulation kernel *GTM-X*, the full order CFD model that is defined in a case file is simulated for the geometry generated by the grid file. The results can be viewed again in X-GUI. This full order GTM-X model gives access to the complete state information but it is not possible to access the governing equations that are coded in the software.

The second part of the software is developed separately in order to automate the extraction and subsequent processing of the data from GTM-X. The

[1]The figure and some part of the software is provided by R. Romijn and L. Ozkan as part of the research collaboration, PROMATCH

automated part performs writing the case files, running them through GTM-X kernel, creation of the geometry, extraction of the generated data, its processing and carrying out data based model reduction techniques which are explained in subsequent chapters. This part of the software was built in software environment of *matlab*.

These software tools were also used to automate and simulate the effect of corrosion of the throat wall in the 2D model. The effect of wearing of throat wall in the form of corrosion is explained in next subsection.

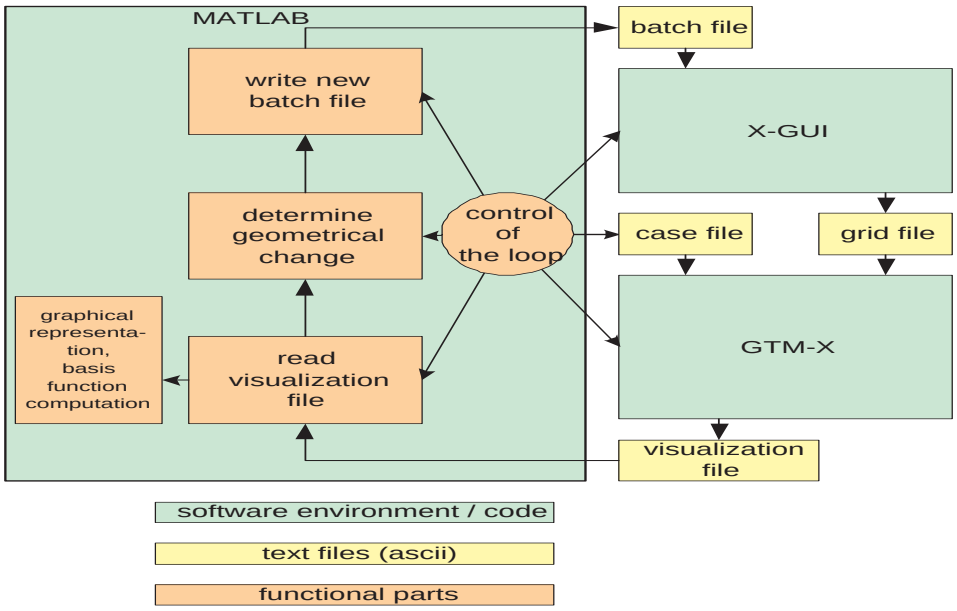

Figure 2.10: Software Architecture

Corrosion of throat wall

In this thesis, apart from approximating the process non-linearity in the reduced order modeling framework, the effect of very slow geometric changes that take place in real $3D$ furnace in the form of throat or dam wall corrosion are also studied. The corrosion of the throat wall is shown in Figure 2.2. Corrosion or wearing of different parts of the furnace walls occurs over the years due to the aggressive nature of the glass at high temperatures and due to the emission of corrosive gases. The effect of corrosion on the furnace

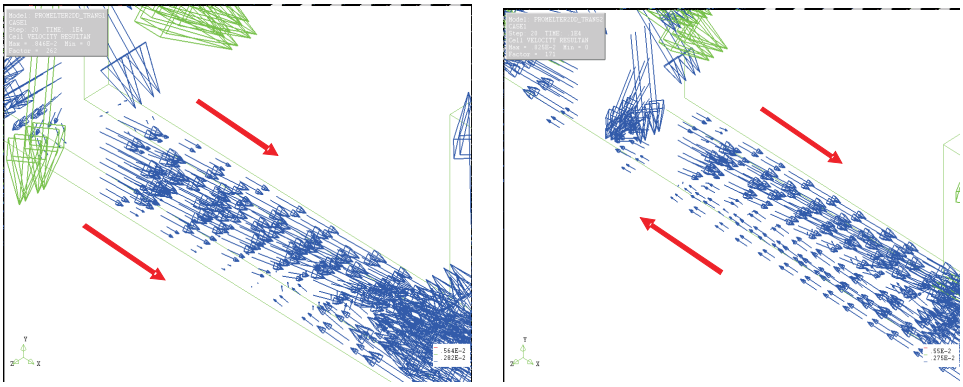

Figure 2.11: Occurrence of back-flow

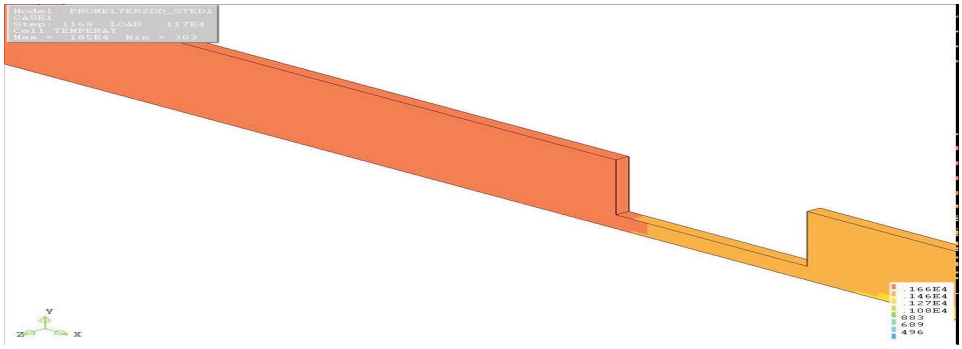

Figure 2.12: Temperature in the throat region, $h_1 = 0.2$

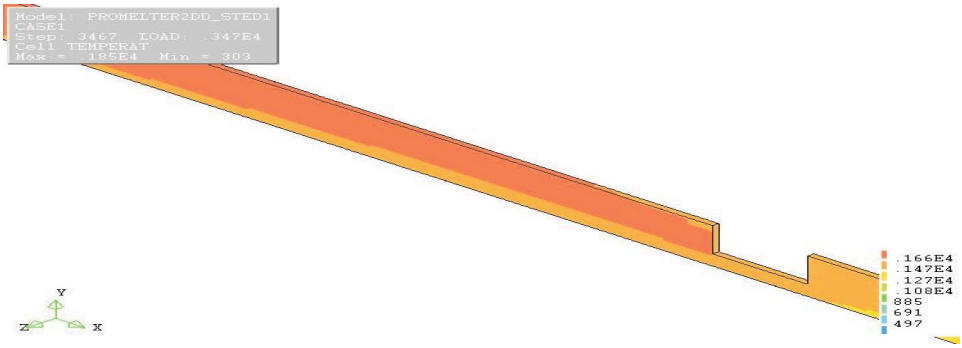

Figure 2.13: Temperature in the throat region, $h_2 = 0.3$

---

dynamics is more prominent near the throat region. In the throat region,

the corrosion results into back-flow of molten glass from the refining zone to the fining zone. Such back-flow behavior causes uncertain changes in the temperature distribution in the furnace which ultimately can lead to the economic losses. For the $2D$ furnace we observe this bifurcation behavior i.e the occurrence of back-flow somewhere between throat heights of 0.2m (h_1) and 0.3m (h_2). Figure 2.11 shows that corrosion of throat wall results into completely different velocity pattern in the throat section of the furnace.

The effect of back-flow can also be verified by viewing Figure 2.12 and Figure 2.13, where the temperature (in Kelvin) plots corresponding to the two cases of h_1 and h_2 is shown. Plot shows that temperature in the melting and fining zone decreases as result of mixing of the cold glass from the refiner section.

3

Tools from Theory

This chapter presents various mathematical tools and system theory concepts from the literature that are relevant for the purpose of this thesis. Some of the presented tools are often used in subsequent chapters. These involve tools from system identification theory and tools from projection and model reduction theory like Proper Orthogonal Decomposition (POD). We include a number of methods where the model reduction problem is represented as an identification problem. Some past methods presented in the literature with similar aim are also briefly presented in this chapter. Based on the available model reduction methods/techniques from the literature and on the thesis objectives discussed in section 1.2, applicability of different methods is compared and discussed in section 3.4.

3.1 System Identification

System Identification is a well known research field developed by the system and control community in order to identify the controller oriented models from plant input-output data. Classical identification techniques include parametric methods where different structures of Linear Time Invariant (LTI) models are proposed. The parameters of these models are estimated using some parameter estimation techniques of Ordinary Least Square (OLS) type. Many well known model structures like Auto-Regressive (ARX), Output Error (OE), Box-Jenkins (BJ) etc. have been treated in this setting. We refer to the literature in standard references including Ljung (1999) and

many others. The overall system identification approach aims at identifying the best model from a given model class, where "best" means the model that optimally explains a given data set. Typically, data is generated by exciting the dynamics of the system whose model needs to be identified. Based on the input and output data, the model parameters are estimated in a specific model class in order to predict the dynamic behavior of the process. There are few non-iterative identification techniques like subspace state space methods. Such methods takes memory effects or the states of a dynamical system into account which are subsequently modeled as the connection between process inputs and outputs. As this method is often used in model reduction techniques that are proposed in this thesis, they are explained in more details in the next subsection.

There are many nonlinear identification techniques as well. Nonlinear identification techniques are usually tailored as per the type of a process and its underlying nonlinearity. Some examples of nonlinear identification techniques are nonlinear auto-regressive, Wiener-Hammerstein configurations, black-box methods (see, e.g. Sjoberg and et. al. (1995)), neural networks, fuzzy logic, support vector machine models (see, Goethals et al. (2005)), grey box models as explained, for instance in Romijn et al. (2008) and many others. A good overview of many nonlinear identification methods in the form of a bibliography is compiled in Giannakis and Serpedin (2001). Lately, the grey-box modeling approaches has drawn lot of attention in the identification community.

System identification techniques that result in LTI models are well suited for analyzing the system properties like stability, convexity, system invariant properties and closed loop performance. Whereas nonlinear models are not very well suited for such a purpose. This has paved a way for identification of Linear Parameter Varying (LPV) systems. Identified LPV models approximates the non-linear behavior on one hand and on the other hand they offer the possibility to extend the notions from classical LTI systems theory as well. Later in this thesis a model reduction framework involving LPV systems is proposed.

3.1.1 Subspace state-space identification techniques

Subspace state space identification techniques have their origin and interpretation in terms of geometry, system theory and linear algebra. The tech-

niques results into model structure in the form of state space matrices. As modern control theory uses a state space description of the system, subspace methods became one of the most favored identification technique. From observed input-output data, the subspace identification methods aim to identify the dominant subspace in which the system dynamics evolve. There is some similarity between the subspace identification method and the POD reduction schemes involving Galerkin projections. POD is primarily used for systems which are distributed in space, and it employs spatio-temporal decompositions of the system solutions. Whereas, the subspace identification is applicable to the systems which are lumped in space and employs a decomposition of the Hankel matrix, which characterizes the temporal evolutions only. The subspace identification method is based on the input-output data, whereas the POD method exploits the availability of state information from the full order model. In our recent work, Wattamwar et al. (2009b) we have proposed a novel method of model reduction which exploits similarity and differences between POD and subspace identification methods. Some standard references about the overview of the system identification methods include Overschee and Moor (1996), Qin (2006),etc. This method has been applied to many MIMO LTI systems. Advantages of subspace methods over prediction error methods are compared in Favoreel et al. (2000) for many industrial applications.

A general linear discrete time-invariant state space system obtained by subspace identification techniques is given by (3.1)

$$\begin{aligned} x(k+1) &= Ax(k) + Bu(k) \\ y(k) &= Cx(k) + Du(k) \end{aligned} \tag{3.1}$$

where $x(k) \in \mathbb{R}^n$ is the state vector, $u(k) \in \mathbb{R}^{n_u}$ is the input vector, $y(k) \in \mathbb{R}^{n_y}$ is the output vector. The subspace identification problem amounts to estimating state space matrices A, B, C, D from observed input-output data. Although for the research work presented in this chapter we have used standard *N4SID* algorithms which are available in various commercial software packages, for the sake of completeness of the presentation we explain this identification method here briefly. Like any other identification technique, the quality of the identified models obtained from subspace identification techniques depend on the input-output data. Usually the input signal is designed such that it excites system dynamics covering a desired frequency range. Pseudo Random Binary Signals (PRBS) or sum of multi-sine signals are often used to excite the underlying process. We elaborate the details of choice for the identification signal in section 5.2. In subspace

identification methods the postulated model (3.1) is used to formulate a 's' step ahead prediction as in (3.2),

$$y^s(k) = \mathcal{O}_s x(k) + \mathcal{T}_s u^s(k), \quad \text{for} \quad k = 1, \ldots, K-s \tag{3.2}$$

where,

$$\mathcal{T}_s = \begin{Bmatrix} D & 0 & 0 & 0 \\ CB & D & 0 & 0 \\ CAB & CB & D & 0 \\ . & . & . & . \\ CA^{i-2}B & CA^{i-3}B & \ldots & D \end{Bmatrix} \in \mathbb{R}^{sn_y \times sn_u} \tag{3.3}$$

is a lower block triangular Toeplitz matrix, and

$$\mathcal{O}_s = \text{col}\left(C, CA, CA^2, \ldots, CA^{s-1}\right) \tag{3.4}$$

is the observability matrix such that $\mathcal{O}_s \in \mathbb{R}^{(sn_y)\times n}$, where, $s \geq n$. In this chapter, the operator *col* stands for the column stacking operator, i.e.

$$\text{col}(a, b) = \begin{pmatrix} a \\ b \end{pmatrix}, \tag{3.5}$$

and

$$u^s(k) = \text{col}\left(u(k)\ u(k+1) \ldots u(k+s-1)\right) \in \mathbb{R}^{sn_u}, \tag{3.6}$$

$$y^s(k) = \text{col}\left(y(k)\ y(k+1) \ldots y(k+s-1)\right) \in \mathbb{R}^{sn_y} \tag{3.7}$$

are stacked input and output column vectors. In matrix form, for $k = 0, 1, ..., K-s$ these equations are given by eq. (3.8)

$$Y_{0,s,K-s} = \mathcal{O}_s X_{0,K-s} + \mathcal{T}_s U_{0,s,K-s}, \tag{3.8}$$

where, $X_{0,K-s}$ is the state matrix, $Y_{0,s,K-s}$ and $U_{0,s,K-s}$ are the output and input Hankel matrices defined by

$$U_{0,s,K-s} = [u^s(0), \ldots, u^s(K-s)] \in \mathbb{R}^{(sn_u)\times(K-s-1)} \tag{3.9}$$

$$Y_{0,s,K-s} = [y^s(0), \ldots, y^s(K-s)] \in \mathbb{R}^{(sn_y)\times(K-s-1)} \tag{3.10}$$

$$X_{0,K-s} = [x(0), \ldots, x(K-s)] \in \mathbb{R}^{n\times(K-s-1)} \tag{3.11}$$

The identification of (A, B, C, D) in (3.1), is carried out in two steps. The first step always performs the (weighted) projection of the row space of the above mentioned Hankel matrices. From this projection the observability

matrix $\mathcal{O}_s$ and/or an estimate $X_{0,K-s}$ can be retrieved, see e.g. Favoreel et al. (2000). In the second step, the system matrices A, B, C, D are determined. In some more detail, the first step of all subspace methods can be briefly described as follows: Find $\mathcal{O}_s X_{0,K-s}$ of (3.8) by the orthogonal projection of the row space of $Y_{0,s,K-s}$ onto $U^{\perp}_{0,s,K-s}$, where

$$U^{\perp}_{0,s,K-s} = I_k - U^T_{0,s,K-s}(U_{0,s,K-s}U^T_{0,s,K-s})^{-1}U_{0,s,K-s} \tag{3.12}$$

is an annihilator of $U_{0,s,K-s}$ in the sense, that

$$U_{0,s,K-s}U^{\perp}_{0,s,K-s} = 0. \tag{3.13}$$

This leads to

$$Y_{0,s,K-s}U^{\perp}_{0,s,K-s} = \mathcal{O}_s X_{0,K-s}U^{\perp}_{0,s,K-s}. \tag{3.14}$$

Eq. (3.14) shows that each column of $Y_{0,s,K-s}U^{\perp}_{0,s,K-s}$ is a linear combination of the columns of $\mathcal{O}_s$, i.e. the column space of $Y_{0,s,K-s}U^{\perp}_{0,s,K-s}$ is contained in the column space of $\mathcal{O}_s$. In the second step we have 2 possible approaches. With the Singular Value Decomposition (SVD), following set of equations can be obtained:

$$Y_{0,s,K-s}U^{\perp}_{0,s,K-s} = (U_1\, U_2)\begin{pmatrix} S_1 & 0 \\ 0 & 0 \end{pmatrix}\begin{pmatrix} V_1^T \\ V_2^T \end{pmatrix} \tag{3.15}$$

$$\text{rank}(Y_{0,s,K-s}U^{\perp}_{0,s,K-s}) = n, \text{i.e. the number of non-zero singular values} \tag{3.16}$$

$$\mathcal{O}_s = U_1 S_1^{1/2} \tag{3.17}$$

$$X_{0,K-s}U^{\perp}_{0,s,K-s} = S_1^{1/2}V_1^T \tag{3.18}$$

Left singular vectors $[U_1\ U_2]$ contain the information about the observability matrix $\mathcal{O}_s$, i.e. (3.17) while the right singular vectors $[V_1\ V_2]$ contain the information about the states $X_{0,K-s}$, i.e. (3.18). Algorithms like *N4SID* and *CVA* uses estimate of states, while *MOESP*, *IV-4SID* uses the extended observability matrix. State space matrices A and C can be determined from observability matrix $\mathcal{O}_s$ as in (3.4). First n_y rows of $\mathcal{O}_s$ gives C,

$$C = \mathcal{O}_s(1 : n_y, :) \tag{3.19}$$

$$\mathcal{O}_s(1 : (s-1)n_y, :)A = \mathcal{O}_s(n_y + 1 : sn_y, :) \tag{3.20}$$

while by solving the overdetermined (if $s > n$) equation (3.20), A is determined. Note that all the state space matrices in subspace identification

algorithms are determined upto a similarity transformation. Once A and C are determined, B, D and initial conditions $x(0)$ can be determined from input-output data by writing it as

$$y(k) = CA^k x(0) + \left(\sum_{\tau=0}^{k-1} u(\tau)^T \otimes CA^{k-\tau-1} \right) \mathrm{vec}(B) + \left(u(k)^T \otimes \mathcal{I}_{n_y} \right) \mathrm{vec}(D). \tag{3.21}$$

Here, $\otimes$ is the Kronecker product and $I_{n_y} \in \mathcal{R}^{n_y}$ is the identity matrix. *vec* operator stacks columns of a matrix over each other, i.e. if $B = [B1\ B2] \in \mathbb{R}^{n \times 2}$, then

$$\mathrm{vec}(B) = \begin{pmatrix} B1 \\ B2 \end{pmatrix} \in \mathbb{R}^{2n \times 1}$$

Equation (3.21) can be written as

$$y(k) = \psi(k)\, \vartheta, \tag{3.22}$$

where,

$$\psi = [CA^k \quad \left(\sum_{\tau=0}^{k-1} u(\tau)^T \otimes CA^{k-\tau-1} \right) \quad \left(u(k)^T \otimes \mathcal{I}_{n_y} \right)] \quad \text{and} \tag{3.23}$$

$$\vartheta = \mathrm{col}\left(x(0), \mathrm{vec}(B), \mathrm{vec}(D) \right) \tag{3.24}$$

and (3.23) consists product of C,A and inputs u. The unknown parameter vector ϑ is usually estimated by using Least Square Estimation Techniques which solves following optimization problem,

$$\min_{\vartheta} \frac{1}{K} \sum_{k=0}^{K-1} ||y(k) - \psi(k)\vartheta||_2^2 \tag{3.25}$$

Considering the complete dataset, (3.25) can be written in matrix form as,

$$\min_{\vartheta} \frac{1}{K} ||Y_K - \Psi_K \vartheta||_2^2 \tag{3.26}$$

Here, $Y_K = [(y(0), \ldots, y(k-1)]$ and $\Psi_K = [\psi(0), \ldots, \psi(k-1)]$. The estimated solution $\hat{\vartheta}$ of the optimization problem in (3.26) is given by,

$$\hat{\vartheta} = \left(\frac{1}{K} \Psi_K^T \Psi_K \right)^{-1} \frac{1}{K} \Psi_K^T Y_K \tag{3.27}$$

For further details of the subspace identification technique, interested readers are referred to Overschee and Moor (1996) and Favoreel et al. (2000). The complete procedure is repeated in the form of an algorithm as follows:

Algorithmic procedure

- Assume the model structure (3.1) and collect the data $u(k)$ and $y(k)$.
- Choose $n > 0$; set $n \leq s < K$. Construct the stacked vectors (3.6), (3.7) and Hankel matrices (3.9),(3.10) and (3.11).
- Construct the annihilator (3.12) and get (3.14).
- Get $\mathcal{O}_s$ as in (3.17) by performing SVD as in (3.15).
- Estimate state space matrices A and C from (3.20) and (3.19) respectively.
- Estimate B, D and $x(0)$ by solving (3.26) whose solution is (3.27).

3.2 Model reduction and POD

As explained in the introductory chapter of this thesis, for some large scale applications, model reduction is necessary for the design of model based controllers. Model reduction can be viewed as a mathematical solution to the dilemma in which on one hand, great details of a process are necessary to understand its dynamic features. While, on the other hand, simpler and computationally efficient models are needed to perform model based optimizations and control system designs. Model reduction therefore involves the crucial trade off between the information that is kept and the information that is thrown away which is irrelevant for the optimization and control purpose. A good model reduction technique therefore tries to keep the necessary information and throws away the unnecessary. This can also be viewed as the retention of the most relevant system memory.

There are different model reduction techniques. Some of them are based on physical insight of the process like compartmental methods, time scale separation methods, traveling waves, flatness based methods, approximate inertial manifolds etc. Such methods, based on the process insight separate the relevant from irrelevant information and suggests to throw away the irrelevante part. There are some other algorithmic methods which do not need any special process insight and can be applied to different type of systems without much extra efforts. Many model reduction techniques suitable for LTI systems like gramian based balancing and truncation, Hankel norm approximation can be categorized under such techniques. Such

methods are based on estimation of dominant subspace in which the system dynamics evolve. Most of them involves, some form of Eigenvalue Decomposition techniques to estimate the dominant subspace that is spanned by the eigenvectors. Such techniques are motivated by the fact that for a linear system, the amount of the energy that is supplied can be recovered if there are no losses. The reduced order models are then inferred by projection of the full order model onto the dominant subspace. This thesis has investigated model reduction techniques to infer reduced order models for the class of systems described by partial differential equations and generally referred to as the Distributed Parameter Systems (DPS). Classical solution techniques amounts to approximating the infinite dimensional system by a finite dimensional one by projecting it on some Hilbert space spanned by finite number of orthonormal basis functions. This is a form of model order reduction, from infinite order to the a finite one. Within this context, the next subsection describes the projection of a generic infinite dimensional system. This is followed by the explanation of method of the model reduction by the Proper Orthogonal Decomposition (POD).

The difference between the POD and any other projection technique lies in the estimation of the projection space. POD based model reduction techniques has many desirable features. The POD method allows nonlinearities in the system and it is suitable for model reduction of spatio-temporal systems. It is data based method, therefore it is empirical in nature. It is physically natural in the sense that it searches for the coherent patterns in the system. Moreover, the method of POD is optimal in the sense that it projects the solution of full order model on a subspace which is optimal with respect to some cost function characterizing the projection residue. However, it has few drawbacks as well. As the method is data dependent, the reduced order models obtained from POD are highly dependent to the input excitation signal. Moreover they are system representation dependent and there are no clear error bounds. Another drawback of the projection based POD method is that the possibly original sparse structure of a DPS is lost during the projection of DPS on the reduced space. While doing so, the resulting reduced order model has a dense structure which needs a significant computation time. Therefore for some applications, the advantage of having a reduced order model by the method of POD does not lead to any remarkable gain in simulation time and the very purpose of having a reduced order model is lost. Nevertheless, many recent developments (see section 3.2.3) in the POD method makes it attractive from computational purpose as well. The methods that are proposed in this thesis in subsequent chapters are also

directed towards the similar purpose. The POD method as explained in next subsection is often used in this thesis while proposing a new model reduction framework.

3.2.1 Model reduction by projection

In this section, discretization of infinite dimensional Partial Differential Equations (PDE) using Galerkin projection is presented. Discretization is treated as a form of model reduction, from infinite dimensional to the finite dimensional. The discretized PDE result into a model in Ordinary Differential Equation (ODE) form. In this thesis the discretized version of original distributed parameter system is referred to as a full order model. The approach that is presented in this subsection is used to propose the model reduction using the POD method in the next subsection.

Consider a system which is governed by a partial differential equation of the generic form

$$\frac{\partial T}{\partial t} = \mathcal{A}(T) + \mathcal{B}(u) + \mathcal{F}(T, u). \tag{3.28}$$

where the solution $T : \Omega \times \mathbb{R} \to \mathbb{R}$ is a function of a spatial configuration variable $z \in \Omega$ and time $t \in \mathbb{R}$. We assume that for all time instants $t \in \mathbb{R}$, $T(\cdot, t)$ belongs to some Hilbert space $\mathcal{H}$ of functions defined on Ω. Here $\mathcal{A} : \mathcal{H} \to \mathcal{H}$ and $\mathcal{B} : \mathcal{U} \to \mathcal{H}$ are linear operators where $\mathcal{U}$ denotes some input space of functions $u : \mathbb{R} \to \mathbb{R}^m$. For a model equation based on conservation laws, $\mathcal{A}$ typically represents convection and diffusion phenomena while $\mathcal{B}$ is an input operator that represents external influences. $\mathcal{F}$ is a non-linear operator depending on T and the input u. Suppose that $\{\psi_j\}_{j=1}^{\infty}$ with $\psi_j \in \mathcal{H}$ is an orthonormal basis of $\mathcal{H}$ in the sense that

$$\langle \psi_i, \psi_j \rangle \; = \; \delta_{ij}. \tag{3.29}$$

Here, δ is the Kronecker delta and $\langle \cdot, \cdot \rangle$ denotes the inner product in the Hilbert space $\mathcal{H}$. A solution T of eq. (3.28) then admits a representation

$$T(z, t) = \sum_{j=1}^{\infty} \alpha_j(t) \psi_j(z), \quad z \in \Omega \tag{3.30}$$

where, for any $t \in \mathbb{R}$,

$$\alpha_j(t) \; = \; \langle T(z, t),\, \psi_j(z) \rangle \quad \text{for} \quad j = 1, \ldots, \infty \tag{3.31}$$

are the *modal coefficients*, associated with the basis. Numerical computation of a solution T invariably requires a spatial discretization of Ω and the approximation of the infinite sum in eq.(3.30) by a finite one. Specifically, for $n > 0$, the truncated expression

$$T_n(z) = \sum_{j=1}^{n} \alpha_j \psi_j(z), \quad z \in \Omega \tag{3.32}$$

is used as approximation of T where the approximation order n is decided based on some accuracy threshold and the basis functions ψ_j, $j = 1, \ldots, n$ are usually taken as indicator functions on a complete partitioning Ω_j of Ω. For the purpose of inferring a finite dimensional model for eq. (3.28), let $\mathcal{H}_n$ be the n dimensional subspace of $\mathcal{H}$ that is spanned by the first n orthonormal basis functions $\psi_1, \ldots, \psi_n$. Define the canonical projection and injection operators

$$\mathcal{P}_n : \quad \mathcal{H} \to \mathcal{H}_n \tag{3.33}$$

$$\mathcal{I}_n : \quad \mathcal{H}_n \to \mathcal{H} \tag{3.34}$$

The projection operator $\mathcal{P}_n$ then maps the solution T of (3.30) to a finite dimensional space $\mathcal{H}_n$ according to $T_n = \mathcal{P}_n T$, which is represented by eq. (3.32). The injection operator $\mathcal{I}_n$ embeds an element $T_n \in \mathcal{H}_n$ into the infinite dimensional space according to $T = \mathcal{I}_n T_n$. Note that $\mathcal{P}_n \mathcal{I}_n$ is the identity operator on $\mathcal{H}_n$.

A finite dimensional model will be obtained from (3.30) by approximating T in (3.30) by $\mathcal{I}_n T_n$ and using projection and injection operations as follows:

$$\mathcal{P}_n \frac{\partial \mathcal{I}_n T_n}{\partial t} = \mathcal{P}_n \mathcal{A}(\mathcal{I}_n T_n) + \mathcal{P}_n \mathcal{B}(u) + \mathcal{P}_n \mathcal{F}(\mathcal{I}_n T_n, u). \tag{3.35}$$

Recall that $\mathcal{A}$, $\mathcal{B}$ and $\frac{\partial}{\partial t}$ are linear operators. Define $\mathcal{A}_n = \mathcal{P}_n \mathcal{A} \mathcal{I}_n$, $\mathcal{B}_n = \mathcal{P}_n \mathcal{B}$ and define $\mathcal{F}_n : \mathcal{H}_n \times \mathcal{U} \to \mathcal{H}_n$ by setting $\mathcal{F}_n(T_n, u) := \mathcal{P}_n \mathcal{F}(\mathcal{I}_n T_n, u)$. Since $\mathcal{P}_n$ projects on a finite Hilbert space, eq. (3.35) becomes an ordinary differential equation as follows:

$$\frac{d\, T_n}{dt} = \mathcal{A}_n(T_n) + \mathcal{B}_n(u) + \mathcal{F}_n(T_n, u). \tag{3.36}$$

Eq. (3.36) is a finite dimensional model which can be equivalently represented in terms of the basis functions $\psi_1, \ldots, \psi_n$ by performing a so called Galerkin projection:

$$\langle \psi_j, \frac{\partial T}{\partial t} \rangle = \langle \psi_j, \mathcal{A}(T) + \mathcal{B}(u) + \mathcal{F}(T, u) \rangle \quad \text{for } j = 1, \ldots, n. \tag{3.37}$$

Due to the linearity of the inner product, eq. (3.37) reduces to

$$\frac{\partial\langle\psi_j, T\rangle}{\partial t} = \langle\psi_j, \mathcal{A}(T)\rangle + \langle\psi_j, \mathcal{B}(u)\rangle + \langle\psi_j, \mathcal{F}(T,u)\rangle \quad \text{for } j = 1,\ldots,n.. \tag{3.38}$$

Substitute in the latter expression the expansion eq. (3.32) for T and use the assumption (3.29) to infer that

$$\frac{d\alpha_j}{dt} = \mathcal{A}_{n,j}(\alpha) + \mathcal{B}_{n,j}(u) + \mathcal{F}_{n,j}(\alpha, u), \quad j = 1,\ldots,r$$

where

$$\begin{aligned}
\mathcal{A}_{n,j}(\alpha) &= \langle\psi_j, \sum_{i=1}^{n} \alpha_i \mathcal{A}(\psi_i)\rangle \\
\mathcal{B}_{n,j}(u) &= \langle\psi_j, \mathcal{B}(u)\rangle \\
\mathcal{F}_{n,j}(\alpha, u) &= \langle\psi_j, \mathcal{F}(\sum_{i=1}^{n} \alpha_i\psi_i, u)\rangle
\end{aligned}$$

and where we stacked the coefficients $\alpha_1,\ldots,\alpha_n$ in a vector $\alpha = \mathrm{col}(\alpha_1,\ldots\alpha_n)$. In vector notation, (3.37) is therefore approximated by the ordinary differential equation

$$\frac{d}{dt}\alpha = \mathcal{A}_n(\alpha) + \mathcal{B}_n(u) + \mathcal{F}_n(\alpha, u). \tag{3.39}$$

with the obvious definitions for $\mathcal{A}_n$, $\mathcal{B}_n$ and $\mathcal{F}_n$. Eq. (3.39) is the full order finite dimensional model as an approximation of the infinite dimensional system (3.28). The number n constitute the number of ODEs, i.e., the order of the full scale model. Note that the *states of the finite dimensional model in eq.* (3.39) *are the time-varying modal coefficients in the finite expansion in eq.* (3.31). Therefore, eq. (3.39) and eq. (3.36) are equivalent expressions. Any solution α of eq. (3.39) defines an approximate solution to the original model though the expansion (3.32).

3.2.2 Low order models by POD

One of the most promising and successful techniques for an efficient reduction of large-scale nonlinear systems in fluid dynamics is the method of Proper Orthogonal Decompositions (POD), also known as the Karhunen-Loève decomposition. The method was independently introduced by Karhunen (1946) (also see Karhunen and Kari (1947)), Loève (1978) (see also, Loève (1945)),

Pougachev (1953), and Obukhov (1954). The method is often applied to large scale data to study the statistical properties. See Lorenze (1956), Lumley (1967) and Holmes et al. (1996) for use of the POD method for PDE based fluid flow models. Kunisch and Volkwein (2002) provide the Galerkin POD method for general equations in fluid dynamics. The work from Sirovich (1987) is about turbulence and coherent patterns. Error analysis for non-linear dynamical systems in finite dimensions were carried out in Rathinam and Petzold (2002). Some work related to the POD method from control perspective is provided in Shvartsman and Kevrekidis (1998), Afanasiev and Hinze (2001), Ly and Tran (2001), Tang et al. (1999). Work related to control of fluid flows using the reduced POD models is presented in Ravindran and Ito (1998) and Ravindran (2000). Relation between the POD method and balancing is provided in Lall et al. (1999), Willcox and Peraire (2002).

The problem of model order reduction using the method of POD amounts to finding approximate solutions T of the infinite dimensional representation (3.28). In practice, this problem usually amounts to first approximating T by a high, but finite n-dimensional, system like the one we derived in eq. (3.39). Then, as a second step, solutions to the high order finite dimensional system are approximated by a low order model of dimension $r < n$. This practice is most common when reduced order models are inferred from finite element or finite volume implementations of infinite dimensional systems.

The POD method is based on the observation that in many processes involving fluid flows, flow characteristics reveal *coherent structures* or *patterns*. This has led to the idea that the solutions T_n may be approximated by T_r by expanding T_r in a small number (r) of dominant coherent structures φ_j, called *modes*. The functions φ_j are inferred in an *empirical* manner from the measurements or from the simulation data. As we are interested in complete state information, we have opted to consider the simulation data from a full scale model as in eq.(3.36). From the simulation data the POD basis functions are obtained as follows.

Let us redefine the solution of the reduced order model T_r as an approximation to the solution T_n of the full scale model (3.36), where $r < n$. Similar to the finite expansion (3.32), T_r is assumed to be represented by

$$T_r(z,t) = \sum_{j=1}^{r} \varphi_j^T(z) a_j(t), \quad z \in \Omega, \tag{3.40}$$

where a_j are the modal coefficients and the functions φ_j, $j = 1, \ldots, r$ define a, possibly different, set of the orthonormal functions in $\mathcal{H}_n$. The derivation of these functions by using the method of model order reduction is elaborated in subsequent paragraphs.

Given an ensemble $\mathbf{T}_n(\cdot)$ of K measurements $\mathbf{T}_n^k(\cdot)$, $k = 1, \ldots, K$ of simulation data of a full scale model, with each measurement defined on the spatial domain Ω, the POD method amounts to assuming that each observation $\mathbf{T}_n^k$ belongs to the Hilbert space $\mathcal{H}_n$ of functions defined on Ω. With the inner product defined on $\mathcal{H}_n$, and a collection $\{\varphi_j\}_{j=1}^n$ such that $\varphi_j \in \mathcal{H}_n$ is an *orthonormal basis* of $\mathcal{H}_n$ if the inner product $\langle \varphi_i \, , \, \varphi_j \rangle = \delta_{ij}$, and if any element, say $\mathbf{T}_r^k \in \mathcal{H}_n$, admits the representation as in eq. (3.40). The approximate solution causes an error $\|\mathbf{T}_n - \mathbf{T}_r\|$ in the norm of the Hilbert space. We will call $\{\varphi_j\}_{j=1}^n$ a *POD basis* of $\mathcal{H}_n$ whenever it is an orthonormal basis of $\mathcal{H}_n$ for which the *total approximation error* over the complete ensemble, i.e when

$$e_r = \sum_{k=1}^{K} \|\mathbf{T}_n^k - \mathbf{T}_r^k\| \tag{3.41}$$

is minimal for all truncation levels r. This is an *empirical basis* in the sense that every POD basis depends on the data ensemble. Using variational calculus, the solution to this optimization problem amounts to finding the normalized eigenfunctions $\varphi_j \in \mathcal{H}_n$ of a positive semi-definite operator $R : \mathcal{H}_n \to \mathcal{H}_n$ which is defined by

$$\langle \xi_1, R\xi_2 \rangle := \frac{1}{K} \sum_{k=1}^{K} \langle \xi_1, \mathbf{T}_n^k \rangle \cdot \langle \xi_2, \mathbf{T}_n^k \rangle \tag{3.42}$$

with $\xi_1, \xi_2 \in \mathcal{H}_n$. Here, R is a well defined and positive semi-definite matrix. A POD basis is obtained from the normalized eigenvectors of R in the sense that the POD basis functions satisfy $R\varphi_j = \lambda_j \varphi_j$ for $j = 1, \ldots, n$ where the non-negative eigenvalues are ordered according to $\lambda_1 \geq \cdots \geq \lambda_n \geq 0$ and where the eigenfunctions φ_j are normalized in the sense that $\langle \varphi_i, \varphi_j \rangle = \delta_{ij}$. See e.g. Astrid (2004).

The modal coefficients a_j in eq. (3.40) are referred to as *POD modal coefficients* and satisfy

$$a_j(t) = \langle \varphi_j, T_n(\cdot, t) \rangle \quad \text{for} \quad j = 1, \ldots, r, \quad t \in \mathbb{R}. \tag{3.43}$$

Subsequently, as explained in section 3.2.1, a Galerkin projection is used to deduce a reduced order model from the full scale model (3.36) by projecting

the model residual on the span of dominant r POD basis functions:

$$\frac{d\,\langle \varphi_j, T_n \rangle}{dt} = \langle \varphi_j, \mathcal{A}_n(T_n) + \mathcal{B}_n(u) + \mathcal{F}_n(T_n, u) \rangle \quad \text{for} \quad j = 1, \ldots, r. \tag{3.44}$$

Substitution of the expansion eq. (3.40) gives that the j^{th} POD modal coefficient a_j satisfies the ordinary differential equation

$$\frac{d\,a_j}{dt} = \mathcal{A}_{r,j}(a) + \mathcal{B}_{r,j}(u) + \mathcal{F}_{r,j}(a, u) \quad \text{for} \quad j = 1, \ldots, r. \tag{3.45}$$

where we stacked the coefficients $a_1, \ldots, a_r$ in the vector a. In vector form, eq. (3.45) reads

$$\frac{d}{dt} a = \mathcal{A}_r(a) + \mathcal{B}_r(u) + \mathcal{F}_r(a, u). \tag{3.46}$$

Eq. (3.46) is a reduced order model (ROM). Note that, *the POD modal coefficient vector a turns out to be the states of the ROM.* This is an important observation and rarely in literature the POD modal coefficients have been interpreted in a similar way. In chapter 7 this knowledge that POD modal coefficients can be viewed as the states of a reduced order model is further employed to identify reduced order models of different nonlinear forms.

As result of the eigenvalue decomposition of the correlation matrix R in (3.42), the POD basis functions and the modal coefficients are arranged as per the order of the maximum gain directions in R. Therefore the reduced r dimensional model exhibits the most dominant system dynamics, in the sense that the j^{th} evolution equation (3.45) is more relevant than the $j + 1^{\text{st}}$ evolution equation. Once the POD modal coefficients are known, the reconstructed solution T_r can be obtained through the expansion eq. (3.40).

The optimization problem to obtain the POD basis from the eigenvalue decomposition of $\mathcal{R}$ from eq. (3.42) can also be equivalently solved for the ensemble $\mathbf{T}_n$ as a singular value decomposition (*SVD*) problem. Precisely, a singular value decomposition $T_{\text{snap}} = U \Sigma V^\top$ of the snapshot matrix $T_{\text{snap}} = \begin{bmatrix} \mathbf{T}_n^1 & \cdots & \mathbf{T}_n^K \end{bmatrix}$ defines the j^{th} POD basis function φ_j in the j^{th} column of the unitary matrix U consisting of the left singular vectors of T_{snap}. From the property of the SVD these basis functions are ordered according to their importance, i.e. the first POD basis corresponds to the direction of maximum energy. Usually a tolerance criterion based on the amount of energy captured in the reduced model is used to decide about the approximation order r of the reduced model. The criterion is usually called the

projection energy and is given by

$$P_{tol} = \frac{\sum_{k=1}^{r} \lambda_k}{\sum_{k=1}^{n} \lambda_k} \tag{3.47}$$

where λ_k is the k^{th} eigenvalue of the correlation operator R defined in eq. (3.42) (or $\sigma_k = \lambda_k^{1/2}$ is the k^{th} singular value of T_{snap}) and r is the desired order of the ROM of eq. (3.45).

3.2.3 Recent developments in model reduction

Some recent work in the field of model order reduction includes- Belzen and Weiland (2008), where a theoretical framework is proposed for the decomposition of multidimensional data objects. Markovinovic (2009) has proposed an iterative method for the development of reduced order models. In his work the author recommends a new procedure to reduce the computation time of full scale models by using a smart guess of initial conditions after a certain simulation horizon. For an application in automobile catalytic converters, Nauta (2008) has proposed model reduction techniques for the kinetic networks of reactions in which wave propagations occur.

Although the lower dimensional models obtained by POD and Galerkin type of projection techniques are smaller in dimension, the reduced order models are dense and they are not necessarily better in computational performance. This is possibly due to the loss of sparsity in the original model structure. Therefore often there is no big advantage of having lower dimensional model, see, e.g. Astrid et al. (2008), Agudelo (2009a), Bos (2006), Huisman (2005), Romijn et al. (2008) and Linhart and Skogestad (2009) and the references therein. The first step of the POD method that is explained in section 3.2.2 involves spectral decomposition which is similar to the Principle Component Analysis (PCA) method used for the analysis of large data sets. Journée et al. (2008) has proposed some new results to infer sparse principal components or in other words, orthonormal POD basis. Extension of this notion of sparse principal component can be very interesting, especially to infer computationally efficient reduced order models.

Towards the purpose of identifying a computationally efficient reduced order model, many novel methods have been proposed in the last few years. Astrid et al. (2008) proposed a new algorithm called 'Missing Point Estimation' (MPE) which suggests to compute a Galerkin projection over an optimally

restricted subset of the spatial domain. MPE takes its inspiration from 'Gappy POD', see Wilcox (2006). Linhart and Skogestad (2009) have compared the effect of different numerical parameters in model reduction setting for a distillation column. Romijn et al. (2008) proposed a grey-box type of model reduction strategy to solve the problem of high computation cost associated with the evaluation of non-linear terms in a full scale model. There, they reduced the linear part by the POD method and approximated the non-linearity in a reduced dimensional space by using a small neural net as a black-box model. Bos (2006) suggested to approximate the non-linear process model by using a blend of linear models based on some weighting function. The resultant pseudo Linear Parameter Varying (pLPV) model is computationally efficient as it does not involve expensive evaluation of non-linear terms.

3.3 Model reduction as an identification problem: Literature overview

This section elaborates on a few model reduction techniques which provided solutions to the problem of model reduction by formulating it as an identification problem, i.e. problem involving some form of parameter estimation. The techniques reviewed here involve either replacement of the full order model or replacement of the computationally expensive non-linear parts alone, by some parameterized model structure. The resulting model structure therefore involved different model forms, e.g. LTI, polynomial, (q)LPV, grey-box etc.

3.3.1 Identification of Kernel using Singular Functions

Like many input-output data based system identification techniques, this technique explores the mapping between the input space to the output space. This identification technique proposes a Singular Value Decomposition (SVD) of an integral equation kernel to approximate the input-output behavior of the system. The technique was first proposed by Gay (1989), (see also Gay and Ray (1995)).

Similar to any other identification techniques (see, Ljung (1999)) this identification method starts with collection of the input and output data $u(\zeta, t)$

and $y(z,t)$ respectively. Here, t is the temporal variable, and $z \subset \mathbb{R}^d$ and $\zeta \subset \mathbb{R}^d$ is the spatial variable that assume values in domain Ω. The method proposes that a distributed parameter system (DPS) can be represented as a mapping from the inputs $u(z,t)$ to the outputs $y(z,t)$. This mapping can be expressed in a Fredholm integral equation of the first kind containing a square-integrable kernel, which may or may not be symmetric (see, Gay and Ray (1995)). That is, the model is represented by

$$y(z,t) = \int_0^\infty \int_\Omega k(z,\zeta,t-\tau)u(\zeta,\tau)d\zeta d\tau \tag{3.48}$$

and $k : \Omega \times \Omega \times \mathbb{R} \to \mathbb{R}$, is the Kernel function. The discussion that follows assumes a single-input-single-output system, i.e. $u(z,t) \in \mathbb{R}$, $y(z,t) \in \mathbb{R}$, for all $z, \zeta \in \Omega, t \geq 0$. Extension to the multi-variable case is straightforward.

Following Gay (1989), and Gay and Ray (1995), the Laplace transform of the above with respect to time yields a transform of the DPS, where s is the Laplace variable,

$$Y(z,s) = \int_\Omega K(z,\zeta,s)U(\zeta,s)d\zeta. \tag{3.49}$$

Here $Y(z,s) = \mathcal{L}(y(z,t))$ is the Laplace transform of $y(z,t)$, $K(z,\zeta,s) = \mathcal{L}(k(z,\zeta,t))$ is the Laplace transform of $k(z,\zeta,t)$ and $U(\zeta,s) = \mathcal{L}(u(\zeta,t))$ is the Laplace transform of $u(\zeta,t)$.

To approximate the input-output data, suitable functions $r_j(z)$ and $q_j(z)$ are selected as the basis functions

$$U(\zeta,s) = \sum_{j=1}^{m} r_j(\zeta)\tilde{a}_j(s), \tag{3.50}$$

$$Y(z,s) = \sum_{j=1}^{p} q_j(z)\tilde{b}_j(s), \tag{3.51}$$

where $m < \infty$ is the number of actuators, $p < \infty$ is the number of the sensors and $\tilde{a}_j$ and $\tilde{b}_j$ are the coefficients which, for a given input-output data and for a chosen basis function $r_j(\zeta)$ and $q_j(z)$ can be computed from (3.50) and (3.51) respectively. It will be shown subsequently that the kernel $k(z,\zeta,t)$ can be expressed in terms of these coefficients $\tilde{a}_j$ and $\tilde{b}_j$.

The kernel in (3.49) can be decomposed using Singular Value Decomposition as,

$$K(z,\zeta,s) = \sum_{i=1}^{\infty} \omega_i(z,s)\sigma_i(s)\overline{\upsilon_i(\zeta,s)}, \tag{3.52}$$

where $\omega_i(z,s)$ is left singular vector, $\overline{\upsilon_i(\zeta,s)}$ is the complex conjugate of the right singular vector, and $\sigma_i(s)$ is the i^{th} singular value. For all practical purposes a finite approximation of (3.52) can be represented as,

$$K(z,\zeta,s) = \sum_{i=1}^{m} \omega_i(z,s)\sigma_i(s)\overline{\upsilon_i(\zeta,s)}. \tag{3.53}$$

The right and left singular vectors in (3.53) can be approximated using a finite set of functions $r_j(z)$ for $j = 1,\ldots,m$ and $q_k(z)$ for $k = 1,\ldots,p$ such that,

$$\overline{\upsilon_i(\zeta,s)} = \sum_{l=1}^{m} r_l(\zeta)\overline{\upsilon_{li}(s)}, \tag{3.54}$$

$$\omega_i(z,s) = \sum_{k=1}^{p} q_k(z)\omega_{ki}(s). \tag{3.55}$$

where $\overline{\upsilon_{li}}(s)$ and $\omega_{ki}(s)$ are input (right) and output (left) basis function coefficients respectively.

To get an expression as a map from the input to the output space in terms of the finite decompositions that is presented above, substitute (3.54), (3.55) in (3.53) to get,

$$K(z,\zeta,s) = \sum_{i=1}^{m}\sum_{k=1}^{p} q_k(z)\omega_{ki}(s)\sigma_i(s)\sum_{l=1}^{m} r_l(\zeta)\overline{\upsilon_{li}(s)}. \tag{3.56}$$

To get a relation between input and output in terms of expansion, substitute (3.56),(3.51) and (3.50) in (3.49), which after some rearrangement gives,

$$\begin{aligned}\sum_{j=1}^{p} q_j(z)\tilde{b}_j(s) &= \sum_{k=1}^{p} q_k(z)\sum_{i=1}^{m}\omega_{ki}(s)\sigma_i(s)\times \\ &\quad \sum_{l=1}^{m}\overline{\upsilon}_{li}(s)\int_{\Omega} r_l(\zeta)\sum_{j=1}^{m} r_j(\zeta)\tilde{a}_j(s)d\zeta \end{aligned}\tag{3.57}$$

Using the output trial basis function q_h for $h = 1,\ldots,p$ in the Galerkin procedure produces the following system of linear algebraic equations:

$$\begin{aligned}\int_{\Omega} q_h(z)\sum_{j=1}^{p} q_j(z)\tilde{b}_j(s) &= \int_{\Omega} q_h(z)\sum_{k=1}^{p} q_k(z)\sum_{i=1}^{m}\omega_{ki}(s)\sigma_i(s)\times \\ &\quad \sum_{l=1}^{m}\overline{\upsilon}_{li}(s)\int_{\Omega} r_l(\zeta)\sum_{j=1}^{m} r_j(\zeta)\tilde{a}_j(s)d\zeta dz \end{aligned}\tag{3.58}$$

The above equation can be represented in matrix form as

$$QW\Sigma\overline{V}R\tilde{a}(s) = Q\tilde{b}(s) \quad \text{or equivalently,} \tag{3.59}$$

$$KU = Y, \quad \text{with} \quad \text{SVD}(K) = W\Sigma\overline{V} \tag{3.60}$$

where, $Q = \int_\Omega q(\zeta)q^T(\zeta)d\zeta$, $R = \int_\Omega r(\zeta)r^T(\zeta)d\zeta$, $\Sigma = \text{diag}\{\sigma_i(s)\}$, $W = \omega_{ki}$ for $k = 1, \ldots, p$, $V = v_{li}$ for $l = 1, \ldots, m$. The kernel is then given by

$$K(s) = W\Sigma\overline{V}R = \overline{B}(s)\tilde{A}^{-1}(s) \tag{3.61}$$

where $\tilde{A}(s)$ and $\overline{B}(s)$ are input and output coefficients, respectively, that come from the Laplace transform of the data presented in (3.50) and (3.51). The input-output data normally contain values that result from small perturbations in the inputs set about the nominal point. These deviations can be interpolated by well behaved functions such as B-splines to give the output, $\tilde{B}(s)$, and input $\tilde{A}(s)$ coefficient matrices, respectively. For further details, readers can refer to Gay and Ray (1995).

Remark 3.3.1 The method presented here is similar to other system identification methods (see, Ljung (1999)) aimed at identifying a map between system inputs and outputs for a lumped system. The unique advantage of the presented method is its applicability to a process which is viewed as a distributed parameter system. Due to its simplicity and finite approximation of kernel, the dynamic models obtained by such an identification method can be used for the control purposes. Unfortunately the method presented here do not present a way to estimate the physically interpretable states of a distributed system and therefore the method do not offer any physical insight of the underlying process. Moreover, the method is not suitable for highly nonlinear processes as it exploits the linear relation between the input and the outputs.

3.3.2 Reduced order Grey-Box modeling

Grey-Box modeling in context of model reduction using POD for Distributed Parameter Systems (DPS) was initially proposed in Romijn et al. (2008) and in Özkan et al. (2007). It extends the notion of grey-box modeling as investigated for lumped systems in Psichogios and Ungar (1992) and later in Thompson and Kramer (2000). The grey-box modeling method for nonlinear processes proposes to separate the linear and non-linear part of a

dynamical system, such that the linear part is derived from the First Principle Modeling techniques while the non-linear part is approximated by using a black box. The black box model in Psichogios and Ungar (1992) is used to approximate unknown relations which determine certain model variables, where as in Thompson and Kramer (2000), the black-box model is used in parallel structure to approximate the model prediction error. Application of grey-box modeling approach in model reduction can be useful, as it avoids expensive evaluation of non-linear functions by replacing these functions by static mappings that allow faster evaluations. Overall grey box reduced order modeling technique amounts to approximating the linear part of a full order model by a low order linear model obtained by some classical projection technique (see Antoulas (2005a)) and to approximate the nonlinear function (or uncertain/un-modeled component) by a simpler function in reduced space. The proposed technique results into computationally efficient models which generally preserves the original sparse model structure. The overall methodology is briefly explained below.

Consider a DPS of the form (3.28), which, as explained in subsection 3.2.1, after some type of spatial discretization can be converted to an ODE system of the form (3.39). Like many other model reduction techniques, grey-box model order reduction starts from the ODE system of the form (3.39). After any chosen method of projection, the full order model (3.39) is converted to (3.46). The grey-box modeling approach proposes to replace the computationally expensive part $\mathcal{F}_r(a,u)$ by using some empirical function of the form $\varepsilon\left(\tilde{a},u,\theta^*\right)$ such that (3.46) will take a form,

$$\frac{d}{dt}\tilde{a} = \tilde{\mathcal{A}}_r(\tilde{a}) + \tilde{\mathcal{B}}_r(u) + \varepsilon\left(\tilde{a},u,\theta^*\right). \tag{3.62}$$

Here, $\tilde{a}$ are the states of the reduced grey box model, $\tilde{\mathcal{A}}_r$ and $\tilde{\mathcal{B}}_r$ are state space matrices corresponding to $\mathcal{A}_r$ and $\mathcal{B}_r$ respectively, as explained in section 3.2.2. $\varepsilon : \mathcal{H}_n \times \mathcal{U} \times \Theta \rightarrow \mathcal{H}_n$ defines a parametrization of the empirical part. An optimal parameter $\theta^* \in \Theta$ is identified, such that certain criterion function $J : \theta^* \rightarrow \mathbb{R}$ is minimized. The criterion can either minimize the approximation error $||\mathcal{F}_r(a,u) - \varepsilon\left(\tilde{a},u,\theta^*\right)||$ or minimize an error on the state trajectory predictions $||a-\tilde{a}||$. The computational advantage comes from the fact that the evaluation of the nonlinear function $\mathcal{F}_r$ involves the prediction of the state trajectory of full scale model i.e. $\mathbb{R}^n$ whereas evaluation of the empirical function ε requires prediction of the state trajectory in the reduced space, i.e. $\mathbb{R}^r$.

Remark 3.3.2 The grey-box reduced order modeling approach presented

here is different than the approach used in Nauta (2008) and in Agudelo (2009b), where positive polynomials are used to approximate the nonlinear functions and state constraints simultaneously in reduced space. This has guaranteed that the concentrations of the species do not drop below zero. There, the nonlinear function is approximated by a polynomial function in an open loop fashion whereas here in grey-box method, the nonlinear part is approximated by a black-box model in a feedback fashion.

Remark 3.3.3 The number of states and the computational load reduces significantly with the grey-box reduced order model structure, but the resulting model structure is difficult for analysis of stability, optimality, convexity and closed loop performance.

3.3.3 PCA based Subspace Identification techniques

Principal Component Analysis (PCA) is central to the study of multivariate data. Although PCA is one of the earliest multivariate techniques, it continues to be the subject of much research, ranging from new model-based approaches to black-box modeling approaches, e.g. in neural networks. It is extremely versatile, with applications in many disciplines. With advancement in sensor and data acquisition technology, large datasets are available and it is becoming more and more important to process data so that it can be properly analyzed. As PCA is one of the widely used modeling technique, many books and articles explain it vividly. Some recent references include Jolliffe (2002), Jakson (2003), Stone (2004), Esbensen and Geladi (2009). Many commercial software packages like Matlab, Mathematica, etc. have build-in rigorous routines to perform Principal Component Analysis. Although there are many variants of PCA based models, methods involving PCA for subspace identification are rare. As both, PCA and subspace state-space identification techniques (see, 3.1.1) involve Singular Value Decomposition (SVD) of the input-output data matrices to find the dominant subspaces in which the original system dynamics evolve, it makes sense to investigate the PCA-type of subspace identification techniques. Some recent work in this direction is proposed by Wang and Qin (2002), Ku et al. (1995), Li and Qin (2001). This work results in identification techniques for LTI models in or without the presence of input/output noise. The same technique is presented here and later its pros and cons are discussed. For the

case of illustration we consider the deterministic case alone, given by

$$\begin{aligned} x(k+1) &= Ax(k) + Bu(k) \\ y(k) &= Cx(k) + Du(k) \end{aligned} \tag{3.63}$$

Consider a general state-space model structure of the form (3.63) with the dimensions of input $u(k) \in \mathbb{R}^l$, output $y(k) \in \mathbb{R}^m$ and state variable $x(k) \in \mathbb{R}^n$. The method imposes assumptions that the system in (3.63) is asymptotically stable, i.e. the eigenvalues of A are strictly inside the unit circle and the system (A, C) is observable. As in section 3.1.1, define input and output Hankel matrices Y_f and U_f as,

$$Y_f = [y_f(k) \quad y_f(k+1) \dots y_f(k+N-1)] \in \mathbb{R}^{mf \times N}, \quad \text{for } k = 1, \dots, N-f \tag{3.64}$$

$$U_f = [u_f(k) \quad u_f(k+1) \dots u_f(k+N-1)] \in \mathbb{R}^{mf \times N}, \quad \text{for } k = 1, \dots, N-f \tag{3.65}$$

where,

$$y_f(k) = \begin{bmatrix} y(k) \\ y(k+1) \\ \vdots \\ y(k+f-1) \end{bmatrix} \in \mathbb{R}^{mf}, \quad \text{for } k = 1, \dots, N-f \tag{3.66}$$

$$u_f(k) = \begin{bmatrix} u(k) \\ u(k+1) \\ \vdots \\ u(k+f-1) \end{bmatrix} \in \mathbb{R}^{lf}, \quad \text{for } k = 1, \dots, N-f \tag{3.67}$$

are stacked input and output variables such that the included lags $f > n$. The system order n is determined by Akaike information criterion (AIC) as given in Akaike (1974), Akaike (1997) and used in Larimore (1990) for subspace model identification. Iterating eq. (3.63) we obtain

$$y_f(k) = \mathcal{O}_f x(k) + \mathcal{T}_f u_f(k) \tag{3.68}$$

and in matrix form,

$$Y_f = \mathcal{O}_f X + \mathcal{T}_f U_f, \tag{3.69}$$

where, $\mathcal{O}_f \in \mathbb{R}^{mf \times n}$ is the extended observability matrix and $\mathcal{T}_f \in \mathbb{R}^{mf \times lf}$ is block-triangular Toeplitz matrix, similar to the one expressed in (3.4), (3.3),

respectively. In order to use PCA for identification, define a stacked variable z_f and Z_f as,

$$z_f = \begin{bmatrix} y_f(k) \\ u_f(k) \end{bmatrix} \in \mathbb{R}^{lf+mf} \tag{3.70}$$

$$Z_f = \begin{bmatrix} Y_f \\ U_f \end{bmatrix} \in \mathbb{R}^{(lf+mf)\times N}. \tag{3.71}$$

Rewrite (3.68) as

$$[I| - \mathcal{T}_f]\, z_f(k) = \mathcal{O}_f x(k), \tag{3.72}$$

where, | separates the two parts of the matrix. In matrix form,

$$[I| - \mathcal{T}_f]\, Z_f(k) = \mathcal{O}_f X(k). \tag{3.73}$$

As this technique of subspace identification is derived from PCA, we use the data matrix Z_f. Classical PCA method involves collection of data (Z_f), its processing (to remove the mean), scaling to avoid the numerical problems and construction of the co-relation matrix as in (3.42). The SVD of the data matrix Z_f results into the separation of the principal (important) and non-principal components. PCA is similar to the POD method (see, 3.2.2 for POD) up to the separation of dominant and non-dominant directions. Both the methods rely on spectral decomposition in the form of eigenvalue decomposition or the singular value decomposition. After the spectral decomposition, next step in POD involves Galerkin projection of equation residuals to infer the reduced order dynamic models, whereas classical PCA do not lead to any dynamic model. Although, recently some variants of PCA (see, Ku et al. (1995)) proposes certain dynamic modeling features. Classical PCA decomposes data matrix $Z_f^\top$ into,

$$Z_f^\top = TP^\top + \tilde{Z}_f^\top = TP^\top + \tilde{T}\tilde{P}^\top \tag{3.74}$$

where T is a score matrix, P is the loading matrix which consists of principal components as the column vectors, and $\tilde{Z}_f^\top$ is the residual matrix whose norm is minimized during the decomposition. $\tilde{T}$ and $\tilde{P}^\top$ are the score and loading matrices corresponding to $\tilde{Z}_f$. If we compare this decomposition to the SVD, then scores are equivalent to singular values and loading matrix consists of the left singular vectors. That is, if SVD of Z_f is given by,

$$Z_f = U\Sigma V^\top = U_1\Sigma_1 V_1^\top + U_2\Sigma_2 V_2^\top. \tag{3.75}$$

Where, singular values in Σ_2 are equal to zero, $P = U_1$, $\tilde{P} = U_2$, $T_1 = \Sigma_1 V_1^\top$ and $T_2 = 0$. The next step in the procedure is to estimate the extended

observability matrix $\mathcal{O}_f$ and $\mathcal{T}_s$. Towards that purpose, define the orthogonal complement of full column rank $\mathcal{O}_f$ as $\mathcal{O}_f^{\perp}$ such that $\mathcal{O}_f^{\perp}\mathcal{O}_f = 0$. The assumption that $f > n$ guarantees the existence of $\mathcal{O}_f^{\perp}$. Multiply (3.73) with $\mathcal{O}_f^{\perp}$ which will give,

$$\mathcal{O}_f^{\perp}\left[I| - \mathcal{T}_f\right] Z_f = 0 \tag{3.76}$$

(3.76) shows that the elements of Z_f are linearly related, i.e. Z_f has zero singular values. It means that in (3.75), we have $\tilde{T} = 0$ as the residual scores. As,

$$\operatorname{rank} Z_f = \operatorname{rank} Y_f + \operatorname{rank} U_f = n + lf, \tag{3.77}$$

we have number of zero singular values of $Z_f = \dim \tilde{P}$ is,

$$\dim \tilde{P} = \dim\left(\text{image space}\, Z_f\right) - \operatorname{rank} Z_f = (mf + lf) - (n + lf) = mf - n. \tag{3.78}$$

Using this knowledge and the decomposition,

$$Z_f = \begin{bmatrix} Y_f \\ U_f \end{bmatrix} = PT^T + \tilde{P}\tilde{T}^T, \tag{3.79}$$

along with (3.76) we have,

$$\begin{bmatrix} \mathcal{O}_f^{\perp} \\ -\mathcal{T}_f^T\mathcal{O}_f^{\perp} \end{bmatrix} = \tilde{P}M = \begin{bmatrix} \tilde{P}_y \\ \tilde{P}_u \end{bmatrix} M. \tag{3.80}$$

Where, $M \in \mathbb{R}^{(mf-n)\times(mf-n)}$ is a non-singular matrix and usually is an identity matrix of proper dimensions. The explanation behind (3.80) is given in Wang and Qin (2002) and follows the logic that dominant system dynamics evolve in the space spanned by column space of $\mathcal{O}_f$ which implies that the residual dynamic evolve in the space spanned by it's orthogonal complement $\mathcal{O}_f^{\perp}$. (3.80) can be splitted as,

$$\mathcal{O}_f^{\perp} = \tilde{P}_y M \tag{3.81}$$

$$\mathcal{T}_f^T\mathcal{O}_f^{\perp} = \tilde{P}_u M \tag{3.82}$$

With $M = \mathcal{I}$, (3.81) can be written as,

$$\mathcal{O}_f = \tilde{P}_y^{\perp}. \tag{3.83}$$

Once $\mathcal{O}_f$ is estimated from (3.83), system matrices A, B, C, D can be obtained as mentioned in the last two steps of subspace identification algorithm from section 3.1.1. Moreover one can obtain B, D by further rearrangement of (3.82), as given in Wang and Qin (2002).

Remark 3.3.4 From the above discussion it is clear that both; the PCA method and other subspace identification techniques as mentioned in section 3.1.1 aim to estimate the dominant subspace where system dynamics evolves. Therefore this method can be viewed as an approach to identify reduced order models, however in practice, it is difficult to use this method to infer reduced order data-driven models. This is due to the end result of this method, which is an LTI model, which might not be adequate for most of the large scale chemical processes. Moreover, the states of the identified model by this identification technique do not have any physical meaning, and therefore do not provide insight into the physics behind the process. For the case of POD, which unlike PCA involves Galerkin projection of equation residuals (see, 3.2.2), a straight forward extension of the same theory as presented here is not possible.

3.3.4 POD based reduced model identification

POD based identification approach to solve the problem of model order reduction for DPS involves two steps. As explained in section 3.2.2, the first step involves separation of spatial and temporal patterns using the SVD of snapshot matrix. The way to infer important spatial patterns i.e. the eigenvectors of spatial correlation operator is presented in (3.42). The method to obtain an expression for POD modal coefficients which can be viewed as dominant temporal evolution patterns, is expressed in eqs. (3.43). The second step of POD based identification involves LTI model identification by proposing some model structure and fitting the model parameters to the temporal patterns obtained in the first step. In the second step Huisman (2005) proposes to treat the POD modal coefficients obtained in (3.43) as an output of some unknown black-box model and then to use classical LTI model identification technique e.g. subspace identification technique (see, section 3.1.1) to identify the reduced order LTI model of the form (3.1). Whereas Bos (2006) has extended the approach presented by Huisman (2005) for nonlinear systems. There, to approximate the temporal evolution of POD modal coefficients, Bos (2006) proposed quasi-Linear Parameter Varying (qLPV) modeling framework. The qLPV framework, due to its increased parameterizations, is better suited to the non-linear systems. However the qLPV method is somewhat complicated and it is validated only on academic/small scale examples.

Due to the drawbacks of both the methods, i.e. the method presented by

Huisman (2005) lacked proper framework to deduce the non-linear reduced order models whereas effectiveness of the qLPV modeling approach for a large scale, complex system is uncertain. In order to overcome the above mentioned drawbacks, two new approaches have been proposed in this thesis. While discussing the new approaches, these techniques are also in greater details.

3.4 Applicability of methods: Comments on literature review

This chapter has elaborated on some of the tools from the theory that are used to propose few new model reduction frameworks in subsequent chapters. Along with the necessary tools from the theory, few methods which have proposed the model reduction problem similar to an identification problem involving some kind of parameter estimation are also briefly explained. Each method has been motivated by a certain type of system and is tailored towards finding a reduced order model for a specific class of system. Therefore each method has its own advantages and pitfalls which are already mentioned in respective subsections. Some of the techniques presented here, meet the few objectives that are mentioned in section 1.2. For example, for very large scale-multidimensional systems, classical POD model reduction technique alone is not able to present computationally efficient, low order models which can be used for the control purpose. This has been concluded as well in the work of Astrid (2004), Nauta (2008), Romijn et al. (2008), Huisman (2005) and many others. For the objectives mentioned in 1.2, hardly any specific approach presented in the literature is suitable. Either most of the methods are not suitable for large scale real life nonlinear processes (e.g. see, Butkovskiy (1969), Butkovskiy (1982), Hoo and Zheng (2001)), or they do not preserve the physical interpretation of the states (e.g. see, Gay (1989),Wang and Qin (2002)), or they need access to the governing equation for projecting them onto lower space using Galerkin projections (e.g. see, Astrid et al. (2008), Holmes et al. (1996) and many other), or the identified reduced model is not easy for analytical treatment for studying stability, convexity, optimality etc. (e.g. see Romijn et al. (2008),Bos (2006)). Among the different approaches presented here, the work of Huisman (2005) satisfies most of the objectives outlined in section 1.2. The work presented there does not need access to the governing system equations and need information of the states of full order model only. The method presented there is based

on a two step approach involving a spectral decomposition and subsequent system identification. Unfortunately, for many real life processes, identification of LTI reduced order models is not sufficient and it becomes imperative to identify reduced order nonlinear models. This thesis tries to address this problem of inferring reduced order nonlinear models. Moreover the question of parameter sensitivity in context of model reduction for lage scale nonlinear systems, which has been rarely explored in the literature is also addressed in this thesis.

4

Detection of Bifurcations in Tubular Reactor using Reduced Order Models

In this chapter a novel methodology to detect the bifurcating dynamics of a tubular reactor is presented. The bifurcation behavior exhibited by the full order process model as result of the parameter variations is approximated by using the detection mechanisms. The detection mechanisms are based on reduced order models obtained by the method of Proper Orthogonal Decompositions. The parameter variation was chosen so as to exhibit a discontinuous dependence of the dynamical responses as function of the parameter (the Damkohler number). A critical value of the Damkohler number causes changes in the steady state response of the system. In an on-line fashion the algorithm allows to detect the process operation regime, viz- before or after the critical bifurcation value. An investigation of the corresponding wave patterns in the reactor shows the difficulty to capture the transition from a lower to a higher steady state in the reduced model. Depending on the possibility of access to the model equations, two types of detection mechanism; a static and a dynamic one, are presented.

The results presented in this chapter are based on the paper, see Wattamwar and Weiland (2008).

4.1 Introduction

Many large scale chemical processes are modeled by using the first principles. These models can be computationally demanding in the sense that due to their large state space dimension they might need significant computation time. Such large computation time may hinder the use of first principle models for the purpose of plant control and optimization. Model reduction to infer computationally efficient process models is therefore an important step towards realizing this goal. The method of Proper Orthogonal Decomposition (POD) is useful to infer the reduced order models. The POD method is explained in chapter 3. Sometimes, for specific combination of process parameters, the lage scale chemical processes exhibit a discontinuous change in the dynamic behavior as result of a continuous change in the process parameter. The process behavior is further characterized such that at certain critical value of the process parameter, the underlying process may show existence of multiple solutions. The situation with simultaneous existence of the two solutions is usually known as bifurcations of system solutions.

Bifurcations constitute an important part of the dynamic behavior of a system. Understanding of bifurcation behavior is necessary especially for the large scale chemical processes characterized by the exothermic reaction kinetics. Any inappropriate operation (e.g. failure of reaction cooling) of such sensitive processes can easily lead to runaway of process reactions. Runaway reactions are never desired and they can pose serious threats to the plant operation. Therefore, for large scale processes with exothermic reactions, it is imperative to analyse the possibility of existence of multiple solutions.

Although, the first principle models can predict the occurrence of bifurcations, the large computation time associated with their dynamic simulations do not allow them to be used in an online fashion. Therefore, along with the faster computation of system solutions while approximating the dynamic behavior of full order process model, the ability to detect and to predict the occurrence of the bifurcations is also desired form the reduced order models. This issue of detection of bifurcations using the reduced order models is addressed in this chapter. The methods that are presented here may have some similarities with respect to the approach of multi-model fault detection. See, e.g. Berec (1998), Bhagwat et al. (2003a), Bhagwat et al. (2003b), Johansen and Foss (1999), Isermann (1984), Himmelblau (1978), Charbonnaud (2001). But with respect to model reduction to detect the bifurcations using the POD reduced order models, the presented mechanism is rarely explored

in the literature.

In this chapter the discontinuous process behavior as result of a continuous parameter variation in a tubular reactor is presented. The method of Proper Orthogonal Decomposition accompanied with Galerkin projection of equation residuals is used to infer the reduced order models. The performance of the reduced order models under such discontinuous process behavior is investigated. The use of POD techniques for obtaining the low complexity models for highly complex dynamic operating conditions of processes is motivated by a number of arguments. Firstly, the method results in reduced order models that are highly accurate and of very low complexity. Secondly, unlike many other methods of model approximation the POD technique captures relevant dynamics of the system in a small number of basis functions by explicitly using observed time series or simulated responses of the system. As such, the method is data dependent. Moreover, the separation of spatial and temporal dynamics in the reduced order models allows a perfect basis for control system design. However, the method of POD is not very well suitable for approximating the extreme process behavior exhibited in the form of bifurcations.

The work presented here is motivated by the fact that similar to the method of POD, many other model reduction techniques do not take model uncertainty or the effect of time-varying model parameters into account while deriving the reduced order models. The validity of the reduced order models is then limited if the model is largely uncertain or if parameter variations lead to discontinuities in the process behavior. Indeed, if system exhibit significant dynamical changes due to the small parameter variations then this usually lead to a large mismatch between the system and its approximation. Such type of discontinuous dependence on system parameters is not at all uncommon in chemical engineering. Process parameters can show bifurcation or trifurcation phenomena of various types. For example, a jump from an extinction to an ignited state is the effect of a bifurcation value of a well defined system parameter. Such effects are widely reported for many chemical processes. See, for example, some early work in Amundson (1970), Aris (1969), Hlavácek and Hoffmann (1970) that provide an analytical treatment to bifurcation phenomena. See also Jensen and Ray (1982) where the occurrence of multiple solutions for many chemical processes is reported. Recently Bizon et al. (2007) studied the performance of reduced model of a tubular reactor. There, the tubular reactor is modeled as a chain of continuous stirred tank reactors (CSTR). The performance of the reduced

order model was studied as effect of inclusion of samples from a steady and an oscillatory regime.

This chapter tries to answer the question on how to define reduced order models for the nonlinear systems that have uncertain time-varying parameters that exhibit strong discontinuities in dynamic responses. This question is of evident interest for questions on model validation. However, our prime motivation amounts to detecting, monitoring and controlling the parameters that cause abrupt changes in the system dynamics. For systems that exhibit bifurcation phenomenon, we propose a hybrid model structure so as to allow a classification of system parameters around their bifurcation values.

Specifically, in this chapter we consider a model of a tubular reactor where the Damkohler number is viewed as the uncertain parameter that varies close to one of its bifurcation values. The bifurcation phenomena is studied for full order and for reduced order models. Changes of the Damkohler number correspond to the transition of the reactor from a lower (extinction) to higher (ignited) states. The detection mechanisms that are proposed here employ the reduced order models obtained from the POD method. The mechanism processes the plant outputs and predicts the region of process operation (below or above the critical bifurcation parameter value).

This chapter is organized by giving some background knowledge about the existence of multiple steady state solutions in a tubular reactor in section 4.2. The benchmark example of the tubular reactor is already explained in section 2.2.2. Section 4.3 proposes the detection mechanism which is based on reduced order models, while section 4.4 presents the results of investigation of bifurcations in context of model order reduction. Section 4.5 concludes the chapter.

4.2 Occurrence of multiple solutions in tubular reactor

In this section we will discuss the occurrence of multiple steady states for the tubular reactor. The details of the tubular reactor model are presented in section 2.2.2. Many tubular reactor models that occur in the literature can be adequately represented by the dimensionless model presented there. The spatial domain of 1 dimensional reactor is discretized in 301 grid points. Considering only the mass and energy balance, the full order model has the

state dimension 602. Temperatures and concentrations are the variable of interest. The spatial gridding into 301 grid points is the result of a continued refinement of discretizations until the numerical solutions do not change further in accuracy. This is usually referred to as a converged Galerkin projection of an infinite dimensional system. Due to extremities in the process behavior as effect of changes of the Damkohler number around the critical point, numerical integrators can easily fail to integrate the system solutions if the grid is too coarse.

In many earlier works, the dynamic analysis of tubular reactor models was performed by a lumping the spatial coordinates and yielding a model structure that is similar to a continuous stirred tank reactor (CSTR) model. In a CSTR, multiple steady states and oscillating solutions are observed when process parameters or process inputs such as inlet temperatures are changed. For a CSTR, the equilibrium between the heat generation and the heat removal defines the steady state at which the process is operating. For a CSTR, a "lower steady state" (extinction) is observed when the reaction kinetics are limiting, i.e. when the heat generation effects (due to the exothermic reaction) are slower than the heat removal effects. Whereas, an "upper steady state" (ignition) is the opposite situation, which implies that the heat exchange is limiting (i.e. a limited cooling). Based on the process operating conditions and the parameter values, the reactor often shows a tendency to jump either to an upper or to a lower steady state.

Similar effects occur in a tubular reactor where due to the large axial dimension, the transportation effects play a major role along with the reaction and heat effects. Parameters in (2.1), like Damkohler number (Da), Peclet numbers (P_{eh}, P_{em} for heat and mass respectively.), Lewis number (Le) etc. determines the effect of contribution of the transportation and the reaction effects in overall dynamic behavior of a tubular reactor. Damkohler number is the ratio of residence time to reaction time. Fast reactions have smaller reaction time and therefore large Damkohler numbers. For large Da values we have almost complete conversion of the reacting species in the given tubular reactor. The Peclet number is the ratio of a flow advection to a flow diffusion. It is defined in a similar way for mass and heat transfer. The Peclet numbers approach to infinity for the plug flow reactors. Whereas for tubular reactors, the Peclet numbers are larger than one. The Lewis number (Le) is the ratio of a physical transport thermal time constant to a physical transport material time constant. For a tubular reactor the Lewis number is equal to one. For a fixed bed reactor, the $Le > 1$. For a tubular reactor, when

the bifurcation effect is studied for the changes in the Damkohler number, then the analysis of one more dimensionless number; Adiabatic temperature rise becomes important. The relation for a adiabatic temperature rise with other numbers is expressed as $\gamma = B \times Da$. Adiabatic temperature rise is the ratio of the heat of reaction and the average heat capacity of the reactants and the products. For a highly exothermic reaction, the adiabatic number is significantly larger than relatively low exothermic or the endothermic reactions. It is perhaps the most important parameter which determines the existence of multiple steady states. Highly exothermic reactions show increased chances of existence of multiple steady or periodic solutions. Often in practise, the parameter values other than the Damkholer number and the Peclet number can hardly influenced by the control action, the bifurcation phenomena are usually studied in the Peclet-Da parameter space. For various values of the adiabatic temperature rise B, different parameter sets can be obtained which may cause bifurcations of the solution set. Although bifurcations can occur for adiabatic or non-adiabatic situation, in this chapter we are assuming the adiabatic case which creates a 'hot-spot' at the (right) reactor end. As the reaction rate is exponentially related to the negative inverse of the reaction temperature, the hot-spot at the reactor end causes a higher reaction rate at that location. This effect persists at the reactor end and at a certain temperature and concentration, it causes a jump from the lower to the higher steady state. This higher steady state will be limited up to the adiabatic temperature rise (B) and will consume all the possible reactant, that is the concentration of the reactants will drop to zero. Due to the presence of the diffusion term in the tubular reactor model, the transition effect from the lower to the higher steady state will lead to the transition at a point just before the reactor end, and so on. And we see that within a short time (with respect to the residence time of the reactants) the total reactor jumps from the lower to the higher steady state. The transition or the bifurcation effect is observed for different combinations of the process parameters. The critical Damkohler value for which this jump of steady states occurs is denoted by Da^*. Lower steady state solutions are observed for Damkohler values $\mathrm{Da} < \mathrm{Da}^*$ and higher steady state solutions are observed for $\mathrm{Da} > \mathrm{Da}^*$. More than sixteen different types of bifurcation structure have been reported in Jensen and Ray (1982). Most of the literature on bifurcations in tubular reactors is devoted to finding conditions for existence of unique solutions, and to find the bounds for the parameter which guarantee the uniqueness of the solutions. Hlavácek and Hoffmann (1970) derived the bound $B < 4$ on the adiabatic temperature rise that guarantees the uniqueness of solutions. Stability analysis of other chemical processes exhibiting

multiple solutions has received major attention as well, see e.g. Jensen and Ray (1982), Shvartsman and Kevrekidis (1998), Hahn et al. (2004). Eigenvalue analysis of a linearized form of the full order nonlinear model around a steady state operating point is one of the easy yet effective ways of the stability analysis. Based on the eigenvalue analysis, predominantly, two types of bifurcations are reported. When the real eigenvalues cross the imaginary axis in a complex plane the resulting bifurcation is known as saddle node. Therefore, the Saddle node type of bifurcation characterize the stability of the steady state solutions. Whereas, when a pair of complex eigenvalues with an imaginary part cross the imaginary axis, the resulting bifurcation is called as the Hopf bifurcation. The Hopf bifurcation characterize bifurcation of periodic solutions. In some cases, the tools like Lyaponov functional, Poincare maps, phase diagram etc. are employed to study the stability of nonlinear systems.

4.3 Methodology: Detection of bifurcations using reduced order models

In this section the overall methodology to detect the bifurcations in a tubular reactor using the reduced order models is presented. The presented methodology uses full scale first principle model (2.1) of the tubular reactor as a replacement of a real life process. The method of POD with Galerkin projection of model equations is used to infer the reduced order models. Detection mechanisms- dynamic and static are presented to detect the operation regime (below or above the critical value) of the process. To make the chapter consistent with the theme, in this section the method of POD, bifurcation analysis of a system and the detection mecshanisms are presented in separate subsections. Although the POD method is already explained in chapter 3, for the sake of continuity it is discussed again briefly and the discussion is directed towards analyzing the influence of parameter variations in overall POD method.

4.3.1 Bifurcations in dynamical systems

Consider a dynamical model of the form

$$\Sigma(\theta) : \dot{T}_{n,\theta} = f\left(T_{n,\theta}, u, \theta\right) \tag{4.1}$$

where, $T^k_{n,\theta} \in \mathbb{R}^n$ is a solution of the model $\Sigma(\theta)$, $k = 0, \ldots, K$ is the temporal variable, $u(k) \in \mathbb{U}$ is the process input vector and $\theta \in \Theta$ is the vector of process parameters. For the given system model of the form (4.1), suppose that the model has a qualitative property $P_1 \in P$ for $\theta \in \Theta_1$ and $P_2 \in P$ for $\theta \in \Theta_2$, where $\Theta_1 \subseteq \Theta$ and $\Theta_2 \subseteq \Theta$ define a partition of Θ. We call $\theta^* \in \Theta$ a bifurcation value, if θ^* lies on the boundary $\partial\Theta_1 \cap \partial\Theta_2$ where, $\partial\Theta_i$ is boundary of $\Theta_i \in \Theta$. Property sets P_1 and P_2 are disjoint sets. Typically P_1 and P_2 denotes different stability properties of fixed point/limit cycles/regions or orbits in a phase plane of $\Sigma(\theta)$. Bifurcation is defined as a discontinuous (from one set to another) change in the property P as result of continuous change in θ. For Linear systems, bifurcations are often characterized by the behavior of eigenvalues of the Jacobian matrix obtained by the linearization of underlying nonlinear system. For nonlinear systems, often the discontinuous changes cannot be computed. Therefore, for the practical reasons, we define bifurcation as a large change in system solutions at the bifurcating parameter value (θ^*), for a small change in the system parameter θ. Bifurcation of the nonlinear system (4.1) is defined as

$$\frac{\partial T}{\partial \theta}|_{\theta^*} \gg \frac{\partial T}{\partial \theta}|_{\theta}; \quad \forall \theta \in \Theta, \text{ and } \theta \neq \theta^* \tag{4.2}$$

Condition in (4.2) implies that the bifurcation is the critical point θ^* in the parameter space where the changes in the system solutions are significantly larger than at any other values of the process parameter.

4.3.2 Problem formulation

The problem of detection of bifurcations (that is, the detection of process operation regime) using the reduced order model for a parametric process model $\Sigma(\theta)$ of the form (4.1), amounts to finding an approximate process model $\tilde{\Sigma}(\theta)$ of the form,

$$\tilde{\Sigma}(\theta) : \dot{\tilde{T}}_{r,\theta} = f_r\left(\tilde{T}_{r,\theta}, u, \theta\right) \tag{4.3}$$

such that the approximation minimizes some cost function

$$J := \sum_{k=1}^{K} \|T^k_{n,\theta} - \tilde{T}^k_{r,\theta}| \tag{4.4}$$

in some norm. Here, $\tilde{T}^k_{r,\theta} \in \mathbb{R}^r$ is a solution of the reduced order model $\tilde{\Sigma}(\theta)$, and f_r is the reduced nonlinear map. The parameter $\theta(k) \in \Theta = \Theta_1 \cup \Theta_2$,

such that Θ_1 is the domain of parameter variation before the bifurcation, i.e. $\theta(k) \leq \theta^*$ for $k = 1, \ldots, K$ as the number of time samples, with θ^* as the critical bifurcation value of the parameter lying on the boundary of Θ_1 and Θ_2. Θ_2 is the domain of parameter variation after the bifurcation point, that is $\theta(k) \geq \theta^*$ for $k = 1, \ldots, K$. This implies that if the full order process model exhibits parameter sensitivity and the bifurcation as per the definition in (4.2), then this parameter sensitive behavior is also expected to be approximated by the reduced order model.

4.3.3 Model reduction for parameter sensitive processes

Towards the solution of the problem 4.3.2, we briefly define model reduction for parameter sensitive process from the point of bifurcations of solutions of dynamical system. The model reduction method that is used in this chapter is Proper Orthogonal Decomposition (POD), which is already explained rigorously in chapter 3. The method is briefly revised here and is formulated so as to accommodate the effect of parameter variations.

The method of POD involves projection of trajectories of full order process model on some lower dimensional space inferred in some optimal way. The solution of the full and the reduced order process models are related by some projection operator Φ such that,

$$\tilde{T}_{r,\theta} = \Phi_\theta T_{n,\theta} \tag{4.5}$$

The projection operator projects the solution of full order process model onto a lower dimensional subspace spanned by some orthonormal basis functions. The method of POD suggests to find the orthonormal basis by the Singular Value Decompositions (SVD) of the ensemble of the trajectories of the full order model known as the snapshot matrix. The snapshot matrix can be represented as

$$T_{snap,\theta} = \left[T^1_{n,\theta}, \ldots, T^K_{n,\theta}\right] \tag{4.6}$$

SVD of $T_{snap,\theta}$ in matrix notations results in,

$$T_{snap,\theta} = U_\theta S_\theta V_\theta^\top \tag{4.7}$$

where,

$$\begin{aligned} U_\theta &= \left[\varphi_{1,\theta}, \ldots, \varphi_{n,\theta}\right], \quad \text{i.e. matrix with left singular vectors,} \\ S_\theta &= \text{diag}\left[\sigma_{1,\theta}, \ldots, \sigma_{n,\theta}\right], \quad \text{i.e. diagonal matrix with singular values,} \\ V_\theta^\top &= \left[v_{1,\theta}^\top, \ldots, v_{K,\theta}^\top\right] \text{i.e. matrix with right singular vectors.} \end{aligned} \tag{4.8}$$

$\varphi_{i,\theta}(z)$ for $i = 1, \ldots, n$ are the POD basis (spatial components), $\sigma_{i,\theta}$ for $i = 1, \ldots, n$ are the singular values and $v_{i,\theta}$, for $i = 1, \ldots, K$ are the temporal basis functions (right singular vectors), $z \in \mathbb{R}^n$ is the spatial coordinate. The solution $T^k_{n,\theta}$ of (4.1)can be represented in terms of finite spectral expansion as,

$$T^k_{n,\theta} = \sum_{i=1}^{n} a_{i,\theta}\varphi_{i,\theta}(z). \tag{4.9}$$

where $a_{i,\theta}$ are the corresponding modal coefficients satisfying the condition,

$$a_{i,\theta}(k) = \langle T_{n,\theta}(z,k), \varphi_{i,\theta}(z)\rangle, \quad \text{for} \quad i = 1, \ldots, n. \tag{4.10}$$

Due to the property of the SVD, the singular values are arranged in a decreasing order. The approximation order r of a reduced order model can be decided by analysing the singular value decay, i.e. the truncation (approximation) order is decided such that 99% of the projection energy is captured using the criterion,

$$P_{tol} = \frac{\sum_{k=1}^{r} \sigma_k}{\sum_{k=1}^{n} \sigma_k}. \tag{4.11}$$

Therefore, the approximate solutions can be presented as,

$$\tilde{T}^k_{r,\theta} = \sum_{i=1}^{r} a_{i,\theta}\varphi_{i,\theta}(z). \tag{4.12}$$

A projection operator Φ_θ is constructed such that $\Phi_\theta = \left[\varphi_{1,\theta}, \ldots, \varphi_{r,\theta}\right]$. Once the projection operator is constructed, the full order model is projected on the lower space using the projection operator to infer $\tilde{\Sigma}_\theta$. The discussion up-to here is valid for a fixed value of the process parameter and the subscript θ shows the dependence of model reduction procedure on a constant value of process parameter. For a parameter sensitive process (without the bifurcation effect) in which the system solution changes continuously for the changes in the parameter value, the dynamics corresponding to the parameter variation that are exhibited by the full order model can be approximated by the reduced order model by storing the trajectories corresponding to the parameter variations in the snapshot matrix. In this approach of capturing the dynamics of process parameter in a reduced model, the parameter vector is treated similar to a process input. The snapshot matrix can then be represented as,

$$T_{snap,\theta} = \left[T^1_{n,\theta_1}, \ldots, T^K_{n,\theta_1}, \ldots, T^1_{n,\theta_h}, \ldots, T^K_{n,\theta_h}\right] \in \mathbb{R}^{n\times(K*h)}. \tag{4.13}$$

Here $\theta_i \in \Theta$ is a finite set, $\Theta = \left[\theta_1, \ldots, \theta_h\right]$. Note that this formulation of parameter variations allows to consider variation of θ among few discrete values. In case θ is a function of time, i.e. $\theta(k)$ with $i = 1, \ldots, K$ then in order to approximate the dynamics due to the parameter variations in a reduced model, the parameter θ needs a similar attention like an process input.

Based on the SVD of the snapshot matrix (4.13), the approximation order l, as decided by the energy norm (4.11) for a parameter varying case can be different than r, that is, for the situation characterized by a fixed value of the parameter. Model reduction makes sense only if $l \ll n$, i.e. if the singular values of the snapshot matrix (4.13) are dropping at significantly fast rate.

For the processes exhibiting bifurcation type of a behavior as explained in section 4.3.1, i.e. when θ varies over the critical bifurcation value θ^*, then the drop in singular values of (4.13) could be very slow. Nonlinear processes can exhibit different types of bifurcation behavior. Here, with respect to model reduction we classify the bifurcation as a 'mild' or a 'strong' bifurcation. For a parameter variation over a critical bifurcation value, a mild bifurcation is characterized by $l \ll n$ and then the above mentioned model reduction strategy is still valid. For a parameter sensitive process, a strong bifurcation is characterized by $l \approx n$. That is, the approximation of bifurcation using reduced order models obtained by the POD method might not be possible. In other words, it might be possible to infer the lower dimensional subspace for each regime $\theta \in \Theta_1$ and $\theta \in \Theta_2$ separately, but it might not be possible to find a lower dimensional subspace for $\theta \in \Theta = \Theta_1 \cup \Theta_2$. The reason for not being able to approximate the transition dynamics at θ^* is possibly due to the existence of non-correlated patterns in the process dynamics at θ^*. And as the method of POD is based on the existence of correlated patterns, the transition from one domain (Θ_1) to another (Θ_2) might not be effectively approximated by the method of POD.

Towards this problem of approximation of full order model exhibiting the bifurcation behavior and the detection of the process operation regime (i.e. if $\theta \leq \theta^*$ or $\theta \geq \theta^*$) using the POD models is explained in subsequent sections.

4.3.4 Detection Mechanisms

In this subsection, the method to detect the bifurcations exhibited by a nonlinear process (here, a full order model) is presented. In case of uncertainty of the process operation regime (i.e. the bifurcating parameter is smaller or large than the critical value) the mechanism which is based on the reduced order models obtained by the method of POD detects the process operation regime. Depending on the availability of the equations of the full order model for the Galerkin projection on the space spanned by the POD basis, two types of detection mechanism are presented here; a static and a dynamic. The idea behind the detection mechanism comes from the observation that there is a partition in state space due to the presence of bifurcations in system solutions at the bifurcation value θ^* of the parameter θ. In other words, it is possible to find the correlated patterns for the parameter variation for different values of bifurcating parameter (either in Θ_1 or Θ_2) other than the critical one.

The mechanism proposes to identify the reduced order model corresponding to each domain of process parameter variation, separately. That is, if the process parameter θ varies in a space Θ and if θ^* is the bifurcation value then the parameter space is partitioned in two; Θ_1 and Θ_2, such that $\Theta_1 \cup \Theta_2 = \Theta$ and $\Theta_1 \cap \Theta_2 = \theta^*$. Moreover, $\theta \in \Theta_1$ or $\theta \in \Theta_2$ and $\theta \neq \theta^*$. Using the procedure explained in section 4.3.3, the two state spaces corresponding to the two parameter variation domains Θ_1 and Θ_2 are used to construct the snapshot matrices T_{snap,Θ_1} and T_{snap,Θ_2}. Subsequently using the SVD, the spatial basis φ_{i,Θ_1}, φ_{j,Θ_2} for $i = 1, \ldots, r_1$ and $j = 1, \ldots, r_2$ corresponding to the two domains are estimated. r_1 and r_2 are the order of the two corresponding reduced order models. The modal coefficients corresponding to the two parts will be a_{i,Θ_1} and a_{j,Θ_2}. Similarly the two reduced order models $\tilde{\Sigma}_{\Theta_1}$ and $\tilde{\Sigma}_{\Theta_2}$ of the form (4.3) can be obtained after the Galerkin projection.

Based on the availability of the equations of the full order model to deduce the reduced order models, the two types of detection mechanisms are explained in following sections.

Remark 4.3.1 In case of mild case of bifurcation which is explained in last few paragraphs of section 4.3.3, there is no need of partition of the state space corresponding to the two parameter variation spaces. Partition is necessary only for the case of strong bifurcation when transition from one operation domain to another results into completely different process dynamics.

Remark 4.3.2 For the case of existence of multiple solutions (tri-furcations, etc.), similar idea of separation of parameter space can be exploited.

Static Detection Mechanism

The static detection mechanism is useful when the governing equations of full order model are not available and only the process (output) measurements are available. This special case is often observed for commercial softwares (simulators) which do not give access to the model equations but they do provide the state information of full order model. For such situations, as explained in earlier sections, the two snapshot matrices T_{snap,Θ_1} and T_{snap,Θ_2} corresponding to the two sides of partition of parameter space are constructed. In stead of process trajectories, the snapshot matrices may consist of the process measurements. If measurements at sufficiently many locations are available then the snapshot matrices will consists of all the underlying correlated patterns i.e. the POD basis functions. As explained in the previous section, a subsequent SVD of the snapshot matrices will give φ_{i,Θ_1}, and φ_{j,Θ_2} for $i = 1, \ldots, r_1$ and $j = 1, \ldots, r_2$. r_1 and r_2 will serve as the number of correlated patterns for the two operation domains. The two projection operators Φ_{Θ_1} and Φ_{Θ_2} consisting of the correlated patterns φ_{i,Θ_1}, and φ_{j,Θ_2} are constructed. If the snapshot matrix consists of the system trajectories then the inferred projection operators are $\Phi_{\Theta_i} \in \mathbb{R}^{r_i \times n}$ for $i = 1, 2$. If the snapshot matrix consist of the measurements (outputs) then the projection operators are $\Phi_{\Theta_i} \in \mathbb{R}^{r_i \times m}$ for $i = 1, 2$. m is the number of outputs. It should be noted that the,

$$\text{rank}\left[\Phi_{\Theta_1}\right] = r_1, \quad \text{and} \quad \text{rank}\left[\Phi_{\Theta_2}\right] = r_2$$

Now, with underlying assumption that the state space can be partitioned in two parts, and the process measurements reflects major (relevant) process dynamics corresponding to the process inputs and the dynamics corresponding to the parameter variations (belonging to either of the partitioned side), then the static detection mechanism amounts to finding the rank of a matrix as follows: If $y(k) \in \mathbb{R}^{1 \times m}$ is the process measurement vector then,

$$\begin{aligned} \text{if, rank} \begin{bmatrix} \Phi_{\Theta_1} \\ y(k) \end{bmatrix} > r_1 \quad \text{then,} \quad & \theta \in \Theta_2 \subset \Theta \\ \text{else,} \quad & \theta \in \Theta_1 \subset \Theta \end{aligned} \tag{4.14}$$

Based on the output information alone, the static mechanism in (4.14) can detect the operation regime (i.e. before of after the bifurcation) of the process. The static detection mechanism is valid only for the input profile which is similar to the one that is used for construction of the snapshot matrices. For any other type of input profile (different frequency content or the one which excites the other process dynamics), the procedure of estimation of Φ_{Θ_i} needs to be repeated. In other words, the proposed method is not possible to extrapolate and the method cannot be used to predict the temporal evolution of process outputs. It can detect the operation regime of the process alone. The static detection mechanism have similarity to the Principle Component Analysis (PCA) based multi model fault detection mechanism. See, e.g. Esbensen and Geladi (2009), Wang and Qin (2002) and references therein for PCA method. Although, multi-model approach is widely reported in fault detection literature, the approach is not often applied to the detection of bifurcations using reduced order models. Moreover, bifurcations can be viewed as the special type of faults in a system. Some references to the fault detection based on multi-model approach is presented in the introductory section of this chapter.

Another static detection mechanism is proposed here which is suitable for the situation when the state information of the full order model is available however the access to the governing model equations is not possible. This static detection mechanism is based on the residue between the snapshot matrix and its reconstruction. Similar to usual situation, the snapshot matrices considered in this second type of static mechanism consists of solution trajectories. If Φ_{Θ_1} and Φ_{Θ_2} are computed for the snapshot matrices T_{snap,Θ_1} and T_{snap,Θ_2} and if $y(k)$ is the process measurement then the second static mechanism is as follows:

$$\begin{aligned} \left(1 - \Phi_{\Theta_1}^{\top} \Phi_{\Theta_1}\right) * T(k) > \epsilon \quad & \text{then,} \quad \theta \in \Theta_2 \subset \Theta \\ & \text{else,} \quad \theta \in \Theta_1 \subset \Theta \end{aligned} \tag{4.15}$$

where, ϵ is some predefined error criterion by the user. The second type of static detection mechanism is also able to predict the operation regime of the process alone (i.e. if Θ_1 or Θ_2). And due to the unavailability of a dynamic model, neither of the static detection mechanism is able to *predict* the dynamic behavior (future response) of the process.

It becomes clear from the discussion presented in this section that both static detection mechanisms exploit the fact that the dynamic behavior corresponding to the two operation domain of the process parameters is uncorrelated

and therefore it can be used to detect the occurrence of the bifurcations exhibited by the process.

To over-come the pitfalls of static detection mechanism i.e. inability to predict the process behavior, in next chapter another method for the detection of bifurcation using the reduced order models is presented. The method is suitable for the situation when the access to the governing full order model equations is not possible, however the state information of the full order model is available. The method proposed there can predict and detect the occurrence of bifurcations and due to the construction of the dynamic reduced order model, the method can also predict the dynamic behavior of the underlying process.

In case of the availability of the full order model equation, one can deduce the reduced order models corresponding to the two parameter spaces (Θ_1 and Θ_2). The mechanism which allows such detection is explained in next subsection.

Dynamic detection Mechanism

The word 'dynamic' suggests that this mechanism is useful in predicting both; the dynamic process behavior and the occurrence of bifurcations. This mechanism is also based on the partition of the parameter space. Based on the two parameter spaces Θ_1 and Θ_2, two reduced order models $\tilde{\Sigma}_{\Theta_1}$ and $\tilde{\Sigma}_{\Theta_1}$ are obtained as per the procedure explained in earlier subsections. From the knowledge of process inputs and outputs, the dynamic detection mechanism amounts to computation of the residue error between the plant and reduced order model outputs. Residue value implies the domain of parameter operation. That is if,

$$\begin{aligned} ||y_{\tilde{\Sigma}_{\Theta_1}}(k) - y(k)|| > \epsilon \quad &\text{then,} \quad \theta \in \Theta_2 \subset \Theta \\ &\text{else,} \quad \theta \in \Theta_1 \subset \Theta \end{aligned} \tag{4.16}$$

where, ϵ is some predefined error criterion by the user, $y_{\tilde{\Sigma}_{\Theta_1}}(k) \in \mathbb{R}^m$ is the output of the reduced order model $\tilde{\Sigma}_{\Theta_1}$ and $y(k)$ is the plant output. Pictorially, the mechanism can be depicted as in Figure 4.1. Figure shows that depending on the output residue information between the plant and reduced model output, the detection mechanism suggests the operation regime of the process.

Remark 4.3.3 In practice, to compensate the effect of noise and disturbances, the reduced order model need to be replaced by the reduced order observers. The results presented here are based on the simulations alone and the effect of real life disturbances is not modeled here. In this thesis we have not addressed the issue of designing of the reduced observers.

4.4 *Discussion of simulation results*

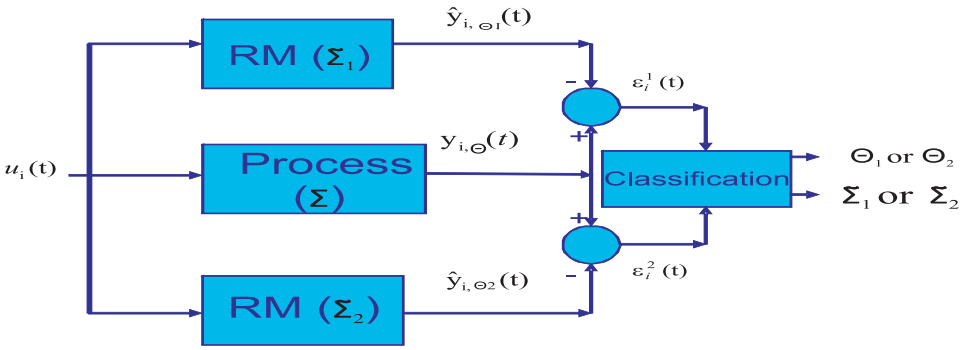

Figure 4.1: Dynamic error detection mechanism.

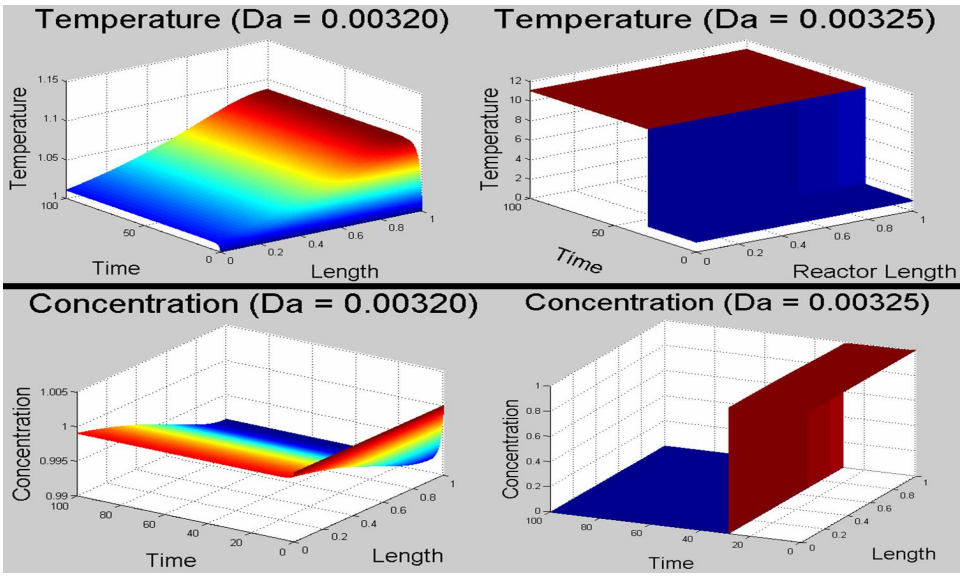

Figure 4.2: Behavior of tubular reactor before and after bifurcation.

This section presents the simulation results on benchmark example of the tubular reactor explained in chapter 2. First, the simulation results of full order model with respect to bifurcation behavior are discussed and then the performance of detection mechanism employing the reduced order models obtained from POD with Galerkin projection techniques are discussed.

4.4.1 Bifurcations exhibited by full order model

The PDEs governing the tubular reactor model in (2.1) were discretized by the numerical technique of method of lines, so as to represent the model as a finite number of differential equations constituting the full order model. The spatial component was discretized into 301 grid points. As there are two variables of interest, viz-temperatures and concentrations, the full order model has state dimension $n = 602$. The wall temperature of the reactor served as the process inputs and they were kept at constant values (=1) during the simulations. The initial conditions were also kept at unity. The full order model is in dimensionless form, therefore all the variables of interest are varied in between 0 to 1. For a constant input profile, the full order model was simulated for different values of bifurcation parameter under study, i.e. for different values of Damkohler numbers (Da). The parameter variation range was $\mathrm{Da} < \mathrm{Da}^*$ and $\mathrm{Da} > \mathrm{Da}^*$, i.e. below and above the bifurcation value Da^*. Figure 4.2 shows the dynamic response of the full order tubular reactor around the bifurcation point. Left side plots corresponds to the parameter values less than the critical bifurcation value, i.e. $\mathrm{Da} < \mathrm{Da}^*$ and right side plots corresponds to $\mathrm{Da} > \mathrm{Da}^*$, i.e. parameter value larger than the bifurcation value. Upper plots show the temperature and lower plots show the concentrations in the reactor. As all the variables are dimensionless, the reactor length varies from 0 to 1. The axis with simulation time is with respect to the residence time, i.e. simulation horizon of 100 shows that the full order model is simulated for a horizon of 100 times that of the residence time of the reactants.

The simulation results are shown in Figure 4.2. For the simulation conditions mentioned in previous paragraph and for the other parameter values given in table 2.2.2, the bifurcation parameter range ($Da^- < Da^* < Da^+$) is ($0.00320 < Da^* < 0.00325$). This implies that for a certain Da^* in the specified parameter window, there exist multiple steady states. The simulations were carried for the adiabatic conditions, i.e. adiabatic reactor with $\mu = 0$ and adiabatic temperature rise $B = 10$. For Damkohler number

$\mathrm{Da} \leq \mathrm{Da}^- = 0.00320$ the full order model shows lower steady state which is characterized by a slow reaction and comparatively lower temperature rise. As the simulation conditions are adiabatic (no cooling), we see the location of the hot-spot at the reactor end (top left plot in figure 4.2). The reaction (exothermic) keeps on increasing the temperature of the content in the reactor and therefore the right end of the reactor becomes a hot spot. For some value of $Da^+ > 0.00320$, the reactor jumps from the lower to higher steady state. In Jensen and Ray (1982), three steady states are reported for these parameter values. However, it is difficult to observe the middle steady state by the dynamic simulations. Similar to a CSTR, the middle steady state is usually said to be unstable. Numerical techniques suggested by Doedel et al. (1997), shows that the middle steady state solutions can also be found out. Sometimes, operating around the middle state could be optimal from the economic point of view but it should be avoided as operating around middle steady state can easily lead to run away of the reaction which is not a desirable situation from point of safety of the process.

4.4.2 Model reduction

As explained in earlier subsections the approximation of bifurcations exhibited by the full order tubular reactor model using a single reduced order model alone is not possible. If the bifurcation window is characterized by three values of Da as mentioned in last paragraph, i.e. $Da^- < Da^* < Da^+$ then as per the discussion presented in the methodology section, the parameter space can be divided into Θ_1 representing a subset of Da values such that $Da \leq Da^-$. The other subset Θ_2 is represented by $Da \geq Da^+$. The bifurcation window $Da^- < Da^* < Da^+$ characterizes the transition from one parameter set to another. This implies that the parameter variation domain characterizing different values of Da can be categorized in three parts; Θ_1, Θ_2 and the bifurcation window. However, for the purpose of validation of the detection mechanisms, only the two subsets, i.e. Θ_1 and Θ_2 are considered here. The transition window, due to its very small size (0.00320 to 0.00325) is ignored. Model reduction is carried out using the method of POD with Galerkin projection of equations of full order model. The model reduction procedure is repeated to infer the two reduced order models corresponding to these two parameter space. In subsequent sections the result of two detection mechanisms based on the reduced order model will be discussed. The difficulty in approximation of the bifurcation behavior of full order model during the transition (bifurcation window) is discussed separately in another

subsection.

Detection of process operation regime for $Da \leq Da^-$ ***and*** $Da > Da^+$

The parameter sets corresponding to $Da \leq Da^-$ and $Da > Da^+$ gives the lower and the higher steady state respectively. The dynamic behavior of full order model corresponding to these sets do not exhibit any discontinuous behavior and therefore it can be lumped in either of these two sets. The procedure of obtaining the reduced order models for the two parameter sets is same. The snapshots matrices corresponding to different values of Da belonging to either of the two parameter sets is constructed. Subsequent step of SVD of these snapshots matrices gave the dominant POD basis functions φ_{i,Θ_1} and φ_{i,Θ_2}. The projection operators Φ_{Θ_1} and Φ_{Θ_2} are constructed using the POD basis functions. Galerkin projection of the full order process model on the space spanned by these projection operators produced two reduced order models $\tilde{\Sigma}_1$ and $\tilde{\Sigma}_2$, each corresponding to either of the parameter set.

The two detection mechanisms; static and dynamic are used to predict the operation window of Da, i.e. smaller or larger than the bifurcation point (if $Da \leq Da^-$ or $Da \geq Da^+$). The full order model of the tubular reactor served as the replacement of the actual process.

Figure 4.3 shows the result of application of static detection mechanism that is explained in subsection 4.3.4, in equation (4.15). As this is a simulation based research work, in stead of error in reconstruction of an individual output signal or a single trajectory, the results are shown for the reconstruction of all spatial signals over the complete simulation horizon (i.e. the snapshot matrix). That is, the figure shows the error in reconstruction of the snapshot matrix obtained for a certain fixed value of Da. The process is distributed in space and time, therefore, to characterize the total error the residue in (4.15) is normed over the space and the simulation horizon. The left side plot shows the error incurred in reconstruction of the temperature snapshots whereas the right side plot shows it for the reconstruction of snapshots of the species concentration. The snapshots corresponding to each parameter regime, i.e. $Da \leq Da^-$ and $Da \geq Da^+$ are constructed. After SVD, the operators Φ_{Θ_1} and Φ_{Θ_2} were constructed. The validation step involved reconstruction of snapshot matrix corresponding to different values of Da. And the error in (4.15) is computed for each case which is plotted in the Figure 4.3. It becomes clear from the plots that the reconstruction error is relatively small for

reconstruction of the snapshot matrix using the projection operator inferred from the SVD of the same snapshot matrix. That is, during validation for different values of $Da \leq Da^{-}$, when a snapshot matrix is reconstructed using the projection and the injection (for reconstructions) operators Φ_{Θ_1} and $\Phi_{\Theta_1}^{\top}$ then the errors are smaller (blue crosses). But if the same snapshot matrix is reconstructed using the operator Φ_{Θ_2} and $\Phi_{\Theta_2}^{\top}$ then the reconstruction error is comparatively bigger. Same holds true for the other validation situation when $Da \geq Da^{+}$ and the error is computed using the operators Φ_{Θ_1} and $\Phi_{\Theta_1}^{\top}$. Therefore, given the knowledge of process output signal or the trajectory, it is possible to detect the process operation regime (i.e. corresponding to before or after a bifurcation point) using the static detection mechanism. The injection operators which gives minimum reconstruction error characterizes the operation regime of the process. Similar explanation holds for the concentrations. It is explained in the methodology section, that this method is not based on the reduced order models in the form of equations, therefore the method is of static nature. That is, only the process operation regime is detected and the process response (outputs) is not predicted. The dynamic detection mechanism overcomes this pitfall and it is discussed in next paragraph.

Understanding the working of dynamic detection mechanism is relatively easier. The full order tubular reactor model served as the plant. The reduced order models were obtained using the method of POD with Galerkin projection. As the mechanism is based on the output residue between the plant and the reduced order models, it suffices to show that at any time instant, the process behavior can be approximated by either of the reduced order model. Figure 4.4 confirms the same thing. The plots in Figure 4.4 show temperatures and concentrations in the middle of the reactor for the full order model (blue line), and for the two reduced order models. The first reduced order model was obtained for the parameter domain $Da \leq Da^{-}$ and it is represented by the red line (RM-Da-minus) whereas the second reduced order model is obtained for the parameter space $Da \geq Da^{+}$ and it is represented by the green line (RM-Da-plus). The maximum value of the temperature that the reactant can observe for the adiabatic case is (Initial condition + Adiabatic temperature rise (B)). The adiabatic temperature rise $B = 10$, and initial condition equal to one, therefore the final temperature in the reactor after crossing the bifurcation point is equal to 11. When the temperature in the reactor reaches its maximum value (adiabatic rise), the reactants are completely consumed and the concentration of the species drop to zero. The lower plateau of the dynamic behavior of the full order

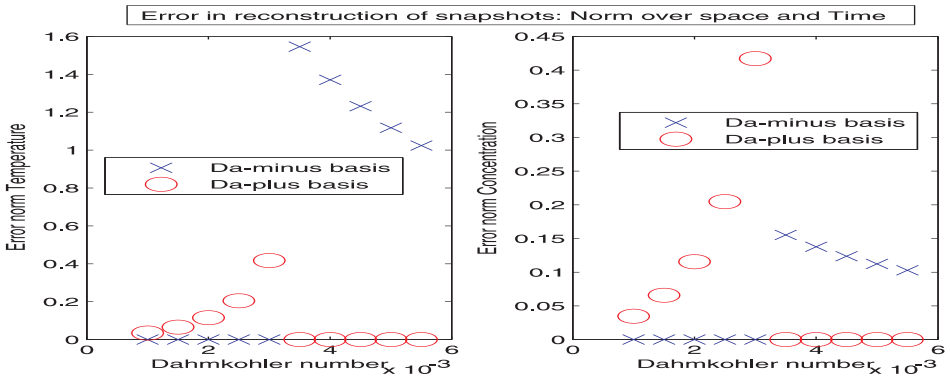

Figure 4.3: Results of static error detection mechanism.

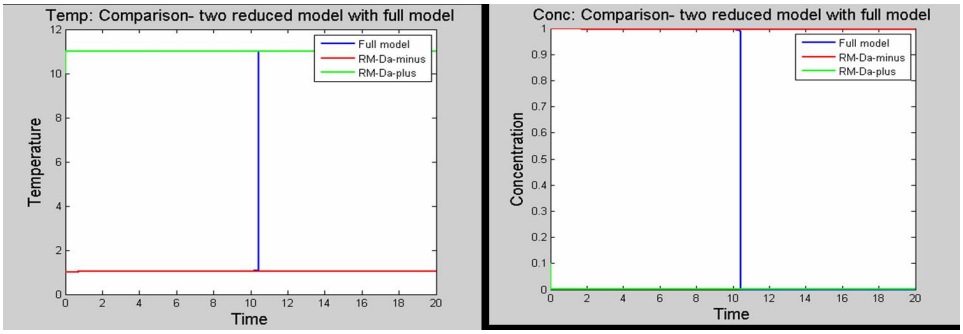

Figure 4.4: Comparison of full scale and two reduced models of tubular reactor

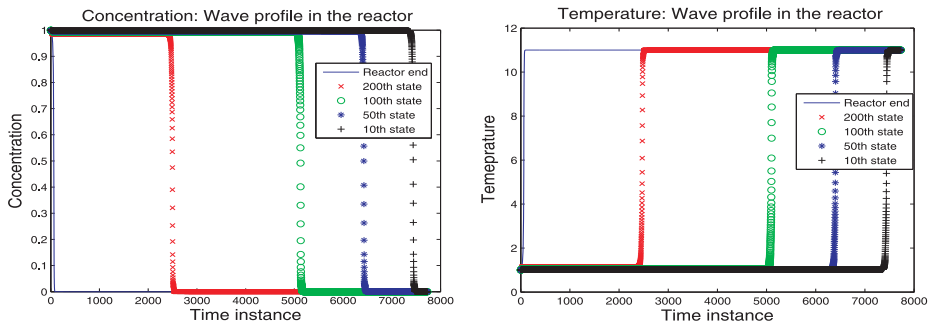

Figure 4.5: Wave pattern in the reactor

model is approximated by the first reduced order model, i.e. corresponding

to the domain $Da \leq Da^{-}$. The higher plateau of the dynamic behavior (i.e. ignition state which occurs after the bifurcation point) is approximated by the reduced order model corresponding to parameter variation domain $Da \geq Da^{+}$. The transition from lower plateau to the higher one is characterized by a special spatio-temporal effect, which is discussed in more detail in next subsection.

Model reduction for $Da > Da^{+}$ ***and for*** $Da \leq Da^{-}$***, i.e the bifurcation window***

The bifurcation window for the full order process model around the critical bifurcation point Da^{*} is $Da > Da^{-}$ and $Da \leq Da^{+}$ is equal to $0.00320 < Da^{*} < 0.00325$. In this parameter range, the full order process model shows the transition from the lower to the higher steady state. Due to the adiabatic nature (no cooling) of the reactor, for the mentioned bifurcation window of the Damkohler number, the temperature at the (right side) reactor end increases significantly. This increase in temperature further increases the reaction rate. This positive loop continues such that at a certain value of temperature and concentration for the mentioned bifurcation window of the Damkohler number, the temperature at the end jumps from the lower to the higher plateau. In comparison to the residence time of the reactants in the reactor, this transition is relatively much faster. As explained in earlier paragraph, the higher plateau (steady state) is determined by the value of the adiabatic temperature rise of the reactor. The higher steady state is the limiting case and the temperature can not be increased there beyond 11 (value of adiabatic temperature rise + initial condition). The concentration drops to zero at this spatial location. The limiting situation implies that the temperature at the reactor end can not be increased further (due to unavailability of the reactants anymore). This results into repetition of same effect at the spatial location which is on the left side of the reactor end, and subsequently the solution at that location also shows transition from the lower to the higher plateau. In a similar way every next spatial location in the tubular reactor starts exhibiting the similar effect. In this way, the diffusion in the reactor carries the transition behavior from the right end of the reactor to the left end in a very short span of time. The word *short* is referred with respect to the residence time of the reactants in the reactor. This spatio-temporal effect of transition in the reactor appears in the form of wave, or sometimes referred to as the 'traveling wave'.

The occurrence of the traveling waves in a chemical unit operations is not uncommon. For example, fixed bed reactors, distillation columns, settling tanks and many other unit operations in chemical process industry show this phenomena. A good account on the information of traveling waves in different chemical unit operations is presented in Marquardt (1990). Model reduction using the method of POD for the processes exhibiting the phenomenon of traveling waves is relatively complex spatio-temporal effect. The usual method of collection of process snapshots and its spectral decomposition to separate the spatial and temporal patterns can still be performed. However, the resulting snapshot matrix is then a triangular matrix with almost full rank. That is, the decay of the singular values for such a snapshot matrix storing the trajectories corresponding to the wave and effect is different than that is observed for any other dynamic process not exhibiting the wave effect. The decay of singular values for a process with a wave effect is very slow and it implies that almost no model reduction is possible. The common notion of truncation of model order to the point where the projection energy content (see, (4.11)) of the reduced model is 99% of the excitation signal does not hold anymore. And therefore, model approximation using a reduced order is not possible anymore. The method of POD is based on correlation of spatial patterns, whereas the wave effect signifies correlation in time. This insight can be useful in inferring a reduced order model by approximating the wave effect using a single temporal pattern. This idea is not further exploited in this thesis. Rather, a similar idea is nicely explored in Nauta (2008). Figure 4.5 shows the wave pattern of temperature and concentration in the reactor during the transition from lower to the higher plateau. The plots in the figure shows that the wave begins at the right end of the reactor from where the product leaves. The wave then travels toward the left end. The plots show that the time instance at which the transition occurs at each location is different and it appears in the form of wave.

4.5 Conclusions and ideas for future research

The work presented in this chapter is motivated by the problem of detection of bifurcations caused by parameters variations in tubular reactor as a benchmark example of large scale processes. The complexity and computation time associated with the full order process model of such a large scale process is the main hurdle for its use in on-line fashion. This chapter provides a practically feasible method as a solution towards this problem. A

novel methodology is presented in this chapter to detect the occurrence of bifurcation and the operation regime of the process. The parameter variation is chosen so as to exhibit a discontinuous dependence of the dynamical responses as function of the parameter (the Damkohler number in the reaction). A critical value of the Damkohler number causes changes in the steady state response of the system. Towards the purpose of detection of parameter regime and occurrence of the bifurcations, two types of detection mechanism; a static and a dynamic are presented in this chapter. The static detection mechanism is based on span of dominant spatial patterns alone and it is useful in detection of bifurcations in the absence of the model equations. The dynamic detection mechanism is based on the output information of the reduced order models obtained by the method of POD with Galerkin projection of equations. The dynamic detection mechanism can be used in an online fashion for the detection of bifurcation occurrence. An investigation into the model approximation using the method of POD for the bifurcation window around the critical parameter value shows the occurrence of the wave pattern in the tubular reactor. The problems associated with model reduction using the method of POD for the process exhibiting the phenomenon of wave is also discussed in this chapter. Due to practical feasible the proposed mechanism should be applicable to other large scale processes. In next chapter we validate the usability of the approach that is presented here on benchmark example of industrial glass manufacturing process.

The wave pattern in the tubular reactor is a temporal effect. Therefore, the possibility of investigating a method based on temporal patterns (right singular vectors) to infer the reduced model can be pursued as the future work. Moreover, for the detection of bifurcations in real life situations, developing a reduced order hybrid observer is more promising. The reduced order observer, are better placed to compensate the effect of process noise and disturbances.

5

Detection of Bifurcation of Flow Patterns in Glass Furnace using Reduced Order Models

---

In this chapter we apply a combination of the method of spectral decomposition and system identification to identify a low dimensional model of a benchmark example representing an Industrial Glass Manufacturing Process (IGMP). The proposed model reduction method does not need the access to the governing equations and relies only on the state information of the full order model. In particular, we infer a reduced model by identifying a linear map from process inputs to the POD modal coefficients by a subspace state-space identification method. Reduced models obtained from such a method are not well equipped to capture the process behavior with time varying uncertain process parameters. For this reason a hybrid detection mechanism, which has been introduced in chapter four is used to approximate the glass manufacturing process (benchmark CFD model) exhibiting non-smooth geometric parameter dependence (corrosion and wear) by using lower dimensional models. Given the state or the output information the mechanisms detect the process parameter operation regime and suggests a computationally faster, lower dimensional model as an approximate for the real process.

The work presented here is based on a paper, see Wattamwar et al. (2008).

5.1 Introduction

This chapter presents the model reduction framework to infer reduced order process models for the 2D glass furnace model exhibiting discontinuous process behavior as result of continuous geometric parameter variations. The problem of model reduction for system exhibiting bifurcations is already discussed in Chapter 4. It is shown there that the reduced model obtained by POD techniques are not well equipped for the processes (tubular reactor) exhibiting non-smooth dependence on process parameters i.e. bifurcation type of a behavior. The problem becomes worse when the physical boundaries of the process domain become uncertain. It is shown in this chapter how the POD basis becomes obsolete when the throat wall of the glass manufacturing furnace (a geometric parameter) wears out over time. See, section 3.2.2 for information on POD method. To address this issue of model reduction for processes exhibiting bifurcations, in this chapter a reduced order modeling framework is proposed. The model reduction technique presented here is similar to the one proposed in Huisman (2005) and it involves two steps. The first step is based on Proper Orthogonal Decomposition (POD) as explained in section 3.2.2 and it involves spectral decomposition of the solutions of the full order model to separate the spatial and temporal patterns. The dominant patterns are then selected to infer the lower dimensional subspace. The second step is different when compared to the usual POD method involving the Galerkin projection of equations. The second step involves approximation of the dominant temporal patterns using the tools from the field of system identification. See section 3.1 for more details about these identification tools. In particular, the subspace state space method of identification is used. It results into LTI models in state space form. The *main contribution* of this chapter is the modification of this data based model reduction method to accommodate the detection of bifurcations of flow patterns in the glass furnace using the detection mechanisms that are proposed in Chapter 4. Based on the state or output residue information between the plant (full order glass furnace model) and the reduced model, the model reduction framework detects the process operation regime (i.e. before or after the bifurcation point) and approximates its behavior using the reduced order models.

The model reduction framework that is proposed here is useful especially when it is difficult to get an access to the governing model equations, in absence of which it is impossible to project the full order process model

onto a lower dimensional subspace spanned by the POD basis. That is, in the absence of modal equations, no model reduction is possible using the classical method of POD with Galerkin projection. Therefore the method that is presented here serves as an alternative to infer the low order process models from the state information of full order process model. The model reduction technique presented here searches for the linear operation regime and results into LTI reduced order models. Due to the linear nature of such models, they are computationally very efficient (more than 1000 times faster) when compared to the full order CFD models used for simulating the glass manufacturing process.

The details about glass manufacturing process, its modeling and wearing of throat wall are explained in section 2.3.6. The wearing out of a throat wall in glass furnace causes initiation of back-flow i.e inversion of the flow direction. This back-flow causes changes of critical process variable (Temperature, Pressure, Velocity...). Occurrence of back-flow is similar to bifurcation or trifurcation happening in many chemical processes exhibiting discontinuous dependence on process parameter. The unit operations in chemical industry which often exhibit the bifurcation behavior are mentioned in Chapter 4.

This chapter is organized in few sections. The overall model reduction framework employing reduced order models, the detection mechanism and the tools from theory is explained in section 5.2. The simulation results are presented in section 5.3 which is followed by the conclusions in section 5.4.

5.2 Methodology: Model reduction and detection of bifurcations

In this section we explain the methodology for identifying smaller dimensional, computationally faster models which can approximate the original full order non-linear process model showing non-smooth geometric parameter dependence. Furthermore this section will explain how to detect the operation regime of the geometric parameter (i.e. below or above bifurcation value) from the obtained reduced model and some process measurements.

This chapter will use the notion of bifurcation, and the concept of detection mechanism to detect the bifurcations from Chapter 4. To avoid the repetition they are not explained in greater details in this chapter. The new contribution from this chapter is the method of inferring the low order models , and

the implementation of the proposed methodology on benchmark example of glass furnace. The method of model reduction that is presented in Chapter 4 is based on the availability of the model equations and it involves projection of model equations on a lower dimensional subspace spanned by the POD basis functions. Whereas, the method of model approximation (reduction) that is presented here is different. It relies on the availability the information of the states of the full order model and therefore does not need the governing equations of the full order model. The method is proposed by Huisman (2005) and it is adapted here for the model reduction of parameter sensitive process and for the detection of bifurcations of flow patterns in 2D glas furnace. The method involves identification of a linear map between process inputs and the modal coefficients that are obtained during the spectral decompositions of the system solutions. For the ease of reading, the overall methodology is presented here in the form of an algorithm. Moreover, the problem formulation that is already presented in Chapter 4 is repeated here for the sake of completeness of the methodology.

5.2.1 Problem formulation

The problem of detection of bifurcations (that is, the detection of process operation regime) for a parametric process model $\Sigma(\theta)$ of the form;

$$\Sigma(\theta) : \dot{T}_{n,\theta} = f\left(T_{n,\theta}, u, \theta\right) \tag{5.1}$$

amounts to finding an approximate process model $\tilde{\Sigma}(\theta)$ of the form;

$$\tilde{\Sigma}(\theta) : \dot{\tilde{T}}_{r,\theta} = f_r\left(\tilde{T}_{r,\theta}, u, \theta\right) \tag{5.2}$$

such that the approximation minimizes some cost function

$$J := \sum_{k=1}^{K} \|T^k_{n,\theta} - \tilde{T}^k_{r,\theta}| \tag{5.3}$$

in some norm. Here, $T^k_{n,\theta} \in \mathbb{R}^n$ is a solution of the model $\Sigma(\theta)$, $u(k) \subset \mathbb{U} \in \mathbb{R}^l$ is the vector of process inputs, $\tilde{T}^k_{r,\theta} \in \mathbb{R}^n$ is a solution of the reduced order model $\tilde{\Sigma}(\theta)$, and f_r is the reduced nonlinear map. The parameter $\theta(k) \in \Theta = \Theta_1 \cup \Theta_2$, such that Θ_1 is the domain of parameter variation before the bifurcation, i.e. $\theta(k) \leq \theta^*$ for $k = 1, \ldots, K$ as the number of time samples, with θ^* as the critical bifurcation value of the parameter on the domain

boundary $\partial\Theta_i$ for $i = 1, 2$. Θ_2 is the domain of parameter variation after the bifurcation point, that is $\theta(k) \geq \theta^*$ for $k = 1, \ldots, K$. This implies that if the full order process model exhibits parameter sensitivity and the bifurcation as per the definition in (4.2) then this parameter sensitive behavior is also expected to be approximated by the reduced order model.

Solution to the problem mentioned earlier can be found by using spectral decompositions as the method of inferring lower dimensional subspace, the method of subspace state-space identification (SID) as explained in section 3.1.1 to approximate the evolution of temporal patterns and the Dynamic Detection Mechanism (DDM) explained in Chapter 4 to accommodate the parameter variation over the bifurcation point. This is explained in subsequent paragraphs as an algorithm. It is assumed here that the full order model is available as a reliable process simulator and the modeling efforts required for the development of the full order model is not discussed here.

5.2.2 Algorithmic procedure

The algorithmic procedure involve two major parts. The first part results into LTI reduced order models and it is explained in the first three steps while the second part involved detection of bifurcations and it is explained in the fourth step.

Step 1: Data collection and processing

Excite the full order process model by the excitation (identification) signal $u(k)$. Construct the snapshot matrix $T_{snap,\theta}$,

$$T_{snap,\Theta_j} = \left[T^1_{n,\theta_{1,j}}, \ldots, T^K_{n,\theta_{1,j}}, \ldots, T^1_{n,\theta_{h,j}}, \ldots, T^K_{n,\theta_{h,j}}\right] \in \mathbb{R}^{n\times(K*h)}. \quad (5.4)$$

Here $\theta_{i,j} \in \Theta_j$ is a finite set, with $i = 1, \ldots, h$ and h is the number of discrete parameter values in a parameter set, j is the number of parameter sets separated by the bifurcation points, i.e. $\Theta_j = \left[\theta_{1,j}, \ldots, \theta_{h,j}\right]$. Here, $j = [1, 2]$. That is, when $j = 1$ represents the situation before the bifurcation and $j = 2$ is the situation after the bifurcation. Therefore the complete parameter variation domain is given by $\Theta = \Theta_1 \cup \Theta_2$, with θ^* as the bifurcation value.

Step 2: Spectral decompositions

$$
\begin{aligned}
U_{\Theta_j} &= \left[\varphi_{1,\Theta_j}, \ldots, \varphi_{n,\Theta_j}\right], \quad \text{i.e. matrix with left singular vectors,} \\
S_{\Theta_j} &= \operatorname{diag}\left[\sigma_{1,\Theta_j}, \ldots, \sigma_{n,\Theta_j}\right], \quad \text{i.e. diagonal matrix with singular values,} \\
V_{\Theta_j}^{\top} &= \left[\upsilon_{1,\Theta_j}^{\top}, \ldots, \upsilon_{K,\Theta_j}^{\top}\right] \text{i.e. matrix with right singular vectors.}
\end{aligned} \tag{5.5}
$$

$\varphi_{i,\Theta_j}(z)$ for $i = 1, \ldots, n$ are the orthonormal basis (spatial components), σ_{i,Θ_j} for $i = 1, \ldots, n$ are the singular values and υ_{i,Θ_j} for $i = 1, \ldots, K$ are the temporal basis functions (right singular vectors), $z \in \mathbb{R}^n$ is the spatial coordinate, with $j = 1, 2$. The solution T^k_{n,Θ_j} of (5.1)can be represented in terms of finite spectral expansion as,

$$
T^k_{n,\Theta_j} = \sum_{i=1}^{n} a_{i,\Theta_j} \varphi_{i,\Theta_j}(z). \tag{5.6}
$$

where a_{i,Θ_j} are the corresponding modal coefficients satisfying the condition,

$$
a_{i,\Theta_j}(k) = \langle T_{n,\Theta_j}(z,k), \varphi_{i,\Theta_j}(z) \rangle, \quad \text{for} \quad i = 1, \ldots, n. \tag{5.7}
$$

Due to the property of the SVD, the singular values are arranged in a decreasing order. The approximation order r of a reduced order model can be decided by analyzing at the singular value decay, i.e. the truncation (approximation) order is decided such that 99% of the projection energy is captured using the criterion,

$$
P_{tol} = \frac{\sum_{k=1}^{r} \sigma_{k,\Theta_j}}{\sum_{k=1}^{n} \sigma_{k,\Theta_j}}. \tag{5.8}
$$

Therefore, the solution of the approximate (reduced order model) can be presented as,

$$
\tilde{T}^k_{r,\Theta_j} = \sum_{i=1}^{r} a_{i,\Theta_j} \varphi_{i,\Theta_j}(z). \tag{5.9}
$$

Step 3: Identification of reduced model

This step involves identification of a LTI reduced model between plant inputs and the modal coefficients, i.e. $u(k) \to a_{\Theta_j}(k)$, with $a_{\Theta_j}(k) = \operatorname{col}(a_{1,\Theta_j}, \ldots, a_{r,\Theta_j})$ as the vector of modal coefficients and col is the column operator stacking the entries over each other. Here, r is the number of modal coefficients

whose temporal evolutions are approximated using the reduced order models. This necessitate a multi-input-multi-output (MIMO) black-box identification method to infer the reduced order models. Moreover, it implies that the modal coefficients $a_{\Theta_j}(k)$ are treated as the outputs of the black-box reduced order LTI model that we aim to identify. The black-box identification method that is chosen to identify this reduced map is a subspace state space identification method. The details about this method can be found in chapter 3. The choice of any other black-box identification method is avoided here as subspace identification method performs better in this special case of treating the POD modal coefficients as the outputs of a black-box model. The reason behind the better performance of the subspace method over the other black-box identification methods lies in the similarity between the functioning of subspace method and the way the modal coefficients are inferred. Both; the way to obtain the modal coefficients and the subspace method involve singular value decomposition. As the modal coefficients are already arranged as per their order of importance, the subspace method becomes the natural choice. This identification step results into black-box LTI models in state space form as,

$$\tilde{\Sigma}(\Theta_j)\begin{cases} x_{\Theta_j}(k+1) & = A_{\Theta_j}x_{\Theta_j}(k) + B_{\Theta_j}u(k) \\ \hat{a}_{\Theta_j}(k) & = C_{\Theta_j}x_{\Theta_j}(k) \end{cases}$$

where, $x \in \mathbb{R}^o$ is the state space dimension of the black-box reduced order model and $j = 1, 2$ i.e. two sides of the partition of parameter space. These states have no physical interpretation. A_{Θ_j},B_{Θ_j} and C_{Θ_j} are the state space parameters of the identified low dimensional model. $\hat{a}_{\Theta_j}(k) \in \mathbb{R}^r$ are the identified modal coefficients obtained by simulating the dynamic model $\tilde{\Sigma}(\Theta_j)$. The reconstructed states $\hat{T}_{r,\Theta_j}$ of the full order model are given by,

$$\hat{T}_{r,\Theta_j}(k) = \Phi_{\Theta_j}^{\top}\hat{a}_{\Theta_j}(k) \in \mathbb{R}^n, \tag{5.10}$$

where, $\Phi_{\Theta_j}^{\top} \in \mathbb{R}^{n\times r}$ is the injection operator constructed from the projection operator $\Phi_{\Theta_j} = \left[\varphi_{1,\Theta_j}^{\top}, \ldots, \varphi_{r,\Theta_j}^{\top}\right]$ constructed from the orthonormal basis functions φ_{i,Θ_j}, where $i = 1, \ldots, r$ and $j = 1, 2$, obtained during the spectral decomposition in second step. The identified outputs (having physical interpretation) of the process are given by,

$$\hat{y}_{r,\Theta_j}(k) = C_T\hat{T}_{r,\Theta_j}(k) \tag{5.11}$$

where, $C_T \in \mathbb{R}^{m\times n}$ is the output matrix.

Step 4: Detection of bifurcations

The detection mechanisms are already explained in Chapter 4. To maintain the continuity, they are briefly explained here once again.

The parameter variation domain Θ is divided into two sets, Θ_1 as the domain in which parameter θ varies before the bifurcation point θ^* and Θ_2 as the domain in which parameter θ varies after the bifurcation point θ^*. Using the first three steps two reduced order black-box models $\tilde{\Sigma}_{\Theta_1}$ and $\tilde{\Sigma}_{\Theta_2}$ corresponding to the two parameter variation domains Θ_1 and Θ_2 are identified. The dynamic behavior of the process is approximated by using either of these reduced order models after comparing the state or the output residue between the reduced order models and the process. If $y(k)$ is the process output and $\hat{y}_{\Theta_j}(k)$ for $j = 1$ or 2, is the output of either of the model, then the residual with respect to the first reduced model is given by,

$$\epsilon_1(k) = ||y_\theta(k) - \hat{y}_{\Theta_1}(k)||_2^2, \tag{5.12}$$

and with respect to the second reduced order model is given by,

$$\epsilon_2(k) = ||y_\theta(k) - \hat{y}_{\Theta_2}(k)||_2^2. \tag{5.13}$$

The dynamic detection mechanism compares these two residuals and detects the occurrence of the bifurcation, i.e. it detects the operation regime of the parameter. That is, if,

$$\begin{aligned} \epsilon_1(k) > \epsilon_2(k) \quad & \text{then,} \quad \theta \in \Theta_2 \subset \Theta, \quad \text{i.e.}\, \theta \geq \theta^*, \\ & \text{else,} \quad \theta \in \Theta_1 \subset \Theta, \quad \text{i.e.}\, \theta < \theta^* \end{aligned} \tag{5.14}$$

5.3 Discussion of simulation results

In this section the results of the application of the proposed detection framework employing the reduced order models is presented. The model reduction framework that is proposed in this chapter is motivated by the industrial application of glass manufacturing process. The glass manufacturing process details are explained in section 2.3.6. The methodology was implemented in order to detect the bifurcations of flow patterns that occur in glass furnace using less complex, computationally efficient reduced order models. The bifurcation of flow patterns in the glass furnace appears as result of the corrosion of the furnace throat wall which is shown in Figure 2.2. The effect of

wearing of the throat wall in the form of corrosion results into back-flow of the glass from the refining section to the fining zone via the throat area. The occurrence of the back-flow is shown in the Figure 2.11. The model reduction and detection framework proposed in this chapter allows to approximate this problem of corrosion resulting into back-flow as a bifurcation problem. The furnace throat height is treated as the bifurcation parameter. For the 2D model of the furnace that is presented in chapter 2, the bifurcation window is observed for the values $h_1 = 0.2[m]$ and $h_2 = 0.3[m]$, where h_i is the throat gap. Increased gap at the throat area from h_1 to h_2 due to the corrosion results into the bifurcation of flow patterns.

Simulation experiments were performed on the $2D$ glass furnace model for two different throat heights for a time horizon of 60 hr. The full order process model is simulated using the Computational Fluid dynamics (CFD) tools coded in software platform *GTM-X* designed by TNO, see TNO (2008). The software serves as a simulator, which means that the inputs can be designed and the CFD model can be simulated with the desired numerical parameter settings, but the access to the full order model equation is not available to the user. As the methodology that is proposed in this chapter is based on the state information of a full order model, the low order models can be still developed to detect the bifurcations of flow patterns.

The data comprising of the full order state information was extracted and imported in MATLAB environment for performing the spectral decomposition of temperatures in the furnace followed by the identification of the low order models. In real life glass furnace, temperature is one of the few important process variables that can be reliably measured. Therefore the results of the proposed methodology are validated on the process temperature alone. From step 1 to step 3 as mentioned in the methodology section are repeated for the two situations, viz. before the bifurcation (h_1) and after the bifurcation(h_2). Two linear models $\tilde{\Sigma}_{\Theta_1}$ and $\tilde{\Sigma}_{\Theta_2}$ are identified corresponding to h_1 and h_2. The identified models are linear in nature and therefore they are comparatively much faster (> 1000 times) in computation of dynamic solutions when compared to the computation time of the full order CFD models. Due to the big mismatch in computation time of the full and the reduced order models, the computational advantages of the identified models over the full order CFD models is not compared in further detail. The lower dimensional linear models were identified between a single input, which is *glass pull rate or the production rate* and three outputs which are first three modal coefficients $a_{i,\Theta_j}(k)$ corresponding to the dominant spatial

patterns $\varphi_{i,\Theta_j}(z)$ with $i = 1, 2, 3$ for the number of modal coefficients and $j = 1, 2$ for the two partitions of the parameter space. Figure 5.1 shows the process input profile (left) and the temporal evolution of the mean temperature in the glass furnace for the two different CFD models, corresponding to the two situations - before and after corrosion. The identification signal was made of steps in positive and negative directions and sampling rate was chosen equal to 8 min. The average temperature plot of the CFD models

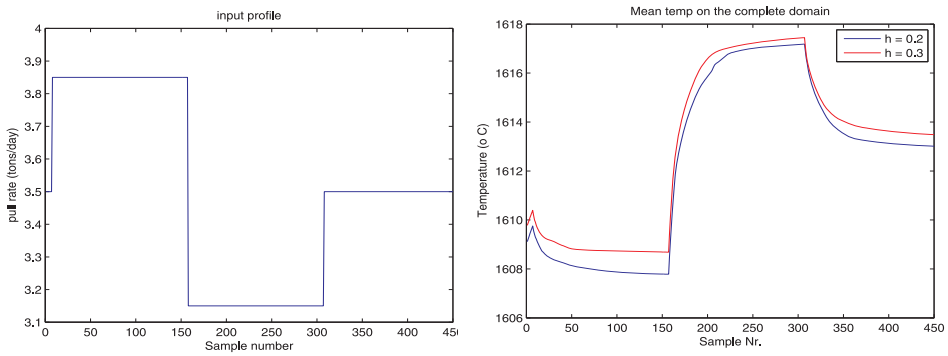

Figure 5.1: Left: Process input, Right: Average temp. profile

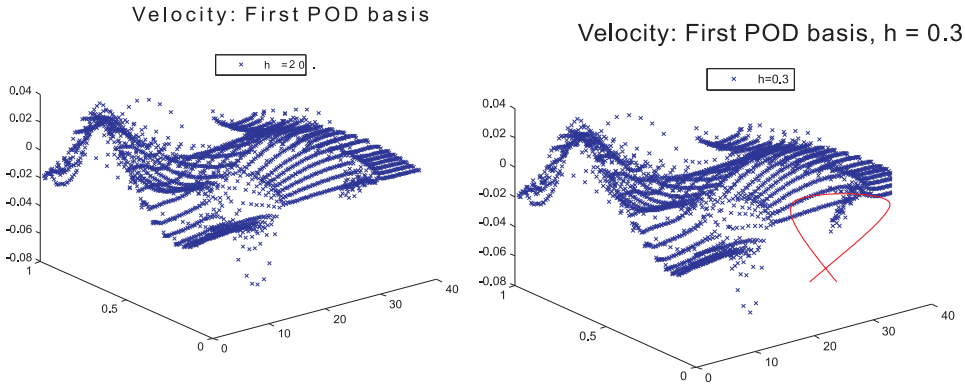

Figure 5.2: Comparison between first velocity basis function. Left: $h = 0.2$, Right: $h = 0.3$

for the two situations (h_1 and h_2) is shown on right hand side plot in Figure 5.1. The response of each furnace (corresponding to the geometry h_1 and h_2) to the changes in feed rate is different and it depends on many factors like furnace capacity, heat content of the molten glass, external heat supply

and many other process variables. Plot shows that even for 1% step around the working point, the process shows nonlinear behavior, as observed by the different gain in positive and negative directions. The plot also shows that the full order CFD model exhibit a similar dynamic behavior for the two situations with relatively small difference. However, the plot shown in Figure 5.1 represent the average (over the complete spatial domain) response of the full order model and it does not show the local influence (in throat region) of the corrosion. Therefore the plot should be used to understand the extent of nonlinearity alone. The difference between the two situation is observed predominantly near the throat section in the furnace, see Figure 2.11 in subsection 2.3.6.

The local influence of the back-flow is also observed in the 1st dominant spatial basis obtained for the velocity variables, and it is shown in Figure 5.2. The spatial basis functions for velocity were obtained by spectral decomposition of the snapshot matrix consisting of x (varying between 0 to 40 [m]) and y (varying between 0 to 1[m]) directional component of velocity. Due to the small width, the basis functions for the velocity component in z-direction is not plotted in the figure, rather in z-direction, the magnitude of the velocity in corresponding grid location is plotted. The first spatial basis represents the most dominant spatial pattern in a process. From Figure 5.2 it is visually observable that around $x = 29\,[m]$ the two plots on either side differs. This region is the throat region. This observation confirms that the orthonormal basis functions obtained by the spectral decomposition is able to depict the effect of strong bifurcations exhibited by a process. Moreover, it also implies that the basis functions obtained after spectral decomposition become obsolete for parameter sensitive processes like glass furnace. That is, the spatial basis functions obtained for the simulation data corresponding to the throat height h_1 will not be able to represent the behavior corresponding to h_2. This necessitates use of the methodology of separation of state space at bifurcation point into two parts.

As in reality one can measure the *temperatures* reliably at a few sensor locations placed at the bottom of the furnace, the performance of the identified reduced order model is compared with the full order CFD model at the selected sensor locations. Identification of the reduced models for the velocity variable is not presented in this chapter. Following are the sensor locations where the performance of the reduced order models are compared. The sensor locations can be viewed in the Figure 2.2.

$S6$ at $x = 25\,m$, i.e. $3m$ left of the throat entrance

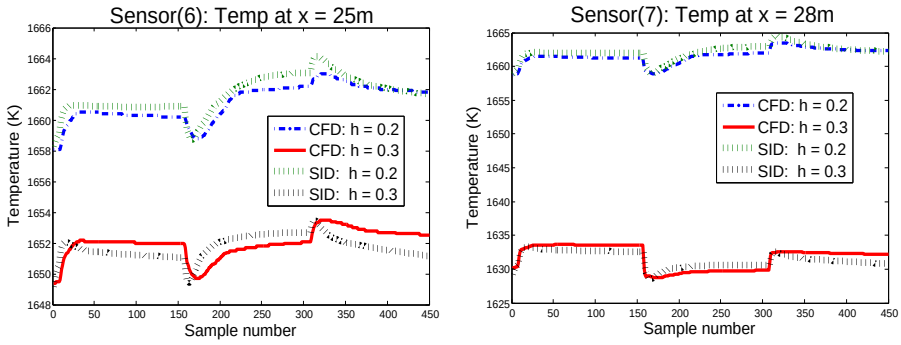

(a) (b)

Figure 5.3: (a) Temperature at S6. (b) Temperature at S7

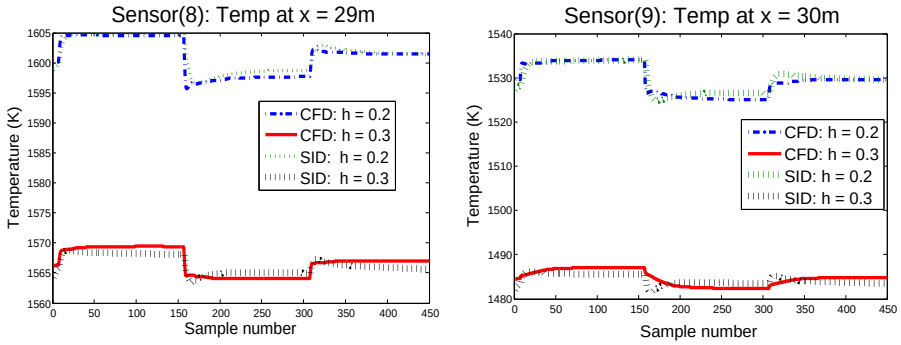

(a) (b)

Figure 5.4: (a) Temperature at S8. (b) Temperature at S9

$S7$ at $x = 28\,m$, i.e. at the throat entrance
$S8$ at $x = 29\,m$, i.e. at the middle of the throat
$S9$ at $x = 30\,m$, i.e. right end of the throat
Figure 5.3 compares the performance of the CFD and the identified reduced model at ($S6$) & at ($S7$), while Figure 5.4 shows the same at sensor ($S8$) & at ($S9$).

Both the identified low dimensional models show a good approximation of the true process (CFD models). They capture the process dynamics reasonably well. Due to the distributed nature of the process we see different

performance quality of the identified models at each sensor locations. At $S6$ the identified model is faster than the real process. The poor performance of the identified models at $S6$ is partly attributed to the spatial location of $S6$ which is strongly influenced by the hot molten glass coming from the upper side of the finning region and the cold glass from the throat region. This makes it difficult to approximate the process behavior at $S6$ using the linear reduced order models.

The detection mechanism that is presented in the methodology part relies on the output residue between the full order and the low order models at any time instant. This implies that it suffices to show that at any time instant, either of the low order models (corresponding to h_1 or h_2) should approximate the full order model. That is, at any time instant it should be possible to fulfill the residual criterion mentioned in (5.14). As the plots in Figure 5.3 and 5.4 satisfy this requirement, it is clear that the detection mechanism based on the computationally efficient low dimensional models can be used to detect the occurrence of the bifurcations (process operation regime) in the flow pattern observed in 2D glass furnace.

5.4 Conclusions

We conclude this chapter with the remark that for a slow parameter variation, it is possible to use the hybrid type of detection mechanism to detect the bifurcations. The detection mechanism employs the low dimensional models obtained using the method of spectral decomposition of process solutions and subsequent identification of a linear map as an approximation of the dynamic evolution of the associated modal coefficients. The proposed framework serves two purposes. First, it explains the methodology to infer lower dimensional process models using the combinations of the spectral decompositions and the subspace identification techniques. The resultant reduced order models are significantly faster in computation than the full order CFD models. Second, by using the hybrid detection mechanism it is possible to detect the process operation regime (before or after the bifurcation point) as result of the uncertain value of bifurcating parameter (throat height). The proposed framework is tried on a benchmark example of large scale industrial application, i.e. a glass manufacturing process. The bifurcations of flow patterns in 2D glass furnace model is detected using the detection mechanism. The results show that it is possible to approximate

the behavior of a large scale process exhibiting extreme parameter sensitivity by using computationally efficient reduced order modeling framework.

The bifurcation in flow patterns in glass furnace as shown in this chapter is function of spatial position. Therefore, the time instance of the occurrence of back-flow is different at different locations in the throat region. This has motivated to consider the corrosion occurring in glass furnace as a continuous phenomena and propose a reduced order modeling framework which will be valid over the complete domain of variations of uncertain parameter. This is achieved by using a framework of Reduced Order - Linear Parameter Varying (RO-LPV) model. This RO-LPV modeling framework is explained in greater details in chapter 6.

6

Identification of Low Order Linear Parameter Varying Models

In this chapter a novel procedure for obtaining low dimensional models of large scale, non-linear fluid flow systems is proposed. The approach is based on the combination of methods of spectral decomposition, black box system identification techniques and nonlinear spline based blending of the local black box models to create a reduced order linear parameter varying model. The proposed method is of empirical nature and gives computationally very efficient low order process models for large scale processes which are modeled by computational fluid dynamic tools. The method proposed here do not need the access to the governing model equations and rely alone on the state information of the full order model. The data dependence of the proposed method make it applicable for other processes. The efficiency of the proposed approach is illustrated on a benchmark problem of an industrial glass manufacturing process where the process non-linearity and non-linearity arising due to the corrosion of refractory materials is approximated using a linear parameter varying model. The results show good performance of the proposed method.
The results presented here are based on the conference paper Wattamwar et al. (2009a) and the journal paper Wattamwar et al. (2009c).

6.1 Introduction

It is explained in Chapter 5 that the singular value decomposition of the solutions of the full order model equations along with the tools from the area of system identification can be used to identify computationally efficient reduced order LTI models. Although the model reduction technique proposed there is able to approximate the linear dynamics, the method is not suitable to approximate the nonlinear behavior that is inherent to many processes. Here, nonlinear behavior is referred to any continuous mapping from the plant inputs to the plant outputs which cannot be expressed by a linear relation. For many chemical processes, it is possible to approximate their dynamic behavior by a linear model in a certain operation window. For such processes, it is also possible to approximate the dynamics of full order model by a reduced order LTI model. Nevertheless, for chemical processes it is also common to see the nonlinear behavior. Nonlinear process behavior can be an outcome of changes in working/operating point or due to the changes in the scheduling variables of a plant. For such processes it is not sufficient to approximate the process dynamics by a linear model and one need a richer model structure. In context of model order reduction, it is worth investigating a nonlinear model reduction technique based on similar ideas that are presented in chapter 5. Such a nonlinear reduced order modeling technique should be able to approximate the nonlinear behavior of the process and should inherit the advantages of the LTI model reduction technique presented in Chapter 5.

To meet the above mentioned requirement by a model reduction technique, in this chapter we present a novel reduced order modeling technique which is able to approximate the nonlinear behavior of a plant. The first part of the technique proposed here is similar to the one explained in Chapter 5 and it results into reduced order LTI models. Therefore, the model reduction method proposed in this chapter also inherit all the benefits of the model reduction technique presented in Chapter 5, e.g. ease of application, simple model structure, possibility of inferring reduced order models in absence of the model equations, applicability of the theory developed for liner system, etc. The contribution of this chapter is to modify the same technique to approximate the process nonlinearity. This is done by proposing a Linear Parameter Varying (LPV) framework that blends different reduced order LTI models corresponding to various process working points into one Reduced Order Linear Parameter Varying (RO-LPV) model. The blending of local

models is performed using weighted splines. The details of this method are explained in subsequent sections. The simplicity of the proposed approach makes it easy to interpret, easy to implement and applicable to very large scale processes in absence of access to the governing equations. The overall problem of identifying a nonlinear model is formulated in terms of parameter estimation in Ordinary Least Square (OLS) sense. The technique proposed here needs information of states of full order model and its inputs.

There are many possible ways to identify LPV models but due to the involved complexity and processing of large amount of simulation data associated with large scale process models, very few LPV identification techniques can really be used effectively. Although the RO-LPV model structure is convex combination of multiple local models, the nonlinear spline that are used for blending the local models make the overall RO-LPV model structure non-convex.

The effectiveness of the proposed model reduction framework is validated on glass manufacturing benchmark example explained in section 2.3.6. Two different types of nonlinear effects are approximated by using RO-LPV framework. First, the problem of corrosion or wearing of throat wall of glass furnace that is explained in Chapter 5 is revisited. Here, the complete domain of parameter (throat height in glass furnace) variation is considered. It is also shown here that such phenomena of corrosion is a type of nonlinear effect. The proposed RO-LPV structure covers larger domain of process operation and is richer in model structure than the hybrid model structure that is presented in chapter 5. Along with the nonlinearity arising due to the wearing of furnace wall, the inherent process nonlinearity arising from changes in the operating point (production rate) is considered as another example of nonlinear behavior. The chapter is organized as follows.

Some of the mathematical tools that are used here are explained in chapter 3. In section 6.2, a generic LPV model identification method is proposed. To solve the above mentioned problem of model order reduction for nonlinear processes under parametric variation, a framework employing POD, local identified (reduced) models and their blending by using two different types of splines is explained in section 6.3. This proposed RO-LPV modeling framework is the main contribution of this chapter. Results of the proposed method on the benchmark example of glass furnace are presented in the section 6.4, which is followed by conclusions in 6.5 that can be drawn form this chapter.

6.2 Linear Parameter Varying (LPV) models

For many processes in chemical process industry, it is necessary to operate at various working points (scheduling variable). Such processes often show smooth, non-chaotic and non-linear behavior as a function of certain scheduling parameters. Often an approximation in the form of Linear Parameter Varying (LPV) systems is sufficient to describe such systems, where the system canonical variables are modeled as nonlinear functions of the scheduling parameters. It is desired that the identified LPV model is able to represent the non-linear process behavior at and during the transition between the operating regimes. A recent overview of LPV modeling techniques is given in Casella and Lovera (2008).

Two common approaches are often used to model LPV systems. The first approach is of a *global* nature, which treats scheduling parameters similar to an input or to a disturbance, i.e. as a continuous function of time that needs to satisfy conditions of persistency of excitation, e.g. see Verdult and Verhagen (2005), Wingerden and Verhagen (2008) for LPV modeling using subspace state space identification technique. The second approach is of a *local* nature and relies on interpolation/convex combination of system invariance properties like poles of a system, Hankel Singular Values (see Lovera and Mercere (2008)) or canonical coefficients. In the second approach towards LPV modeling, it is always assumed that the given system is a convex polytope whose vertices correspond to the local linear model obtained for a constant value of the scheduling variable. The second approach is similar to the local Jacobian linearization. The models identified by the local approach are interpolated to depict the continuous dependence on the scheduling parameter. It is necessary in the second approach that the order of the local identified model is the same. In practice, it is difficult to satisfy this condition of having the same order of identified models for varying values of scheduling parameter. This problem also arises during the identification of reduced order (RO)LPV models as proposed in this chapter, where the optimal number of POD modal coefficients and therefore the order of subspace identified models could be different. The method proposed here allows different order of the local LTI models to blend into one LPV model. Recently LPV modeling techniques using orthonormal basis functions is explained in Tóth (2008).

Another variant of merging the local models is superposition of the local identified models. This is based on a weighted combination of outputs and

leads to the concatenation of the local state space models. As a result, the state space of the LPV model will be a combination of the state space of the local models. Various methods like e.g. Gain scheduling (see Rugh and Shamma (2000)) and spline based interpolation are among the typical forms of such LPV identification. A recent paper (see Zhu and Xu (2008)) discusses the practical aspects of LPV identification methods. It is shown there that for a smooth and non-chaotic non-linear process, a LPV approximation can be useful from control point of view. The method of LPV model identification is described in detail in the following paragraphs.

Throughout, we take the variable h as a scheduling parameter, and assume $h \in \Theta \subset \mathbb{R}^+$. Further, let $\mathcal{H} \subset \Theta$ be a finite set $\mathcal{H} = \{h_j\}$ for $j = 1, \ldots, M$ with $M > 0$, discrete values. Subscript h and h_j shows the implicit parameter dependence while explicit dependence on the parameter is shown in brackets as (h) or (h_j). As this method is based on matching input-output behavior, for the purpose of illustration we present it in the form of transfer functions.

For a given set of local linear time-invariant (LTI) parameterized models $G_{h_j}(q), j = 1, \ldots, M$, the j^{th} input-output relation can be represented as:

$$y_{h_j}(k) = G_{h_j}(q)u(k) := \sum_{l=0}^{\infty} G_{l,h_j} u(k-l) \quad \text{for } j = 1, \ldots, M. \tag{6.1}$$

Here $G_{h_j}(s) \in \mathcal{R}^{n_y \times n_u}(s)$, $G_{l,h_j} \in \mathcal{R}^{n_y \times n_u}$, n_u and n_y are number of inputs and outputs respectively, M is the number of local LTI models which on weighted blending gives LPV model. In other words, if we interpret M models as M vertices of a polytope in which the original nonlinear system dynamics evolve, then the LPV model describes the original nonlinear system behavior in the polytopic region defined by the convex combination of the identified local LTI models as follows:

$$y_{lpv,h}(k) = \sum_{j=1}^{M} \alpha^j(h) y_{h_j}(k), \quad \text{or equivalently} \tag{6.2}$$

$$y_{lpv,h}(k) = \sum_{j=1}^{M} \alpha^j(h) G_{h_j}(q)u(k), \quad \text{or equivalently,} \tag{6.3}$$

$$G_{lpv,h}(s) = \sum_{j=1}^{M} \alpha^j(h) G_{h_j}(s) \quad \forall\, h \subset \Theta. \tag{6.4}$$

Equation (6.4) also defines $G_{lpv,h(t)}(s)$, as long as $h(t) \in \Theta$.
Here α^j are the weights such that $\alpha^j : \Theta \to \mathbb{R}$, which are used for the convex combination of the local LTI models which need to be determined. Interesting results about LPV modeling using various types of nonlinear orthogonal splines are presented in (Zhu and Xu (2008)) and references therein.

By convex combination we mean,

$$\sum_{j=1}^{M} \alpha^j(h) = 1 \quad \text{and} \quad \alpha^j(h) \geq 0, \forall h \in \Theta \tag{6.5}$$

A general spline structure can now be presented as

$$\alpha^j(h) = \sum_{i=1}^{k_n} \theta_i^j \varphi_i^j(h) \tag{6.6}$$

where $\theta_i^j \in \mathcal{R}$ are the spline coefficients and $\varphi_i^j(h)$ are the basis functions, and $h \in \Theta \subset \mathbb{R}^+$ is the scheduling parameter. The scheduling parameter can be a working point/operating point of the process. In-stead of spline in (6.3), other type of scheduling function, for instance, radial basis function as used in Verdult (2002) or membership functions from fuzzy modeling as explained in Babuska (1998) can be used.

In this chapter we present two types of splines viz. cubic and trigonometric. They have different properties. The cubic spline is of the form,

$$\alpha^j(h) = \beta_1^j + \beta_2^j h + \sum_{i=2}^{k_n} \beta_{i+1}^j |h - b_i|^3. \tag{6.7}$$

$b_i \in \mathbb{R}^{k_n}$ are spline knots which are distributed in k_n different (disjoint) elements, over an interval $[h_{min}, h_{max}]$ such that $h_{min} \in \Theta$ and $h_{max} \in \Theta$, and $h_{min} < h_{max}$.
β_i^j are the spline coefficients corresponding to each knot.
Here we define unknown spline coefficients as a parameter vector as,

$$\theta^j = \text{col}(\beta_1^j, \ldots, \beta_{k_n}^j) = \text{col}(\theta_i^j, \ldots, \theta_{k_n}^j). \tag{6.8}$$

Note that there can be various possible spline structures other than the cubic spline as shown in equation (6.7). The knots distribution can be of various

types as well. The simplest knot distribution is an equidistant covering the whole domain of scheduling parameters, as in eq. (6.7). However the spline in eq. (6.7) does not guarantee the following condition of consistency:

Definition 6.2.1 Given $\mathcal{H} = \{h_1, \ldots, h_M\} \subset \Theta \subset \mathcal{R}^+$, and models G_{h_j}; for $j = 1, \ldots, M$. Then the LPV model $G_{lpv,h}$ defined in (6.4) is consistent with the set $\{G_{h_j}\}_{j=1,\ldots,M}$ if $G_{lpv,h_j} = G_{h_j}$ for all $j = 1, \ldots, M$.

Observe, in view of (6.6), consistency of LPV model with respect to the local models is obtained if and only if

$$\alpha^j(h_i) = \begin{cases} 1, & \text{if } i = j \\ 0, & \text{if } i \neq j \end{cases} \tag{6.9}$$

Desired condition in eq. (6.9) means when $h = h_j$, then blended LPV model has 100% contribution from j^{th} model and no contribution from other models. This property is desirable as it gives an idea about the performance quality of LPV model. In this chapter we propose another spline structure which guarantee the condition in (6.9), i.e. $\alpha^j(h_i) = 0$

$$\alpha^j(h) = \beta^j \, cos(h - h_j) \prod_{i=1}^{M} (h - h_i) \tag{6.10}$$

The spline structure in eq.(6.10) preserves the second condition in (6.9) alone, whereas the condition $\alpha^j(h_i) = 1$ is not guaranteed in this spline either. But this second spline is easier to adopt and to interpret.
If all the necessary info to identify a LPV model viz. y_{plant}, y_{h_j}, h_j, $G_{h_j}(q)$ and $u(k)$ is available then the problem of LPV identification can be transformed into a problem of estimation of spline coefficients β_i^j, see eq. (6.8). The quality of an identified LPV model will then be decided by the accuracy of estimation of spline parameters, θ_i^j. For this purpose we define the output error of the LPV model as follows:

$$e_h(k) = y_{plant}(k) - y_{lpv,h}(k) = y_{plant}(k) - \sum_{j=1}^{M} \alpha^j(h) y_h^j(k), \tag{6.11}$$

or equivalently,

$$e_h(k) = \; y_{plant}(k) - \sum_{j=1}^{M} \sum_{i=1}^{k_n} [\varphi_i^j(h) \, y_h^j(k)] \, \theta_i^j. \tag{6.12}$$

It is desired to minimize the error in (6.12) by formulating an optimization problem as

$$\hat{\theta} := \arg\min_{\theta} \sum_{k=1}^{K} ||e_h(k)||_2^2 \tag{6.13}$$

As the error model (6.12) is linear in the spline parameters θ_i^j, we can attain a solution of the optimization problem (6.13) in least square sense as:

$$\hat{\theta} = [\Phi^T \Phi]^{-1} \Phi^T Y \tag{6.14}$$

where, $Y = \mathrm{col}\,(y(1), \ldots, y(N))$ and

$$\Phi = \begin{bmatrix} \varphi_1^1(h)\, y(1) & \cdots & \varphi_i^1(h)\, y(1) & \cdots & \varphi_i^j(h)\, y(1) \\ \vdots & & & & \vdots \\ \varphi_1^1(h)\, y(K) & \cdots & \varphi_i^1(h)\, y(K) & \cdots & \varphi_i^j(h)\, y(K) \end{bmatrix} \tag{6.15}$$

$\hat{\theta}$ is the estimated value of θ. From (6.15) it is clear that the splines are dependent on the process data. This suggests that it is necessary to have plant data sufficiently rich to capture the plant dynamics corresponding to the complete space in which parameters vary. This can be achieved only when the plant data contains the information of transition from one working point to another, i.e.there should be an excitation signal during the transition as well.

There are some technical aspects, e.g it is assumed that identified models are stable and inputs are persistently exciting. As RO-LPV model is linear combination of local ROM, stability of local identified ROM ensures stability of RO-LPV model. The second condition of persistency of excitation ensures that the rank of the matrix Φ is equal to the dimension of the vector θ. This guarantees that $\Phi^T\Phi$ is not rank deficient. Moreover if the outputs of each local model that is used for blending is not sufficiently different then at least the knot distribution in splines should be different in order to guarantee that $\Phi^T\Phi$ has full rank.

Eq. (6.3) of LPV model can be written in usual state space form as in eq. (6.16). The spline weight can be included either in the matrix B or

in C but not in both.

$$\begin{aligned} x_{lpv}(k+1) &= A_{lpv}\ x_{lpv}(k) + B_{lpv}\ u(k) \\ y_{lpv,h}(k) &= C_{lpv,h}\ x_{lpv}(k) \end{aligned} \tag{6.16}$$

Where,

$$A_{lpv} = \begin{bmatrix} A^1 & & & \\ & A^2 & & \\ & & . & \\ & & & A^M \end{bmatrix},\ B_{lpv} = \begin{bmatrix} B^1 \\ B^2 \\ . \\ B^M \end{bmatrix}$$

$$C_{lpv,h} = [\alpha^1(h)C^1\ \alpha^2(h)C^2, \ldots, \alpha^M(h)C^M] \text{ and } x_{lpv} = \text{col}\left(x^1\ x^2\ \ldots x^M\right)^T \tag{6.17}$$

6.3 Reduced order LPV modeling framework

For the methodology presented in this section we assume that the knowledge of the scheduling parameter is available. The overall strategy is presented at the end of this section as an algorithm. The problem can be formulated as follows:

For a given parameterized process Σ with parameter $h \in \Theta \subset \mathbb{R}^+$, such that

$$\Sigma : T_h(z, k+1) = f\left(T_h(z,k), u(k), h\right), \tag{6.18}$$

identify, for a varying parameter $h(k)$ and input u a reduced order (RO) LPV model $\hat{\Sigma}$ of the form (3.1), such that the norm of the error between the solution of the original full order (CFD) model and the reduced identified model given by,

$$\min \sum_{k=0}^{K} ||T_h(z,k) - \hat{T}_h(z,k)||_2^2 \tag{6.19}$$

is minimal when ranging over all values of $h \in \Theta$. Here,
k : is time instance, z : is spatial position, h : is the value of the scheduling parameter,
$T_h(z,k)$: is temperature, which is a solution at time k and position z of the real process i.e. CFD model (Σ),
$\hat{T}_h(z,k)$: is temperature, which is a solution at time k and position z of the LPV model in reduced space ($\hat{\Sigma}$).

The error minimization criterion of (6.19) means that we are interested in finding an approximate model such that under parameter variations $h(k)$, the solution of the RO-LPV model approximately matches the large scale process model. For a very slow parameter variation, there are many possible ways to formulate the LPV problem, e.g. see Casella and Lovera (2008).

In this section we present a method to obtain a solution to the problem in equation (6.19) by using POD (see, 3.2.2) to infer a reduced dimensional space, system identification technique (see, 3.1.1) to approximate the temporal evolution (POD modal coefficients) and framework to blend local RO-LTI models into an RO-LPV model as described in section 6.2. The complete methodology is explained below in further detail.

For the input sequence $\{u(k)\}_{k=1}^{K}$, the full order (CFD) simulation model is excited. The snapshots of the solution, e.g. temperature snapshots $T_{snap} \in \mathbb{R}^{n \times K}$ are collected. From this snapshot sequence an optimal POD basis ϕ_i and corresponding modal coefficients a_i for $i = 1, \ldots, r$, with r as order of reduced model, are determined by setting $R = T_{snap} {T_{snap}}^T$, in eq. (3.42).

The length of the snapshot matrix i.e. number of snapshots K, is decided based on the settling time of the process, which is residence time in the case of glass manufacturing. The duration of the experiment should be planned so that it should be larger than the settling time of the process.

After computing the POD basis vectors ϕ_i, which represent the spatial patterns, and modal coefficients $a_i(k)$, which characterize the temporal evolution, on the basis of data $(u(k), a_i(k))$, $i = 1, \ldots, r$ we proceed to the system identification by applying the subspace state space identification algorithms. By doing so, state space matrices A,B,C,D are identified as a map between the process inputs u and dominant POD modal coefficients $a(k) = \mathrm{col}\,(a_1(k), \ldots\ a_r(k))$ corresponding to the dominant spatial patterns $\varphi_1, \ldots, \varphi_r$, see e.g. Huisman (2005). While identifying a black-box reduced order LTI models we are treating the dominant POD modal coefficients as if they are the outputs of certain unknown system. We reconstruct the states of the full order model by projecting back the identified model on the space spanned by dominant POD basis functions $[\varphi_i]_{i=1}^{r}$. In this way a local RO-LTI model is obtained for each constant value of the scheduling parameter, h_j for $j = 1, \ldots, n_e$, with $h_{min} \leq h_1 < h2 < \ldots < h_{ne} \leq h_{max}$ and n_e is the number of experiments or dynamic simulation run of full order CFD model. Now we proceed to construct a RO-LPV model.

Out of these n_e local reduced models also referred to as SID models, M models were chosen to construct the LPV model ($M \leq n_e$), see section 6.2. The M values of parameter h_j should be chosen such that the process shows non-linear behavior as result of transition from one value of scheduling variable to the other. The data set corresponding to $n_e - M$ experiments is considered as transition data between M values of scheduling variable. Note that this approach is similar to the gain scheduling i.e. there are few working points (n_e). More about gain scheduling can be found in Rugh and Shamma (2000). This approach is different than the approach used by Verdult and Verhagen (2005).

As the full scale model is not able to change the physical boundary dynamically, to emulate corrosion, the model proposed here uses RO-LTI models corresponding to discrete values of h_j to identify RO-LPV model, whereas the data corresponding to $h_j,\ j \neq M$ is used as data corresponding to transition from one working point to another. Nevertheless, the method is generic any can be used for identification of RO-LPV model of any process.

In subsequent subsections design of excitation inputs and overall method is explained as an algorithm.

6.3.1 Input design

The input signal that is used for the excitation during the identification step decides the dynamics that are excited and these dynamics are reflected in snapshot matrix which subsequently determines the POD basis. Therefore while designing the input signal for large scale dynamical systems from model reduction perspective, care must be taken. There are different ways that are used in the actual practise to design the input signal. But the overall goal is to excite both - fast and slow dynamics. For this reason we have used two types of input signals. First type is multi-step input signal in positive and negative direction (increase and decrease), and it is further imposed by PRBS (Pseudo Random Binary Signal). PRBS with fast switching excites the dynamics corresponding to high frequencies while different step amplitude excites the non-linearities and slow dynamics. The second input type, that is presented here, is the PRBS at one nominal value of the input. The average switching time of such an input is equal to the average time constant of the distributed system. The minimum switching time of such an input is usually equal to $1/5^{th}$ of the minimum time constant of the process.

In section 6.4, the input signals are discussed in more detail. The overall methodology can be explained in four steps algorithm in subsequent paragraphs. Step 1 to 3 are repeated M times, which corresponds to the number of discrete values taken by the scheduling parameter. Step 4 which involves blending of the local reduced models is performed once only.

6.3.2 Algorithmic procedure

The first three steps of the algorithmic procedure that is explained here are similar to the procedure explained in Chapter 5 and they result into identification of reduced order LTI models. The step is different and it is directed towards inferring a RO-LPV model.

Step 1: Data collection

Collect the data $T(z, k, h_j)$ and store it into a snapshot matrix T^j_{snap} from the measurements or from the simulation of full order model for a given value of scheduling parameter h, such that, $z \in \mathcal{Z} \subset \mathbb{R}^d$: spatial coordinate, $k = 1, \ldots, K$, time instant, $h_j \in \mathcal{H} = \{h_1, \ldots, h_M\}$: scheduling parameter. The process is repeated for M discrete values of h_j i.e., $j = 1, \ldots, M$. Use the data corresponding to the experiments h_i for $i = 1, \ldots, n_e$ $i \neq j$, and $j = 1, \ldots, M$ as the transition data during the identification of spline parameters.

$$T^j_{snap} = \begin{bmatrix} T(z_1, k_1, h_j) \ldots T(z_1, k_K, h_j) \\ . \qquad\qquad . \\ . \qquad\qquad . \\ T(z_n, k_1, h_j) \ldots T(z_n, k_K, h_j) \end{bmatrix} \in \mathbb{R}^{n \times K}, \text{ for } j = 1, \ldots, M.$$

Step 2: Spectral decomposition

Spectral decomposition of the snapshot matrix obtained in step 1 or the eigenvalue decomposition of the covariance matrix $R = T^j_{snap} {T^j_{snap}}^T$, as explained in section 3.2.2 gives spatial and temporal patterns arranged in order of importance. Readers can refer to section 3.2.2 for more details of spectral

decomposition. Thus,

$$T^j_{h_j}(z;k) = \sum_{i=1}^{n} a_{i,h_j}\, \phi_{i,h_j}(z)$$

$$\text{with, } a_{i,h_j}(\text{k}) := \left\langle T^j_{h_j}(z,k), \phi_{i,h_j}(z) \right\rangle,\ z \in \mathcal{Z},\ h_j \in \mathcal{H},\ j = 1,\ldots,M$$

Here, $a_{i,h_j}(k)$ are the modal coefficients and $\phi_{i,h_j}(z)$ are the spatial basis. Both, the modal coefficients and the spatial basis are parameter dependent. Out of n patterns, only first r patterns corresponding to the maximum energy are used to infer the reduced order model. This step is repeated M times.

Step 3: Identification of local RO-LTI models

Third step involves identification of a model between system inputs and first r modal coefficients obtained in step 2, i.e. $u \rightarrow \text{col}(a_{1,h_j},\ldots,a_{r,h_j})$; $j = 1,\ldots,M$. By using the subspace state space algorithms explained in the section 3.1.1, we get linear reduced order model for a specific value h_j of scheduling parameter. Although the model is obtained from the data which is dependent on the scheduling parameter; the model structure does not have an explicit scheduling parameter dependent term. The model structure as result of identification is of the following form.

$$\begin{aligned} \hat{x}_{h_j}(k+1) &= A_{h_j}\ \hat{x}_{h_j}(k) + B_{h_j}\ u(k) \\ \hat{a}_{h_j}(k) &= C_{h_j}\ \hat{x}_{h_j}(k) \end{aligned} \tag{6.20}$$

Here, $A_{h_j}, B_{h_j}, C_{h_j}$ are the state space matrices corresponding to a specific value of parameter $h_j \in \mathcal{H}$ and $\hat{x}_{h_j}(k)$ are the states of identified reduced order local model.

The identified modal coefficients $\hat{a}_{h_j}$, after an outer product with spatial bases $\phi_{i,h_j}(z)$ gives the reconstructed states $\hat{T}^j_{z,h_j}(k) \in \mathbb{R}^n$ of full order model.

$$\hat{T}^j_{z,h_j}(k) = \sum_{i=1}^{r} \hat{a}_{i,h_j}(k)\, \phi^T_{i,h_j}(z) \quad ; j = 1,\ldots,M. \tag{6.21}$$

The LPV modeling framework is based on weighted blend of outputs $\hat{y}_{h_j}$,

$$\begin{aligned} \hat{y}_{h_j}(k) &= C_T\, \hat{T}_{h_j}(z,k) \quad \text{or} \\ \hat{y}_{h_j}(k) &= G_{h_j}(q)\, u(k) \end{aligned} \tag{6.22}$$

Step 4: Identification of RO-LPV model

As mentioned in the section 6.2, the RO-LPV model is the weighted blend of M local ROM. The weights are in the form of splines whose coefficients are obtained from minimization of the output error between the plant (full order model) and RO-LPV model. The output of RO-LPV model can be represented as

$$\hat{y}_{lpv,h} = \sum_{j=1}^{M} \alpha^j(h)\, \hat{y}_{h_j}(k) \quad \text{i.e} \tag{6.23}$$

$$\hat{y}_{lpv,h} = \sum_{j=1}^{M} \alpha^j(h)\, [G_{h_j}(q)\, u(k)] \tag{6.24}$$

where, $G_{h_j}(q)$ is the local reduced order identified model in transfer function form and $\alpha^j(h)$ are the spline weights. As mentioned in last step and from (6.22), it is clear that to get a RO-LPV model as a blend of local models in state space form, spline weights must be introduced in state space matrix $C_{lpv,h}$ and not in B_{lpv} of equation (6.17).

6.4 Discussion of simulation results: 2D Glass furnace

A $2D$ benchmark CFD model to illustrate the method of the previous section, for a glass manufacturing process is considered as a replacement of the real Industrial Glass Manufacturing Process. More details of the process can be found in section 2.3.6. The proposed RO-LPV approach is used to approximate the non-linear effect as result of changes in nominal throughput (pull-rate) of the process and the non-linear effects arising due to the corrosion of the furnace wall (geometric parameter variation).

6.4.1 Non-linearity due to the corrosion

For the identification of RO-LPV model we use corrosion level as the working point or scheduling variable. By 'corrosion level' we mean the gap at the throat region as shown in the Figure 2.2. The space of interest for this scheduling variable covers the interesting range from no-back flow to back flow of glass from refiner to the melter zone. Due to the difficulty of

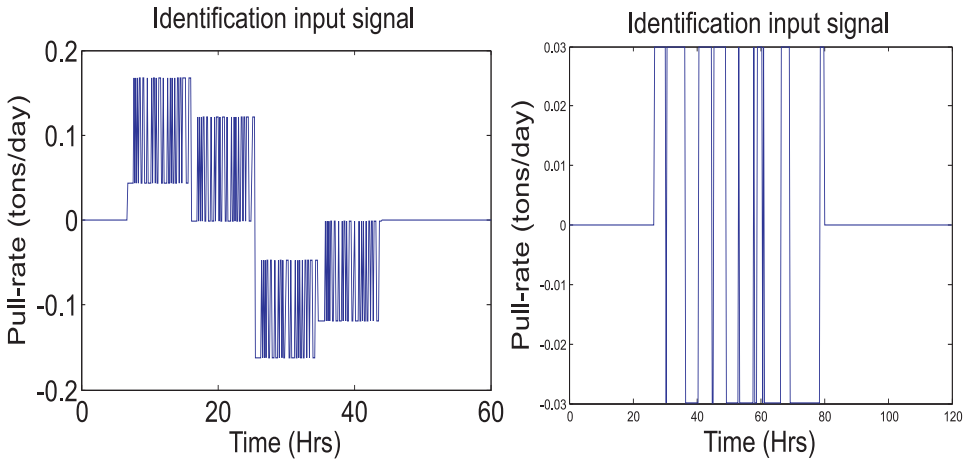

Figure 6.1: Identification Input Signals: Left plot belongs to the corrosion experiments while the right plot belongs to the experiments of excitation of process non-linearity due to the changes in the production-rate.

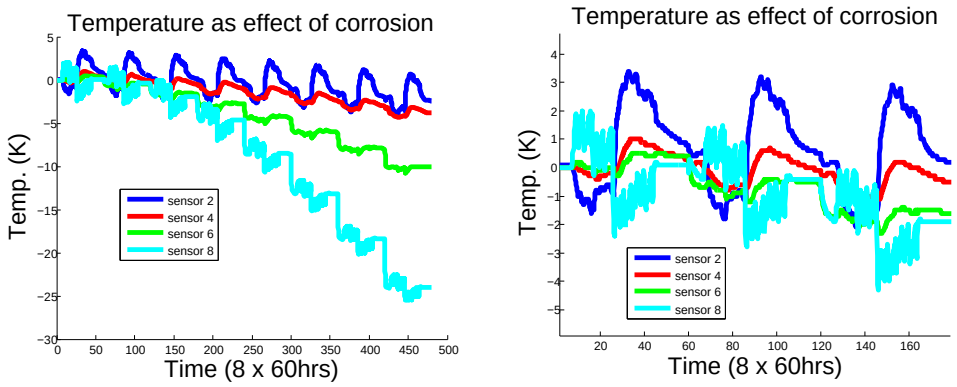

(a) Corrosion

(b) Corrosion, zoomed

Figure 6.2: Effect of corrosion on the temperature in the furnace

---

modeling corrosion as a continuous phenomenon in CFD software, we divide the (corrosion) parameter space into eight discrete elements. For this reason, simulation experiments were performed for eight different throat heights (i.e. $n_e = 8$) of the $2D$ glass furnace model, equally distributed from 0.2 [m] to 0.27 [m], i.e. $h_j \in \mathcal{H} = \{0.20, 0.21, \ldots, 0.27\}$. The first experiment corresponding to the throat gap of $h_1 = 0.20$ $[m]$ was initiated with a steady state solution as an initial condition. The second experiment starts with the

(converged) solution of first experiment as its initial condition. Similarly all subsequent experiments have converged solution of the previous experiment as an initial condition. The data set corresponding to these eight experiments was concatenated to resemble the continuity in the corrosion. The boundary conditions were fixed and they are different for each region of the 2D furnace. The goal of the present work is to present the results of the proposed model reduction techniques, therefore the details about the first principle modeling of the glass is not explained.

Each simulation experiment was aimed at identifying a good local reduced order model (corresponding to constant throat height). The input identification signal chosen was pull-rate/production rate and it is shown in Figure 6.1, left hand side plot. The identification input signal consisted in multiple step in both positive and negative direction and each step was imposed by a high frequency PRBS signal. The steps were supposed to excite the slower dynamics whereas the PRBS signal was supposed to excite the faster dynamics. The full order process model does not contain any explicit disturbances.

The time horizon of each experiment was sixty hours with a sampling interval of eight minutes. The 2D glass furnace shows average residence time of 30-40 hours. Therefore the experiment horizon of 60 hours is sufficient. Care should be taken, as large data might be difficult to handel during the construction of RO-LPV which needs concatenation of the data sets corresponding to all experiments.

The effect of corrosion is shown in Figure 6.2 by concatenating the datasets corresponding to the eight experiments. The figures show change in temperature with respect to the steady state solution of the nominal case ($h = 0.20$ $[m]$) at four sensor locations as shown in Figure 2.2. The Figure on the right hand side is the zoomed version of the figure on the left. The throat region shows the biggest effect of the corrosion. The glass mixes at the hot spot location with the glass coming from the melting zone, and therefore do not influence temperature in the melting zone. During the back-flow, the cold glass from the refining zone mixes with the hot glass in melting zone and it leads to the temperature drop, as seen in the figures. Most of the variables like temperature, pressure, velocity are coupled to each-other. Therefore the temperature changes that result from the back-flow (or corrosion) can have a bigger impact than one can anticipate. At the current status of this research, we have not yet investigated the effect of corrosion on variables other than temperature in the RO-LPV modeling framework.

The data was extracted from the CFD environment and imported in the MATLAB for processing and for carrying out POD, subspace identification, spline parameter identification and finally for LPV model blending. The identified models are very fast in simulation (> 1000 times faster than the CFD simulations). The detailed analysis of the computational performance of the identified model and the original CFD model is not presented here. The lower dimensional models were identified as a map from single input (production/pull rate) and outputs which were the first few (r) POD modal coefficients corresponding to the dominant singular values. The order of each reduced order model was different and usually it was less than ten, i.e. ($r < 10$). The three local models ($M = 3$) corresponding to throat height $h = 0.20\,[m]$, $h = 0.23\,[m]$ and $h = 0.27\,[m]$ were used to construct an LPV model and then the spline parameters corresponding to each local model were identified as mentioned in section 6.2. The identified LPV model was then validated for a throat height $h = 0.22\,[m]$ i.e. corresponding to the situation without back flow and $h = 0.26\,[m]$, the situation with back-flow.

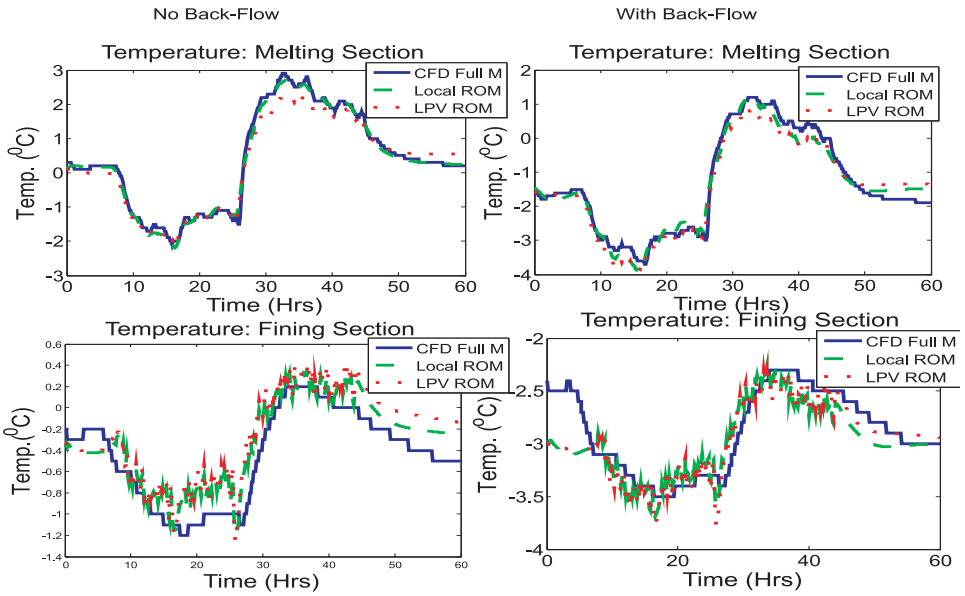

Figure 6.3: LPV approximation 1: Performance of RO-LPV model in reproducing the temperature dynamics under the corrosion effect. Upper plots: Melting zone, Lower plots: Fining zone.Left hand side plots:'No back-flow'(h=0.22m).Right hand side plots: 'With back-flow'(h=0.26m).

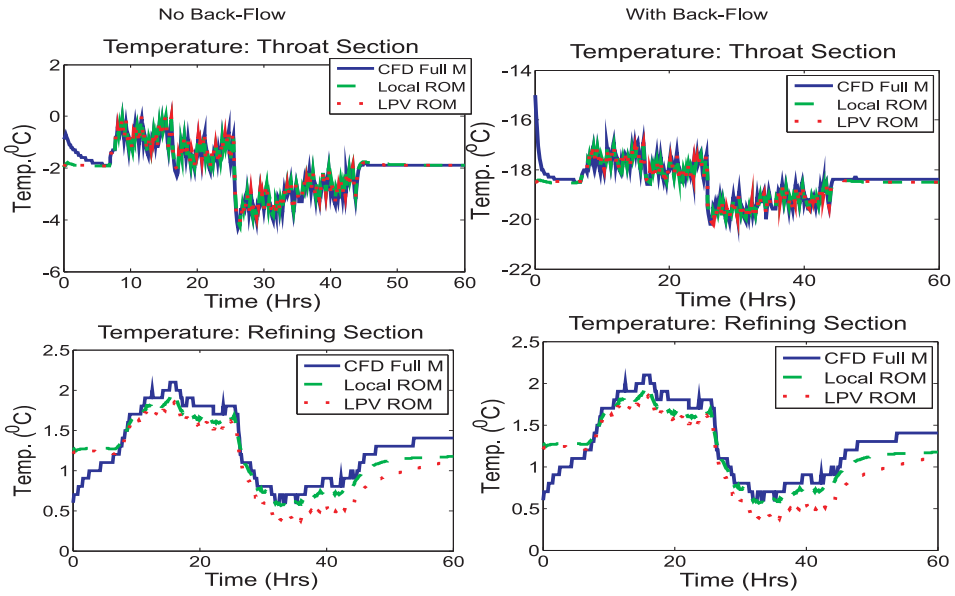

Figure 6.4: LPV approximation 2: Performance of RO-LPV model in reproducing the temperature dynamics under the corrosion effect. Upper plots:Fining zone zone, Lower plots:Refining zone.Left:'No back-flow'(h=0.22m).Right: 'With back-flow' (h =0.26m).

Figure 6.3 shows the validation results for the melting and the fining zones.

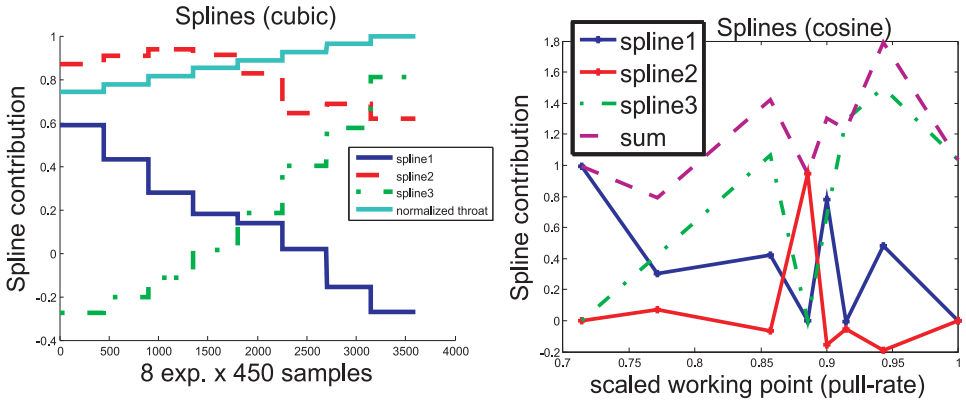

Figure 6.5: Splines: Left: Corrosion experiments, Right: Expe. of pull-rate change

Figure 6.4 results for the throat and for the refining zone are shown for the cases of 'No back-flow' (left side plots) and 'With back-flow'. Plots are shown for the original plant (CFD), local reduced SID models corresponding to the validation throat height and the global RO-LPV model covering complete domain of the scheduling parameter. The local ROM should work better than the RO-LPV model as a local ROM is identified on the basis of a data set corresponding to a specific throat height, where as the the RO-LPV model is of global nature (i.e. approximated over complete domain of corrosion). The performance of the RO-LPV model is very good except for the refining section in the case of 'With back-flow'. See figure 6.4.

The performance of LPV model in the refining section is poor because the back-flow has instantaneous and largest effect in the throat and fining zones, while refining zone shows a delayed effect of the back-flow. The performance of the LPV model can be further improved by using a longer simulation horizon and by removal of the dynamics due to the corrosion in the identification of local SID/reduced model.

The spline in equation which define the contribution of each ROM for the construction of the RO-LPV model is shown in Figure 6.5, left side plot. The plot shows spline weights obtained from the data corresponding to the simulation experiments carried to study corrosion effect. The plot on the right side corresponds to non-linearity due to throughput and it is explained in next section. Continuing the discussion of the plot on the left, the cubic spline were obtained by using the method as explained in the section 6.2, see eq. (6.7). Along with the splines the normalized value of varying parameter (throat gap) corresponding to each experiment is also shown in the plot. For any experiment, the throat gap is fixed. Therefore the plot shows two things - spline as a map, $\alpha : time \rightarrow \mathcal{R}$ and normalized throat gap as a map, $h : time \rightarrow \mathcal{R}^+$. As corrosion is irreversible process, the throat gap is increasing with every experiment. The eight constant values of throat gap corresponding to eight experiments is concatenated to show corrosion as a continuous effect. This means that when the throat gap is smaller (case of no-back flow) the RO-LPV model will be dominated by the first ROM which corresponds to $h = 0.20\,[m]$. For the case when back-flow is mild i.e. upto $h = 0.23\,[m]$ the contribution of the second spline is more, as compared to it's (spline 2) contribution for any other value of h . As expected, the second spline shows a behavior which is an average of the two other splines. With increasing value of the throat gap, i.e. increased intensity of the back-flow we get more contribution of the third ROM (corresponding

to $h = 0.27\,[m]$) in the RO-LPV model. Summarizing the discussion, for increasing corrosion effect (i.e.increasing throat gap), contribution of spline 1 decreases, contribution of spline 2 increases first and then decreases while spline 3 contribution to RO-LPV model keeps on increasing. The cubic splines used here do not impose either of the condition of consistency, as formulated in eq. (6.9). In the next subsection we will discuss the use of trigonometric spline as formulated in eq. (6.10) which partially obeys the condition of consistency.

From this discussion it becomes clear that the proposed model reduction methodology is useful in dealing with large scale complex problems.

6.4.2 Process non-linearity

For most of the chemical processes it is possible to find an operation range of the process inputs such that a linear model can be used to approximate the non-linear process behavior. The accuracy of such a linear model is limited and depends on the operation range of process inputs and disturbances. For the industrial glass manufacturing process it is very difficult to find the process operation range in which linear models are sufficiently accurate. Within the range of 1% of process input variation around the steady state value, the process can be reasonably approximated by using local reduced order linear models. Multiple reduced order models are then obtained for various operating points of the process inputs. As mentioned in section 6.3, local reduced order models are then blended to form RO-LPV model.

The simulation experiments involved the identification of local linear models at eight nominal operating points of pull-rate/production rate, which is considered as working-point/scheduling variable for the construction of RO-LPV model. These eight local models have been blended to construct RO-LPV model. The eight values of the working points were $h_j \in \mathcal{H} = \{2.5, 2.7, 3.0, 3.1, 3.15, 3.2, 3.3, 3.5\}$, in tons/day. The time horizon of each experiment was 120 hours. The identification signal was Pseudo Random Binary Signal (PRBS) with average switching time equal to the 'average time constant' of the process (2D model) which is approximately equal to 4 hours. IGMP is a distributed process and it shows different transient and steady state behavior in each region of the manufacturing furnace. Therefore the average of time constants in each region is considered. The minimum switching time of the input signal was 8 min, which is approximately equal to $1/5^{th}$ of the fastest process time constant. The amplitude of the PRBS

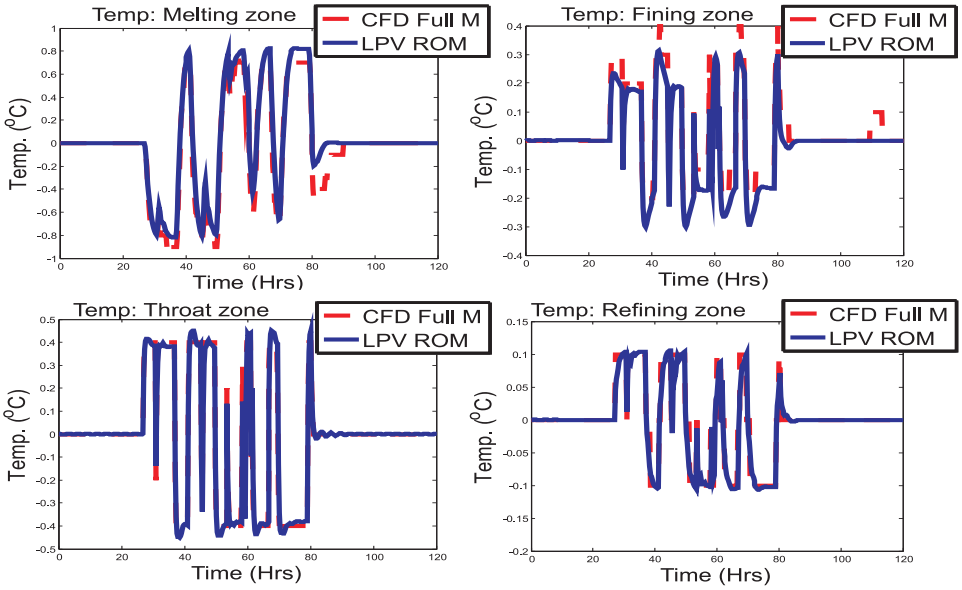

Figure 6.6: Performance of RO-LPV to the identification signal

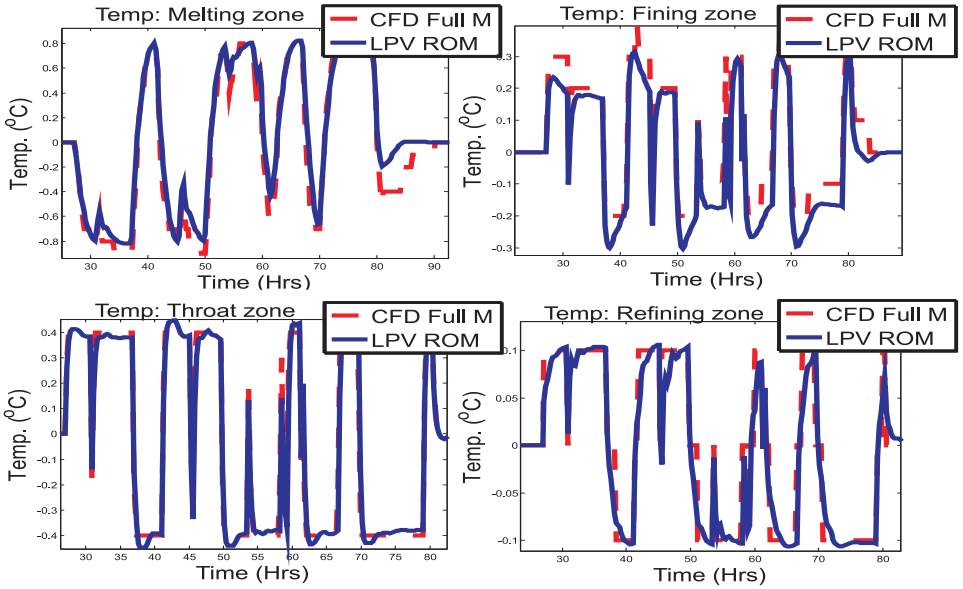

Figure 6.7: Performance of RO-LPV to the identification signal, zoomed

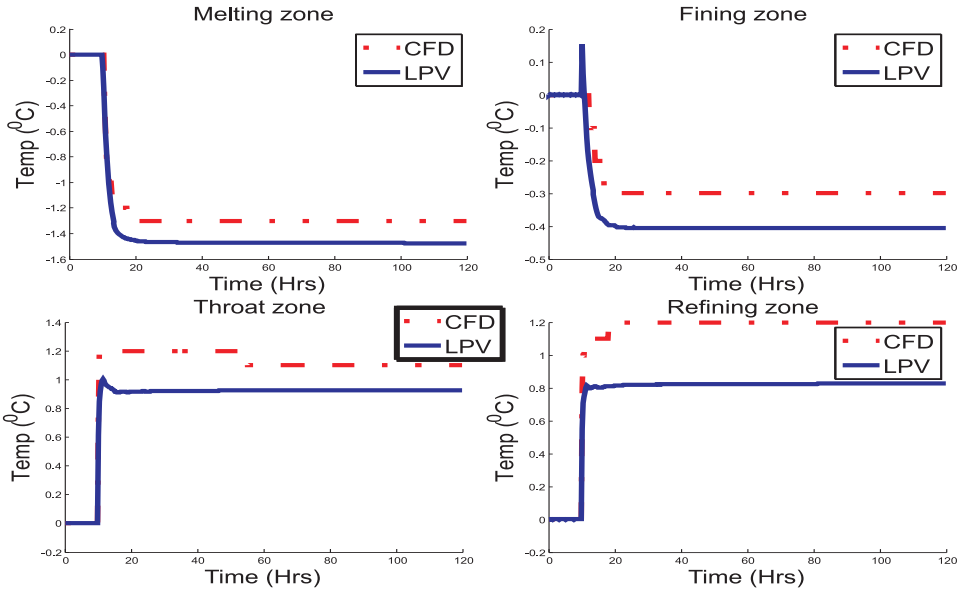

Figure 6.8: Performance of RO-LPV to the validation signal

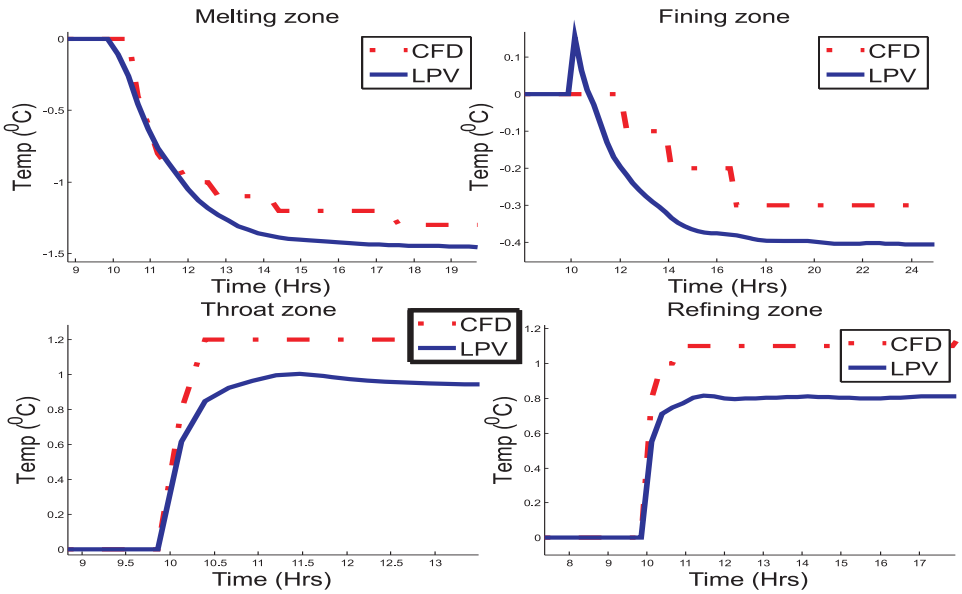

Figure 6.9: Performance of RO-LPV to the validation signal, zoomed

was 1% of the nominal value.

The order of the reduced order model was decided based on the best possible fit to the first five POD modal coefficients. The best fit resulted into different order of the reduced models. The order of all the reduced models was less than 10. As the non-linear effects start emerging in lower modal coefficients, it becomes difficult to fit a linear model to more than five modal coefficients. The three local RO models ($M = 3$) corresponding to pull rate 2.5, 3.0 and 3.5 were used to construct the RO-LPV model. The data corresponding to the other values of pull-rate was used as transition data. Figure 6.6 shows the fit of the RO-LPV model to the full scale CFD model for the identification signal. Figure 6.7 shows the enlarged version of figure 6.6. Output 2 alone is used to construct the RO-LPV model as it shows the largest sensitivity to the process input.

Unlike the last sub-section (6.4.1), the splines used to get RO-LPV model are not cubic, but they are trigonometric (cosine), see eq. (6.10). The optimized spline functions are shown in the right hand side of the Figure 6.5. The plot shows splines as a map, i.e.$\alpha : h \rightarrow \mathcal{R}$, with h as a scaled working point, i.e.pull-rate. Each spline shows the contribution (weight) of the corresponding local model in the construction of the RO-LPV model. The splines satisfy one of the conditions of consistency as mentioned in eq. (6.9). When the value of the working point (pull-rate) is equal to either of the local ROM which is used to form the RO-LPV model, then the contribution of the other two splines as per the condition of consistency in eq. (6.9) is forced to zero.

The RO-LPV model was validated by using step input signals with 3% amplitude changes from their nominal value as the step size. The validation results are shown in Figure 6.8. Figure 6.9 shows the important dynamics of Figure 6.8 in enlarged form. Four plots are shown in that figure where each plot corresponds to a different region in the glass manufacturing furnace, see Figure 2.2. It is clear from Figure 6.8, that the performance of the RO-LPV model varies in different regions. In all the regions the RO-LPV model shows good fit but it fails to match the final steady state gain. This is because of the involved error at different stages of the identification of the RO-LPV model. The largest contribution of this discrepancy is due to the quality of the identified local reduced order LTI models used to identify RO-LPV. Indeed, most of the local RO models could approximate $< 80\%$ of the projection energy which is not sufficient. Usually the RO model performance is good if it captures approximately 99% of the projection energy. This turned out to be impossible by linear model approximation. However, for the size

and involved complexity, the results seem to be promising.

6.5 Conclusions

This chapter has presented a data based practical approach to solve the problem of model reduction for large scale nonlinear processes. Due to the large order and involved process complexity, the model reduction strategy proposed in this chapter involved multi pronged strategy incorporating spectral decomposition, subspace state space LTI model identification and linear parameter varying modeling framework. The practical aspects of such a model reduction procedure are also explained which can be useful while applying this procedure to other large scale processes. The method proposed here can be considered as an alternative to classical Galerkin type of projections to infer reduced order models. To validate the effectiveness of the proposed method, it is implemented on industrial glass manufacturing as a benchmark example. In case of glass manufacturing, the proposed RO-LPV model approximates the process nonlinearity as result of transition between operation regimes and nonlinearity arising out of geometric parameter variations. The results presented here are very encouraging and data based nature make it of generic nature.

Due to the data based nature of the method it is applicable for other large scale energy intensive processes in chemical industry, e.g. cement, oil, steel, paper, fertilizers etc. to obtain reduced order models which can be used for real-time control and optimization purposes. The LPV model identification technique explained in this chapter, in stead of reduced order models, can also be used to identify black-box LPV models from the input-output data of actual plant. In the proposed method, nonlinear splines capture the process nonlinearity that arise during a transition between the working points. In stead of nonlinear splines, if linear splines are used then the resulting RO-LPV model will be convex. Convex nature of a RO-LPV model allows extension of the notions from the LTI system theory.

From the discussion presented in section 6.4, it is clear that for a complex chemical process like glass manufacturing, it is difficult to find a linear operation range of the process. For such cases, in stead of identifying a local LTI reduced model, it is more rewarding to have a non-linear reduced order model. In next chapter this issue of identification of non-linear reduced order model using spectral decomposition will be addressed.

7

Identification of Low Order Non-linear Models

In this chapter a novel procedure for obtaining low order linear and non-linear models of large scale non-linear fluid flow systems is proposed. The approach is based on the combination of the methods of spectral decompositions, and non-linear system identification techniques. Here, the model reduction problem for non-linear processes is formulated as a parameter estimation problem. The first step of this model reduction technique is similar to the one proposed in other chapters and involves separation of spatial and temporal patterns. In the second step, a model structure of tensorial (multivariable polynomial) expansions is selected to describe linear or non-linear time evolutions of modal coefficients. The proposed model reduction strategy explores the observation made in the Chapter 3, that, for a certain class of PDE the modal coefficients obtained by the spectral decomposition can be viewed as the states of the reduced order model. With the knowledge of the POD modal coefficients and the process inputs, different model structures are proposed to relate the input and the states (i.e the modal coefficients). In particular, a tensorial representation of the vector field of the system is proposed. This generalizes the usual LTI setting in a nice manner to a different model class of nonlinear systems. An ordinary least squares method is then used to efficiently estimate the model parameters. The simplicity of the proposed method gives computationally very efficient linear and non-linear low order process models for large scale processes. During the whole

procedure the physical interpretation of the states is preserved. The (state) data based nature of the method make it generic. The efficiency of the identification method is illustrated on large scale benchmark examples of an industrial tubular reactor and the 2D glass furnace model. The chapter also presents the comparison between the identification and the projection based approaches. Moreover, for the implementation purpose, guidelines about the experiment design are also presented in this chapter.

To evaluate the Lyapunov stability of the proposed tensorial systems at a fixed point, sufficient conditions are presented. Tools from the Linear Matrix Inequalities (LMI) and the semi-definite programming are used to establish these conditions. Moreover, this chapter also characterize the dissipativity of the tensorial systems for a quadratic supply function.

Some of the results from this chapter are presented at a conference, see Wattamwar et al. (2009b) for further detail.

7.1 Introduction

In last few chapters a few different ways to approximate the large scale systems using reduced order modeling framework employing the tools from spectral decomposition theory and from system identification theory are presented. It is shown in Chapter 6 that the process non-linearity as result of changes in the process operating conditions may be approximated using a Reduced Order-Linear Parameter Varying (RO-LPV) framework. The RO-LPV modeling framework has its own advantages and drawbacks. The advantages of the method are its practically applicable procedure and simple model structure that is suitable for system theoretic analysis. One of the drawback of that method is its inability to make an apriory estimation about the involved error. This was due to the overall nature of the method which was based on combinations of many tools which induced some approximation error at every stage. Moreover, the RO-LPV method is suitable to approximate the process nonlinearity arising from the transitions of working point.

It is also shown in Chapter 6 that sometimes for large scale nonlinear processes, it is almost impossible to find a linear range of process operation to identify a local (corresponding to a constant value of the scheduling parameter) LTI reduced model. It is therefore rewarding to identify a local model

that can approximate the process non-linearity. Moreover, it is also desired that the reduced order nonlinear model should have a structure which is easy for analysis and for the extension of the concepts from linear system theory like stability, disspativity, observability etc. In literature, many nonlinear identification techniques have ben proposed so far. For example, Wiener-Hammerstein configurations, black-box methods (see, e.g. Sjoberg and et. al. (1995)), neural networks, fuzzy logic, support vector machine models (see, Goethals et al. (2005)), grey box models as explained, for instance in Romijn et al. (2008) and many others. A good overview of many nonlinear identification methods in the form of a bibliography is compiled in Giannakis and Serpedin (2001). Most of these nonlinear identification methods do not propose a model structure that is suitable for extending the system theoretic properties of LTI systems.

In this chapter a non-linear reduced order modeling technique that meets the above mentioned desired properties and the objectives mentioned in section 1.2 is proposed. The proposed technique involves two steps. The first step is similar to the method proposed by Huisman (2005) and Wattamwar et al. (2008), which is discussed in detail in Chapter 5 and 6 and it involves spatio-temporal decomposition of dynamic process variables by using the POD method or the spectral decomposition of system solutions. The second step is different from the method that is proposed in last few chapters. The difference lies in the fact that the method presented in last few chapters treats POD modal coefficients as outputs of a reduced order (black-box) model that needs to be identified, whereas in the approach presented in this chapter treats the modal coefficients as the states of a reduced model that needs to be identified. The reason and mathematical framework behind this idea is already explained in section 3.2.2 and further elaborated in section 7.2. The observation made in section 3.2.2 that the POD modal coefficients can be viewed as the states of a reduced order model that is to be identified, has motivated to formulate the model reduction problem as a parameter estimation problem. As the states of the model to be identified are known, one can use different model structures to approximate the state evolutions. Among many possible different model structures, LTI and tensorial (multi-variable polynomial) type of model structures are selected. Tensorial models appear as a natural choice due to their origin in Taylor series expansion of a nonlinear function. Simulation results of the reduced LTI and the tensorial type of models are presented in this chapter. It is also shown here that the tensorial type of reduced order models due to increased parameterizations, approximate the dynamics of full order model better than the linear reduced

model. Further, it is explained in this chapter that both the approaches; viz- the identification of reduced order black box model and the classical approach of inferring reduced order models from Galerkin projection of full order model equations are related. The method that is proposed here is similar in its motivation and the reduced order model structure to the work of Perret et al. (2006). There, they have proposed a method to identify a polynomial model for POD based low order model. But the work that is presented there lacks rigorous mathematical formulation and does not present a reasoning for treating the POD modal coefficients as the states of a reduced order model. Moreover the approach presented there was aimed at autonomous systems.

Meeting the objectives mentioned in the first chapter of this thesis, the method proposed in this chapter do not need access to the governing PDEs that are formulated as ODEs in CFD softwares and rely only on the states information of the full order CFD model. The method proposed in this chapter therefore avoids the laborious programming efforts which are required in model reduction techniques based on Galerkin Projections. Similar to the other model reduction techniques presented in last few chapters, the identification based approach presented here can be very useful in practice, since it allows to use the available full-scale first principle based non-linear process model in the form of commercial software as an replacement of the original plant. The reduced nonlinear identified models are computationally very efficient, they may be used for analysis of process dynamics and also for the purpose of design of the process controller and optimizer. Therefore the proposed method minimizes the dependence on the expensive testing of the plant required for the controller design.

This chapter is organized as follows. The proposed model reduction method is based on spectral decomposition step of POD that is explained in section 3.2.2. The overall methodology is explained in section 7.2. The two approaches- identification of reduced model as proposed in this chapter and the method of POD with Galerkin projection of model equations are compared in section 7.3. The practical guidelines related to the implementation are explained in section 7.4. The proposed methods are validated on two large scale benchmark examples; viz- the tubular reactor and the 2D glass furnace model. The benchmarks are already explained in section 2.2.2 and 2.3.6, respectively. The validation results of the proposed method on the benchmark examples are presented in section 7.5. To characterize the stability of the tensorial models, Lyapunov test using the LMI tools is proposed in

section 7.6. The dissipativity of the tensorial models for a quadratic supply function is explained in section 7.7. The last section presents the conclusions.

7.2 Methodology for reduced order modeling

The main contribution of this chapter, a new model reduction method, is explained in this section. The proposed method is a combination of tools from system identification and the usage of proper orthogonal decompositions to separate spatial and temporal patterns or signals. Moreover, the relation between the two different approaches, identification and projection is elaborated here. In the first subsection, a brief connection is made to the POD method explained in section 3.2.2 and later the model reduction techniques to obtain LTI and nonlinear models in polynomial form are derived in subsequent subsections.

7.2.1 Identification of reduced order LTI models

Assume that only *data* from the full-scale model (3.36) is available but not the equations (3.36) itself. This situation is relevant when the full-scale (3.36) is an implementation of a finite element model whose equations are not available for making Galerkin-type of projections. To infer low-order models, in this subsection an identification algorithm is proposed. The proposed technique estimates a functional relation between the inputs (u, d) of the system (3.36) and the POD modal coefficients a as they appear in (3.46). The identification is carried out under the assumption that a model order r and a POD basis of orthonormal functions φ_j, $j = 1, \ldots, r$, defined on the spatial configuration space Ω has been decided upon or, otherwise, has been computed from simulated data $\mathbf{T}_n^k$, $k = 1, \ldots, K$. The orthonormal functions can be computed by defining a correlation operator as in (3.42) and its subsequent eigenvalue decomposition. The orthonormal basis can also be computed from SVD of the ensemble $\mathbf{T}_n$

The POD method with Galerkin projection of model equations transforms the full order nonlinear model from (3.36) to (3.46). For linear systems, the nonlinear term $\mathcal{F}_r$ in eq. (3.46) vanishes in which case eq. (3.46) becomes a linear dynamical system that, after a suitable discretization over

time,assumes the form

$$a(k+1) = A_d a(k) + B_d u(k). \tag{7.1}$$

Here, $a(k)$ and $u(k)$ are shorthand for $a(t_k)$ and $u(t_k)$ with $t_k \in \mathbb{R}$ the k^{th} time-sample and the j^{th} coefficient of $a(k)$ actually satisfies $a_j(k) = \langle \varphi_j, T_n(t_k) \rangle$, with $j = 1, \ldots, r$. With data $(a(k), u(k))$ given on a sampled time axis, the system matrices A_d and B_d can be inferred from an identification algorithm for linear system identification. Ordinary Least Square (OLS) parameter estimation technique can be used to estimate A_d and B_d. This is possible due to the linear in parameter nature of the (7.1). The observation that POD modal coefficients are the states of the reduced order model in (3.46) is the key to infer reduced order LTI model. OLS is used in next subsection as well and discussed in more detail. From this discussion, it is clear that, it is possible to infer a LTI reduced order models from the knowledge of states and inputs of full order model. Conceptually, the LTI reduced order model inferred here and in Chapter 6 are similar. Both the methods try to estimate the space in which the system dynamics can be approximated by a linear mappings. Once the state space matrices A_d and B_d are estimated, the reconstructed states of full order model can be obtained by outer product,

$$\hat{T}_r(z,k) = \sum_{j=1}^{r} \varphi_j^T(z) \hat{a}_j(k), \quad z \in \Omega, \tag{7.2}$$

where, $\hat{a}(k) \in \mathbb{R}^r$ are the estimated POD modal coefficients and $\hat{T}_r(z,k) \in \mathbb{R}^n$ are the reconstructed states (approximate solution) of the full order model.

If the governing equations eq. (3.46) are nonlinear, the above strategy may be less successful for systems in which strong nonlinearities affect the behavior. The literature on input-output based identification methods describes many methods to approximate the non-linearities in (3.46). Some examples of nonlinear identification techniques are nonlinear auto-regressive, Wiener-Hammerstein configurations, black-box methods (see, e.g. Sjoberg and et. al. (1995)), neural networks, fuzzy logic, support vector machine models (see, Goethals et al. (2005)), grey box models as explained, for instance in Romijn et al. (2008) and many others. A good overview of many nonlinear identification methods in the form of a bibliography is compiled in Giannakis and Serpedin (2001).

Apart from the input data $u(k)$, the POD basis allows to use the coefficients $a_j(k)$, for $j = 1, \ldots, r$ to be available for model identification purposes. The observation made earlier that the modal coefficients can be viewed as the states of the reduced order model (3.46) that is aimed to identify can be useful again. Once a good quality model is identified for the mapping $u \mapsto a$, the approximate solution $\hat{T}_r$ of the full scale model are obtained from eq. (7.2). A novel procedure for identification of the nonlinear map $u \mapsto a$ is explained in subsequent sections.

7.2.2 Identification of non-linear Tensorial models

It is well known that Taylor series expansions of a nonlinear function allow accurate approximations of a non-linear smooth function nearby an arbitrary point. It is therefore remarkable that the identification of terms in the Taylor series expansions of the mappings $\mathcal{A}_r$, $\mathcal{B}_r$ and $\mathcal{F}_r$ in (3.46) are not often considered in classical input-output identification methods. Evidently, this is mostly due to the lack of access of information about the state variable a. However, as explained earlier, in the case of model order reduction for the model (3.36), the sampled states $a(k)$ are accessible for identification. Taylor series expansions of the mappings $\mathcal{A}_r$, $\mathcal{B}_r$ and $\mathcal{F}_r$ in (3.46) results in tensorial or multi-variable polynomial system equations which allow a more tractable analytical treatment of the model than many other approximations of the process non-linearities. Some interesting extensions of notions from linear system theory to scalar valued polynomial systems can be found in Ebenbauer et al. (2005).

Taylor and tensor series expansions

For a *scalar valued* and p times continuously differentiable function $f : \mathbb{R} \to \mathbb{R}$ the pth order Taylor series approximation of the nonlinear flow $\dot{x} = f(x)$ in a point $x^* \in \mathbb{R}$ is given by

$$\dot{\xi} = f(x^*) + f^{(1)}(x^*)\xi + \frac{1}{2}f^{(2)}(x^*)\xi^2 + \cdots + \frac{1}{p!}f^{(p)}(x^*)\xi^p. \tag{7.3}$$

Here, $\xi = x - x^*$ and $f^{(p)}$ denotes the pth derivative of f.

For *vector valued* functions one need a slightly more rigorous treatment. Suppose that $f : X \to Y$ is an p times continuously differentiable function

with X and Y (finite dimensional) normed vector spaces. Let $x^* \in X$ be a fixed point in the interior of X and denote by $\mathcal{L}(X,Y)$ the set of all linear mappings from X to Y. The mapping f is said to be *Fréchet differentiable at* x^* if there exists a linear operator $A \in \mathcal{L}(X,Y)$ with the property that

$$\lim_{\|\xi\|\to 0} \frac{\|f(x^*+\xi) - f(x^*) - A\xi\|}{\|\xi\|} = 0.$$

Here, $\xi \in X$ and the norm $\|\xi\|$ is the norm in the vector space X. It is well known that, whenever A exists, it is uniquely defined. The unique linear operator A that satisfies this limit, is denoted $f^{(1)}(x^*)$ and is called the *Fréchet derivative of* f *at* x^*. Clearly, $A = f^{(1)}(x^*)$ admits a matrix representation a_{ij} with $1 \le i \le \dim(Y)$ and $1 \le j \le \dim(X)$ which is given by the partial derivatives $a_{ij} = \frac{\partial f_i}{\partial x_j}(x^*)$. This coincides with the usual Jacobian of f at x^*. If f is Fréchet differentiable at each point in X then for each $x^* \in X$ the derivative $f^{(1)}(x^*)$ is a linear operator. In that case, the mapping $f^{(1)} : X \to \mathcal{L}(X,Y)$ is called the Fréchet derivative of f.

In a similar fashion, the *second Fréchet derivative of* f *at* x^* is defined as the Fréchet derivative of $f^{(1)} : X \to \mathcal{L}(X,Y)$ at the point $x^* \in X$. Specifically, let $\mathcal{L}(X,Y)$ become a normed space with the operator norm $\|A\| := \sup_{0\neq x\in X} \frac{\|Ax\|}{\|x\|}$. Then f is said to be twice Fréchet differentiable at x^* if there exists a linear operator $B \in \mathcal{L}(X, \mathcal{L}(X,Y))$ such that

$$\lim_{\|\xi\|\to 0} \frac{\|f^{(1)}(x^*+\xi) - f^{(1)}(x^*) - B(\xi)\|}{\|\xi\|} = 0.$$

Here, the norm in the numerator is the operator norm of $\mathcal{L}(X,Y)$, the norm in the denominator is the norm in X and $B(\xi) \in \mathcal{L}(X,Y)$. With some abuse of notation, B will be identified with the bilinear function $B : X \times X \to Y$ in the sense that the element $[B(\xi)](\zeta)$ in Y will mean the same thing as $B(\xi, zeta)$. The unique bilinear operator $B : X \times X \to Y$ is the second Fréchet derivative of f at x^* and will be denoted by $f^{(2)}(x^*)$. Hence, $f^{(2)}(x^*) = [f^{(1)}]^{(1)}(x^*) = B$. To simplify notation, let us denote by $\mathcal{T}_2$ the set of bilinear functions $B : X \times X \to Y$. That is, B is a linear function in each of its arguments. If the mapping $f^{(1)}$ is Fréchet differentiable at each point $x^* \in X$ then the second Fréchet derivative $f^{(2)}$ becomes a mapping $f^{(2)} : X \to \mathcal{T}_2$.

Continuing this way, the pth Fréchet derivative of $f : X \to Y$ is recursively defined as the Fréchet derivative of $f^{(p-1)}$ and, whenever it exists at each

point $x^* \in X$, becomes a mapping $f^{(p)} : X \to \mathcal{T}_p$ where $\mathcal{T}_p$ denotes the set of all multi-linear functions $C : X \times \cdots \times X \to Y$. That is, $\mathcal{T}_p$ is the set of vector-valued functions that are linear in each of its p arguments. $\mathcal{T}_p$ will be referred to as the set of pth order *tensors on* X[1].

Similar to (7.3), if $f : \mathbb{R}^n \to \mathbb{R}^n$ is a mapping that is p times Fréchet differentiable, then the multi-variable nonlinear system $\dot{x} = f(x)$ admits the pth order tensor expansion

$$\dot{\xi} = f(x^*) + [f^{(1)}(x^*)](\xi) + \frac{1}{2}[f^{(2)}(x^*)]\,(\xi,\xi) + \cdots + \frac{1}{p!}[f^{(p)}(x^*)](\underbrace{\xi,\ldots,\xi}_{p \text{ times}})$$

in the point $x^* \in \mathbb{R}^n$, where $\xi = x - x^*$. Likewise, tensor expansions can be inferred for nonlinear systems of the form $\dot{x} = f(x,u)$ with $f : \mathbb{R}^{n+m} \to \mathbb{R}^n$.

Least squares identification of tensor expansions

Recall that the Kronecker product of two vectors $a, b \in \mathbb{R}^n$ is the vector $a \otimes b = \mathrm{col}(a_1 b, \ldots, a_n b)$ in $\mathbb{R}^{n^2}$ and that the Kronecker product of multiple vectors is distributive, i.e., $a \otimes (b \otimes c) = (a \otimes b) \otimes c$. The following result is basic but crucial.

Lemma 7.2.1 *Let $f : X \to Y$ be p times Fréchet differentiable. Then $f^{(p)}(x^*)$ is a tensor in $\mathcal{T}_p$ that admits the representation*

$$[f^{(p)}(x^*)](x_1, \cdots, x_p) = A(x_1 \otimes x_2 \otimes \cdots \otimes x_p) \tag{7.4}$$

where A is a linear operator in $\mathcal{L}(X^p, Y)$ and where $x_1 \otimes \cdots \otimes x_p$ is the Kronecker product of $x_1, \ldots, x_p \in X$.

Proof: The result is trivial for $p = 1$ as $f^{(1)}(x^*) \in \mathcal{L}(X,Y)$. For $p = 2$, consider the tensor $B = f^{(2)}(x^*) \in \mathcal{T}_2$. Then $B(x,y)$ is linear with respect to x and linear with respect to y. Define $z := x \otimes y$. Then

$$[f^{(2)}\,(x^*)](x,y) = \begin{bmatrix} \sum_{k=1}^{n}\sum_{j=1}^{n} \frac{\partial^2 f_1(x^*)}{\partial x_k \partial y_j} x_k y_j \\ \vdots \\ \sum_{k=1}^{n}\sum_{j=1}^{n} \frac{\partial^2 f_n(x^*)}{\partial x_k \partial y_j} x_k y_j \end{bmatrix} \tag{7.5}$$

[1]Strictly speaking, the set of pth order (covariant) tensors is the set of multi-linear *functionals* $C : X_1 \times \cdots \times X_p \to \mathbb{R}$ defined on p vector spaces $X_1, \ldots, X_p$, but we will adhere to the present terminology here.

which shows that $f^{(2)}(x^*)$ is a linear function of z. In a recursive fashion, one proves that the tensor $[f^{(p)}(x^*)](x_1, \ldots, x_p)$ can be written as a linear function of $z = x_1 \otimes \cdots \otimes x_p$. ■

Now consider the nonlinear model of eq. (3.46) and let $f : \mathbb{R}^{r+m} \to \mathbb{R}^r$ be defined by

$$f(a, u) := \mathcal{A}_r(a) + \mathcal{B}_r(u) + \mathcal{F}_r(a, u)$$

An pth order tensor expansion of eq. (3.46) in a stationary point (a^*, u^*) for which $f(a^*, u^*) = 0$ then reads

$$\dot{x} = [f^{(1)}(a^*, u^*)] \begin{pmatrix} x \\ v \end{pmatrix} + \cdots + [f^{(p)}(a^*, u^*)] \left(\begin{pmatrix} x \\ v \end{pmatrix}, \cdots, \begin{pmatrix} x \\ v \end{pmatrix} \right)$$

where,

$$\begin{aligned} x &:= a - a^*, \quad \text{and} \\ v &= u - u^* \end{aligned} \tag{7.6}$$

Using Lemma 7.2.1, a second order tensor expansion assumes the more explicit form

$$\begin{aligned} \dot{x}(t) &= Ax(t) + Bu(t) + A_1(x(t) \otimes x(t)) \\ &\quad + B_1(v(t) \otimes v(t)) + Q(x(t) \otimes v(t)) \\ y(t) &= Ix(t) \end{aligned} \tag{7.7}$$

where, A, B, A_1, B_1 and Q are matrices in $\mathbb{R}^{r \times r}$, $\mathbb{R}^{r \times m}$, $\mathbb{R}^{r \times r^2}$, $\mathbb{R}^{r \times m^2}$ and $\mathbb{R}^{r \times rm}$, respectively.

In a similar fashion, a discrete time second order tensor approximation of the system (3.46) can be written as:

$$\begin{aligned} x(k+1) &= Ax(k) + Bv(k) + A_1(x(k) \otimes x(k)) \\ &\quad + B_1(v(k) \otimes v(t)) + Q(x(k) \otimes v(k)) \\ y(k) &= Ix(k) \end{aligned} \tag{7.8}$$

(with different matrices A, B, A_1, B_1 and Q). For the problem of identification of the model (3.46) it is assumed that a suitable sampling time has been decided upon and we will focus on the identification of the second order tensor approximation (7.8). Note that the tensor expansion in the right-hand side of (7.8) is non-linear in the states and the inputs but it is linear in all the system parameters. If N consecutive samples of the states x and inputs

u are known, this allows us to identify the matrices A, B, A_1, B_1 and Q in an optimal manner by minimizing the criterion

$$J(A, B, A_1, B_1, Q) := \sum_{k=1}^{N} \|e(k)\|^2$$

where $e(k) := x(k+1) - Ax(k) - Bv(k) - A_1(x(k) \otimes x(k)) - B_1(v(k) \otimes v(t)) - Q(x(k) \otimes v(k))$ is the *prediction error* at time k. In particular, if we define

$$\xi_k := \mathrm{col}(x(k), v(k), x(k) \otimes x(k), x(k) \otimes v(k), v(k) \otimes v(k))$$

then $e(k) = x(k+1) - \Theta\xi_k$ where

$$\Theta = \begin{pmatrix} A & B & A_1 & B_1 & Q \end{pmatrix}$$

and the problem to minimize $J(\Theta)$ over all parameters Θ becomes an ordinary least squares estimation problem. Note that $\Theta \in \mathbb{R}^{r \times (r+m+r^2+m^2+rm)}$. In matrix notation, let

$$E = \begin{bmatrix} e(1) & \cdots & e(N) \end{bmatrix}, \quad X = \begin{bmatrix} x(2) & \cdots & x(N+1) \end{bmatrix},$$
$$\Xi = \begin{bmatrix} \xi_1 & \cdots & \xi_N \end{bmatrix}$$

Then

$$E = X - \Theta\Xi \tag{7.9}$$

and the optimization problem amounts to finding Θ such that $\|E\|^2 = \langle E, E \rangle$ is minimal. The optimal solution to this problem is given by

$$\Theta^* = X\,\Xi^\top\,(\Xi\,\Xi^\top)^{-1} \tag{7.10}$$

Here, the system parameter matrix Θ may become rank deficient due to the involved Kronecker product. Nevertheless, there are some simple ways to estimate the parameters for rank deficient problem. Here, only the standard routines for the computation of the pseudo-inverse are used.

Once the system parameters (state space matrices) are estimated from (7.10), the POD modal coefficients can be estimated after adjusting the offset in (7.6), from (7.8). The approximate solution of the full order model can be obtained as in (7.2).

Remark 7.2.1 The above analysis focuses on least squares estimates of second order tensor expansions. Generalization to higher order tensor expansions is straightforward and left to the reader.

Remark 7.2.2 Large scale parameter varying systems can basically be identified in the same manner as described. If knowledge of the variation of time-varying parameters is available, the uncertain parameter can be treated as a process input and the above method applies to this setting.

Remark 7.2.3 The above least squares estimation method may lead to an unstable system. To overcome the drawback of possible instability, one might try different orders, or to impose stability during the identification of the model by using a regularization method. However, regularization methods often lead to the loss of performance of the identified models. Typically for linear subspace identification techniques, regularization is imposed by forcing the eigenvalues of the identified model to lie in the unit circle, e.g. see Gestel et al. (2000). In this chapter the problem of imposing the stability in the identification process is not solved. The research in tensorial systems is still relatively new and imposing the stability in the identification procedure involving tensors, will need considerable amount of further efforts. Nevertheless, characterization of the stability of such a tensorial system is performed in later part of this chapter.

7.2.3 Algorithmic procedure

In this subsection, we explain the overall procedure to identify low order models in algorithmic form. It is assumed that the full order model is available for simulations.

- Excite the full order model after designing the experiment as per the guidelines presented in section 7.4.
- Collect the snapshots to construct the snapshot matrix T_{snap}.
- Perform singular value decomposition of the snapshot matrix T_{snap} or eigenvalue decomposition of the correlation matrix R as in (3.42). Use the criterion in (3.47) to decide the order of the reduced model.
- Collect the dominant patterns in the form of POD spatial basis functions and the modal coefficients.
- Fix a model structure of the form (7.1) or of nonlinear form as in (7.8).
- Estimate the model parameters using the least square estimation technique as explained in section 7.2.2.

7.3 Comparison: Identification and projection methods

In this subsection we compare the model reduction techniques obtained by the two different approaches. That is, we compare the identification methods that are proposed in this thesis with the method of POD using Galerkin projection of equations. In particular, the similarities and the differences between the two methods are compared here.

Similarity

- Both the techniques are motivated by a common goal of removing the redundancy from the first principle models used for fluid flow systems.
- The first step of both the methods is same and it involves the spectral decomposition of the system solutions to infer the dominant spatial and temporal patterns.
- As showed in the subsection 7.2.1, both the methods have similar model structures for discrete LTI systems.

Differences

- The second step is different for the two methods. The second step of the identification methods that are proposed here exploits the fact that the POD modal coefficients can be viewed as the states of a reduced order model (see subsection 7.2.1). Subsequently, the method involves estimation of the parameters of a proposed (linear/nonlinear) model structure. Therefore, the identification based method does not need access to the governing equations. Whereas, the second step of POD with Galerkin projection method involves projection of the governing equations on the lower dimensional subspace spanned by the dominant POD spatial basis functions.
- Reduced order modeling by POD with Galerkin projection is explained in section 3.2. The procedure involve model reduction of a full order finite dimensional ODE model to a reduced order model (3.39). Whereas, the identification based model reduction method proposes model structure of LTI form as in (7.1), or of nonlinear form as in (7.8).

- Nonlinear terms in the reduced order model obtained by the method of POD with Galerkin projection is similar to the full order model and therefore such a reduced order model is more accurate. Whereas, the nonlinear terms in the identification based approach is approximated by a Taylor series tensorial expansion whose accuracy depends on the truncation level.
- In the method of POD with Galerkin projection, due to the evaluation of nonlinear terms in a full dimensional space, the method does not offer substantial gain in computational speed over a full order model. Whereas, in identification based approach, the evaluation of nonlinear terms is performed in a reduced space. Therefore, the identification based model reduction method offers distinct advantage in terms of computation speed.

7.4 Experiment design

In this section, practical aspects with respect to the design of experiments for inferring optimal reduced order models for a large scale distributed process are explained. The identification signal used to excite a full order model and the details about the construction of a snapshot matrix are discussed in more detail. The concepts and the reasoning from the field of classical system identification (see, e.g. Ljung (1999)) is used to design the experiments for inferring a good reduced order model.

7.4.1 Input design

The input signal that is used for the excitation during the identification step determines the dynamics that are excited and these dynamics are reflected in the snapshot matrix which is subsequently used to infer the POD basis functions. In other words, an identification signal determines the quality of a reduced model. For the same reason, POD based methods are often classified as empirical methods of model reduction. Thus, while designing an identification signal for the identification of reduced order models of large scale dynamical systems, care must be taken. There are different ways that are used in actual practice to design an identification signal. The overall goal is to excite the dynamics that are relevant for the purpose of controller design.

The input identification signal that is used in this paper is a Pseudo Random Binary Signal (PRBS) around its nominal operating value. PRBS aims at exciting the dynamics of underlying system corresponding to certain frequency range. Based on the physical insight of the process, the PRBS is a binary signal with switching between the sign is adjusted such that the average switching time of the signal is equivalent to the average time constant of the process. PRBS satisfies the condition of persistency of excitation while identifying an LTI system. Especially in Subspace state space LTI model identification techniques, it is necessary to fulfill certain mathematical conditions. For these identification techniques, readers are referred to the work presented by, Overschee and Moor (1996), Qin (2006).

Often, it is of interest to approximate the steady state behavior along with some relevant dynamics of the process. This translates into discarding the very fast dynamics during the model reduction step. Large scale industrial applications are characterized by wide distribution of dynamics. Sometimes each spatial region can show different time constants as well. Therefore, while designing an identification signal, the distributed nature and the presence of wide range of dynamics (very fast to very slow) of the process has to be considered.

To address the distributed nature of the process, in this paper, the average switching time of such an identification signal is chosen equal to the average (of different spatial regions) time constant of the distributed process. The minimum switching time of such an input is usually less than the smallest time constant (fastest dynamics) of the process. In section 7.5, the input signals with respect to the specific process time constant are discussed in more detail for each benchmark example.

7.4.2 Design of a snapshot matrix

As explained in the section 3.2.2, the POD basis functions are obtained from a Singular Value Decomposition (SVD) of a snapshot matrix or by an eigenvalue decomposition of a correlation matrix. The *choice of an input identification signal* explained in 7.4.1 decides the richness of the dynamics contained in the snapshot matrix. From SVD of the snapshot matrix, these dynamics are reflected in terms of the POD spatial basis functions (*spatial patterns*) and the modal coefficients (*temporal patterns*).

The duration of an experiment should be based on the settling time of that

process, which can be residence time for some applications in the process industry. The duration should be planned such that it is longer than the settling time of the process. The Simulation horizon much longer than the settling time is not desirable either, as this will lead to problems while data processing. If the contribution of the steady states in the snapshot matrix is more, then the reduced order model will not be able to approximate the transient (dynamic) behavior of the process, whereas the steady state approximation may be satisfactory.

The *sampling time* should be chosen such that it is smaller than the fastest dynamics. It is common to have a sampling time equal to $1/5^{th}$ to $1/10^{th}$ of the smallest time constant of the process. Again, for a given simulation horizon, an increased sampling rate may lead to the problems associated with data processing.

The effect of an *initial condition* on a reduced order model is minimized by considering the steady state solution as an initial condition during the simulation of a full order model. Further, before SVD of the snapshot matrix, the non-zero initial condition is subtracted from the solution trajectories.

Often it is helpful to *numerically condition* the snapshot matrix. This is performed by scaling it with respect to the maximum value of the system solution, considered over the complete spatio-temporal domain.

7.5 Discussion of simulation results

The simulation results that are presented here are based on the CPU with configuration - Intel Core 2 CPU, T7200 @ 2.00 GHz, 2.00 GB of RAM, Microsoft Windows XP operating system.

The discussion hereafter presented often use the term 'order' in different context. An order of a full (rigorous) scale model and a reduced identified model is their state space dimensions. The order of a reduced model is same as the number of POD modal coefficients whose time evolution is approximated using the identified model. The order of a tensor is the number of unfolding that are necessary to represent it as a matrix. Therefore, a Hessian matrix is a tensor of first order.

7.5.1 Tubular reactor

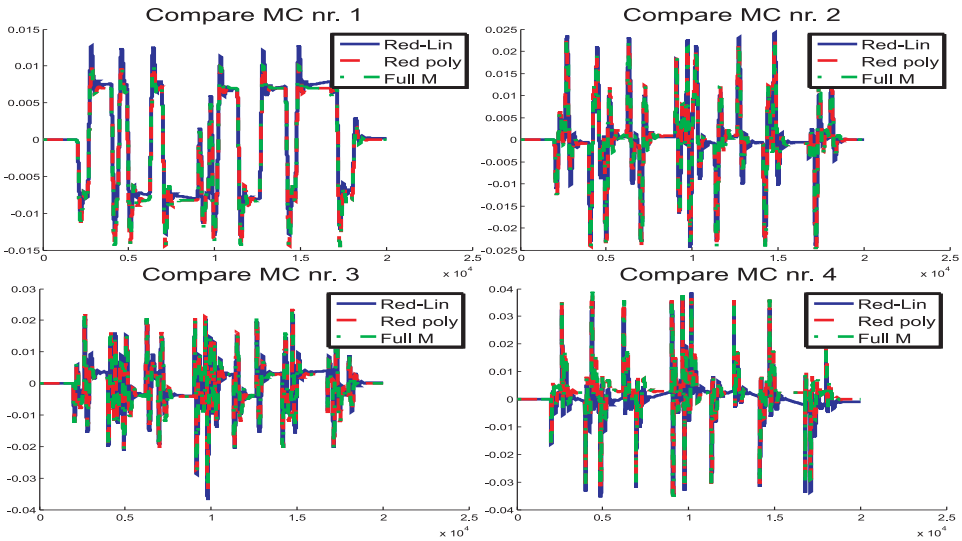

Figure 7.1: Identification: Model fit to the Modal coefficients (MC) of the Tubular reactor. Red-Lin: Reduced Order Linear Model, Red-poly: Reduced Order Polynomial Model, Full M: Full Order Non-linear Model, nr.: Number.

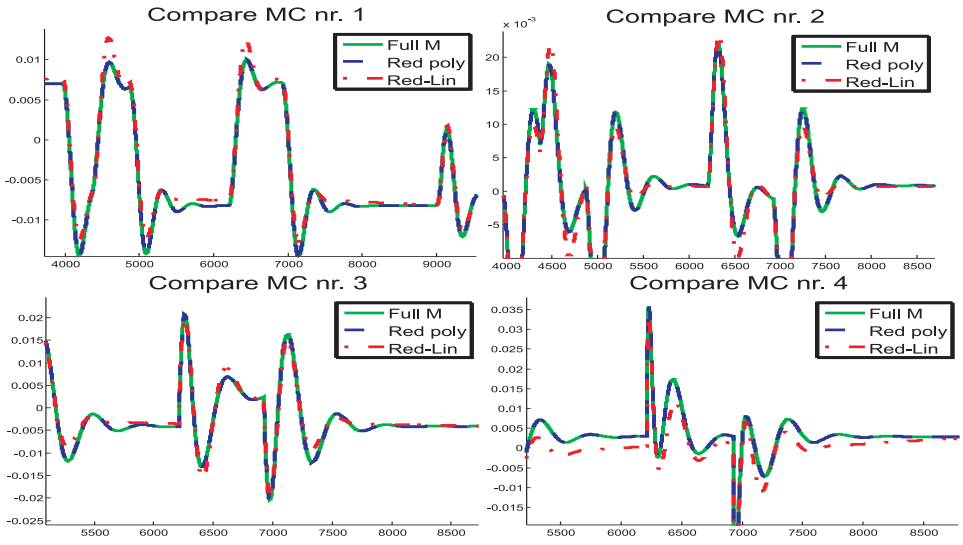

Figure 7.2: Identification: Model fit to the Modal coefficients (MC) of the Tubular reactor, zoomed.

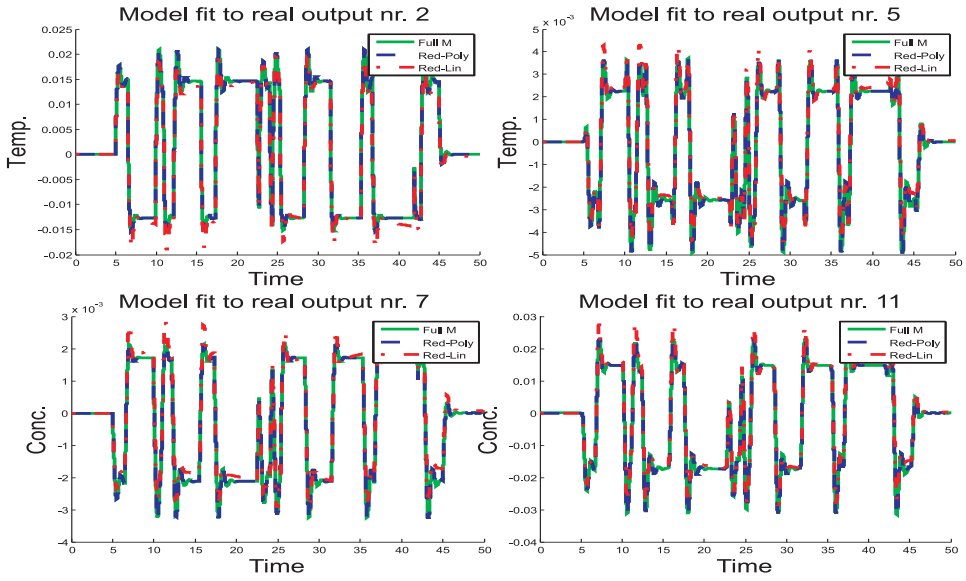

Figure 7.3: Identification: Model fit to the real outputs of the Tubular reactor.

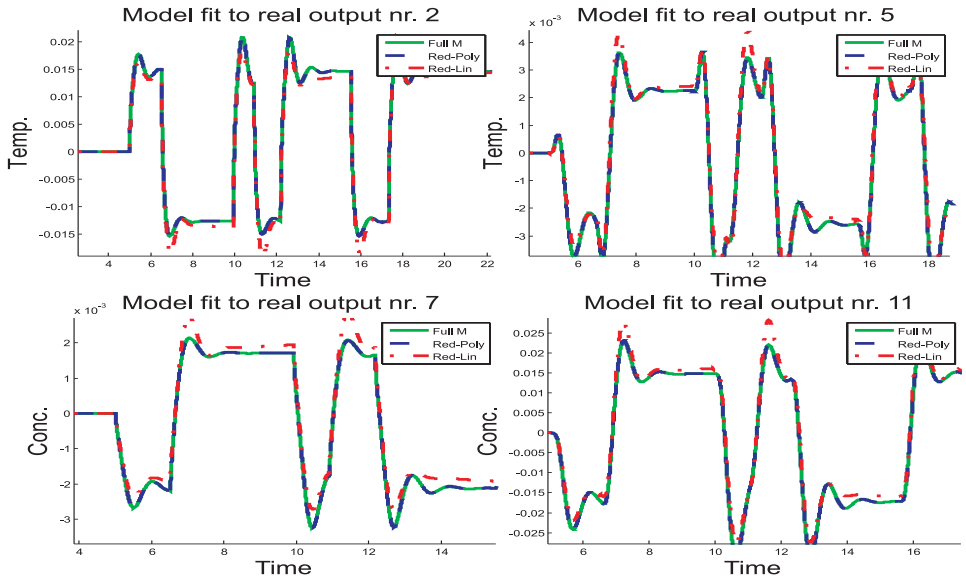

Figure 7.4: Identification: Model fit to the real outputs of the Tubular reactor, zoomed.

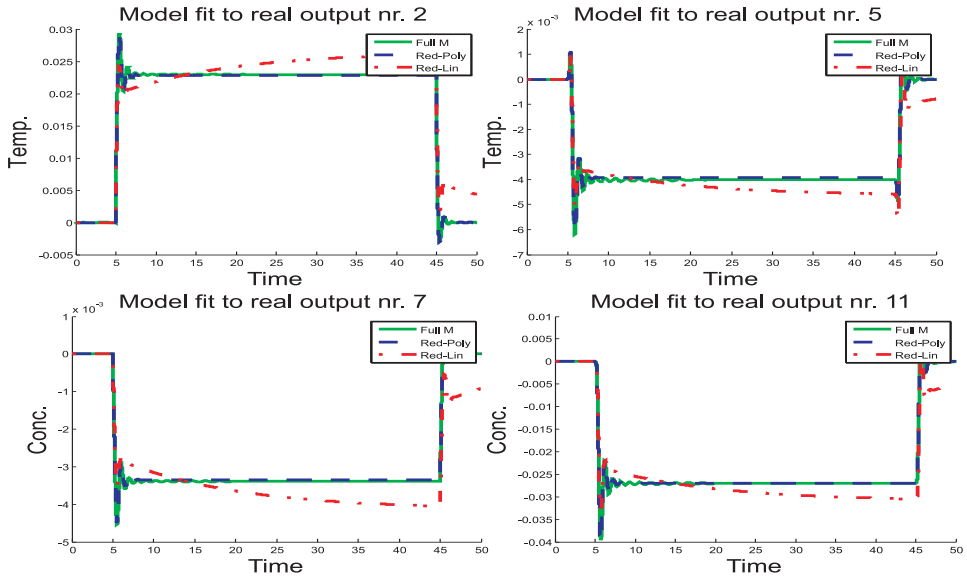

Figure 7.5: Validation: Model fit to the real outputs of the Tubular reactor.

The spatial discretization of the 1-dimensional tubular reactor has been carried out with 100 grid cells. Since there are two states variables, temperature T and concentration C, the full scale model is of order $n = 200$. All variables in the equation (2.1) are represented in dimensionless form. The reaction kinetics is of first order. The full order model has been simulated on a time horizon that corresponds to 50 times the residence time of the reactants in the reactor. The reaction was sampled for 20000 time samples. The time samples have been collected in a snapshot matrix and the POD basis functions have been computed. The results presented here belong to the multi-variable case which means that the temperature and concentration state variables are stacked over each other in the snapshot matrix before computing the POD basis and the modal coefficients. This ensures the coupling of the two state variables. We identified a linear model and a nonlinear first order tensor expansion model of the form (7.8) that maps inputs to modal coefficients.

Obviously, the quality of the identified model depends on the quality of the data. Therefore the data should be generated by input signals which excite the full scale model in the frequency range which is of the interest from a control point of view. The full model was excited with a Pseudo Random Binary Signal (PRBS) on T_i. The average switching time of such an identification signal should be equivalent to the process time constant.

However, as all the variables are dimensionless, the time constant of the tubular reactor is small with respect to time constant of a real-life tubular reactor. Therefore, the average switching of PRBS signal is adjusted to 1/20 of the total simulation horizon. The initial condition is the steady state profile of temperature and concentration. In real life situations, transition in working point excites the process nonlinearity. Such transitions are often implemented in the form of step inputs. Therefore, the validation signal that is considered here is a step input on T_i. The physical parameters of the full scale model are very close to an unstable operating condition. This is evidenced when the full order model is perturbed by 3% change of its nominal value. For the same reason, the amplitude of the input signal used for the validation is limited to 2% of the nominal value.

The fit of a reduced linear and a tensor model to the first 4 modal coefficients, is shown in Figure 7.1 and 7.2. The blue line represents the reduced linear model (Red-lin), the dash green line is reduced tensor model (Red-poly) and the dash-dot green line is the full order model (Full M). The reduced tensor model can fit 12 modal coefficients without becoming unstable. However, 8 modal coefficients are sufficient as they corresponds to $> 99\%$ of the projection energy as specified by the criterion in (3.47). Estimating the parameters of a polynomial model does not take much computation time. But the computation time for evaluating the solutions of resulting reduced model can become significant if the state space dimension of a polynomial model is increased a lot. For this reason we fit the tensor expansion model to only 8 modal coefficients. The plot shows that the linear reduced model does not fit as good as the reduced tensor model. Although evolution of modal coefficients can be conceptually understood as the temporal dynamics, they can not be physically interpreted. Therefore the units are omitted in mentioned figures.

The performance of the identified models in predicting the dynamic evolution of the process outputs are shown in Figure 7.3 and 7.4. The validation of the identified model is performed by using the step input signal. The results of validation are shown in Figure 7.5. The results presented here are based on the software simulation alone and we assume that both; the temperatures and the concentrations can be measured at any location in the reactor. In all the figures the top plots show temperature and the lower plots show concentration in the reactor. Sensors 2^{nd} and 7^{th} are located at 10% of the reactor length from the left entrance while the sensors 5^{th} and 11^{th} are located at 20% from the reactor end i.e. the end on the right hand

side in Figure 2.1. Each identification plot shows the response of the three models- viz. the linear, the tensorial and the full order model. Although both reduced order models show good performance, the reduced order tensorial model approximates the full scale model better than the linear model. The validation plots confirm the same conclusion. The reduced tensor model is also able to approximate the oscillations quite satisfactorily.

As explained in the previous paragraph, depending on the number of modal coefficients fitted by the tensorial model, the computation time of the reduced order tensorial model can vary. For the tubular reactor, when 8 modal coefficients are fitted, the simulation time is approximately 30% that of the full order model. Although, the gain in saving the computation time by the reduced order tensorial model is satisfactory (70% only) over the full order tubular reactor model, it is shown in the next subsection that for the glass manufacturing process, the reduced order tensorial model is computationally very efficient and the associated computational efforts are fraction of the computational efforts needed for the full scale model. The difference of gain in savings of computational effort for the two benchmarks can be explained from the fact that the redundancy in modeling of full order tubular reactor is less when compared to a glass furnace model. Therefore, tubular reactor offers lesser opportunity to invent a computationally efficient reduced order model as compared to the glass furnace. Redundancy in a model can come from unnecessary (large) model dimension of its state space, or unnecessary inclusion of the physical effects, or too small convergence threshold during the computation of the solutions, etc.

7.5.2 Glass manufacturing process

In this paper a $2D$ benchmark CFD model of the original process is considered as a full scale model. The full scale CFD model has 3000 grid cells (spatial discretization). It has many variables like temperature, velocity, concentration, pressure, etc. in each grid cell. Although most of the variables are coupled, for the results presented here we have considered temperature alone as the variable of interest, and we have not used the multi-variable approach that is used in the earlier example of a tubular reactor. Therefore the order of the full scale model is 3000. From the method explained in section 7.2, a reduced linear and a tensorial model is identified. The state space dimension of the linear model is 10 whereas the state space dimension of the tensorial model is 6. The tensorial model is of the form (7.8), i.e.

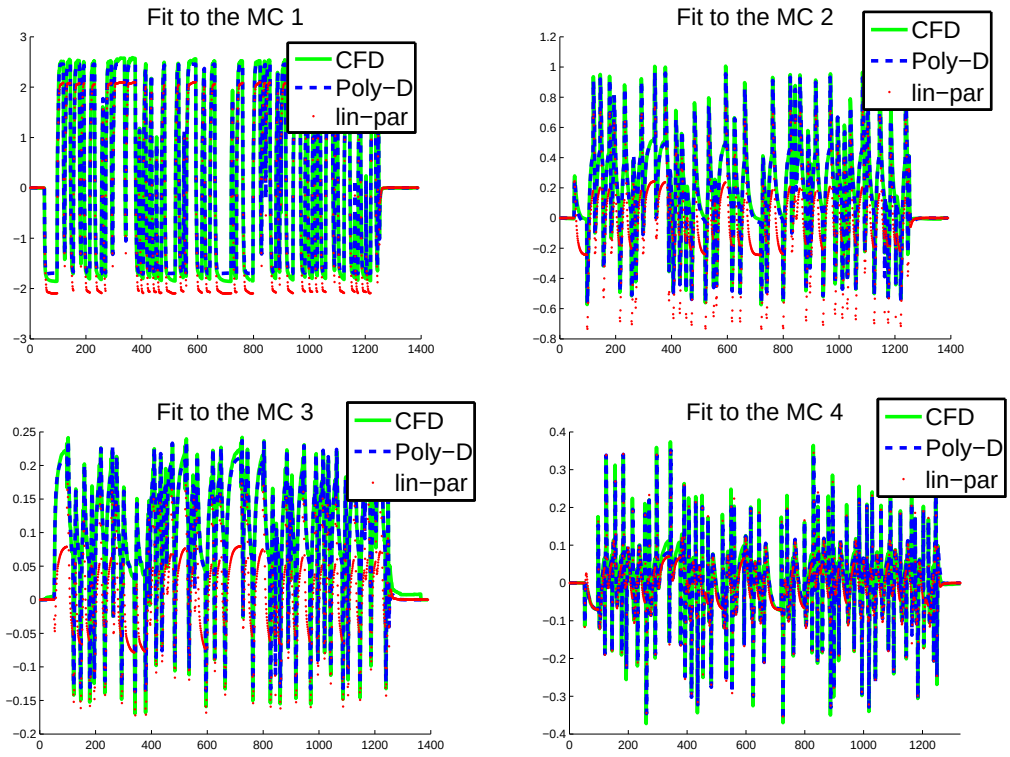

Figure 7.6: Identification: Model fit to the modal coefficients of the glass furnace. CFD: Full order CFD model, Poly-D: Reduced order discrete polynomial model, Lin-par: Reduced order discrete LTI model

---

only the first order tensors are considered here. The identification of a linear model involves fitting the modal coefficients to the linear model obtained by considering the Jacobian terms alone. An order larger than 6 results in an unstable reduced order polynomial model. The notion of stability is used in the sense of divergence of the numerical simulations. For the linear model as well, there is not much improvement in its performance for the approximation order larger than 10. This means that for a linear reduced model, it is not possible to improve its performance merely by increasing the order, and there is need for a non-linear reduced order model. The six POD modal coefficients corresponds approximately to 70% of the total projection energy. This is not sufficient. For a good performance of the reduced order model, it is desired to capture approximately 99% of the total projection energy. But due to the stability limitation we can not satisfy this requirement. As

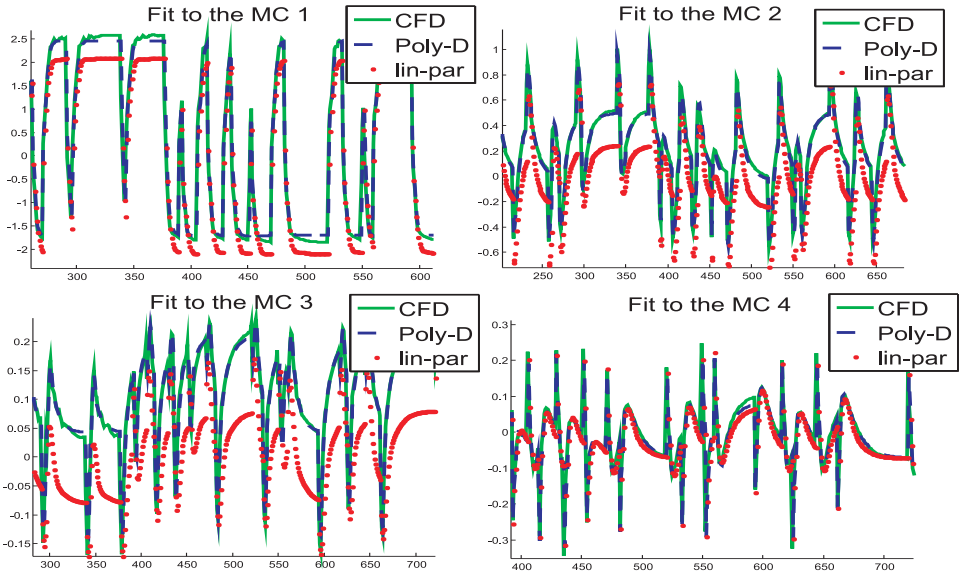

Figure 7.7: Identification: Model fit to the modal coefficients of the glass furnace, zoomed.

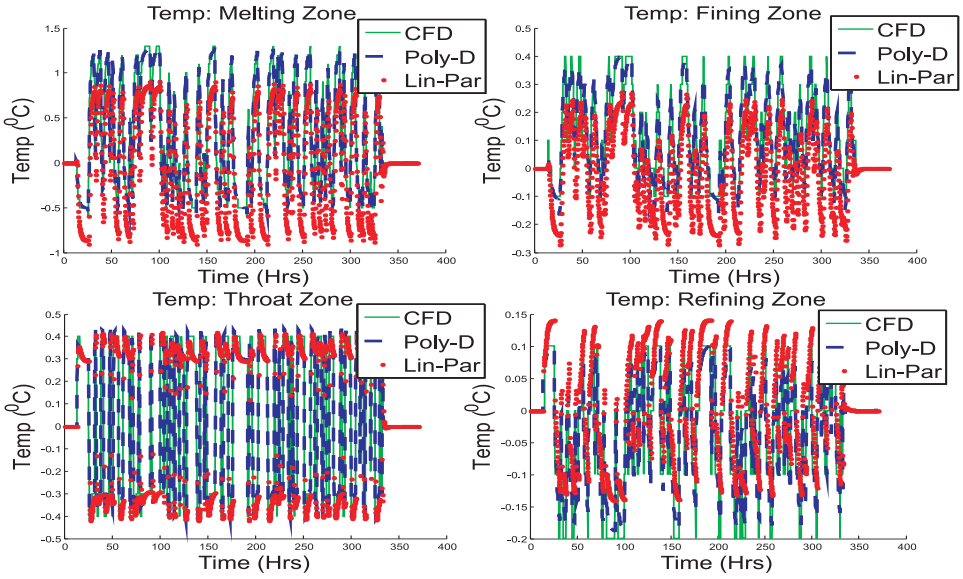

Figure 7.8: Identification: Model fit to the process outputs of the glass furnace.

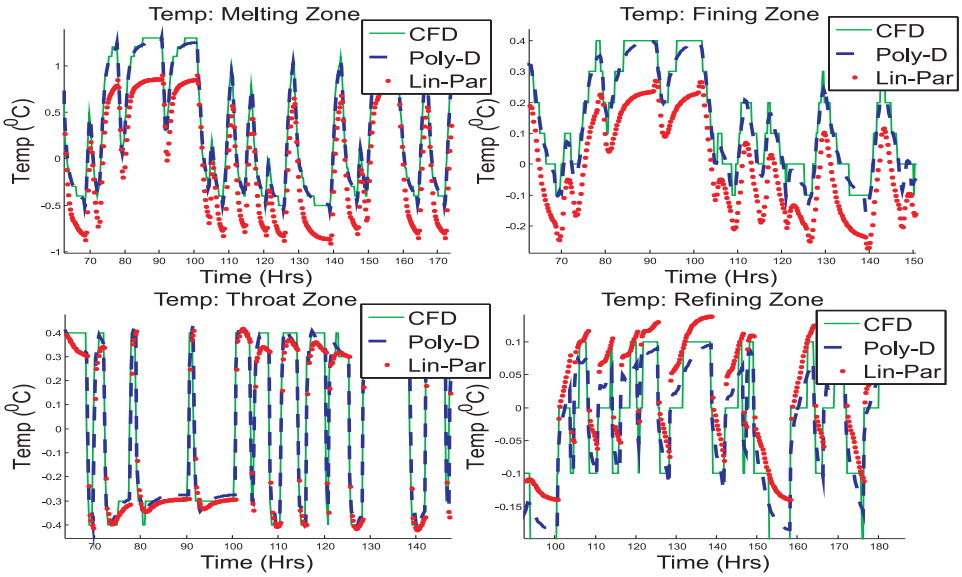

Figure 7.9: Identification: Model fit to the process outputs of the glass furnace, zoomed.

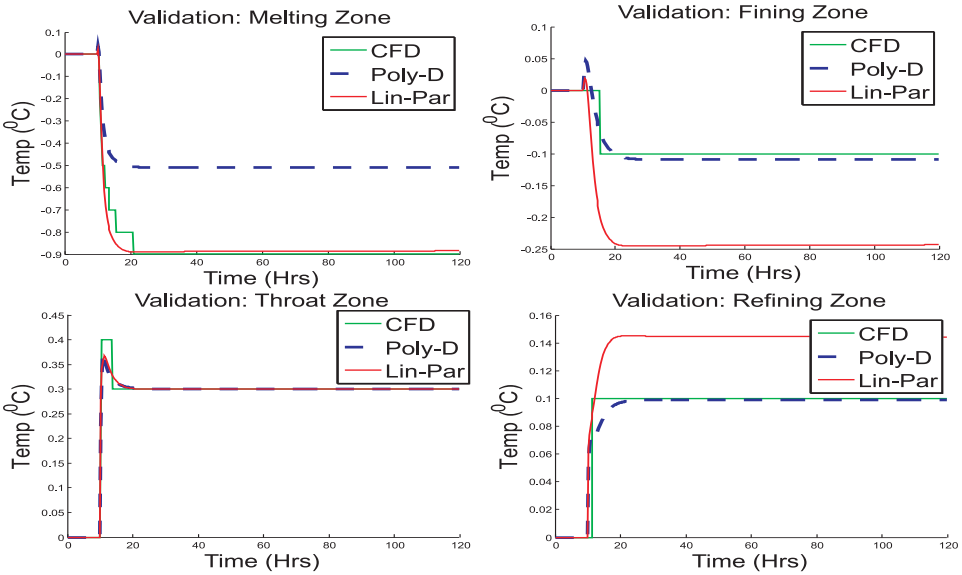

Figure 7.10: Validation: Model fit to the process outputs of the glass furnace.

reduced order tensorial model can approximate the evolution of 6 modal coefficients alone, its performance is expected to be limited as well. Had the tensorial reduced order model approximated the evolution of more number of POD modal coefficients, without becoming unstable, its performance would have been improved.

The input considered for the identification purpose is pull-rate(feed rate) in terms of tons/day, which varies 1% around the nominal value in the form of Pseudo Random Binary Signal (PRBS). The identification experiments are planned as per the discussion presented in section 7.4. The average switching time of the PRBS was adjusted to 4 hours which is equal to the average time constant of the 2D CFD glass process model. The simulation horizon is 370 hours and sampling time is 16 mins, therefore we have 1390 snapshots. Due to slow computation speed of 2D CFD model (although it is much faster when compared to the 3D model), necessary data processing efforts and associated system memory problems, we limited the simulation horizon of the experiments to 370 hours only.

Figure 7.6 and 7.7 shows the dynamic evolutions of the first four modal coefficients as computed by the full order and the reduced linear and nonlinear (tensorial) models. It shows that the tensorial model approximates the dynamic response of the full order CFD model better than the linear one. This shows that even for 1% perturbation, glass exhibits nonlinear behavior. Figure 7.8 and 7.9 shows the identification result in reproducing the plant outputs. Plot shows the result for four outputs which are temperatures at the bottom of refractory material in four main zones of a glass furnace- viz. Melting, Fining, Throat and Refining section. This mimics the real life situation. The readers can refer to Figure 2.2 for sensor locations. $S1$ to $S9$ are the sensors in the figure. In each plot, the green line shows the outputs of CFD model, the dashed blue line (Poly-D) shows the results of discrete form of the identified reduced order tensorial model and the dotted red line are the simulation results of the linear model. The identification plot shows that both models approximate the overall trend very well, but the linear model fails to approximate the PRBS dynamics when compared to the tensorial model.

Figure 7.10 shows the performance of the identified models on the validation signal, which is a step input on the raw-material feed rate. Often, the controller input is in the form of step signals, therefore the step signal is used for the validation purpose. Plot shows that both models follows the trend very well, but both models failed to approximate the steady state gain in some

zone. The reduced order tensorial model performed better in three zones whereas the reduced order linear model did well only in two zones. This is possibly due to the two reasons. First, this is a distributed system and the identification signal is designed by considering the average time constant of the complete glass furnace and it was not designed to approximate the four sensor locations alone. The second reason for the mismatch of the final gain is that these reduced order models could not capture $> 70\%$ of the projection energy. One can expect smaller offset if the approximation order of the reduced model is higher. Unfortunately, due to the stability problem associated with the identification of tensorial models, the approximation order can not be increased above 6^{th} for the tensorial reduced model. Nevertheless, for the size and involved complexity in the glass manufacturing process, even the current results seems to be very interesting.

7.6 Stability test for Tensorial systems

In section 7.2.2, we discussed that higher order approximations of state evolutions result in systems of the form,

$$\dot{x} = A_1 x + A_2 (x \otimes x) + \ldots + A_N (x \otimes \ldots \otimes x); \quad x(0) = x_0 \tag{7.11}$$

where $x \in \mathcal{D} \subset \mathbb{R}^n$. For the first order case (n =1), this simplifies to an ordinary homogenous polynomial equation as,

$$\dot{x} = a_1 x + a_2 x^2 + \ldots + a_N x^N. \tag{7.12}$$

In this section we verify the stability of the fixed points of the autonomous system in (7.11). First, we will focus on the quadratic case, i.e. $n = 2$. Also make the observation that (7.11) defines multiple fixed points x^* as the equation

$$0 = A_1 x + A_2 (x \otimes x) + \ldots + A_N (x \otimes \ldots \otimes x); \tag{7.13}$$

generally has multiple solutions. In fact, depending on the dimension of x, the system (7.11) may have limit cycles, chaotic behavior, etc.

The notion of stability of polynomial systems is addressed here using Lyapunov stability criterion and is verified numerically based on the tools from Linear Matrix Inequalities (LMI) and semi definite programming.

Definition 7.6.1 Let $x^* = 0$ be a fixed point of (7.11). Call x^* Lyapunov stable, if $\forall \epsilon > 0$, $\exists\ \delta > 0$ such that whenever x_0 satisfies $||x_0 - x^*|| < \delta$ then

$||x(t;x_0)|| < \epsilon, \forall\ t \geq 0$. Here, $x(t;x_0)$ is a solution of (7.11). This implies that for a fixed point x^*, if system trajectories start within a circle of radius $\delta > 0$ of the initial condition x_0 then they stay within the circle of radius $\epsilon > 0$, for all time $t \geq 0$.

It is well known that x^* is Lyapunov stable if there exists a non-negative function $V : \mathcal{D} \to \mathbb{R}$ continuous in an open set $\mathcal{D} \subset \mathbb{R}^n$ that contains x^* such that V is decreasing along trajectories $x(t;x_0)$ of (7.11) for all $x_0 \in \mathcal{D}$. Lyapunov function is usually interpreted in terms of energy of a system which is a positive function of the state of the system and is decreasing over time. A quadratic form of Lyapunov function can be expressed as,

$$V(x) = x^\top X x; \quad \text{where,} \quad X = X^\top > 0. \tag{7.14}$$

then the condition, $\frac{d}{dt}V(x) \leq 0$ implies

$$\frac{d}{dt}V\left(x(t)\right) = \frac{dV}{dx}(x(t))\dot{x}(t) = \left[\nabla V(x(t))\right]^\top \dot{x}(t) \leq 0; \quad \forall t \geq 0, \tag{7.15}$$

or equivalently,

$$\dot{V}(x) = \dot{x}^\top X x + x^\top X \dot{x}\ \leq 0, \quad \forall t \geq 0. \tag{7.16}$$

Theorem 7.6.1 *If there exists $X = X^\top$ that satisfies the Linear Matrix Inequalities,*

$$\begin{array}{rcl} X & > & 0 \\ \begin{bmatrix} A_1^\top X + X A_1 & X A_2 \\ A_2^\top X & 0 \end{bmatrix} & \leq & 0. \end{array} \tag{7.17}$$

then the origin $x^* = 0$ is a fixed point of the quadratic system

$$\dot{x} = A_1 x + A_2(x \otimes x) \tag{7.18}$$

is a stable fixed point of the quadratic system .

Proof: Suppose (7.17) holds. Claim is that $V(x) = x^\top X x$ is the

Lyapunov function. Indeed, $X > 0$ implies $V \geq 0$ and

$$\begin{aligned}\frac{d}{dt}V\left(x(t)\right) &= \dot{x}^\top X x + x^\top X \dot{x}, \\ &= \left[(x \otimes x)^\top A_2^\top + x^\top A_1^\top\right] X x + x^\top X \left[A_1 x + A_2 (x \otimes x)\right] \\ &= x^\top [A_1^\top X + X A_1] x + [x \otimes x]^\top A_2^\top X x + x^\top X A_2 (x \otimes x) \\ &= \begin{bmatrix} x \\ x \otimes x \end{bmatrix}^\top \begin{bmatrix} A_1^\top X + X A_1 & X A_2 \\ A_2^\top X & 0 \end{bmatrix} \begin{bmatrix} x \\ x \otimes x \end{bmatrix} \leq 0, \quad \forall x, \end{aligned} \tag{7.19}$$

Lyapunov stability condition in (7.15) is therefore implied by $X > 0$ and,

$$\begin{bmatrix} A_1^\top X + X A_1 & X A_2 \\ A_2^\top X & 0 \end{bmatrix} \leq 0.$$

■

More generally, for the system (7.11) we have,

Theorem 7.6.2 *If there exists $X = X^\top$ that satisfies the Linear Matrix Inequalities,*

$$\begin{aligned} X &> 0 \\ \begin{bmatrix} A_1^\top X + X A_1 & X A_2 & \cdots & X A_N \\ A_2^\top X & 0 & \cdots & 0 \\ \vdots & \vdots & \vdots & \vdots \\ A_N^\top X & 0 & \cdots & 0 \end{bmatrix} &\leq 0. \end{aligned} \tag{7.20}$$

then the origin $x^* = 0$ is a stable fixed point of the quadratic system (7.11)*.*

Proof: The proof follows the same line of reasoning as the proof of theorem 7.6.1. Indeed (7.19) now generalizes to,

$$\frac{d}{dt}V(x(t)) = \begin{bmatrix} x \\ x \otimes x \\ \vdots \\ x \otimes \ldots \otimes x \end{bmatrix}^\top \begin{bmatrix} A_1^\top X + X A_1 & X A_2 & \cdots & X A_N \\ A_2^\top X & 0 & \cdots & 0 \\ \vdots & \vdots & \vdots & \vdots \\ A_N^\top X & 0 & \cdots & 0 \end{bmatrix} \begin{bmatrix} x \\ x \otimes x \\ \vdots \\ x \otimes \ldots \otimes x \end{bmatrix} \leq 0.$$

■

For the discrete form of (7.11) following theorem are useful.

Theorem 7.6.3 *If there exists $X = X^\top$ that satisfies the Linear Matrix Inequalities,*

$$\begin{aligned} X &> 0 \\ \begin{bmatrix} A_1^\top X A_1 - X & A_1^\top X A_2 \\ A_2^\top X A_1 & A_2^\top X A_2 \end{bmatrix} &\leq 0. \end{aligned} \tag{7.21}$$

then the origin $x^* = 0$ is the stable fixed point of the quadratic system

$$x(k+1) = A_1 x(k) + A_2 \left(x(k) \otimes x(k)\right); \quad x\left(0\right) = x_0 \tag{7.22}$$

and n=2.

Proof: The proof is similar to the proof of 7.6.1 and is obtained by substituting (7.22) in the discrete version of (7.15), where we need that $V(x) \geq 0$ and

$$V(x(k+1)) - V(x(k)) \leq 0. \tag{7.23}$$

Substituting (7.22) in (7.23) gives,

$$\begin{aligned} V(x(k+1)) - V(x(k)) &= \left[A_1 x + A_2(x \otimes x)\right]^\top X \left[A_1 x + A_2(x \otimes x)\right] - x^\top X x \leq 0, \\ &= \begin{bmatrix} x \\ x \otimes x \end{bmatrix}^\top \begin{bmatrix} A_1^\top X A_1 - X & A_1^\top X A_2 \\ A_2^\top X A_1 & A_2^\top X A_2 \end{bmatrix} \begin{bmatrix} x \\ x \otimes x \end{bmatrix} \leq 0, \end{aligned}$$

■

Theorem 7.6.4 *If there exists $X = X^\top$ that satisfies the Linear Matrix Inequalities,*

$$\begin{aligned} X &> 0 \\ \begin{bmatrix} A_1^\top X A_1 - X & A_1^\top X A_2 & \cdots & A_1^\top X A_N \\ A_2^\top X A_1 & A_2^\top X A_2 & \cdots & A_2^\top X A_N \\ \vdots & \vdots & \vdots & \vdots \\ A_N^\top X A_1 & A_N^\top X A_2 & \cdots & A_N^\top X A_N \end{bmatrix} &\leq 0. \end{aligned} \tag{7.24}$$

then the origin $x^* = 0$ is a stable fixed point of the general nonlinear system

$$x(k+1) = A_1 x(k) + A_2 \left(x(k) \otimes x(k)\right) + \ldots + A_N (x(k) \otimes \ldots \otimes x(k)); \tag{7.25}$$

Proof: The proof is similar to the proof of 7.6.3 and is obtained by substituting (7.25) with n terms in discrete version of (7.15). ■

Remark 7.6.1 The stability results provide sufficient condition only. IF $N = 1$, the conditions are necessary as well.

Remark 7.6.2 All the proofs from 7.6.1 to 7.6.4 rely on the existence of quadratic Lyapunov functions. Conditions for other type of Lyapunov functions will be different.

Remark 7.6.3 The Lyapunov stability proofs are valid for the stability of the fixed point $x^* = 0$ only. There is no claim on general stability of the systems (7.11) or (7.25), or claims on stability of other fixed points.

Remark 7.6.4 The Lyapunov stability condition in theorem 7.6.2 for the continuous tensorial system in (7.11) or the equivalent condition in 7.6.1 for $n = 2$, are not strictly definite, i.e. the corresponding Lyapunov function is not strictly decreasing, it is rather non increasing function. Such a non decreasing function do not guarantee the asymptotic stability of (7.11). Another implication of such a semi-definite condition is the numerical problems that might arise to find a $X = X^\top > 0$. Moreover, for such a semi-definite inequality, strong duality does not hold (Staler's constraint qualification does not hold). It might be possible to transfer such a semi-definite problem into a definite one by using any other Lyapunov function, as suggested in the work of Parrilo (2000) (chapter 7).

Remark 7.6.5 If $x^* \neq 0$ is a fixed point of a system of form

$$\dot{x} = A_0 + A_1 x + A_2(x \otimes x) + \ldots + A_N(x \otimes \ldots \otimes x) \tag{7.26}$$

then one can easily construct matrices $B_1, \ldots, B_N$ such that with the state transformation $\overline{x} := x - x^*$ we have that (7.26) is equivalent to

$$\dot{\overline{x}} = B_1\overline{x} + B_2\overline{x} \otimes x + \ldots + B_N(\overline{x} \otimes \ldots \otimes \overline{x}) \tag{7.27}$$

where $B_0 = 0$, and where $\overline{x}^* = 0$ is a fixed point. A sufficient LMI test to infer stability of x^* in (7.26) can now be performed for the system (7.27) by using the result, of Theorem 7.6.2. Indeed,

$$\begin{aligned}\overline{V}(\overline{x}) :=& \overline{x}^\top X \overline{x} \\ =& (x - x^*)^\top X (x - x^*) \\ =& x^\top X x - {x^*}^\top X x - x^\top X x^* + {x^*}^\top X x^*\end{aligned}$$

is a Lyapunov function for the origin of (7.27) if and only if

$$V(x) := (x - x^*)^\top X (x - x^*)$$

is a Lyapunov function in a neighborhood of x^* for (7.26).

7.7 Dissipativity of Tensorial systems

Dissipativity is a system property that generalizes the notion of stability for systems with inputs. Physical interpretation of dissipativity is that the amount of the energy released by a system never exceeds the sum of energy that is stored in the system and that has been supplied to it externally. The part of energy that is not available for direct use is dissipated in the form of heat, friction, increased internal energy or entropy. Study of Dissipativity of LTI system allows analysis of stability, stabilization, robustness and for control design. Mathematical framework for dissipativity can be expressed in the form of Linear Matrix Inequalities.

Based on the notion of Lyapunov stability as expressed in section 7.6, first the conditions for the dissipativity of LTI systems are established in this section. This is then extended to the tensorial system introduced in section 7.2.2 and further investigated for stability at a fixed point in section 7.6. The tools from Linear Matrix Inequalities (LMIs) are used here again. The LMI conditions are expressed in terms of the positive real matrix $X = X^\top > 0$ which can be computed using tools from semi definite programming.

Consider a nonlinear system Σ of the form

$$\Sigma : \begin{cases} \dot{x} = & f(x,u) \\ y = & g(x,u) \end{cases} \tag{7.28}$$

with $x(t) \in \mathbb{R}^n$ are states, $u(t) \in \mathbb{U}$ are inputs and $y(t) \in \mathbb{Y}$ are the outputs. Suppose that $\mathcal{S}(u,y)$ is a supply rate, i.e. $\mathcal{S} : \mathbb{U} \times \mathbb{Y} \to \mathbb{R}$ indicates with $\mathcal{S}(u(t),y(t))$, is the amount of power delivered to the system at time instant t.

Dissipativity of Σ with respect to the supply function $\mathcal{S}(u,y)$ is defined as follows:

Definition 7.7.1 A system Σ in (7.30) is dissipative with respect to the supply rate $\mathcal{S}(u,y)$ if $\exists\ V : \mathbb{R}^n \to \mathbb{R}$, such that,

$$V(x(t_0)) + \int_{t_0}^{t_e} \mathcal{S}(u(\tau),y(\tau))d\tau \geq V(x(t_e)); \tag{7.29}$$

holds for all $t_0 \leq t_e$ and for all trajectories $(u(t),y(t),x(t))$ that satisfy (7.28).

Now suppose that (7.28) is a LTI system of the form,

$$\Sigma : \begin{cases} \dot{x} = & Ax + Bu \\ y = & Cx + Du \end{cases} \tag{7.30}$$

and $\mathcal{S}(u, y)$ is a supply function in quadratic form, i.e.

$$\mathcal{S}(u, y) = \begin{bmatrix} u \\ y \end{bmatrix}^\top \begin{bmatrix} Q & S \\ S^\top & R \end{bmatrix} \begin{bmatrix} u \\ y \end{bmatrix} \tag{7.31}$$

then we have the following characterization.

Theorem 7.7.1 *The LTI system Σ of the form* (7.30) *is dissipative with resect to the quadratic supply $\mathcal{S}$ as in* (7.31)*, if and only if there exists $X = X^\top$ that satisfies the Linear Matrix Inequality*

$$\mathcal{F}(X) := \begin{bmatrix} A & B \\ I & 0 \end{bmatrix}^\top \begin{bmatrix} 0 & X \\ X & 0 \end{bmatrix} \begin{bmatrix} A & B \\ I & 0 \end{bmatrix} - \begin{bmatrix} 0 & I \\ C & D \end{bmatrix}^\top \begin{bmatrix} Q & S \\ S^\top & R \end{bmatrix} \begin{bmatrix} 0 & I \\ C & D \end{bmatrix} \leq 0 \tag{7.32}$$

Proof: Assume that the storage function in definition 7.7.1 is the quadratic formulation $V(x) = x^\top X x$. ■

The proof of the theorem holds only for the storage functions of the quadratic forms, i.e. $V(x) = x^\top X x$. The LMI condition in Theorem 7.7.1 is worked out here. Note that the dissipation inequality (7.29) can be written as

$$\lim_{t_e \downarrow t_0} \frac{V(x(t_e)) - V(x(t_0))}{t_e - t_0} \leq \lim_{t_e \downarrow t_0} \int_{t_0}^{t_e} \mathcal{S}(u(\tau), y(\tau)) d\tau; \quad \forall x, u, y \quad \forall t_0 \leq t_e \tag{7.33}$$

Using notions from calculus, for a small time window (7.33) can be equivalently written in a continuous form as,

$$\left[\nabla V(x)\right]^\top f(x, u) \leq \mathcal{S}(u, y); \quad \forall x, u, y, \tag{7.34}$$

For LTI system in (7.30) and quadratic supply in (7.31), this is equivalent to:

$$2\left[Xx\right]^\top \left[Ax + Bu\right] \leq \begin{bmatrix} u \\ y \end{bmatrix}^\top \begin{bmatrix} Q & S \\ S^\top & R \end{bmatrix} \begin{bmatrix} u \\ y \end{bmatrix} \quad \forall x, u \tag{7.35}$$

Which, in fact, (7.35) implies condition (7.32). Hence a dynamical system in (7.28) is dissipative with respect to $\mathcal{S}(u, y)$ if and only if (7.34) holds. The

dissipativity condition of theorem 7.35 is based on the the lecture note, see Scherer and Weiland (2009). Due to the linearity of state space matrices, the results from theorem 7.7.1 can be extended to the tensorial system introduced in the section 7.2.2 which is presented here again. Thus, consider the system

$$\Sigma : \begin{cases} \dot{x} = & A_1 x + A_2(x \otimes x) + B_1 u + B_2(u \otimes u) + L(x \otimes u); \quad x(0) = x_0, \\ y = & C_1 x + C_2(x \otimes x) + D_1 u + D_2(u \otimes u) + M(x \otimes u); \end{cases} \tag{7.36}$$

Suppose, again $\mathcal{S}(u, y)$ is a quadratic supply function as in (7.31),

Theorem 7.7.2 *For a tensorial system of the form* (7.36)*, suppose that there exists* $X = X^\top$ *such that*

$$\mathcal{F}(X) \leq 0, \tag{7.37}$$

with $\mathcal{F}(X)$ *defined as the affine function,*

$$\begin{aligned} &\begin{bmatrix} A_1^\top & I \\ A_2^\top & 0 \\ B_1^\top & 0 \\ B_2^\top & 0 \\ L^\top & 0 \end{bmatrix} \begin{bmatrix} 0 & X \\ X & 0 \end{bmatrix} \begin{bmatrix} A_1 & A_2 & B_1 & B_2 & L \\ I & 0 & 0 & 0 & 0 \end{bmatrix} \\ &- \begin{bmatrix} 0 & C_1^\top \\ 0 & C_2^\top \\ I & D_1^\top \\ 0 & D_2^\top \\ 0 & M^\top \end{bmatrix} \begin{bmatrix} Q & S \\ S^\top & R \end{bmatrix} \begin{bmatrix} 0 & 0 & I & 0 & 0 \\ C_1 & C_2 & D_1 & D_2 & M \end{bmatrix} \end{aligned} \tag{7.38}$$

then (7.36) *is dissipative with respect to* $\mathcal{S}$*.*

Proof: It suffices to prove that, $V(x) = x^\top X x$ is a storage function that satisfies (7.34). ■

Similar to the theorem 7.7.1 the proof of theorem 7.7.2 is valid for the quadratic storage function alone. The LMI condition in theorem 7.7.2 is obtained in a similar way to the LTI case explained in the last paragraph. The quadratic supply function in (7.31) is modified to accommodate the

dynamics of tensorial system of the form (7.36) as,

$$\mathcal{S}(u,y) = \begin{bmatrix} x \\ x\otimes x \\ u \\ u\otimes u \\ x\otimes u \end{bmatrix}^{\top} \begin{bmatrix} 0 & C_1^{\top} \\ 0 & C_2^{\top} \\ I & D_1^{\top} \\ 0 & D_2^{\top} \\ 0 & M^{\top} \end{bmatrix} \begin{bmatrix} Q & S \\ S^{\top} & R \end{bmatrix} \begin{bmatrix} 0 & 0 & I & 0 & 0 \\ C_1 & C_2 & D_1 & D_2 & M \end{bmatrix} \begin{bmatrix} x \\ x\otimes x \\ u \\ u\otimes u \\ x\otimes u \end{bmatrix} \tag{7.39}$$

The dissipativity condition in (7.34) for the tensorial system in (7.36) is given by replacing the dynamics of LTI system in (7.35) by the tensorial system and it is given by,

$$\begin{aligned}
&\Rightarrow \left[\nabla V(x)\right]^{\top} f(x,u) - \mathcal{S}(u,y) \\
&= 2\left[Xx\right]^{\top} A_1 x + A_2(x\otimes x) + B_1 u + B_2(u\otimes u) + L(x\otimes u) \\
&- \begin{bmatrix} u \\ y \end{bmatrix}^{\top} \begin{bmatrix} Q & S \\ S^{\top} & R \end{bmatrix} \begin{bmatrix} u \\ y \end{bmatrix} \\
&= \begin{bmatrix} x \\ x\otimes x \\ u \\ u\otimes u \\ x\otimes u \end{bmatrix}^{\top} \begin{bmatrix} A_1^{\top} & I \\ A_2^{\top} & 0 \\ B_1^{\top} & 0 \\ B_2^{\top} & 0 \\ L^{\top} & 0 \end{bmatrix} \begin{bmatrix} 0 & X \\ X & 0 \end{bmatrix} \begin{bmatrix} A_1 & A_2 & B_1 & B_2 & L \\ I & 0 & 0 & 0 & 0 \end{bmatrix} \begin{bmatrix} x \\ x\otimes x \\ u \\ u\otimes u \\ x\otimes u \end{bmatrix} \\
&- \begin{bmatrix} x \\ x\otimes x \\ u \\ u\otimes u \\ x\otimes u \end{bmatrix}^{\top} \begin{bmatrix} 0 & C_1^{\top} \\ 0 & C_2^{\top} \\ I & D_1^{\top} \\ 0 & D_2^{\top} \\ 0 & M^{\top} \end{bmatrix} \begin{bmatrix} Q & S \\ S^{\top} & R \end{bmatrix} \begin{bmatrix} 0 & 0 & I & 0 & 0 \\ C_1 & C_2 & D_1 & D_2 & M \end{bmatrix} \begin{bmatrix} x \\ x\otimes x \\ u \\ u\otimes u \\ x\otimes u \end{bmatrix} \\
&= \begin{bmatrix} x \\ x\otimes x \\ u \\ u\otimes u \\ x\otimes u \end{bmatrix}^{\top} \mathcal{F}(X) \begin{bmatrix} x \\ x\otimes x \\ u \\ u\otimes u \\ x\otimes u \end{bmatrix} \\
&\leq 0
\end{aligned} \tag{7.40}$$

Condition in (7.40) implies condition in Theorem (7.7.2).

Remark 7.7.1 The definition of dissipativity in 7.7.1 also holds for nonlinear systems. A quadratic storage function is $V(x)$ is found for the given supply function under the condition (7.38).

Remark 7.7.2 The LMI conditions presented here are for quadratic supply functions. For other supply functions the LMI conditions wil be different.

Remark 7.7.3 The LMI conditions presented in this section has assumed quadratic storage function. For other form of storage function, e.g. $V(x) = \begin{bmatrix} x \\ x \otimes x \end{bmatrix} [X] \begin{bmatrix} x \\ x \otimes x \end{bmatrix}$ the LMI conditions need to be reformulated.

7.8 Conclusions

In this chapter we have proposed a new model reduction method and demonstrated its application on two large scale industrial processes. The proposed method is promising and is well suited for the identification of large scale processes where complexity reduction by using physical insights alone is not possible. The proposed method is rigorously formulated and it shows the relation between two seemingly different approaches of model reduction, viz. identification type of approach as proposed in this chapter and an approach involving Galerkin type of projection of model equations. The dependence of the method on the state information of full order model alone makes it applicable to other large scale processes. The proposed technique eliminates the expensive and laborious programming efforts that are required for the model order reduction techniques based on Galerkin projections. Due to the fast computations, the inferred reduced order models can be used as a substitute to the expensive identification tests that are carried out in a plant. The proposed method has few pitfalls. The dependence of the presented approach on the (state) data makes the identified reduced models difficult to extrapolate beyond the identification domain. As explained in the section 7.2, the obtained reduced order models can lead to numerically diverging solutions. This problem can be partly avoided by using fewer parameters in the tensorial model. Towards this purpose, methods to detect the Lyapunov stability of continuous and discrete tensorial systems at a fixed point is presented. Tools from theory of Linear Matrix Inequalities (LMI) and semi-definite programming are used to formulate a sufficient conditions to detect the Lyapunov stability. Along with the stability analysis, dissipativity of the tensorial systems for a quadratic supply function and a storage function is also presented. The linearity of system parameters in the tensorial model allows extension of classical stability and dissipativity theory from linear systems to tensorial systems. Similar to the stability and dissipativity analysis, extension of other notions like observability, controllability,

robustness, etc. from LTI system theory to the tensorial systems should be pursued in future.

8

Conclusions and Recommendations for Future Research

In this chapter we present the concluding remarks based on the research presented in this thesis. Along with the conclusions, some research directions for the future are also presented.

8.1 Contributions

The main contributions of this thesis are listed here and they are discussed in greater detail in the subsequent subsections.

- Presentation of a model reduction problem as an identification problem.
- A novel data based method to infer a reduced order nonlinear model is presented.
- Methods to characterize the stability and dissipativity of nonlinear systems beloning to the class of tensorial (multi-variable polynomial) systems is presented.
- A novel data based method to identify reduced order - linear parameter varying (RO-LPV) models is presented.
- A novel method to detect bifurcations in large scale applications using reduced order models is presented.

- An investigation of the proposed model reduction methods on a large scale benchmark example of an industrial glass manufacturing process is presented.

8.1.1 Identification of reduced order nonlinear models

This thesis has presented a novel data based method for the identification of reduced order nonlinear models. The model reduction problem for non-linear processes is formulated as a parameter estimation problem. Based on the state information, the first step of the proposed model reduction technique involve a separation of spatial and temporal patterns. In the second step, a model structure of tensorial (multi-variable polynomial) expansions is selected to describe linear or non-linear time evolutions of modal coefficients. The proposed model reduction strategy explores the observation made in section 3.2 and further explored in Chapter 7, that the POD modal coefficients can be viewed as the states of a reduced order model that needs to be identified. With the knowledge of the POD modal coefficients from the spectral decomposition of the system solutions and with the knowledge of process inputs, different model structures are proposed in Chapter 7 to relate the input and the states (i.e the modal coefficients). In particular, a tensorial (multi-variable polynomial) representation of the vector field of the system is proposed. This generalizes the usual LTI setting in a nice manner to a different model class of nonlinear systems. An ordinary least squares method is then used to efficiently estimate the model parameters. The simplicity of the proposed method gives computationally very efficient linear and non-linear low order process models for large scale processes.

The proposed method is promising and is well suited for the identification of very large scale processes where complexity reduction by using physical insights alone is not possible. The proposed method does not need access to the governing model equations and the state information of the full order model and the process input data is enough to infer reduced order nonlinear models. The proposed method is rigorously formulated and it shows the relation between two seemingly different approaches of model reduction based on identification as presented in this thesis and the classical POD approach involving Galerkin projections of model equations. In fact, for a linear discrete time system, one can estimate the system parameters (state space matrices) of the reduced model consistently. The method is of generic nature and can be easily applied to infer reduced order linear and non-linear models from

large scale process models which are often used in process industry. The proposed technique, in principle, is independent of the model equations, and allows to circumvent the expensive and laborious efforts required in classical Galerkin type of equation based model order reduction. Due to the high computational efficiency, the inferred reduced order models can be used as a substitute to the expensive identification tests that are carried out in a plant in order to identify a control relevant black box model.

The proposed model reduction technique has some drawbacks, e.g. the resultant tensorial reduced order model can become unstable. Moreover, when compared to the POD implementation of model equation, the reduced tensorial models offer limited possibility of extrapolation.

8.1.2 Characterization of stability and dissipativity of Tensorial systems

In Chapter 7 a method to identify reduced order non linear models belonging to the class of tensorial (multi-variable polynomial) expansions is presented. In general, it is very difficult to identify a system belonging to the general class of nonlinear systems from input-output data alone. But in the model reduction framework presented in Chapter 7, the states (POD modal coefficients) are known, which makes it possible to identify a model structure in the form of tensorial systems. The identified model parameters fit very well to the data, but sometimes, simulations of identified tensorial models may lead to a non converging solution. It was therefore of interest to investigate the stability of tensorial systems. As the model parameters of a tensorial system appear linearly in the model equations, it becomes easy to extend the notions from LTI system theory to tensorial systems. Using the tools from Linear Matrix Inequalities, sufficient conditions for Lyapunov stability of a fixed point of continuous and discrete tensorial systems are formulated. Along with the conditions for Lyapunov stability, a sufficient condition to guarantee the dissipativity of a tensorial system for a quadratic external supply function is also presented. These results show that tensorial systems are an important class of nonlinear systems with a special feature of 'linear in parameter'.

8.1.3 Identification of reduced order linear parameter varying models

In this thesis one more novel procedure for obtaining low dimensional models of large scale, non-linear, fluid flow systems is proposed. The proposed method formulates the model reduction problem as a parameter estimation problem. The approach is based on the combination of methods of proper orthogonal decomposition, black box system identification techniques and nonlinear spline based blending of the LTI black box models to create a reduced order linear parameter varying (RO-LPV) model. Spectral decompositions of system solutions is used to infer dominant temporal patterns. The dominant patterns that are obtained as result of spectral decompositions are then treated as the outputs of an unknown LTI model that is to be identified. A model structure of the LTI state space form is subsequently fitted to these dominant temporal patterns using subspace state space identification techniques. This process is repeated for various values of the scheduling variable to infer local reduced order models corresponding to each value of scheduling variable. The last step of the proposed model reduction framework involved a weighted blending of the local reduced order LTI models into a reduced order LPV model. The weighted blending is carried out using two different types of splines - orthogonal and trigonometric. The parameters of the spline are estimated by minimizing the output residue between the full order and the RO-LPV model.

The RO-LPV modeling method along with the two spline types, is explained with more detail in Chapter 6. The proposed method does not need the usual Galerkin type projection of equation residuals to obtain the reduced order model and the method is of generic nature. Only the information of the states of the full order model and the process inputs is sufficient to infer reduced order models and therefore the proposed approach can work in the absence of access to the governing equations. The proposed method is of empirical nature and gives computationally very efficient low order process models for large scale processes which are modeled using Computational Fluid Dynamic (CFD) tools. The efficiency of the proposed approach is illustrated on a benchmark problem of an industrial glass manufacturing process where the process non-linearity and non-linearity arising due to the corrosion of refractory materials is approximated using the proposed reduced order linear parameter varying model. The practical aspects of the method are also discussed in Chapter 6.

The proposed RO-LPV modeling technique is intuitional and it is close to the real life situation when changes in the scheduling variables excite the process nonlinearities. The proposed RO-LPV identification technique can also be used to identify not only reduced order LPV models but also for identifying LPV models from input-output data obtained by excitation of actual plant.

The 'linear in system parameters' structure of the proposed RO-LPV model offers similar advantages as those of an LTI system in terms of extension of notions of LTI system theory like analysis of stability, dissipativity, robustness, observer design, controller design, etc. Although not presented in this thesis, the analysis of Lyapunov stability of RO-LPV model obtained by linear combination of LTI models at a fixed point could be on the same line of deriving the Lyapunov stability conditions for tensorial systems which is presented in Chapter 7. However, RO-LPV model obtained by nonlinear splines that are used in this thesis, the similar analysis will need extra efforts.

8.1.4 Detection of bifurcations in large scale processes using reduced order models

This thesis has proposed a hybrid detection framework, which, based on state or output residue between plant (full order model) and the reduced order model, can detect the occurrences of bifurcations. The proposed mechanism suggests an optimal reduced order model to approximate the process exhibiting bifurcations using reduced order models.

Historically, bifurcations are viewed as a discontinuous change in system solutions for a continuous change in system parameters. Large scale processes often show significant sensitivity of the process solutions to a small, continuous changes in process parameters. Such a behavior is difficult to characterize as a bifurcation in terms of changes in eigen-values of linearizations. Usually bifurcation effects are studied for changes in physical parameters of a governing model equation. It is shown in this thesis that similar to the changes in physical process parameters, changes in the geometric parameter of a process equipment in the form of a physical boundary can also lead to bifurcations. It is difficult to detect the bifurcations in real time in large scale applications using the rigorous process models due to the large state dimensions and slow computations associated with the rigorous process models. To overcome this problem, in this thesis, we developed a strategy to detect the bifurcations

exhibited by a full order model using the combination of detection mechanism based on reduced order models. Chapter 4 and 5 have presented the details of this method.

Moreover, it is shown in this thesis that the reduced order model obtained by using spectral decompositions of system solutions and subsequent projections of model equations on the space spanned by dominant patterns becomes obsolete as result of bifurcations of the system solutions. Therefore, to approximate the behavior of a large scale system exhibiting bifurcations, a framework employing combination of reduced order models and a hybrid detection mechanism is proposed in this thesis. In the proposed framework, the reduced models can be inferred by any suitable model reduction technique. For example, reduced models can be obtained by using Galerkin projection of equation residuals on the dominant subspace, as shown in Chapter 4 or by using an identification based approach that is proposed in Chapter 5. Two types of hybrid detection mechanisms are proposed here - a static and a dynamic one. The hybrid detection mechanisms, based on the state or output residue information between the plant (full order model) and the reduced order model, detects the operation regime of the process and suggests an optimal reduced order model.

In particular, the results of the overall framework involving reduced order models and the detection mechanism are presented on the benchmark examples of a tubular reactor and an industrial glass manufacturing process. The benchmark applications are explained in Chapter 2. The benchmark examples serve as full order models which are modeled using tools from Computational Fluid Dynamics (CFD). The bifurcation effect as result of changes in the Damkohler number for a tubular reactor is presented in Chapter 4. It is shown that the reduced order models along with either of the detection mechanism can approximate the bifurcations exhibited by the full order model. An investigation of the corresponding wave patterns in the reactor shows the difficulty to capture the transition from lower to higher state in the reduced model.

In Chapter 5, the applicability of the proposed detection mechanisms is demonstrated on an industrial glass manufacturing process. The effect of corrosion of the throat wall in a glass furnace results into a bifurcation type of behavior. This behavior was approximated using the framework employing reduced order models and the dynamic detection mechanism. The proposed framework was able to detect the occurrence of bifurcations in the flow patterns in the 2D model of a glass furnace. The model reduction method, that

is presented, employed LTI reduced order models. The LTI reduced order models are obtained by a two step mechanism involving spectral decomposition of system solution and subsequent approximation of temporal patterns using the tools from system identification area.

8.1.5 Application of developed model reduction techniques on large scale benchmarks

This thesis has presented a few novel model reduction techniques. As mentioned in the objectives of this thesis in Chapter 1, the techniques that are investigated here are motivated by their applicability on large scale industrial examples. Towards this goal, two benchmark examples of industrial chemical processes are considered in this thesis. The benchmark examples are presented in Chapter 2. Although every real life application has unique features, the processes that are considered in this thesis have in common that they belong to the class of distributed parameter systems and are modeled using Computational Fluid Dynamic (CFD) tools. The two benchmark examples that are considered here is a 1D tubular reactor and an industrial glass manufacturing process.

Due to its small system order, for the tubular reactor, it is easy to verify the applicability of a developed model reduction techniques. The tubular reactor is used as a benchmark to study the bifurcation effect in Chapter 4 and in Chapter 7 to study the applicability of the reduced order model in the form of a tensorial system.

The benchmark example of glass manufacturing is more complex than the tubular reactor. The geometry considered here depicts a 2D slice (i.e. small width) taken along the length of 3D industrial glass furnace. In Chapter 5, this 2D benchmark of glass furnace is used to develop a data based mechanism to detect the bifurcations of flow patterns in a glass furnace using reduced order models. In particular, the effect of changes in the geometry of the furnace wall is studied in more detail. In Chapter 6 the benchmark glass furnace 2D model is used to develop a (state) data based Reduced Order-Linear Parameter Varying (RO-LPV) framework. The nonlinear effect due to corrosion of the throat wall, and process nonlinearity as result of changes in working point, are approximated using a RO-LPV model. In Chapter 7, the process is used to study the applicability of a reduced order modeling technique which resulted into a model structure in the form of a tensorial

system.

It is observed in this thesis that it is difficult to find the linear range of process operation of a glass furnace. The difficulty arises due to the complex nature of the process, which involved various physical effects. Therefore, it is better to identify a nonlinear reduced order model of glass furnace than a linear one.

8.1.6 General conclusions

This thesis aimed to address the objectives mentioned in the first Chapter. In the following we summarize the conclusions with respect to the thesis objectives.

- *Reduction in model complexity.*

  This thesis has addressed the complexity of process models in Chapters 4, 5, 6 and in Chapter 7.

- *Reduction in model order.*

  The methods proposed in this thesis resulted in large reduction of system dimension, from 3000 to 10 state variables for a 2D benchmark example of a glass furnace.

- *Maintaining the model accuracy.*

  The model reduction techniques that are presented here with increasing accuracy are - Model reduction technique resulting into reduced order LTI model (Chapter 5), model reduction technique resulting into RO-LPV model (Chapter 6), model reduction technique resulting into tensorial models (Chapter 7).

- *Approximation of process nonlinearities.*

  The approximate models; RO-LPV and reduced order tensorial models that are investigated in this thesis can approximate the process nonlinearity in a certain nonlinear range of process operation.

- *Improved computational efficiency.*

  As all the model reduction techniques that are proposed here are linear in parameters and have a small system order, they all are computationally more efficient (>1000 times) than the full order CFD model.

- *To develop approximate process models which are optimal in some sense.*

  The model reduction techniques proposed here are based on spectral decompositions of the system solutions which gives spatial and temporal patterns which are optimal in representing the system solutions.

- *To develop a model approximation technique which can approximates bifurcation behavior nearby critical parameter values as exhibited by the original process model and to detect its occurrence.*

  The techniques proposed in Chapter 4 and 5 addressed the issue of detection of bifurcations using reduced order models for large scale processes.

- *To infer an approximate model in the absence of an explicit mathematical expressions of the model.*

  The techniques presented in this thesis are able to infer reduced order models in the absence of access to the governing equation and the techniques can be viewed as an alternate to the model reduction techniques which are based on the physical insight or as an alternative to projection based approach.

- *To develop model approximation techniques with minimum implementation efforts.*

  One of the major advantage of the model reduction techniques proposed in this thesis is that they are (state) data based and need very small programming efforts in comparison to the other model reduction techniques tailored for large scale processes. This translate into less programming efforts and ultimately into an economically less expensive method to apply.

8.2 Scope for Future Research

Based on the research that is carried out during this thesis, a few open research questions and recommendations for the future research are presented in this section. The recommendations are briefly presented here which are explained in more detail in subsequent subsections.

- Further investigation into system theoretic properties of tensorial systems, especially its identification on the line of subspace identification techniques.
- Investigation of the model quality of the different model structures that are proposed in the thesis.
- Synthesis of observer and controller for each type of reduced order model using tools from LMI and semi-definite programming.
- Investigation of identification of reduced order models from the spectral decomposition using High-Order Singular Value Decomposition (HO-SVD) and subsequent system parameter estimation leading to nonlinear tensorial models that are proposed in this thesis.
- Application of proposed techniques on 3D model of glass manufacturing process.
- Investigation of the applicability of the model reduction techniques proposed here on systems which are modeled using Differential Algebraic Equations (DAEs).

8.2.1 Investigation into Tensorial systems

Based on the proposed model reduction method that is presented in Chapter 7, it will be rewarding to further investigate the tensorial system. Tensorial systems allow approximation of process nonlinearity and at the same time their structure is better suited for analytical treatment, i.e. for studying the system theoretic properties and for extension of the notions from the theory of LTI systems. It is of immediate interest to design an observer and a model based controller for such a system. For many real life chemical processes, this can be highly rewarding. The 'linear in parameter' feature of such a system will be exploited in synthesizing an observer and a controller.

On the lines of subspace identification techniques, the identification of tensorial system need to be investigated. As the underlying systems are often stable, it is worth to investigate the possibility of imposing the stability in tensorial system using some regularization tricks.

Application of the model reduction technique resulting into a tensorial structure should be tried on 3D glass model and systems of DAE model form.

8.2.2 Investigation of bifurcations in Large scale system

Based on the results presented in Chapter four, it would be worth to investigate the problem of model reduction by using POD for parameter sensitive processes. To be precise, bifurcation phenomena should be investigated for 2D and 3D model of a tubular reactor. The mathematical formulation of the hybrid detection mechanism using the notions and concepts from *Hybrid Systems Theory* and will further improve the usability of the proposed detection mechanisms. It is also interesting to design a reduced order observer which can guarantee the convergence of the states under parametric uncertainties. As the processes starts oscillating near bifurcating points, from economic point of view, it might be interesting to operate the process close to bifurcating value, provided the process safety is guaranteed.

8.2.3 Reduced order modeling for 3D glass furnace

While presenting the results in this thesis, the benchmark examples that are considered are tubular reactor and a 2D model of industrial glass manufacturing process. It is shown in this thesis that there are different model reduction techniques that can approximate the nonlinear behavior of a 2D model of industrial glass furnace. Extension of these ideas to a 3D model of glass furnace might be easy and can be useful from the point of designing an observer, controller and a dynamic optimizer. A 3D glass furnace model has different flow patterns than a 2D glass furnace model. This might demand changes in the reduced modeling technique that are presented in this thesis. The problem that might arise for a 3D furnace model is its large system order. Data storage, data processing and spectral decomposition can be a difficult task for glass furnace models approximately of order $10^5 - 10^8$.

In Chapter 7, it is shown for the benchmark example of tubular reactor that considering interactions among different dynamic variables (i.e. a multi-variable case) gives a better reduced order tensorial model. This could be attributed to the coupled dynamics of temperature and concentration in a tubular reactor. During the spectral decomposition for a multi-variable data set, the estimated dominant eigenvectors corresponds to the maximum energy with respect to all the variables. This idea can be useful for developing reduced order tensorial models for a 3D glass manufacturing or to any other process, where various correlated variables like pressure, temperature, velocity, thermal conductivity, concentration etc. interacts dynamically.

Availability of reliable reduced order, computationally efficient reduced order models for glass process can be useful for synthesis of model based controller and for dynamic optimization purposes.

8.2.4 Investigate model reduction techniques using HO-SVD and Tensorial systems

High Order - Singular Value Decomposition or HO-SVD (see, Belzen and Weiland (2008)) is a spectral decomposition method suited specifically to a process belonging to a higher (2 or 3) Dimensional geometry. The idea is based on inferring correlated patterns in all spatial directions. As most of the physical geometries in real life are 3D objects, it makes sense to consider HO-SVD for inferring dominant spectral directions. This idea can also be useful for inferring correlated patterns of multi-variable process. Application of model reduction framework from Chapter 7, to the dominant temporal patterns obtained from such a HO-SVD can be interesting from model reduction point of view. Early results in this directions are very encouraging.

8.2.5 Investigation of the model quality

State data-based methods that are proposed in this thesis resulted into reduced models belonging to different class of systems. These models are not thoroughly investigated for preservation of the invariant properties of original model, with respect to stability, robustness, conservation of physical quantities, physical constraints, dissipativity, controllability, observability, achievable closed loop performance etc. Assessment of these properties for the reduced order models that are inferred in this thesis will improve their usability.

8.2.6 Observer and controller design

Often, the full order process models are not an exact representation of the underlying process and therefore the inferred reduced order models also deviate from the actual process behavior. In practice, the discrepancy between a black-box identified model and the plant is compensated by using an observer. Similarly, the discrepancy between reduced order process models and the plant could be compensated by designing the reduced (order) observers.

In future the design of a reduced observed and its closed loop performance should be investigated in further detail.

8.2.7 Some other research topics

- To impose orthogonality during the identification of POD modal coefficients in system identification approach that is proposed in this thesis.
- To investigate the methods for inferring sparse spatial POD basis, which can lead to sparse reduced order models.
- To further investigate the similarity and difference between model reduction by projection and by identification as proposed in this thesis.
- To characterize the parameter sensitivity of a reduced model using POD basis function.

Bibliography

Afanasiev, K., Hinze, M., 2001. Adaptive control of a wake flow using proper orthogonal decomposition. Lect. Notes Pure Appl. Math. 216, 317–332.

Agudelo, M., 2009a. The application of proper orthogonal decomposition to the control of tubular reactors, PhD thesis. Faculty of Engineering, K.U.Leuven (Leuven, Belgium),Lirias number: 246238.

Agudelo, M., 2009b. Positive polynomial constriants for pod-based model predictive controllers. IEEE Transactions on Automatic Control, Special issue on Positive Polynomials in Control 54, 988–999.

Akaike, H., 1974. A new look at the statistical model identification. IEEE Trans. Auto. Cont. 19, 716–723.

Akaike, H., 1997. Factor analysis and aic. Psychometrica 52, 317–332.

Amundson, N., 1970. Berichte Bunsen-Gesel 74, 90.

Antoulas, A., 2005a. Approximation of large-scale dynamical systems, illustrated Edition. Cambridge University Press, London.

Antoulas, A., 2005b. An overview of approximation methods for large-scale dynamical systems. Annual Reviews in Control 29 (2), 181–190.

Aris, R., 1969. On stability criteria of chemical reaction engineering. Chemical Engineering Sceince 24 (1), 149–169.

Astrid, P., 2004. Reduction of Process Simulation Models- A proper Orthogonal Decomposition Approach. PhD thesis, Technical University of Eindhoven.

Astrid, P., Weiland, S., Willcox, K., Backx, A., 2008. Missing point estimation in models described by proper orthogonal decompositions. IEEE Transactions on Automatic Control 53(10), 2237–2251.

Babuska, R., 1998. Fuzzy Modeling for Control. Kluwer Academic.

Backx, A., 2002. Model-Based Glass Melter Control. Chapter 2, pages: 137-155. In Mathematical Simulation in Glass Technology, eds: H.Loch and D.Krause. Springer-Berlin.

Belzen, F. V., Weiland, S., 2008. Reconstruction and approximation of multi-dimensional signals described by proper orthogonal decompositions. IEEE Transactions on Signal Processing 56 (2), 576–587.

Berec, L., 1998. A multi-model method to fault detection and diagnosis:bayesian solution. an introductory treatise. International Journal of Adaptive Control and Signal Processing 12, 81Ũ92.

Bhagwat, A. M., Srinivasan, R., Krishnaswamy, P. R., 2003a. Fault detection during process transitions: A model-based approach. Chemical Engineering Science 58, 309Ũ325.

Bhagwat, A. M., Srinivasan, R., Krishnaswamy, P. R., 2003b. Multi-linear model-based fault detection during process transitions. Chemical Engineering Science 58, 1649–1670.

Bizon, K., Continillo, G., Russo, L., Smula, J., 2007. On pod reduced models of tubular reactor with periodic regimes. Computers and Chemical Engineering 32(6), 1305–1315.

Bos, R., 2006. Monitoring of Industrial Processes using Large Scale First Principles Models. Delft University, Delft.

Butkovskiy, A., 1969. Distributed Control Systems. New York:Elsevier.

Butkovskiy, A., 1982. Green's function and transfer functions handbook. Chichester, NY: Ellis Horwood.

Carvalho, M., Speranskaia, N., Wang, J., Nogueira, M., 1997. Modeling of glass melting furnaces: applications to control, design and operation optimization. Ceramic Transactions 82, 109–135.

Casella, F., Lovera, M., 2008. Lpv/lft modeling and identification: overview, synergies and a case study. Proceedings, IEEE MSC.

Charbonnaud, P., R. F. . M. S., 2001. Process operating mode monitoring: Switching online the right controller. IEEE Transactions on Systems, Man, and CyberneticsŮPart C: Applications and Reviews 31(1), 77Ũ86.

Doedel, E., Chapneys, A., Fairgrieve, T., Kuznetsov, Y., Sandstede, B., Wand, X., 1997.

Ebenbauer, C., Renz, R., Allgower, F., 2005. Polynomial feedback and observer design using nonquadratic lyapunov function. Conference on Decision and Control.

Esbensen, K. H., Geladi, P., 2009. Principal component analysis: Concept, geometrical interpretation, mathematical background, algorithms, history, practice. Chemical and Biochemical Data Analysis 2, 211–216.

Favoreel, W., Moor, B. D., van Overschee, P., 2000. Subspace state space system identification for industrial processes. Journal of Process Control 10, 149–155.

Gay, D. H., 1989. Distributed Parameter Sysetms by means of the singular value decomposition, PhD thesis. University of Wisconsin-Madison, Madison, WI.

Gay, D. H., Ray, W., 1995. Identification and control of distributed parameter systems by means of the singular value decomposition. Chemical Engineering Science 50(10), 1519–1539.

Gestel, T. V., Suykens, J. A. K., Dooren, P. V., De Moor, B., 2000. Imposing stability in subspace identification by regularization. Proceedings of IEEE-CDC.

Giannakis, G., Serpedin, E., 2001. A bibliography on nonlinear system identification. Signal Processing 81, 533–580.

Goethals, I., Pelckmans, K., Suykens, J., Moor, B., 2005. Identification of mimo hammerstein models using least squares support vector machines. Automatica 41, 1263–1272.

Hahn, J., Monnigmann, M., Marquardt, W., 2004. A method for robustness analysis of controlled nonlinear systems. Chemical Engineering Science 59, 4325–4338.

Himmelblau, D. M., 1978. Fault detection and diagnosis in chemical and petrochemical processes. Chemical engineering monograph.New York: Elsevier 8.

Hlavácek, V., Hoffmann, H., 1970. Modeling of chemical reactors Ů xvii steady state axial heat and mass transfer in tubular reactors numerical investigation of multiplicity. Chemical Engineering Sceince 25, 187–199.

Holmes, P., Lumley, J. L., Berkooz, G., 1996. Turbulence, coherent structures, dynamical systems and symmetry. Cambridge University Press: In Cambridge monograph on mechanics.

Hoo, K. A., Zheng, D., 2001. Low-order control relevant models for a class of distributed parameter systems. Chemical enginering Science 56, 6683–6710.

Hoo, K. A., Zheng, D., 2002. Low-order model identification for implementable control solutions of distributed parameter systems. Computers and Chemical Engineering 26 (7:8), 1049–1076.

Huisman, L., 2005. Control of Glass Melting Processes based on Reduced CFD Models. PhD thesis, Technical University of Eindhoven.

Isermann, R., 1984. Process fault detection based on modeling and estimation methodsŮa survey. Automatica 20, 387Ű404.

Jakson, J. E., 2003. A User's Guide to Principal Components. Wiley-Interscience.

Jensen, K., Ray, W., 1982. The bifurcation behavior of tubular reactors. Chemical Engineering Science 37 (2), 199–222.

Johansen, T. A., Foss, B. A., 1999. Multiple model approaches to modeling and control. International Journal of Control 72(7,8), 575.

Jolliffe, I., 2002. Principal Component Analysis; 2nd edition. Springer.

Journée, M., Nesterov, Y., Richtarik, P., Sepulchre, R., 2008. Generalized power method for sparse principal component analysis. ArXiv.
URL `http://arxiv.org/abs/0811.4724`

Karhunen, K., 1946. Zur spektraltheorie stochastischer prozesse. Ann. Acad. Sci. Fennicae. Ser.A1 34.

Karhunen, K., Kari, 1947. Über lineare methoden in der wahrscheinlichkeitsrechnung. Ann. Acad. Sci. Fennicae. Ser. A. I. Math.-Phys. 37, 1–79.

Krause, D., Loch, H., 2002. Mathematical Simulation in Glass Technology. Schott Series on Glass and Glass Ceramics, Springer, 1st edition.

Ku, W., Storer, R., Georgakis, C., 1995. Disturbance detection and isolation by dynamic principal component analysis. Chem. Intell. Lab. Sys. 30, 179–196.

Kunisch, K., Volkwein, S., 2002. Galerkin proper orthogonal decomposition methods for a general equation in fluid dynamics. SIAM Journal on Numerical Analysis 40(2), 492–515.

Lall, S., Marsden, J., Glavaski, S., 1999. Empirical model reduction of controlled nonlinear systems. In: Proceedings of the IFAC Congress F, 473–478.

Lapidus, L., Pinder, G., 1982. Numerical Solution of Part Differential Equations in Science and Engineering. Wiley, New York.

Larimore, W., 1990. Cannonical variate analysis in identification, filtering and adaptive control. In proc. Conference on decision and control. Honolulu, Hawaii.

Li, W., Qin, S., 2001. Consistent dynamic pca based on errors-in-variables subspace identification. Journal of Process Control 11, 661–678.

Linhart, A., Skogestad, S., 2009. Computational performance of aggregated distillation models. Computers & Chemical Engineering 33(1), 296–308.

Ljung, L., 1999. System Identification: Theory for the Users. Prentice Hall PTR; 2 edition.

Lorenze, E. N., 1956. Empirical orthogonal functions and statistical weather prediction. In Statistical Forecasting Project. MIT Press, Cambridge, MA.

Loève, M., 1945. Funcions aleatoire de second ordre. Comptes Rendus Acad. Sci. Paris 220.

Loève, M., 1978. Probability theory. Vol. II, 4th ed., Graduate Texts in Mathematics. Springer-Verlag, Vol. 46.

Lovera, M., Mercere, G., 2008. Identification for gain-schesduling: A balanced subspace approach. Proceedings, IEEE MSC.

Lumley, J., 1967. The structure of inhomogeneous turbulence. In Atmospheric Turbulence and Wave Propagation, Yaglom and V.I. Tatarski (eds). Nauka, Moscow, 166–178.

Ly, H., Tran, H., 2001. Modelling and control of physical processes using proper orthogonal decomposition. Mathematical and Computer Modeling 33, 223–236.

Markovinovic, R., 2009. System-TheoreticalModel Reduction for Reservoir Simulation and optimization. Delft University, Delft.

Marquardt, W., 1990. Traveling waves in chemical processes. International Chemical Engineering 30 (4), 585.

Nauta, M., 2008. Model Reduction of a Lean NOx Trap Catalyst Model. PhD thesis, Eindhoven University of Technology, Netherlands.

Obukhov, A. M., 1954. Statistical description of continuous fields. Trudy Geo-phys. Int. Aked. Nauk. SSSR 24, 3–42.

Overschee, P. V., Moor, B. D., 1996. Identification for Linear Systems: Theory, Implementation, Applications. Kluwer Academic, Dordrecht, The Netherlands.

Özkan, L., Romijn, R., Weiland, S., Marquardt, W., Ludlage, J., 2007. Model reduction of non-linear systems: A grey-box modeling approach. in Proc. 7th IFAC sysmposium on Nonlinear Control Systems, Praetoria.

Parrilo, P. A., 2000. PhD thesis. Structured Semidefinite Programs and Semialgebraic Geometry Methods in Robustness and Optimization. California Institute of Technology, Pasadena, California.

Patankar, S. V., 1980. Numerical Heat Transfer and Fluid Flow. Hemisphere.

Perret, L., Collin, E., Delville, J., 2006. Polynomial identification of pod based low-order dynamical system. Journal of Turbulence 7/17.

Post, L., 1988. Modeling of Flow and Combustion in a Glass Melting Furnace. PhD thesis, Technical University of Delft.

Pougachev, V. S., 1953. General theory of the correlations of random functions. Izv. Akad. Nauk. SSSR. Math. Ser., 17:401-2.

Psichogios, D., Ungar, L., 1992. A hybrid neural network-first principles approach to process modeling. AIChE Journal 38 (10), 1499–1511.

Qin, S., 2006. An overview of subspace identification. Computers and Chemical Engineering 30, 1502–1513.

Rathinam, M., Petzold, L., 2002. Dynamic iteration using reduced order models: a method for simulation of large scale modular systems. SIAM J. Numer. Anal. 40, 1446–1474.

Ravindran, S., 2000. Reduced-order adaptive controllers for fluid flows using pod. Journal of Scientific Computing 15(4), 457–478.

Ravindran, S., Ito, K., 1998. A reduced order method for simulating and control of fluid flows. Journal of Computational Physics 143(2), 403–425.

Romijn, R., Ozkan, L., Weiland, S., Marquardt, W., Ludlage, J., 2008. A grey-box modeling approach for the reduction of nonlinear systems. Journal of Process Control 18 (9), 906–914.

Rugh, W., Shamma, J., 2000. Research on gain scheduling. Automatica 36 (10), 1401–1425.

Scherer, C., Weiland, S., 2009. Lecture notes on Linear Matrix Inequalities in Control. Dutch Institute of Sysetms and Control.

Shvartsman, S. Y., Kevrekidis, I. G., 1998. Nonlinear model reduction for control of distributed parameter systems: A computer assisted study. AIChE Journal 44 (7), 1579–1595.

Sirovich, L., 1987. Turbulence and the dynamics of coherent structures, parts i-iii. Quart. Appl. Math. XLV, 561–590.

Sjoberg, J., et. al., 1995. Nonlinear black-box modeling in system identification: a unified overview. Automatica 31, 1691–1724.

Stone, J. V., 2004. Independent Component Analysis: A Tutorial Introduction. The MIT Press.

Tang, K., Graham, W., Peraire, J., 1999. Optimal control of vortex shedding using low-order models. i: Open loop model development.ii: Model based control. Int. J. Numer. Methods Eng. 44, 945–990.

Thompson, M., Kramer, M., 2000. Modeling chemical processes using prior knowledge and neural networks. AIChE Journal 40 (8), 1328–1340.

TNO, 2008. GTM-X manual.
URL `http://www.tno.nl`

Tóth, R., 2008. Modeling and Identification of Linear Parameter Varying Systems, an Orthonormal Basis Function Approach. University of Delft, The Netherlands.

Verdult, V., 2002. Nonlinear System Identification - A State-Space Approach, PhD Thesis. University of Twenty, The Netherlands.

Verdult, V., Verhagen, M., 2005. Kernel method for subspace identification of multivariable lpv and bilinear systems. Automatica 41 (9), 1557–1565.

Wang, J., Qin, S. J., 2002. A new subspace identification approach based on principal component analysis. Journal of Process Control 12, 841–855.

Wattamwar, S., Weiland, S., 2008. Detection algorthm for bifurcations in dynamical systems using reduced order models. Proceedings of IFAC World Congress, Seoul, Korea.

Wattamwar, S., Weiland, S., Backx, T., 2008. Identification of low dimensional models for slow geometric parameter variation in an industril glass manufacturing process. Proceedings of IEEE MSC (CCA).

Wattamwar, S., Weiland, S., Backx, T., 2009a. Identification of low dimensional parameter varying models for large scale systems. Proceedings of IFAC SYSID.

Wattamwar, S., Weiland, S., Backx, T., 2009b. Identification of low order models for large scale systems. Proceedings of International Symposium on Advanced Control of Chemical Processes(ADCHEM).

Wattamwar, S., Weiland, S., Backx, T., 2009c. Identification of low-order parameter-varying models for large-scale systems. Journal of Process Control. Article in Press. doi:10.1016/j.jprocont.2009.11.010.

Wilcox, K., 2006. Unsteady flow sensing and estimation via the gappy proper orthogonal decomposition. Comput. Fluids 35(2), 208–226.

Willcox, K., Peraire, J., 2002. Balanced model reduction via the proper orthogonal decomposition. AIAA Journal 40(11), 2323–2330.

Wingerden, J., Verhagen, M., 2008. Subspace identification of multivariable systems: A novel approach. Proceedings, IEEE MSC.

Zheng, D., Hoo, K. A., 2002. Low-order model identification for implementable control solutions of distributed parameter systems. Computers and Chemical Engineering 26 (7:8), 1049–1076.

Zhu, Y., Xu, Z., 2008. An lpv model identification for control. IFAC World Congress, Seoul, Korea.

Notations

Abbreviations

CSTR	Continuously Stirred Tank Reactor
CFD	Computational Fluid Dynamics
DAE	Differential Algebraic Equations
DDM	Dynamic Detection Mechanism
DPS	Distributed Parameter Systems
FEM	Finite Element Methods
FVM	Finite Volume Methods
IGMP	Industrial Glas Manufacturing Process
LMI	Linear Matrix Inequalities
LPV	Linear Parameter Varying Methods
LTI	Linear Time Invariant systems
MPC	Model based Predictive Control
MPE	Missing Point Estimation
MRT	Model Reduction Technique
ODE	Ordinary Differential Equations
OLSE	Ordinary Least Square Estimation
PCA	Principal Component Analyis
PDE	Partial Differential Equations
PFR	Plug Flow Reactor
POD	Proper Orthogonal Decompositions
R-MPC	Rigorous Model based Predictive Control
RO-LPV	Reduced Order - Linear Parameter Varying systems
ROM	Reduced Order Models
SID	System Identification
SDM	Static Detection Mechanism
SVD	Singular Value Decompositions
TR	Tubular Reactor

Latin Symbols

A,B,C,D	State space matrices
K	Number of temporal Samples
M	a system model
P	system property
S	Matrix of singular values
T	Temperature
U	Left singular vectors
V	Right singular vectors
H	Enthalpy content
ΔH	Heat of reaction
$\hat{T}$	Estimated solution of a full order model
$\tilde{T}$	Truncated solution of a full order model
$\mathbf{T}^k$	Solution at k^{th} instance in an ensemble
$\top$	Transpose
T_{snap}	Snapshot matrix
a	Modal Coefficient
$\tilde{a}$	Estimated modal coefficients
h	Throat height
i	Sample number
j	Sample number
k	Sample number
l	Number of inputs
m	Number of outputs
n	State space dimensions
n_u	Number of inputs
n_y	Number of outputs
r	State space dimension of reduced model
s	Number of Shifts
t	time instance
u	Vector of Inputs
x	State vector
y	Vector of outputs
z	Spatial variable

Functions and Operators

arg	the argument of a function
col	operator stacking the elements
grad	gradient operator
div	divergence operator
dim	dimension, i.e. the length of a vector
max	the maximum of
min	the minimum of
rank	rank of a matrix
span	the set of all linear combination
$\mathcal{O}_s$	Observability matrix
$\mathcal{T}_s$	Toeplitz matrix
X	matrix stacking the state trajectories
Y	matrix stacking the output trajectories
$\mathcal{R}$	correlation operator
$\mathcal{P}$	projection operator
$\mathcal{I}$	injection operator
$\mathcal{F}$	nonlinear function
$\mathcal{J}$	Jacobian operator
$\langle \cdot, \cdot \rangle$	inner product
$\|\| \cdot \|\|$	norm
∇	the del operator

Greek Symbols

ρ	mass density
λ	eigenvalue
σ	singular value
ϕ	orthonormal POD basis
ψ	orthonormal basis
θ	system paramter
β	spline parameters
α	spline weights
υ	velocity
q_ϕ	source/sink term
$\geq$	greater than or equal to

$\leq$	less than or equal to
Ω	spatial domain
∞	infinity
ξ	states in term of deviations around a point
$\otimes$	Kronecker product
Γ	diffusion coefficient
$\perp$	orthogonal compliment
τ	time delay
$\hat{\theta}$	estimated parameters
δ	Kronecker delta
$\rightarrow$	mapping
ϵ	residue or error
Ξ	output error matrix
Π	product
$\exists$	there exists
$\approx$	approximately equal to
$*$	critical value
Σ	a system model
Φ	operator spanned by POD basis
Ψ	operator spanned by orthonormal basis
ϑ	vector of system parameters
ζ	spatial variable

Sets and set operators

$\forall$	for all
$\in$	an element of
$\subset$	subset of
$\subseteq$	subset to equal
$\cup$	union of two sets
$\cap$	intersection of two sets
Θ	set of system paramters
$\mathcal{H}$	infinite dimensional Hilbert space
$\mathcal{H}_n$	finite dimensional Hilbert space
$\mathcal{M}$	set of model class
$\mathbb{R}$	the set of real numbers
$\mathbb{R}^+$	the set of all positive real numbers

$\mathbb{T}$	time domain
$\mathcal{U}$	set of admissible input signals

Acknowledgements

Time flies! Especially during a PhD period. Last four years belonged to the fastest period of my life. Even in its fast pace, many faces appear prominently in front of my eyes to whom I wants to say 'thank you!'

In spite of having a different educational background, I jumped into the PhD project only with sheer belief in personal abilities. But when the actual journey started, I realized that without the help from others, the goal can not be easily achieved. And I must say, I was lucky! I got help from many people during last four years.

I take this opportunity to thank my family; without whose support it would have been impossible to have reached this stage of life. Mom, dad and my other family members, I am thankful to you, for your love, moral support and trust in me, throughout my life.

I am very thankful to my promoter Prof. Ton Backx, for giving me an opportunity to pursue PhD in a research stream that is different than my educational background. Ton, your genial and liberal nature during our technical meetings helped me to get a better understanding of the problems and to pursue the topics of my liking.

I am also thankful to my co-promoter Siep Weiland, for our weekly technical discussions and his continuous support towards the development of my ideas. It definitely helped me to groom from a master to a PhD student. Siep, from so many corrections that I got from you, I tried to learn the art of writing a presentable scientific work. Without your help, writing this thesis would have been a very difficult thing.

I am thankful to Prof. Paul van den Bosch for creating a cordial work environment in our group. I am sure, despite being thousands of miles away from their country of origin, every new PhD student feels comfortable here. Like any other PhD student I am thankful to Barbara not just for her efforts to find slots in busy agendas but also for helping me as an international student in all possible way. Your presence makes this group complete.

I am also thankful to Prof. W. Marquardt, Prof. O. Bosgra and Prof. S. Skogestad for their time to read my thesis diligently and for making important suggestions. It has definitely helped me to improve the thesis quality. I also thank Prof. Paul van den Hof and Prof. Paul van den Bosch for being members of the extended committee.

I also thank my old and new colleagues for maintaining a supportive work culture. Maarten, Mark, Haiko, Alexander, Michel it seems like yesterday when you were here. Maarten, you are a nice friend. I learned many 'small small' and 'big big' things from you in initial phase of my PhD. Mark, I will remember you for indirectly teaching me 'relaxed, cheerful but still productive way of working'. I learned many aspects of the Dutch culture from you.

I thank you Andrej, for being my good friend for all these years. Your technical inputs were always useful to me. I always enjoyed your company. Moreover, it was fun with the new team in the group. Thanks guys, for your lively presence in the group! Michal, Patrick, Jasper, Femke, Jochem, Joris, Chenyang, Mark, Jaron, Mohammed, Ralph, Rob and Andelko, your company makes a new person feel comfortable in the group. Michal and Klarka, thank you for being my nice social friends. Jochem, thanks for being an active room-mate and an amiable person. Jasper, I enjoyed the conference that we attended together.

I am also very grateful to other colleagues. Leyla, your leading role and technical contribution within our PROMATCH cluster was useful to me. Will Hendrix, you are very gentle and helpful person. You helped me in many small things related to PROMATCH. Udo, I am thankful to you for the support you always offered cheerfully. Yucai, I express my thanks to you for the technical discussions that we had. Your practical approach to the scientific problems has been motivating to me.

I was also lucky to have many international friends during the last four years. Arvind, Jiri, Patricio, Sam, Karin, Shantanu I thank you all for making my social life eventful and enjoyable.

I am also thankful to PROMATCH cluster members - Reinout and Jobert. Reinout, you are a nice friend and a helpful person. I also thank the other members of PROMTACH team - Lynn, Andreas, Di-

ago, Omar, Stephan and Pablo. The social events after our progress meetings were a great fun for me. I will always cherish those moments.

This PhD work is supported financially by Eindhoven University of Technology and the European Union within the Marie-Curie Training Network PROMATCH. I express my deep thanks for the same. Moreover, I also express my thanks to TNO glass group for providing the GTM-X software and related support.

I am thankful to all those odd people whom I met in conferences or in DISC courses or at other places in last four years. Knowingly and unknowingly they greatly improved my understanding about the systems and control theory apart from giving me the flavor of international culture.

The last person whom i want to express my deep thanks is newest member in my life, my wife Deepali. I know, probably I spent less time with you Deepali, especially when we are *recently married*. Your continuous support, love, affection and understanding nature made it easy for me to focus on my crucial phase of PhD.

At the end, I want to express my gratitude to the supreme almighty, God Shri Krishna. Your message inspires the existence of my living!

Satyajit Kishanrao Wattamwar
Eindhoven, Jan. 2010

Curriculum Vitae

Satyajit Kishanrao Wattamwar was born on 12^{th} June 1980, Manwath, in the state of Maharashatra, India. In 2001, he received his Bachelors of Engineering degree with specialization in Chemical Engineering from University of Pune, India. In October 2005 he received his M.Sc. degree in Chemical and Process Engineering from University of Magdeburg, Germany. During his M.Sc. thesis he worked on experimental optimization of a polymerization reaction in cooperation with Max-Plank Institute, Magdeburg, Germany and Schirm A.G., Germany.

Since January 2006 he is working towards his Ph.D. degree at Eindhoven University of Technology. His prime research interests include model reduction for large scale dynamical systems, system identification and applications in chemical processes. He was one of the researchers involved in the PROMATCH project, which was financially supported by the European Union.

In 2009, he received certificate from “Dutch Institute of Systems and Control" for successfully completing the graduate course work.